Application of indigenous microbial biofilms for bioremediation of polycyclic aromatic hydrocarbon contaminants of the Indian Sundarbans

Thesis submitted for

THE DEGREE OF DOCTOR OF PHILOSOPHY

JADAVPUR UNIVERSITY

2023

By

Saranya Balu

Index No: D-7/ISLM/97/19

School of Environmental Studies

Jadavpur University, Kolkata-700032, India

Dedicated to
My Father

THESIS DETAILS

1. Title of the Thesis: Application of indigenous microbial biofilms for bioremediation of polycyclic aromatic hydrocarbon contaminants of the Indian Sundarbans

2. Index No. and Date of Registration: D-7/ISLM/97/19 registered on November 1, 2019

3. Name, Designation, and Institution of the Supervisor: Dr. Joydeep Mukherjee

Professor

School of Environmental Studies

Jadavpur University

Kolkata- 700032, India

4. E-mail ID of the Supervisor: joydeep.mukherjee@jadavpuruniversity.in

5. List of Publications:

(a) Publications Related to Doctoral Work -

i. Assessment of polycyclic aromatic hydrocarbon contamination in the Sundarbans, the world's largest tidal mangrove forest and indigenous microbial mixed biofilm-based removal of the contaminants. **Saranya Balu**, Shantanu Bhunia, Ratan Gachhui, and Joydeep Mukherjee. **Environmental Pollution** (2020): 115270. https://doi.org/10.1016/j.envpol.2020.115270

ii. Polycyclic aromatic hydrocarbon sequestration by intertidal phototrophic biofilms cultivated in hydrophobic and hydrophilic biofilm-promoting culture vessels. **Saranya Balu**, Shantanu Bhunia, Ratan Gachhui, and Joydeep Mukherjee. **Journal of Hazardous Materials** (2022): 129318. https://doi.org/10.1016/j.jhazmat.2022.129318

6. List of Patents: Nil

7. List of Presentations in National/International Conferences/Workshops:

i. Presented a poster entitled **"Removal of polyaromatic hydrocarbon contaminants applying indigenous microbial-based mixed biofilms from Sundarbans tidal mangrove forest"** authored by **Saranya Balu**, Shantanu Bhunia, Ratan Gachhui, Joydeep Mukherjee, at the 6th Annual International E-Conference of Indian Network for Soil Contamination Research (INSCR) on "Microbes in sustainable development" (November 15 to 18, 2021) .

STATEMENT OF ORIGINALITY

I **SARANYA BALU** registered on **1ST NOVEMBER 2019** do hereby declare that this thesis entitled "***Application of indigenous microbial biofilms for bioremediation of polycyclic aromatic hydrocarbon contaminants of the Indian Sundarbans***" contains literature survey and original research work done by the undersigned candidate as part of doctoral studies.

All information in this thesis have been obtained and presented in accordance with existing academic rules and ethical conduct. I declare that, as required by these rules and conduct, I have fully cited and referred all materials and results that are not original to this work.

I also declare that I have checked this thesis as per the "Policy on Anti Plagiarism, Jadavpur University, 2019", and the level of similarity as checked by iThenticate software is 10 %.

Signature of Candidate: Saranya Balu.

Date: 16/01/2023

Certified by Supervisor: 16/1/23

(Signature with date, seal)

Dr. Joydeep Mukherjee
M. Tech.(Biotechnology) Ph.D.(Engg)
Professor
School of Environmental Studies
Jadavpur University, Kolkata 700 032

CERTIFICATE FROM THE SUPERVISOR

This is to certify that the thesis entitled **Application of indigenous microbial biofilms for bioremediation of polycyclic aromatic hydrocarbon contaminants of the Indian Sundarbans** submitted by Smt **SARANYA BALU**, who got his/her name registered on **1st November 2019**.for the award of **Ph.D. (Science)** degree of **Jadavpur University**, is absolutely based upon her own work under the supervision of **Dr. Joydeep Mukherjee** and that neither her thesis nor any part of the thesis has been submitted for any degree/ diploma or any other academic award anywhere before.

16/1/23

Dr. Joydeep Mukherjee
M. Tech.(Biotechnology) Ph.D.(Engg)
Professor
School of Environmental Studies
Jadavpur University, Kolkata 700 032

(Signature of the Supervisor and date with Office Seal)

Dr. Joydeep Mukherjee

Professor

School of Environmental Studies

Jadavpur University

Kolkata 700032

India

DECLARATION

I do hereby declare that the thesis entitled '**Application of indigenous microbial biofilms for bioremediation of polycyclic aromatic hydrocarbon contaminants of the Indian Sundarbans.**' submitted by me for the fulfilment of the continuous assessment of Ph.D. degree course in Science from Jadavpur University, Kolkata, India. The thesis embodies research work carried out by me at School of Environmental Studies, Jadavpur University, Kolkata under the supervision of Dr. Joydeep Mukherjee, Professor, School of Environmental Studies, Jadavpur University, Kolkata 700032 Neither this thesis nor any part of it has been submitted for either any degree/diploma or any other academic award anywhere before.

Saranya Balu

Registration no.: D-7/ISLM/97/19 of 2019-2020

School of Environmental Studies

Jadavpur University

Kolkata-700032

India

ACKNOWLEDGEMENT

Successful completion of this thesis could not have been possible without the collective association of many people during each step of the research work. Therefore, I take this opportunity to acknowledge the people who were always there for me when I needed them most during my research period and extend my sincere gratitude toward them.

I would like to embrace my profound gratitude to my Ph.D. supervisor **Dr. Joydeep Mukherjee**, for giving me this opportunity to fulfill my dream. I wholeheartedly express my gratitude for the constant guidance, immensely valuable suggestions, patience, and kind encouragement during my Ph.D. study and for providing the correct conditions and freedom to do research. I thank you for your motivation, patience, support, and trust and for inspiring me to be disciplined, punctual, and hardworking.

I embrace the opportunity to express my deep sense of gratitude to **Dr. Tarit Roychowdhury**, **Dr. Subarna Bhattacharyya** and **Dr. Reshmi Das**, faculty of School of Environmental Studies, and **Dr. Ratan Gachhui**, Department of Life Science and Biotechnology, Jadavpur University for the support, valuable advice and suggestions given by them during their busy schedule.

I also take this opportunity to thank the office staff and all other support staff members of our department, who, through their meticulous services, made my research journey a smooth sail.

I am also indebted to the **Department of Biotechnology, Government of West Bengal,** and **Jadavpur University** for financial assistance and my fellowship disbursement during the research period.

I express my gratitude to **Mr. Shantanu Bhunia**, my fellow mate and brother, for his efficient and laborious sampling and careful handling of samples during the journey from Sundarbans. I am thankful for his support and contribution in every step during my toughest period and also for the successful publications. I would also like to thank my seniors Kaushik Biswas, Riddhi Mahansaria, Sayak Bhattacharya, Veerabadhran Maruthanayagam, Sandeep Chakraborty, and especially Dhruba Bhattacharya for invaluable assistance during my journey. I would also like to thank my lab mates Ankita Bhowmik, Arup Ratan Roy, Shayontani Basu, Tanaya Bhowmick, Chiradeep Basu, and Anirban Chaudhuri for their constant support and assistance. I profoundly appreciate them for providing me with dynamic discussions, a gracious atmosphere, and bearing with me during the good and bad times during my wonderful days of my Ph.D.

I express my indebtedness to my parents **N.K Balakrishnan** and **T Radha Balu**, and my brother **Lt Cdr. Visakh Balu**, sister-in-law **Lt Cdr. Pooja**, niece **Nyra Nair** and my in-laws **M.Venugopalan**, **Usha Venugopal**, **Nisha**, **Pradeep,** and nephews **Krishnaraj** and **Karnajith**, for their love, affection, and support during every moment in my life. And also my gratefulness towards my husband **Naveen Venugopal** for his endless love, everlasting indispensable help, support, and patience. Very special gratitude to my dearest daughter, **Nihira Naveen** for the priceless love.

Finally, last but not least, my sincere gratitude to my department, **School of Environmental Studies,** and my university, **Jadavpur University,** for providing all the opportunity to fruitfully complete my thesis work.

Above and beyond all, my heartfelt gratitude to **God almighty**, my family, and my friends for giving me more than I can say.

-Saranya Balu

INDEX

List of abbreviations

%	Percentage
≤	less than or equal to
°C	Degree Celsius
°C/min	Degree Celsius per minute
µg/L	Micro gram per Litre
Ace	Acenaphthene
Acy	Acenaphthylene
ANOVA	Analysis of variance
Ant	Anthracene
As	Arsenic
ASN III	Artificial seawater medium
B(a)A	Benzo (a) anthracene
B(a)P	Benzo (a) pyrene
B(b)F	Benzo (b) fluoranthene
B(g,h,i)P	Benzo (g,h,i) perylene
B(g,h,i)P	Benzo (g,h,i) perylene
BBM	Bold's basal media
BG 11	Blue green algal media
bp	base pair
CD	Czapek Dox
Cd	Cadmium
Chl *a*	Chlorophyll a
Chl *b*	Chlorophyll b

Chl *c*	Chlorophyll c
Chl *d*	Chlorophyll d
Chr	Chrysene
Co	Cobalt
CPS	capsular/bound polymeric substances
Cu	Copper
D(a,h)A	Dibenzo(a,h)anthracene
DCM	Dichloromethane
EPS	Extracellular polymeric substance
ERL	Effects range low
ER-L	Effects range-low value
ERM	Effects range median
ER-M	Effects range-medium
ES-CCF	Enhanced Surface Area Conico Cylindrical Flask
Fla	Fluoranthene
Flu	Fluorene
GC FID	Gas chromatograph flame ionization detector
GPS	Global Positioning System
GYM	glucose yeast maltose
H_2SO_4	Sulfuric acid
HMW	High-molecular weight
Hrs	Hours
HTL	High tide level
IARC	International Agency for Research on Cancer
Ind	Indeno (1,2,3-cd) pyrene

ITS	Intergenic Transcribed Spacer
$K_2Cr_20_7$	Potassium dichromate
Kk	Kakdwip
Km	Kilometre
Km/hr	Kilometre per hour
K_{ow}	Octanol-water partition coefficient
LiP	Lignin peroxidase
LMW	Low-molecular weight
LOD	limit of detection
LTL	Low tide level
m^3/sec	Cubic meter per second
Mg/ml	Milligram per milliliter
MHHW	Mean highest high water level
Min	Minute
ml	Milliliter
Ml/min	Millilitre per minute
MLHW	Mean lowest high water level
Mm	Millimetre
MnP	Manganese peroxidase
mS/cm	Milli siemens per centimetre
Mt	Maipit
MTL	Mid-tide level
NA	Not applicable
Nap	Naphthalene
ND	Not detected

ng/L	Nano gram per Litre
Nk	Namkhana
NTU	Nephelometric Turbidity unit
OC	Organic carbon
OM	Organic Matter
OTUs	operational taxonomic units
PAHs	Polycyclic aromatic hydrocarbons
Pb	Lead
PCBs	Polychlorinated biphenyls
Pg	Purba Gurguria
Phe	Phenanthrene
PMMA	polymethyl methacrylate
POPs	Persistent organic pollutants
Pp1 and Pp2	Patharpratima
ppm	Parts per million
ppt	Parts per trillion
Pyr	Pyrene
QIIME	Quantitative Insights into Microbial Ecology
rpm	Revolutions per minute
RPS	Released polymeric substances
SEM	Scanning electron microscopy
Sq.km / Km sq.	Square Kilometre
US EPA	US Environmental Protection Agency
Zn	Zinc
µ mol	Micromoles

List of Figures

List of Tables

…….

ABSTRACT

The Sundarbans, the world's largest mangrove tidal forest, is a typical and unique ecosystem with rich biodiversity. However, over the past few decades, the most important environmental concern has been the presence of toxic and recalcitrant pollutants coming down through the rivers from India, Bangladesh, Nepal, and Bhutan via the Ganga- Mehgna- Brahmaputra (GMB) river network due to various anthropogenic activities. As a result, the estuary has become vulnerable to chemical pollutants such as heavy metals, polychlorinated biphenyls (*PCBs*), and polycyclic aromatic hydrocarbons (*PAHs*). Among the diverse amount of pollutants available, PAHs are one of the toxic wastes that affect the environmental health and the population who depend on the Sundarbans mangrove ecosystems. With the rising realization of the harmful effects of PAH pollutants on the environment and human health, internationally, more attention has been received for the remediation of such chemicals. Bioremediation using microbial biofilms is the most promising technique compared to other remediation processes.

In this study, the polycyclic aromatic hydrocarbons (PAHs) distribution of surface water and sediments collected from various geographical locations of the Indian Sundarbans were ascertained. The total concentration of 16 priority PAH pollutants of water and sediments fluctuated from non-detectable to 125 ng/ml and 4880 to 2×10^4 ng/g dry weight, respectively. The concentrations of individual PAHs in Sundarbans water were much higher than the limit proposed by WHO. The total PAH concentration of sediments surpassed the Effects Range

Low (ER-L) and the recommended Effects Range-Median (ER-M) values, indicating that the PAHs might adversely affect the Sundarbans' biota. The source identification studies using PAH ratios indicated the pyrogenic and petrogenic contaminations in the Sundarbans sediments. A weak positive correlation of PAHs with organic carbon and organic matter indicated continuous inflow of PAHs.

This study also focused on intertidal microbial biofilms of the Sundarbans and how these biofilms can be exploited to remove PAH contaminants. Six heterotrophic, as well as phototrophic, stably-growing, robust, and well-formed biofilms, were selected, each representing the different geographical locations: (Pg) Purba Gurguria, (Mt) Maipit, (Pp1 and Pp2) Patharpratima, (Nk) Namkhana and (Kk) Kakdwip. These indigenous biofilms were cultivated in two sets of the patented biofilm-promoting culture vessel possessing a hydrophilic glass surface and hydrophobic polymethyl methacrylate (PMMA) surface, containing liquid media spiked with 16 priority PAHs. All media attained 97-100% removal efficacy of 16 PAHs through the heterotrophic biofilm-mediated process. The mean residual PAH from the media collected from hydrophobic and hydrophilic flasks showed no significant difference. However, residual amounts of certain PAHs such as Acenaphthene (Ace), Anthracene (Ant), Benzo(b)Fluorathene [B(b)F], Benzo(ghi)perylene [B(ghi)P], and Benzo (a) pyrene [B(a)P] exhibited differences in their sequestration when cultivated in flasks with hydrophobic and hydrophilic surfaces. The mean residual amounts of total PAHs in biofilm biomasses were in the order Pp1<Kk < Nk < Pp2<Mt < Pg. Composition, structure, and abundances of indigenous heterotrophic microbial communities in PAH-sequestering biofilms by amplicon-based metagenomics established bacterial phyla such as *Proteobacteria*, *Firmicutes*, *Actinobacteria* *Bacteroidetes*, *Planctomycetes,* and *Chloroflexi*, and members of *Ascomycota* phylum of fungi. In addition, the dominance of *Clostridium butyricum*, *Sphingobacterium multivorum*, *Candida tropicalis,* and *Paecilomyces fulvus* were proven.

Phototrophic biofilm attained 98-100% removal efficiency of individual PAHs in all media except for Pg_p biofilm. Significant differences were observed between mean residual PAHs obtained from the liquid media and phototrophic biofilms cultured in PMMA and glass flasks. The biofilm phototrophic community composition did not alter when challenged with PAH; production of biofilm biomass and photosynthetic pigments synthesis and extracellular polymeric substances (EPS) were enhanced. Increased production of EPS was observed in the biofilms treated with PAHs, and a change in the production of capsular polysaccharide (CPS) and released polysaccharide (RPS) was also studied. The ratios of RPS proteins to polysaccharides increased during the biodegradation, whereas the ratios of CPS proteins to polysaccharides were almost constant. The correlation between hydrophobicity and uronic acid contents of EPS was evident in this study. SEM image showed the accumulation of EPS on the surface, and the structure of the biofilms was clustered and embedded within the EPS matrix at the end of the experiment. Morphological analyses of these PAH degrading biofilms showed the presence of purple sulfur bacteria, pennate diatoms, cyanobacteria (*Gleocapsa* sp., *Chloroidium* sp., *Microcystis* sp. and *Phormidium* sp.) as well as *Closterium* sp. like green algae.

CHAPTER 1

INTRODUCTION

The world has come across the most critical environmental concern during the last decades: contaminants with toxic and recalcitrant properties caused by various anthropogenic practices. The presence of xenobiotic compounds caused by solid waste deposits, inorganic contaminants like heavy metals, persistent organic pollutants (POPs), namely polycyclic aromatic hydrocarbons (PAHs), polychlorinated biphenyls (PCBs), pesticides, and unprocessed industrial effluents causes critical environmental as well as health problems (Singh and Haritash, 2019). Direct and indirect release of these compounds into the environment leads to water, soil, and air pollution and further enters the food chain. Among the diverse amounts of pollutants available, PAHs are one of the toxic, noxious wastes affecting aquatic and terrestrial ecosystems adversely.

PAHs are a ubiquitous group of environmentally persistent chemicals with numerous structures with two or more aromatic rings. PAHs cause toxic, mutagenic, and carcinogenic effects on living beings. PAHs are broadly dispersed and repositioned in the environment because ofincomplete combustion of organic matter, coal combustion, and automobile exhausts. PAHs infiltrate the ecosystem through diverse routes and are usually found as an assortment of two or more similar compounds, e.g., soot (Abdel-Shafy and Mansour, 2016). Above 100 unique PAHs are extensively distributed in the surroundings; the U.S. Environmental Protection Agency (US EPA) has reported 16 PAHs as priority pollutants based on their toxicity (Shukla et al. 2014). Some of them are categorised as human carcinogens by US EPA and European Union (Singh and Haritash, 2019). They are hydrophobic with low water solubility, which tends to bind with soil/sediment organic matters, making them recalcitrant in soil. Due to this, PAHs are difficult to degrade compared to other organic pollutants. With the rising realization of the harmful effects of hazardous pollutants on the environment and human health, internationally, more attention has been received for the remediation of such chemicals.

Several methods have been established for the remediation of the contaminated sites, and they include physical (solvent extraction, thermal desorption, and air sparging), chemical (oxidation using ozone, photocatalytic degradation), and biological methods (microbial, land-farming, phytoremediation, and composting,). The remediation methods selected depend on several factors, such as the nature of contaminants present, the type of soil, interference of other compounds, and the risk associated with the technique adopted (Singh and Haritash, 2019). Of these, the biological method of remediation (bioremediation) has several advantages over physical and chemical methods, including avoidance of harsh chemicals, minimum or no disruption of land or wildlife in and around the treated site, and also they are economically efficient (Mitra and Mukhopadhyay, 2016).

Several microorganisms, such as bacteria, fungi, yeast, and microalgae, have the potential to use and mineralize different types of PAHs. They can convert PAHs into less toxic compounds/water and carbon dioxide (Alexander, 1994). Bacteria and fungi are capable of readily degrading low-molecular-weight (LMW) PAHs (two-three ringed structures) such as naphthalene (Nap), phenanthrene (Phe), and anthracene (Ant) (Peng et al., 2008). Due to low bioavailability and strong adsorption into the soil organic matter, high- molecular-weight (HMW) PAHs (four or more rings) are the most persistent, and all the microbes cannot easily degrade them. However, microorganisms release some enzymes for the detoxification and mineralization of PAHs. Indigenous microorganisms isolated from polluted sites illustrate more degradation potential since they have survived contaminants' toxicity and adapted to the polluted environment (Singh and Haritash, 2019).

From time to time, studies show that specific microorganism lacks the genes required for the enzyme synthesis involved in the complete mineralization of PAHs. These findings led the researchers to focus on developing microbial consortia to degrade pollutants completely. The different microbial species in the consortia of biofilms possess different metabolic

degradation pathways and can collectively or individually remove PAHs (Ghosal et al., 2016). Biofilm-mediated degradation of PAHs is more efficient than single microbes since they have a high tolerance toward hazardous pollutants. Biofilms canassimilate, immobilize, and metabolize environmental pollutants (Mitra and Mukhopadhyay, 2016). As PAHs in the environment are found in mixtures, wide varieties of microbial species in the indigenous population exhibit differential gene expression leading to a complex phenomenon known as co-metabolism. The metabolism of one PAH in the mixture possibly has a synergistic effect on the metabolism or degradation of other PAHs (Van Herwijnen et al., 2003).

Microbial species are encapsulated by an extracellular polymeric substance (EPS) matrix to form a mat or biofilm; EPS provides a beneficial structure to the microbes in the biofilms and protects the microbes from environmental stress, U.V damage, desiccation, and high concentrations of toxic chemicals and pollutants. EPS composition varies with the type of species present, environmental status, growth conditions, availability of nutrients, and surface to which microbes are attached. EPS can immobilize the PAHs or any pollutants and aid the degradation process. In addition, EPS constituents act as biosurfactants that can enhance hydrophobic compounds' solubilization. Extracellular enzymes within the EPS also aid in the decontamination of organic pollutants and heavy metals (Mitra and Mukhopadhyay, 2016).

Most of the research was concentrated on the biodegradation of substrate (PAH) under aerobic conditions, but in reality, PAHs are present in a mixture or coexist with other pollutants. Studies also suggest that the coexistence of PAHs sometimes enhances or inhibits the degradation of other PAHs. For example, the removal efficiency of microbes is more robust when acenaphthene (Ace), fluorene (Flu), phenanthrene (Phe), anthracene (Ant), and pyrene (Pyr) are present concurrently compared to the degradation when the PAHs are present separately, and this could be because the existence of PAHs together provides more carbon

source for the microorganisms thereby increasing the rate of biodegradation (Yuan et al., 2002)—compared with bacteria and fungi only a lesser attention is paid to the PAHs biodegradation by microalgae (cyanobacteria, diatoms). Therefore, we aimed to isolate indigenous intertidal biofilms from the PAH-polluted regions of Indian Sundarbans estuaries and identify heterotrophic and phototrophic biofilms with PAH degradation potential.

1.1. Polycyclic aromatic hydrocarbons (PAHs)

PAHs are a group of hazardous organic pollutants arranged in linear, angular, or cluster form. They consist of compounds with two to seven fused carbon rings with substituted groups attached to them (Adeniji et al., 2018). The simplest form of PAHs is Nap with two rings. They are relatively less soluble in water on the other hand highly lipophilic in nature. majority of PAHs have low vapor pressure, are readily adsorbed to the particles in the air, and are globally dispersed in terrestrial, atmospheric, and aquatic ecosystems. The vapor pressure and solubility of PAHs decrease with the addition of a ring and increase in molecular weight, whereas the resistance towards the oxidation and reduction of PAHs increases (Abdel-Shafy and Mansour, 2016). PAHs are classified into two categories based on the number of aromatic rings, LMW PAHs with two to three rings and HMW PAHs with four to six-ringed structures (Figure 1).

1.1.1. Sources of PAHs

Sources of PAHs can be classified into two major types: natural sources and anthropogenic origins. Natural sources include forest fires, petroleum seeps, agricultural burning, decomposition of vegetative litter falls, erosion of sedimentary rocks containing petroleum hydrocarbons, volcanoes, and bacterial and algal synthesis (Abdel-Shafy and Mansour, 2016). Anthropogenic sources consist of two groups, namely pyrolytic and petrogenic. Exposure of

organic substances to high temperatures under less or no oxygen leads to the formation of pyrogenic PAHs. In contrast, petrogenic PAHs are formed during crude oil maturation or the release of petroleum-related products. The sources of pyrolytic PAHs are the incomplete combustion of fuels, combustion of woods in the forest, and fireplace reuse and incineration. Significant sources of petrogenic PAHs include the release of oil, gasoline, and related petroleum products during transportation, ocean, and freshwater oil spills, and road construction materials such as the production of coal tar and carbon black (Brazkova and Krastanov, 2013).

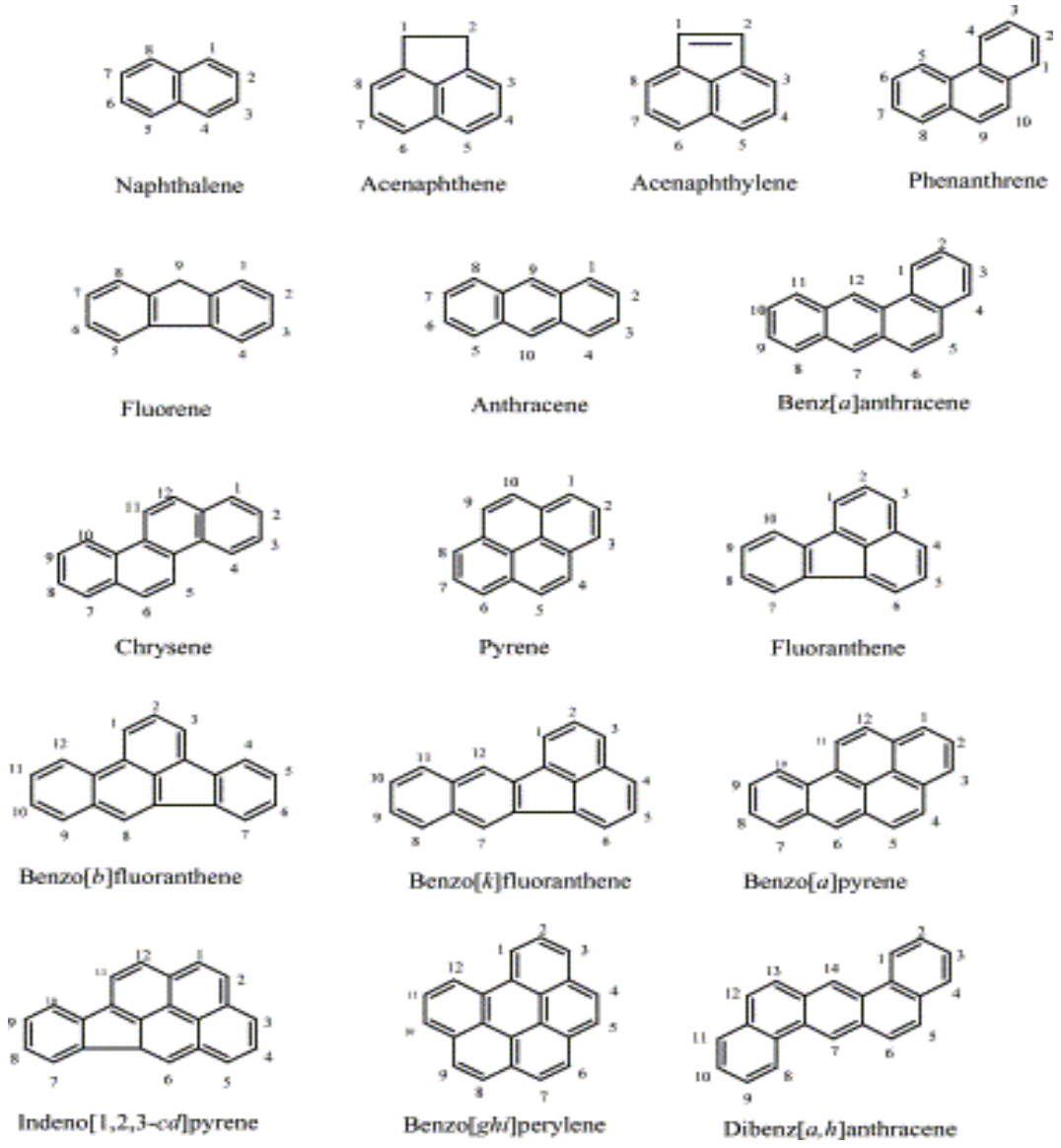

Figure 1: Structure and nomenclature of 16 priority PAHs. (Yan et al., 2004)

1.1.2. Fate of PAHs in the environment

Once emitted into the atmosphere by incomplete combustion of organic matter, PAHs are present in two distinct phases, namely a vapor and a solid phase. PAHs with low vapor pressure readily get adsorbed to atmospheric particulates. Differences in the vapor pressure of each PAH cause the individual PAHs to disperse between vapor and solid phases in different concentrations (Ravindra et al., 2008). Dry or wet deposition causes continuous deposition of atmospheric PAHs to the earth. PAH deposition can either be from nearby sources like automotive exhaust or a distant source carried through the air. Although most of the PAHs deposited will be bound to the soil particles, the sorption of PAHs to the soil depends on the physical properties of the PAHs and soil.

The PAHs octanol-water partition coefficient (K_{ow}) is another critical parameter in deciding the PAHs sorption ability to soil (Schwarzenbach et al., 1993). The aqueous solubility decreases and the sorption of PAHs to soil particles increase with an increase in $K_{ow.}$ Dry and wet deposition of atmospheric PAHs also causes the distribution of PAHs on the surface of water bodies which eventually get integrated with sediments. PAHs enter the water bodies from sewage effluents, storm, and surface runoff water; some PAHs get sorbed to the sediment particles. PAHs with low molecular weight, which are soluble in the water, get incorporated into the pore water and increase the bioavailability of PAHs in water (Abdel-Shafy and Mansour, 2016).

The presence of PAHs in water and sediments makes them available to aquatic and terrestrial living beings. Due to bioaccumulation, PAH concentration in aquatic life, such as fish, mollusks, and shellfish, is predicted to be higher than in their environment. Through several routes like inhalation, ingestion, and dermal contact PAHs get absorbed into mammals (Dong et al., 2012, Burchiel and Luster. 2001). PAH accumulation in groundwater, soil, or

/and sediments enhances the absorption of PAHs by plant roots and is further translocated to different parts of the plants (Patel et al., 2020).

1.1.3. Route of PAH exposure

Most of the population is exposed to PAHs from workplaces, such as smoke from coal, automotive, and road dust (Lee, 2010). However, non-workplace-based exposure also occurs, and exposure occurs via consuming food and water containing PAHs, use of grilled and smoked food, and cigarette smoke; for non-smokers, 70% of exposure is related to food and diet (Suman et al., 2016). Food processing such as roasting, grilling, barbecuing, and frying may cause PAH in food. PAH content in drinking water varies between 1ng/L and 11µg/L; according to WHO, the acceptance value of benzo (a) pyrene [B (a) P] is 0.7 µg/L. Fruits and vegetables grown in soil contaminated with PAHs may also contain PAH contaminants due to atmospheric deposition (Patel et al., 2020). According to the German Environment Agency, PAH is present in our daily life products such as toys, bathing shoes, mousepads, bicycle handles, and many sports items (Brandt and Einhenkel, 2016).

1.1.4. Health effects of PAHs on human

The effect of PAHs on an individual's health depends on various factors like the concentration of PAHs to which an individual is exposed, the extent and route of exposure, and the toxicity of PAHs (Dahlstrom and Bloomhuff, 2014). Depending on the extent of exposure, health effects have been seperated into acute (short-term effects) and chronic (long-term effects). The short-term health effects of PAHs in human is not very much evident. Exposure to high concentrations of certain PAHs shows symptoms like eye irritation, nausea, diarrhoea, vomiting, skin irritation, and inflammation (Unwin et al., 2006). Nap is known to cause direct and instant skin irritation, but Ant and B(a)P initiate allergic reactions in humans and animals.

Chronic exposure to PAHs leads to cataracts, kidney and liver damage, lung abnormalities, reduced immune function, cancer, and genetic mutations. US EPA has categorized 16 PAHs as priority pollutants because of their attribution to the environment and human health (Table 1). Based on carcinogenic tendencies PAHs are generally classified into four groups by the International Agency for Research on Cancer (IARC). Group one belongs to substances with the highest carcinogenic potential; B (a) P is the only PAH in this group and is the primary environmental carcinogen discovered. Group 2A PAHs are probably carcinogenic to humans, e.g., dibenzo (a,h) anthracene [D(a,h)A], group 2B are potentially carcinogenic to humans, and group 3 is not acknowledgeable as carcinogenic to humans (Ghosal et al., 2016).

Table 1: 16 priority PAHs enlisted by US EPA

PAH	Chemical Formula	Molecular weight (g/mol)	IARC group	ERL (µg/kg)	ERM (µg/kg)
Naphthalene (Nap)	$C_{10}H_8$	128.17	2B	160	2100
Acenaphthylene (Acy)	$C_{12}H_8$	152.21	NA	44	640
Acenaphthene (Ace)	$C_{12}H_{10}$	152.20	3	16	500
Fluorene (Flu)	$C_{13}H_{10}$	166.22	3	19	540
Phenanthrene (Phe)	$C_{14}H_{10}$	178.23	3	240	1500
Anthracene (Ant)	$C_{14}H_{10}$	178.23	3	843	1100
Fluoranthene (Fla)	$C_{16}H_{10}$	202.26	3	600	5100
Pyrene (Pyr)	$C_{16}H_{10}$	202.26	3	665	2600
Benzo (a) anthracene (B(a)A)	$C_{18}H_{12}$	228.29	2B	261	1600
Chrysene (Chr)	$C_{18}H_{12}$	228.29	2B	384	2800
Benzo (b) fluoranthene (B(b)F)	$C_{20}H_{12}$	252.32	2B	NA	NA
Benzo (k) fluoranthene (B(k)F)	$C_{20}H_{12}$	252.32	2B	NA	NA
Benzo (a) pyrene (B(a)P)	$C_{20}H_{12}$	252.32	1	430	1600
Indeno (1,2,3-cd) pyrene (Ind)	$C_{22}H_{14}$	278.35	2A	63.4	260
Dibenz (a,h) anthracene D(a,h)A	$C_{22}H_{12}$	276.34	2B	NA	NA
Benzo (ghi) perylene B(ghi)P	$C_{22}H_{12}$	276.34	3	N.A.	NA
ΣPAHs				**4000**	**44,792**

NA: not applicable, IARC: International Agency for Research on Cancer; ERL: effects range low; ERM: effects range median; (Adeniji et al., 2018)

In rodents, PAHs can induce immune suppression reactions, but specific mechanisms of how PAH induces immune toxicity are still not precise. Studies conducted in in-vitro mammalian cell lines illustrated that PAH, when metabolized to diol epoxides, reacts with DNA, inducing genetic damage. Genotoxicity plays a major role in developing cancer in humans. Laboratory studies conducted using B(a)P, benzo (a) anthracene [B(a)A], and Nap demonstrated the embryonic effects of PAHs in experimental animals (Patel et al., 2020).

1.2. The Sundarbans ecosystem

Sundarbans, the world's largest deltaic tidal halophytic mangrove forest, occupies an area of 10,200 sq. km, spreading across India (41%) and Bangladesh (59%) (Figure 2). This largest delta is formed from sediments deposited by the rivers the Ganges, Brahmaputra, and Meghna which converge on the Bengal Basin (Ghosh et al., 2010). The Indian Sundarbans mangrove tidal forest in the estuarine phase of the River Ganges with an area of 9630 km^2, of which 4264 km^2 is considered a Reserve Forest. UNESCO declared this largest delta covering about 2.84% of the global mangrove area (15×10^4 sq. km) as a World Heritage site (1997) (Ray et al., 2011) and also declared it as Ramsar site no. 2370 in 2019.

Indian Sundarbans is known as the Hoogly-Matla estuary; although other than Hoogly and Matla rivers, there are numerous big and small rivers across the Sundarbans, namely Bidya, Saptamukhani, Raimangal, Muriganga, Thakuran, Gomor. Sundarbans are interconnected by a complex system of mudflats, tidal waterways, and small islands of salt-tolerant mangrove forests (Manna et al., 2012). The tidal waterways are sustained mainly by the diurnal tidal flow. The build-ups brought down to the sea are thrust back into the channels and deposited to form beds; a steady rise in the bed ultimately blocks the water flow, gradually developing into small islands (Bhattacharya, 1989). Macrotidal effects make the Sundarban mangrove one

of the top morphogenetically distinct ecosystems in the world (Zanardi-Lamardo et al., 2019). The mudflats are formed at the estuaries and on the deltaic island where the low velocity of river and tidal current occurs. The core parts of the mudflats are magnificent homes for the lush mangroves. The food chain in the estuarine ecosystem is controlled by the Sundarbans mudflat (Bose, 2004).

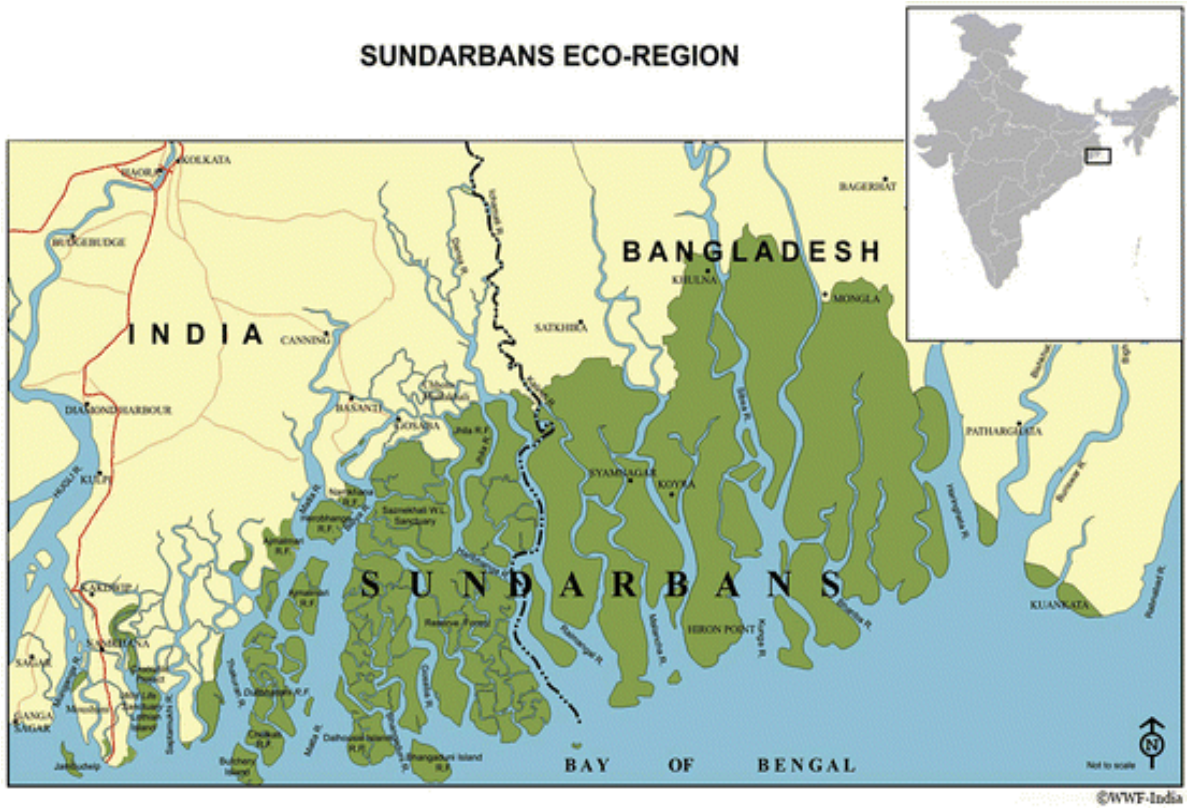

Figure 2: Map of the Sundarbans mangrove ecosystem (Gopal and Chauhan, 2018)

1.2.1. Climate

The seasonal climate of the Sundarbans ecosystem are well divided into pre-monsoon (March-June) with no rainfall and the highest temperature (42 °C), monsoon (July to October) with maximum rainfall and average temperature, and post-monsoon having the lowest temperature of 10°C (November –February). Sundarbans receive about 1500-2000 mm of total annual rainfall. Cyclonic high-intensity storms occur during May but are frequently linked with

monsoon rainfall. The maximum wind velocity experienced during April –June is 16.7-50 km/hr, and the minimum is 10.7-11.8 km/hr (December – February) (Chakraborty, 2011).

1.2.2. Tidal waves and their amplitude

Sundarbans's mean sea level is about 3.30 m, the mean highest high water level (MHHW) is observed to be 5.94 m, and the mean lowest high water level (MLHW) is 0.94 m. The large tidal amplitude and gentle slope of the coast help tidal water to penetrate at an average distance of 110 km inward from the shoreline; in some other areas, the tidal effect is felt over 300 km inland (Selvam, 2003). Different phases of tidal cycles are created based on the seasonal and annual variation of the location Sun, moon, and earth. Intertidal regions are divided into three, high tide level (HTL), mid-tide level (MTL), and low tide level (LTL). The uppermost part of the intertidal zone is the HTL, and the lowermost part represents the LTL. In contrast, any intertidal zone between the uppermost part of the LTL and the lowermost border of HTL represents the MTL (Chakraborty, 2011). Sundarbans experience two flood tides (inflow) and ebb tides (outflow) with semi-diurnal nature that occurs at 12 hrs intervals and twice a day (Chakraborty et al. 2009).

1.2.3. Nature of soil

The Sundarban delta exhibits silt clay loams, sandy clays and loams, soil with organic and peaty deposits, and swampy and marshy soil, also known as mangrove soil (Mandal and Ghosh, 1989). Parental deposits of Sundarbans are rich in calcium, magnesium, or half-decomposed organic matter. The quantity of freshwater influx and the monsoon rainfall alters the surface soil salinity and its adjacent water bodies. The active delta's soil pH varied from 6.5-8.1 (Gupta, 1987). During pre-monsoon, soil salinity, temperature, organic carbon (O.C.), and sand contents were higher, but during monsoon, the maximum amount of available potassium (K), nitrogen (N_2), and phosphorus (P) were found. Moderate levels of all the above parameters and the lowest temperature, available

K, P, and N_2 were the characteristic feature of soil during post-monsoon. Texture analysis conducted by Gupta (1987) revealed that Sundarbans mangrove soils were mainly silty clay.

1.2.4. Biodiversity of Sundarbans ecosystem

In 1989, the Government of India declared 9630 sq. km of Sundarban, including the Sundarban Tiger Reserve, as Sundarban Biosphere Reserve because of its enriched flora and fauna. Sundarbans is the only mangrove ecosystem in the world, having the famous Royal Bengal Tiger (*Panthera tigris*) among its denizens. Sundarbans is considered a luxuriant habitat for aquatic and terrestrial living beings. The biodiversity of the Sundarban ecosystem makes it the most critical biotic region; biodiversity includes algae, fungi, bacteria, different species of plants, mangrove and tidal marshes, fishes, prawns, Royal Bengal Tiger, and estuarine crocodiles (Das, 2010).

Flora is limited to the forested tracts of the mangrove delta, commonly called Mangrove Tidal Forests (Selvam, 2003). Out of fifty mangrove species present in the world, about 35 species and 117 other halophytic mangrove-associated species are found in Sundarbans (Naskar and Ghosh, 1989). Sundarbans mangrove harbors about 163 fungal species, 150 algal species, 32 lichen species , and 40 species of mangrove associates (Chakraborty, 2011). The name Sundarbans originated from the tree species *Heritiera fomes,* which the locals call the Sundari (Beautiful) tree. Valid mangrove species in the Sundarbans include *Bruguiera cylindrica Rhizophora apiculata, Avicennia marina, Excoecaria agallocha, Sonneratia apetala, Acanthus ilicifolius. Sarcolobus carinatus, Suaeda maritima, Pandanus tectorius* represent the mangrove-associated plant associates (Chakraborty, 2011). Phytoplankton species include *Nitzschia* sp., *Rhizosolenia* sp., *Peridinium* sp., *Ceratium* sp., *Thalassiosira* sp., *Planktoniella* sp, *Gosslorilla* sp., *Ditylum* sp., *Triceratium* sp., *Diploneis* sp., *Fragilaria* sp., *Gyrosigma* sp., *Navicula* sp., *Dynophysis* sp., *Oedegonium* sp, (Annon, 2003). Out of 150

species of algae documented, 50 belong to *Cyanophyta* species, 39 belong to *Chlorophyta* species, 2 belong to *Pheophyta* species, 44 belong to *Chrysophyta* species, of which 42 species are diatoms, and 15 belong to *Rhotophyta* species (Naskar et al. 2004). Additionally, 48 bacterial strains with a significant role in the ecosystem's total nutrient cycle were also recorded. Along the sides of 31 large and abundant narrow streams and tidal inlets in the vicinity of 48 major mangrove islands cherishes the mangrove-associated palm species (Das, 2010).

Sundarbans is an abode for a variety of faunal species; out of 1586 faunal species recorded, 215 species belong to fishes, 7 belong to amphibia species, 59 belong to reptiles species, more than 200 belong to birds species, 39 species belong to mammals, besides numerous species of zooplankton , phytoplankton, ichthyoplankton, benthos, soil-inhabiting, and mangrove plants dependant insects are also included (Chaudhuri and Choudhury, 1994). The Royal Bengal tiger occupies the top list of the mangrove ecosystem. Several mammalian species are declared endangered, including famous estuarine crocodiles, smooth Indian otters, Gangetic and Irrawadi dolphins, fishing and leopard cats, and Black porpoise. Predator birds are the common birds in Sundarbans; some are the white-bellied sea eagle, fishing eagle, osprey, Bramhani kites, Monsoon herons like open bill stork. Migratory birds like curlew, whimbrel, plover, goliath and heron also breed in the mangroves of Sundarbans (Das, 2010).

1.2.5. Pollution in the Sundarbans

Sundarbans ecosystem is in crisis mainly due to natural and anthropogenic activities. Change detection analysis conducted in the Sundarban mangrove ecosystem shows that there is small-scale land loss and gain, mainly due to the natural internal dynamics occurring in the mangrove ecosystem. Studies suggested that due to erosion, there is depletion in the land on the eastern sides, and new islands were developed along the Hoogly river channels towards the west. In the past, the rate of erosion and aggradation was more or less balanced, but recently

erosion rates were found to be higher (Ghosh et al., 2015). Twelve sea-facing southern islands, including the world's largest delta, and Sagar island at the west to Bhangaduni in the east are the most prominent erosion-prone regions; an aerial loss of 30 km sq. with marginal accretion due to bulk erosion was already reported in Sagar island. Over thirty years, the total erosion is estimated to be 162.879 km sq. (Hazra et al., 2002). Meltwater from the Himalayan glaciers also increases erosion and increases sediment deposition.

The increased human population is also a major threat to mangrove ecosystems' flora, fauna, and health. Exploiting mangrove forests and land reclamation for human dwellings and agriculture destroy forest areas, enhancing erosion. Construction of drainage and irrigation canals interfere with the natural flow of water bodies; also, the setting up of industries and fisheries along the estuarine and river banks results in a rise in the salinity of the water. Anthropogenic activities threaten flora and fauna and affect the ecosystem's natural balance, disrupting the complex food chain (Bose, 2004). The effluents released from fertilizer, chemicals, paper, and other industries cause a series of adverse effects on the water quality, productivity, and regeneration of mangroves. Agricultural runoff water results in eutrophication, leading to algal blooms and pesticide accumulation in water and sediments. Along with the domestic waste generated by 3.2 million populations of Sundarbans, untreated wastes (397 tons per day) reach the Sundarbans from the Kolkata Municipal Area, which is about 130 km away (Sampath, 2003).

Industrial and municipal effluents lead to the accumulation of pesticides, heavy metals, and other organic pollutants. Several instances of oil spillage have been reported in the Bay of Bengal over the years, and the oil spillage has affected a considerable part of Sundarban mangroves and its resources. The physical and chemical nature of oil showed its effect on aquatic life. Soluble fractions of oil, such as benzene, phenols, and toluene, are toxic to flora and fauna, and low molecular weight aromatic compound affects the cellular membrane of

mangrove roots. Heavy metal contaminants were reported in water as well as sediments. Cadmium, copper, chromium, nickel, mercury, lead, and arsenic are the most common heavy metal pollutants. Bioaccumulation of heavy metals in shrimp, fishes, and other benthic animals. Agrochemical contaminants often destroy the mangrove plants and disturb the soil ecology; they travel through the food chain and accumulate in the biota. These pollutants affect the mangrove's health and the nearly 4 million population who depend on the Sundarban ecosystem (Rahman et al., 2009).

1.2.6. Problems in the management of pollutants

In the last few years, the growing social economy, urbanization, and industrialization have polluted the mangrove ecosystem severely. Some major problems during the management and conservation of pollutants are the lack of available literature and up-gradation of data regarding the pollution index and the lack of strategic acclimatization of environmentally sustainable methods for prevention, control, and remediation of pollutants in the Sundarban ecosystem. Furthermore, lack of knowledge regarding the long-term effect of low concentrations of pollutants on the mangrove species is another drawback in managing pollutants. Furthermore, corruption, lack of accountability at different levels of management, and lack of expertise in pollution management negatively influence the conservation of the mangrove ecosystem (Rahman et al., 2009).

1.3. Bioremediation of polycyclic aromatic hydrocarbons

Environmental pollution has increased tremendously in the last few decades, especially due to anthropogenic activities such as population explosion, deforestation, urbanization, industrialization, unsafe agricultural practices, and exploitation of natural resources. Due to their toxicity, heavy metals, pesticides, herbicides, greenhouse gases, and PAHs are some of the major toxicant pollutants of environmental and public health concerns. The third world

network reports that beyond 450 million kilograms of contaminants are released into the water, air, and soil globally (Megharaj et al., 2011). Conventional techniques such as flocculation, soil washing, adsorption, chemical oxidation, pyrolysis, landfilling, and incineration have removed contaminants from polluted sites. However, these methods are expensive, energy and time-consuming, non-eco-friendly, and do not provide a permanent solution. To overcome this crisis, biological-based removal of contaminants was established for the biodegradation and detoxification of pollutants to restore the pollutant site to its original form.

Bioremediation is a biological process of decontaminating a polluted environment utilizing living organisms, especially microorganisms, green plants, and their enzymes (Tyagi and Kumar, 2021). Bioremediation helps to degrade, mineralize, transform, detoxify and remove the hazardous xenobiotic compounds present in the environment into mild or non-toxic forms. This technique was proven more effective, reliable, eco-friendly, and cost-effective than conventional remediation methods (Sharma, 2020). In the past two decades, new techniques in bioremediation have been developed tremendously to restore the polluted environment. Indigenous or non-indigenous microorganisms can be used for the bioremediation process. Indigenous microbes in polluted sites play a vital role in the bioremediation and biodegradation of pollutants (Khan et al., 2015). Various methods are involved in the bioremediation process, such as degradation, eradication, immobilization, or detoxification of xenobiotic compounds present in the environment through microorganisms (Figure 3).

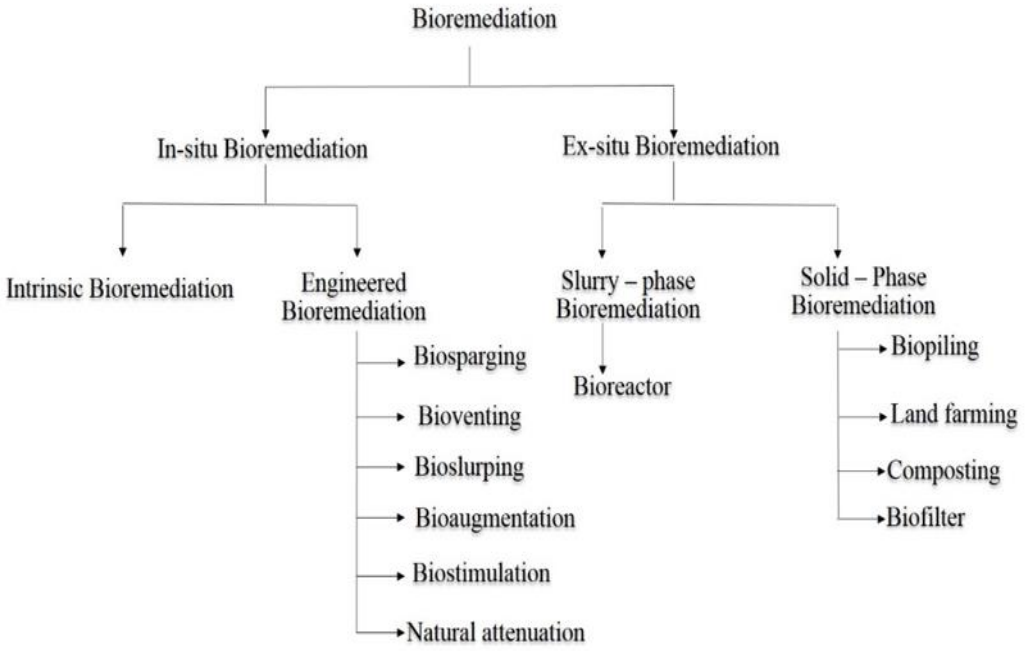

Figure 3: Different bioremediation techniques used for environmental clean-up (Sharma, 2020)

The bioremediation approach also has certain drawbacks. One of the major drawbacks is that not all microorganisms can degrade a broad spectrum of pollutants. Till now, no such microbe has been identified which has the potential to remove a large percentage of these pollutants. Another drawback is that bioremediation is a time cosuming technique. These drawbacks can be solved by identifying new microbial species with high bioremediation potential towards a wide range of toxicants; another solution is using genetically engineered microorganisms to obtain new strains and thereby enhance their bioremediation potential. Use certain enhancers or formulations that can biochemically fortify the biochemical pathways involved in the bioremediation and help increase the bioremediate population. Microbial consortia are the synchronous use of two or more microorganisms that can directly or indirectly increase the bioremediation efficiency (Sardrood et al., 2011).

1.3.1. Factors affecting the bioremediation of PAHs

Microbial bioremediation of PAHs is determined by many physical, chemical, and biological factors (Micky, 2006). Various physical and chemical factors involved in the biodegradation of PAHs, are soil, pressure, temperature, humidity, salinity, nutrient availability, pH, and bioavailability (Gupte et al., 2016) (Figure 4). Generally, PAH-degrading heterotrophic bacteria and fungi perform best at a neutral pH (pH 7). Nutrient availability plays a major role in PAH degradation; concentrations of carbon, nitrogen, and phosphorus concentrations are highly crucial because they greatly affect the growth, cellular metabolism, and PAH degradation potential of the microbes (van Hamme et al., 2003; Gupte et al., 2016). Temperature highly influences the in situ degradation of PAHs by microorganisms; higher temperature, bioavailability, solubility, and rate of diffusion enhance the biodegradation of PAHs (Gupte et al., 2016). The oxygen concentration is considered the rate-limiting parameter in the biodegradation pathway of cyclic and aromatic hydrocarbons by bacteria and fungi. Oxygenase enzymes that require molecular oxygen play a crucial role in the PAH degradation process (Van Hamme et al., 2003). Anaerobic degradation of PAHs occurs at a very nominal rate compared to aerobic degradation, and they are limited to halogenated aromatic compounds (Gupte et al., 2016). Even though a positive correlation is observed between the salinity and rate of mineralization of PAHs, hypersalinity leads to a decrease in microbial metabolic rate (Micky, 2006).

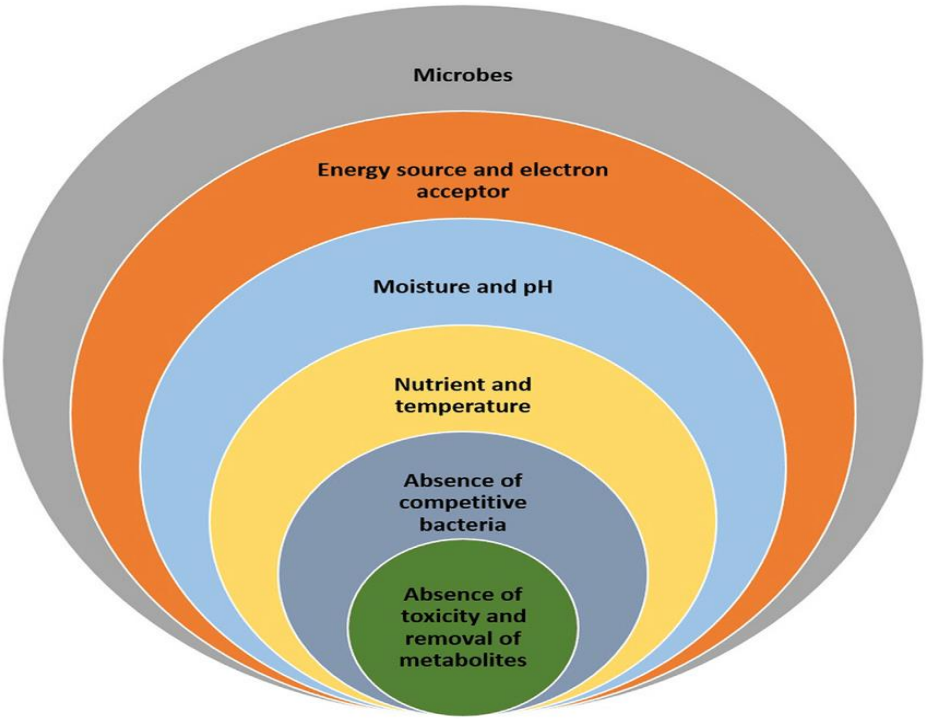

Figure 4: Factors affecting the degradation of PAHs (Tyagi and Kumar, 2021)

1.3.2. Bacterial degradation of PAHs

Several species of bacteria having the ability to degrade PAH contaminants have been identified. Bacteria degrade PAHs by an assimilative process leading to the mineralization of PAHs, and carbon dioxide and water are formed as the by-products, which can be further utilized for their growth (Winquist et al., 2014). Numerous pathways involved in PAH degradation have been recorded, and the degradation of Phe and Nap has been widely studied. The general pathway for the degradation of the PAHs is illustrated in Figure 5 (Sayara and Sánchez, 2020). Activation and oxidation by enzymes that catalyze oxygen fixation is the principal mechanism of bacterial PAH metabolism (Gupte et al., 2016). Aerobic degradation of PAHs by the bacteria is mediated via oxygenase enzyme, either monooxygenase or dioxygenase. Dioxygenase is a multicomponent enzyme comprising ferredoxin, reductase, and terminal oxygenase subunits (Mallick et al., 2011). The first step in aerobic degradation is the hydroxylation of an aromatic ring leads to the formation of *cis*-dihyrodiol, the re-aromatization

of *cis*-dihyrodiol forms a diol intermediate by the action of dehydrogenase enzyme. Catechol intermediates are formed from diol intermediate by the action of intra-diol or extra-diol ring-cleaving dioxygenases through either an ortho-cleavage or meta-cleavage pathway; catechols are ultimately converted to TCA cycle intermediates. Bacterial PAH degradation also occurs via the cytochromeP450-mediated pathway, where *trans*-dihydrodiols are the products formed or under anaerobic conditions (under nitrate-reducing conditions) (Ghosal et al., 2016).

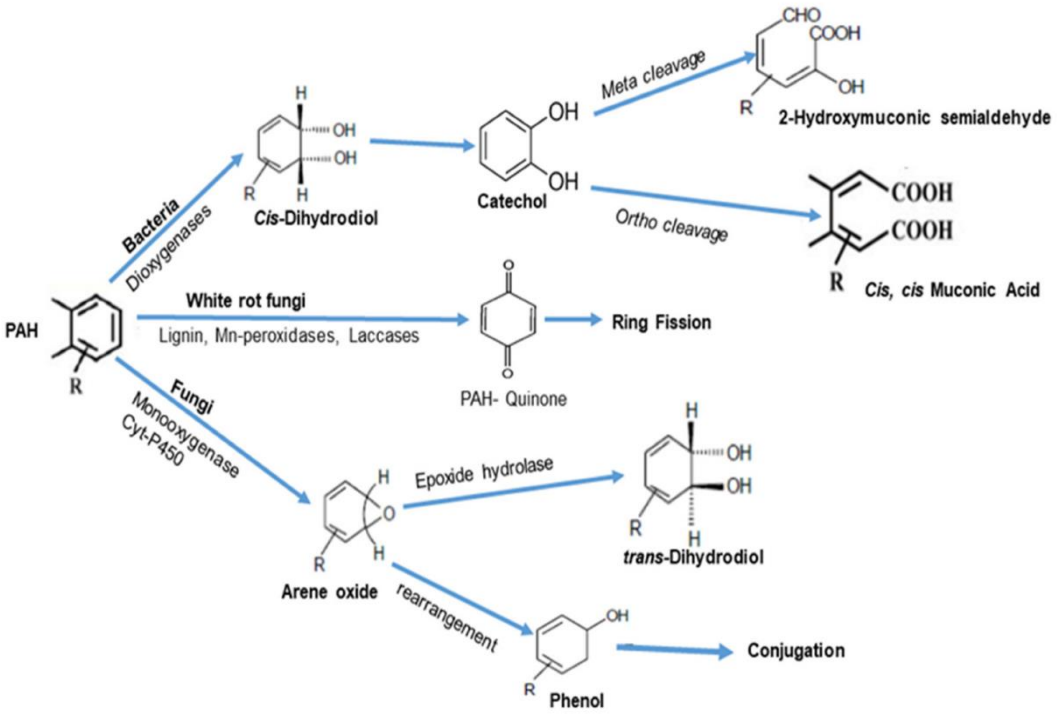

Figure 5: Bacterial and fungal pathways of PAH degradation (Sayara and Sánchez, 2020).

Many bacterial species capable of degrading PAHs have been reported; a few among them are as follows: *Achromobacter* sp., *Arthrobacter* sp., *Bacillus* sp., *Mycobacterium* sp., *Burkholderia* sp., *Pseudomonas* sp., *Rhodococcus* sp., *Stenotrophomonas maltophilia*, *Sphingomonas* sp., *Xanthamonas* sp. *Burkholderia* (β- proteobacteria). Gram-negative bacteria, can easily degrade LMW PAHs, while gram-positive bacteria, such as *Mycobacterium*, can degrade higher-ring PAHs more efficiently (Johnsen et al., 2005). PAHs with four or more rings (Phe, Pyr, and Fluoranthene (Fla)) have been degraded by

Mycobacterium. Fla degradation is mainly by bacteria *Mycobacterium* and *Alcaligenes*. *Acinetobacter* sp. isolated from municipal waste-contaminated soil was reported to degrade Ace and acenaphthylene (Acy) (Gupte et al., 2016).

1.3.3. Fungal metabolism of PAHs

Like bacteria, the biodegradation potential of PAHs in nature by fungi has been studied widely in the past few years, and numerous fungal species have been identified. However, fungi can mineralize PAH as the sole source of carbon. These fungi can be classified into two groups: ligninolytic and non-ligninolytic fungi (Cerniglia, 1997). Ligninolytic or white rot fungi can produce lignin peroxidase (LiP), manganese peroxidase (MnP), and laccases enzymes which can degrade the lignins. In contrast, non-ligninolytic fungi secrete cytochrome P450 monooxygenase-like enzymes (Ghosal et al., 2016), and they can metabolize PAH contaminants in the soil (Figure 6). When cultured under ligninolytic and non-ligninolytic conditions, white rot fungi showed the ability to degrade PAHs.

The genera of *Phanerochaete*, *Trametes*, *Bjerkandera*, and *Pleurotus* are some of the widely studied ligninolytic fungi with considerable potential for the degradation of PAH (Hamman, 2004). Ligninolytic fungi produce extracellular enzymes capable of degrading lignin, namely peroxidases (lignin peroxidases and manganese peroxidases) and laccases (Hammel, 1995; Cerniglia and Sutherland, 2010). These peroxidases and laccases were believed to have PAH degradation potential (Mester and Tien, 2000; Cerniglia and Sutherland, 2010). However, lignin peroxidases can oxidize PAHs, and not all can be degraded by the peroxidases (Hammel, 1995). Peroxidase enzymes transform PAHs into hydroxyl free radicals by donating one electron, which can oxidize the PAH ring (Sutherland, 1995), leading to the formation of PAH-quinones and acids instead of dihydrodiols. Pyr, Ant, Flu, and B(a)P oxidation by the LiP and MnP of white-rot fungus *Phanerochaete chrysosporium* to their

corresponding quinines were reported by Boganetal. (1996 a,b). Laccase catalyzes one-electron oxidation of PAHs such as Ant and B(a)P (Gupte et al., 2016). PAH degradation efficiency of wood-rotting fungi *Plrurotus ostreatus* and *Antrodia vaillantii* was determined in artificially contaminated soil with Flu, Phe, Pyr, and B(a)A, even though *P. ostreatus* can significantly increase the PAH degradation, but they eventually accumulate the toxic metabolites of PAHs such as 9-fluorenone, benzo[a]anthracene-7,12-dione, and two compounds identified as 4-hydroxy-9-fluorenone and 4-oxapyrene-5-one (Andersson et al.2003). Andersson et al. (2003) also suggest that these white-rot fungi have a negative effect on the indigenous microbial communities present in the soil, which may inhibit the complete mineralization of PAHs.

The PAH degradation pathway by non-ligninolytic fungi has been well studied. The PAH degradation by non-ligninolytic fungi involves the oxidation of aromatic rings by Cytochrome P-450 monooxygenase. These enzymes catalyze the ring epoxidation reaction to form an unstable arene oxide, which further undergoes an epoxide-hydrolase reaction to form *trans*-dihydrodiol (Sutherland, 1995). Non-enzymatic rearrangement of arene oxide results in the formation of phenol and further conjugated with glucose, xylose, glucuronic acid, and sulfate (Mueller et al., 1996; Pothuluri et al., 1996). *A. niger, C.elegans, and P. janthinellum* are some non-ligninolytic fungi that secrete Cytochrome P 450 monooxygenase for the oxidative degradation of PAHs.

1.3.4. Microalgal-mediated PAH degradation

Microalgae are considered major primary producers in the aquatic environment; they play a vital role in the fate of PAHs. However, very little attention has been given to microalgal (cyanobacteria and diatoms) mediated biodegradation of PAHs compared to bacteria and fungi. Photosynthetic unicellular prokaryotes or eukaryotes, such as cyanobacteria, green, brown, and

red algae, are considered potential agents for the bioremediation process due to their high biomass production and growth efficiency. Several microalgal species from freshwater and marine ecosystems have been identified that can degrade hydrocarbons. The use of marine photosynthetic microbes for bioremediation has several advantages over freshwater microalgae, which include the ability of marine microalgae to convert the solar energy four-time efficiently than freshwater photosynthetic microbes and also their capability to use salt water for cultivation instead of freshwater (Dell'Anno et al., 2021).

Effective degradation of PAHs, such as Nap, Phe, B(a)P, and Pyr by microalgae belonging to the genera *Selenastrum, Scenedemus,* or *Chlorella* have been demonstrated by various studies (Garcia de Llaseraet al., 2016; Takacova et al., 2014). Exopolysaccharides (EPS) secreted by the phototrophic microbes play a major role in the PAH removal mechanism; they facilitate the uptake of PAHs or other xenobiotic compounds on the cell surface, thereby reducing the bioavailability and toxicity of the contaminants (Liu et al., 2016). Oxidation of Nap to 1- naphthol under phototrophic conditions by *Oscillatoria* sp. strain JCM and their metabolic pathways was illustrated by Cerniglia et al. (1980a) (Figure 6). Cerniglia et al. showed that cyanobacteria and other eukaryotic microalgae could metabolize Nap to four major non-toxic metabolites, such as 1-naphthol, 4-hydroxy-4-tetralone, cis-naphthalene dihydrodiol and trans-naphthalene dihydrodiol. Cerniglia et al. (1980b) also demonstrated the potential of nine cyanobacteria (blue-green algae), five green algae, one red alga, and one brown alga; two diatoms to metabolize Nap under phototrophic conditions.

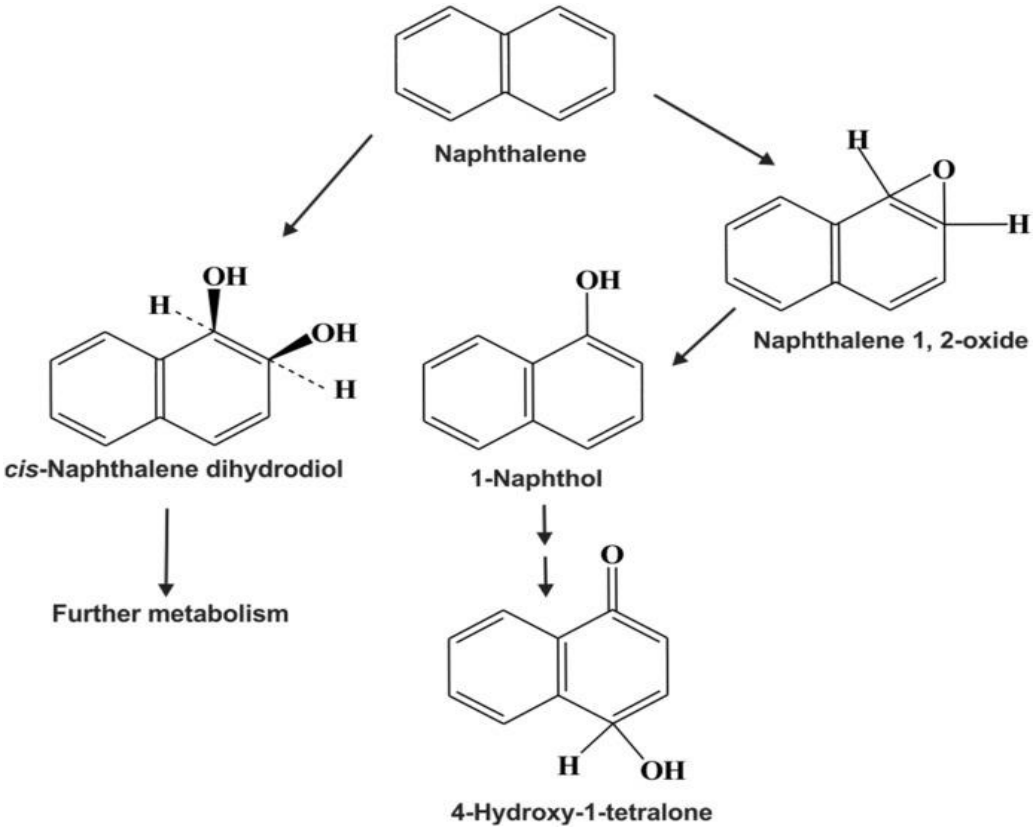

Figure 6: Metabolic pathway of Nap by *Oscillatoria* sp. strain JCM under phototrophic conditions proposed by Cerniglia et al. (1980a).

Further studies using several microalgae sp. suggest that they possess a high potential for the bioremediation of crude oils in the water. Experiments conducted using the achlorophyllous alga *Prototheca zopfii* showed 38–60% degradation of the saturated aliphatic hydrocarbons and 12–41% degradation of the aromatic compounds in Louisiana crude oil, whereas in the motor oil degradation percentage was found to be 10–23% and 10–26% for saturated aliphatic hydrocarbons and aromatic compounds respectively (Walker et al., 1975). The green microalgae *Chlorella vulgaris* could degrade petroleum hydrocarbons up to 98% from water in just 14 days (Das and Deka, 2019). In addition, 24 to 92% reduction in the concentrations of different hydrocarbons present in the oil refinery wastewater by five blue-green algae species isolated from the Iraqi aquatic environment (*Westiellopsis prolific,*

Anabaena variabilia, Oscillatoria pranceps, *Phormidium mucicola*, and *Lyngbya digueti*) has been reported (Al-Hussieny et al., 2020). Hong et al. (2008) studied the accumulation and biodegradation of Phe and Fla by two diatom sp. such as *Skeletonema costatum* and *Nitzschia* sp.; this study just showed that *Nitzschia* sp. has higher accumulation and degradation ability compared to *S. costatum*. The degradation of Fla by both diatoms was found to be lower, implying that Fla was more recalcitrant than Phe. They also showed higher removal efficiency of the Phe-Fla mixture compared to the individual PAHs indicating that one PAH can stimulate the degradation in a mixture and hence the degradation efficiency. In the environment, O_2 released by the microalgae can be utilized by aerobic bacteria, which can degrade hazardous pollutants (Munoz et al., 2003).

1.3.5. Microbial consortia

Several bacteria, fungal and microalgal genera capable of metabolizing LMW and HMW PAHs under aerobic and anaerobic conditions have been identified. However, in the soil, microorganisms rarely present as individual organisms; instead, they occur in complex microbial communities with different degrees of interaction which may immensely influence PAH degradation efficiency. The microbial consortium has advantages over single microbial species in the efficient degradation of PAH mixture because no single microbial sp. can degrade both LMW and HMW PAHs (Zafra et al., 2017). Each microorganism in the consortia has a special role in degradation steps, and the intermediates produced by one microbe are utilized by other microbial members (Ghosal et al., 2016).

Bacteria in the bacterial-fungal consortia enhance the PAH compounds' bioavailability; thereby, white-rot fungi can easily metabolize PAH. Generally, fungi cannot degrade HMW PAHs completely due to a lack of certain enzymes, but the extracellular enzymes secreted by them can form polar metabolites, which the bacteria can further metabolize in the consortia

(Sutherland, 1992). Indigenous mixed bacterial culture can mineralize the degradation product of Ant formed via the white-rot fungal metabolic pathway, and the efficiency of Ant degradation has been increased rapidly rather than the degradation done individually by the bacterial species (Meulenberg et al., 1997). Reports suggest that bacterial-fungal consortia can significantly enhance the degradation of HMW PAHs, such as Chry, B(a)A, and D(a,h)A (Ghosal et al., 2016).

Similar to bacterial-fungal consortia, a consortium of algae and bacteria also showed efficient PAH degradation. Studies suggest that microalgal growth and enzymatic activities have been enhanced in the presence of Pyr-degrading bacteria, thereby increasing PAH degradation (Dell'Anno et al., 2021). Algal-bacterium consortium of *Chlorella sorokiniana* and *Pseudomanas migulae* under photosynthetic conditions and in the absence of an external source of oxygen showed degradation of Phe. Under the photosynthetic condition, the algal bacterial consortium showed accelerated Pyr degradation. Studies indicate that a defined microbial consortium may provide better remediation in the contaminated site rather than treating the contaminant with single isolates. Developing a potential microbial consortium with a strong PAH degrading potential will help reduce the contaminants from the environment more efficiently than treating them with bacteria, fungi, or algae alone (Ghosal et al., 2016).

References

Abdel-Shafy, H.I. and Mansour, M.S., 2016. A review on polycyclic aromatic hydrocarbons: source, environmental impact, effect on human health and remediation. Egypt. J. Pet.m, 25(1), pp.107-123.

Adeniji, A.O., Okoh, O.O. and Okoh, A.I., 2018. Analytical methods for polycyclic aromatic hydrocarbons and their global trend of distribution in water and sediment: a review. Recent insights in petroleum science and engineering, 10.

Alexander, M., 1994. Bio-degradation kind bioremediation academic. San Diego, Calif, pp.1-7.

Al-Hussieny, A.A., Imran, S.G. and Jabur, Z.A., 2020. The use of local blue-green algae in the bioremediation of hydrocarbon pollutants in wastewater from oil refineries. Plant Arch, 20, pp.797-802.

Andersson, B.E., Lundstedt, S., Tornberg, K., Schnürer, Y., Öberg, L.G. and Mattiasson, B., 2003. Incomplete degradation of polycyclic aromatic hydrocarbons in soil inoculated with wood-rotting fungi and their effect on the indigenous soil bacteria. Environ. Toxicol. Chem., 22(6), pp.1238-1243.

Annon, 2003. Mangrove ecosystem: Biodiversity and its influence on the natural recruitment of selected commercially important finfish and shellfish species in fisheries. National Agricultural Technology Project (NATP). Indian Council of Agriculture Research (ICAR). Principal Investigator: George, J.P.; Co-PI: Chakraborty, S.K. and Damroy, S.N.: 1 – 514.

Bhattacharya, A.K., 1989. Coastal geomorphology, processes and hazards: a note on management measures. Coast zone management of West Bengal. Sea Explorer's Institute, Calcutta, pp.D49-D61.

Bogan, B.W., Lamar, R.T. and Hammel, K.E., 1996a. Fluorene oxidation in vivo by Phanerochaete chrysosporium and in vitro during manganese peroxidase-dependent lipid peroxidation. Appl. Environ. Microbiol, 62(5), pp.1788-1792.

Bogan, B.W., Schoenike, B., Lamar, R.T. and Cullen, D., 1996b. Expression of lip genes during growth in soil and oxidation of anthracene by Phanerochaete chrysosporium. Appl. Environ. Microbiol, 62(10), pp.3697-3703.

Bose, S., 2004. The Sunderbans biosphere: a study on uncertainties and impacts in active delta region. In Proceedings of 2nd. APHW Conference .Vol. 1, pp. 475-483.

Brandt, M. and Einhenkel-Arle, D., 2016. Polycyclic Aromatic Hydrocarbons–Harmful to the Environment! Toxic! Inevitable. German Environ. Agency, pp.1-24.

Brazkova M, Krastanov A., 2013. Polycyclic aromatic hydrocarbons: Sources, effects and biodegradation. In: Proceedings of the International Scientific Conference of University of Ruse, Razgrad, Bulgaria; 52(10.2):1-5

Burchiel, S. W., and Luster, M. I. 2001. Signaling by environmental polycyclic aromatic hydrocarbons in human lymphocytes. Clin. Immunol. 98, 2–10.

Cerniglia, C.E. and Sutherland, J.B., 2010. Degradation of polycyclic aromatic hydrocarbons by fungi. In Handbook of hydrocarbon and lipid microbiology.

Cerniglia, C.E., 1997. Fungal metabolism of polycyclic aromatic hydrocarbons: past, present and future applications in bioremediation. J. Ind. Microbiol. Biotechnol., 19(5-6), pp.324-333.

Cerniglia, C.E., Gibson, D.T. and Van Baalen, C., 1980b. Oxidation of naphthalene by cyanobacteria and microalgae. Microbiology, 116(2), pp.495-500.

Cerniglia, C.E., Van Baalen, C. and Gibson, D.T., 1980a. Metabolism of naphthalene by the cyanobacterium Oscillatoria sp., strain JCM. Microbiology, 116(2), pp.485-494.

Chakraborty, S.K., 2011. Mangrove ecosystem of Sundarbans, India: biodiversity, ecology, threats and conservation. Mangroves: Ecology, Biology and Taxonomy. Ed. Metras JN: NOVA publisher, USA, pp.83-112.

Chakraborty, S.K., Giri, S., Chakravarty, G. and Bhattacharya, N., 2009. Impact of eco-restoration on the biodiversity of Sundarbans Mangrove Ecosystem, India. Water Air Soil Pollut., 9(3), pp.303-320.

Chaudhuri, A.B. and Choudhury, A., 1994. Mangroves of the Sundarbans-Vol. 1. India. The IUCN Wetlands Programme, Bangkok, Thailand, 247pp.

Dahlstrom, D.L. and Bloomhuff, A.B., 2014. ACGIH (American conference of governmental industrial hygienists), pp 178-179.

Das GK (2010) Biodiversity in Sunderbans. In: Dwivedi AK, Tripathi SC (eds) Environment and biodiversity, environmental pollution and risk to biodiversity. Lambert Academic Publishing AG & Co., Saarbrucken, pp 1–34.

Das, B. and Deka, S., 2019. A cost-effective and environmentally sustainable process for phycoremediation of oil field formation water for its safe disposal and reuse. Scientific reports, 9(1), pp.1-15.

Dell'Anno, F., Rastelli, E., Sansone, C., Brunet, C., Ianora, A. and Dell'Anno, A., 2021. Bacteria, fungi and microalgae for the bioremediation of marine sediments contaminated by petroleum hydrocarbons in the omics era. Microorganisms, 9(8), p.1695.

Dong, C.D., Chen, C.F. and Chen, C.W., 2012. Determination of Polycyclic Aromatic Hydrocarbons in Industrial Harbor Sediments by GC-MSInt. J. Environ. Res. Public Health, 9, pp.2175-2188.

García de Llasera, M.P., Olmos-Espejel, J.D.J., Díaz-Flores, G. and Montaño-Montiel, A., 2016. Biodegradation of benzo (a) pyrene by two freshwater microalgae Selenastrum capricornutum and Scenedesmus acutus: a comparative study useful for bioremediation. Environ. Sci. Pollut. Res.., 23(4), pp.3365-3375.

Ghosal, D., Ghosh, S., Dutta, T.K. and Ahn, Y., 2016. Current state of knowledge in microbial degradation of polycyclic aromatic hydrocarbons (PAHs): a review. Front. Microbiol., p.1369.

Ghosh, A., Dey, N., Bera, A., Tiwari, A., Sathyaniranjan, K.B., Chakrabarti, K. and Chattopadhyay, D., 2010. Culture independent molecular analysis of bacterial communities in the mangrove sediment of Sundarban, India. Saline systems, 6(1), pp.1-11.

Ghosh, A., Schmidt, S., Fickert, T. and Nüsser, M., 2015. The Indian Sundarban mangrove forests: history, utilization, conservation strategies and local perception. Diversity, 7(2), pp.149-169.

Gopal, B. and Chauhan, M., 2018. The transboundary Sundarbans mangroves (India and Bangladesh). The wetland book. Springer, Dordrecht.

Gupta, S.K., 1987. Some mangrove soils of the Sundarbans ecosystem. UNESCO Reg Introductory Train Course Estuar Res, Calcutta, 2, pp.105-112.

Gupte, A., Tripathi, A., Patel, H., Rudakiya, D. and Gupte, S., 2016. Bioremediation of polycyclic aromatic hydrocarbon (PAHs): a perspective. Biotechnol. J, 10(1).

Hamman, S., 2004. Bioremediation capabilities of white rot fungi. Biodegradation, 52(16), p.11.

Hammel, K.E., 1995. Organopollutant degradation by ligninolytic fungi. Microbial transformation and degradation of toxic organic chemicals, pp.331-346.

Hazra, S., Ghosh, T., Das Gupta, R. and Sen, G., 2002. Sea level and associated changes in the Sundarbans. Science and culture, 68(9/12), pp.309-321.

Hong, Y.W., Yuan, D.X., Lin, Q.M. and Yang, T.L., 2008. Accumulation and biodegradation of phenanthrene and fluoranthene by the algae enriched from a mangrove aquatic ecosystem. Mar. Pollut. Bull, 56(8), pp.1400-1405.

Islam, M.T., 2014. Vegetation changes of Sundarbans based on Landsat Imagery analysis between 1975 and 2006. Landscape & environment, 8(1), pp.1-9.

Johnsen, A.R., Wick, L.Y. and Harms, H., 2005. Principles of microbial PAH-degradation in soil. Environ. Pollut.133(1), pp.71-84.

Lee, B.K., 2010. Sources, distribution and toxicity of polyaromatic hydrocarbons (PAHs) in particulate matter. In Air pollution. IntechOpen.

Liu, L., Pohnert, G. and Wei, D., 2016. Extracellular metabolites from industrial microalgae and their biotechnological potential. Marine drugs, 14(10), p.191.

Mallick, S., Chakraborty, J. and Dutta, T.K., 2011. Role of oxygenases in guiding diverse metabolic pathways in the bacterial degradation of low-molecular-weight polycyclic aromatic hydrocarbons: a review. Crit.Rev.Microbiol., 37(1), pp.64-90.

Mandal, A.K. and Ghosh, R.K., 1989. Sundarban: a socio bio-ecological study. Bookland.

Manna, S., Chaudhuri, K., Sarma, K.S., Naskar, P., Bhattacharyya, S. and Bhattacharyya, M., 2012. Interplay of physical, chemical and biological components in estuarine ecosystem with special reference to Sundarbans, India. Ecological Water Quality—Water Treatment and Reuse, pp.206-238.

Megharaj, M., Ramakrishnan, B., Venkateswarlu, K., Sethunathan, N. and Naidu, R., 2011. Bioremediation approaches for organic pollutants: a critical perspective. Environ. Int, 37(8), pp.1362-1375.

Mester, T. and Tien, M., 2000. Oxidation mechanism of ligninolytic enzymes involved in the degradation of environmental pollutants. Int. Biodeterior. Biodegrad., 46(1), pp.51-59.

Meulenberg, R., Rijnaarts, H.H., Doddema, H.J. and Field, J.A., 1997. Partially oxidized polycyclic aromatic hydrocarbons show an increased bioavailability and biodegradability. FEMS Microbiology Letters, 152(1), pp.45-49.

Micky, V., 2006. Microbial bioremediation of polycyclic aromatic hydrocarbons (PAHs) in oily sludge wastes. J. of Biochem., Microbio. and Biotechnol, 1(1), pp.1-12.

Mitra, A. and Mukhopadhyay, S., 2016. Biofilm mediated decontamination of pollutants from the environment. Aims Bioengineering, 3(1), pp.44-59.

Mueller, J.G., Cerniglia, C.E. and Pritchard, P.H., 1996. Bioremediation of environments contaminated by polycyclic aromatic hydrocarbons. Biotechnology Research Series, 6, pp.125-194.

Munoz, R., Guieysse, B. and Mattiasson, B., 2003. Phenanthrene biodegradation by an algal-bacterial consortium in two-phase partitioning bioreactors. Appl. Microbiol. Biotechnol, 61(3), pp.261-267.

Naskar, K. and Ghosh, A., 1989. Mangrove forest of the Sundarbans: Its impact on estuarine fisheries. Proceeding in Coast Zone Management of West Bengal, Sea Explores Institute, Calcutta, pp.47-59.

Naskar, K., Sarkar, N.S., Ghosh, A., Dasgupta, M. and Sengupta, B., 2004. Status of the mangroves and mangrove ecosystem of Sundarbans in West Bengal: its impact on estuarine wetland fisheries. Bulletin of the Central Inland Fisheries Research Institute, Barrackpore, (134), p.53.

Patel, A.B., Shaikh, S., Jain, K.R., Desai, C. and Madamwar, D., 2020. Polycyclic aromatic hydrocarbons: sources, toxicity, and remediation approaches. Front. Microbiol, p.2675.

Peng, R.H., Xiong, A.S., Xue, Y., Fu, X.Y., Gao, F., Zhao, W., Tian, Y.S. and Yao, Q.H., 2008. Microbial biodegradation of polyaromatic hydrocarbons. FEMS microbiology reviews, 32(6), pp.927-955.

Pothuluri, J.V., Evans, F.E., Heinze, T.M. and Cerniglia, C.E., 1996. Formation of sulfate and glucoside conjugates of benzo [e] pyrene by Cunninghamella elegans. Appl. Microbiol. Biotechnol, 45(5), pp.677-683.

Rahman, M.M., Chongling, Y., Islam, K.S. and Haoliang, L., 2009. A brief review on pollution and ecotoxicologic effects on Sundarbans mangrove ecosystem in Bangladesh. Int. J. Environ. Eng 1(4), pp.369-383.

Ravindra, K., Sokhi, R. and Van Grieken, R., 2008. Atmospheric polycyclic aromatic hydrocarbons: source attribution, emission factors and regulation. Atmos. Environ, 42(13), pp.2895-2921.

Ray, R., Ganguly, D., Chowdhury, C., Dey, M., Das, S., Dutta, M.K., Mandal, S.K., Majumder, N., De, T.K., Mukhopadhyay, S.K. and Jana, T.K., 2011. Carbon sequestration and annual increase of carbon stock in a mangrove forest. Atmos. Environ 45(28), pp.5016-5024.

Sampath, V. 2003. National Report on the Status and Development Potential of the Coastal and Marine Environment of the East Coast of India and Its Living Resources. FAO/BOBLME Programme. 288 pp.

Sardrood, B.P., Goltapeh, E.M. and Varma, A., 2013. An introduction to bioremediation. In Fungi as bioremediators (pp. 3-27). Springer, Berlin, Heidelberg.

Sayara, T. and Sánchez, A., 2020. Bioremediation of PAH-contaminated soils: Process enhancement through composting/compost. Appl. Sci., 10(11), p.3684.

Schwarzenbach, R.P., Gschwend, P.M. and Imboden, D.M., 1993. Vapour pressure. Environ.Org. Chem., pp.56-75.

Selvam, V., 2003. Environmental classification of mangrove wetlands of India. Curr. Sci., 84(6), pp.757-765.

Sharma, I., 2020. Bioremediation techniques for polluted environment: concept, advantages, limitations, and prospects. In Trace Metals in the Environment-New Approaches and Recent Advances. IntechOpen.

Shukla, S.K., Mangwani, N., Rao, T.S. and Das, S., 2014. Biofilm-mediated bioremediation of polycyclic aromatic hydrocarbons. In Microbial biodegrade. and bioremed. (pp. 203-232).

Singh, S.K. and Haritash, A.K., 2019. Polycyclic aromatic hydrocarbons: soil pollution and remediation. Int J Environ Sci Technol, 16(10), pp.6489-6512.

Suman, S., Sinha, A. and Tarafdar, A., 2016. Polycyclic aromatic hydrocarbons (PAHs) concentration levels, pattern, source identification and soil toxicity assessment in urban traffic soil of Dhanbad, India. Sci. Total Environ.545, pp.353-360.

Sutherland, J.B., 1992. Detoxification of polycyclic aromatic hydrocarbons by fungi. J. Ind. Microbiol. Biotechnol. 9(1), pp.53-61.

Sutherland, J.B., 1995. Mechanisms of polycyclic aromatic hydrocarbon degradation. Microbial transformation and degradation of toxic organic chemicals, pp.269-306.

Takáčová, A., Smolinská, M., Ryba, J., Mackuľak, T., Jokrllová, J., Hronec, P. and Čík, G., 2014. Biodegradation of Benzo [a] Pyrene through the use of algae. Cent. Eur. J. Chem., 12(11), pp.1133-1143.

Tyagi, B. and Kumar, N., 2021. Bioremediation: principles and applications in environmental management. In bioremediation for environmental sustainability (pp. 3-28). Elsevier.

Unwin, J., Cocker, J., Scobbie, E. and Chambers, H., 2006. An assessment of occupational exposure to polycyclic aromatic hydrocarbons in the U.K. Ann Occup Hyg, 50(4), pp.395-403.

Van Hamme, J.D., Singh, A. and Ward, O.P., 2003. Recent advances in petroleum microbiology. Microbiol. Mol. Biol. Rev., 67(4), pp.503-549.

Van Herwijnen, R., Wattiau, P., Bastiaens, L., Daal, L., Jonker, L., Springael, D., Govers, H.A. and Parsons, J.R., 2003. Elucidation of the metabolic pathway of fluorene and cometabolic pathways of phenanthrene, fluoranthene, anthracene and dibenzothiophene by Sphingomonas sp. LB126. Microbiol. Res. 154(3), pp.199-206.

Walker, J.D., Colwell, R.R. and Petrakis, L., 1975. Degradation of petroleum by an alga, Prototheca zopfii. Appl. Microbiol., 30(1), pp.79-81.

Winquist, E., Björklöf, K., Schultz, E., Räsänen, M., Salonen, K., Anasonye, F., Cajthaml, T., Steffen, K.T., Jørgensen, K.S. and Tuomela, M., 2014. Bioremediation of PAH-contaminated soil with fungi–From laboratory to field scale. Int. Biodeterior. Biodegrad., 86, pp.238-247.

Yan, J., Wang, L., Fu, P.P. and Yu, H., 2004. Photomutagenicity of 16 polycyclic aromatic hydrocarbons from the US EPA priority pollutant list. Mutation Research/Genetic Toxicology and Environmental Mutagenesis, 557(1), pp.99-108.

Yuan, S.Y., Shiung, L.C. and Chang, B.V., 2002. Biodegradation of polycyclic aromatic hydrocarbons by inoculated microorganisms in soil. Bull Environ Contam Toxicol., 69(1), pp.66-73.

Zafra, G., Absalón, Á.E., Anducho-Reyes, M.Á., Fernandez, F.J. and Cortés-Espinosa, D.V., 2017. Construction of PAH-degrading mixed microbial consortia by induced selection in soil. Chemosphere, 172, pp.120-126.

Zanardi-Lamardo, E., Mitra, S., Vieira-Campos, A.A., Cabral, C.B., Yogui, G.T., Sarkar, S.K., Biswas, J.K. and Godhantaraman, N., 2019. Distribution and sources of organic contaminants in surface sediments of Hooghly river estuary and Sundarban mangrove, eastern coast of India. Mar. Pollut. Bull., 146, pp.39-49.

AIM AND OBJECTIVES

The Sundarbans are the world's largest single-tract intertidal mangrove forest with rich biodiversity. Environmental pollution in the Indian Sundarbans has been the greatest concern in recent years due to natural and anthropogenic activities such as human settlement, deforestation, tourism development, and increased aquaculture and agricultural practices. A pronounced ecological change in the estuarine environment is due to the discharge of untreated domestic and industrial effluents from the tributary rivers. The delta has become vulnerable to chemical pollutants such as heavy metals, polychlorinated biphenyls (PCBs), and polycyclic aromatic hydrocarbons (PAHs), which may have affected the estuarine geochemistry and the quality of the local coastal environment. PAHs are ubiquitous pollutants, and uptake and accumulation are a threat to the flora and fauna as well as human beings. Bioremediation using microorganisms is the most promising technique compared to other remediation processes. The definite objectives behind this work were as follows

(i) Quantitative determination of PAH levels in water and sediments

Collection of water and sediment samples from various geographical regions of Indian Sundarbans and quantitative estimation of 16 priority PAH pollutants present in both water and sediment samples.

(ii) Isolation of indigenous microbial biofilm mats collected from different regions of Sundarbans.

Collection of biofilm samples from the Sundarban by scrapping the biofilms from the sediment surface, further isolation and culturing of heterotrophic and phototrophic indigenous microbial biofilm mats in different modified culture media at laboratory conditions.

(iii) In vitro estimation of PAH bioremediation by heterotrophic biofilms cultured in the patented biofilm-promoting enhanced surface area conico-cylindrical flasks (ES-CCF)

Culturing the isolated heterotrophic biofilms in two sets of patented ES-CCF possessing hydrophilic glass surface and hydrophobic polymethyl methacrylate (PMMA) surface with enrichment media. Quantification of mean residual PAH to determine the PAH removal efficiency after 30 days of incubation with different concentrations of PAHs spiked into the media.

(iv) Study of the community composition of selected heterotrophic biofilms. Metagenomic sequencing to study the bacterial and fungal community of the selected biofilm, which possesses high PAH degradation potential.

(v) Evaluation of PAH degradation efficiency of phototrophic biofilm and study of the effect of PAHs on characteristic features of selected biofilms.

Culturing the isolated phototrophic biofilms in hydrophilic glass and hydrophobic polymethyl methacrylate (PMMA) ES CCF with modified media and estimating mean residual PAH to determine the PAH degradation potential of the biofilms after 21days of incubation with different concentrations of PAHs spiked into the media. Effect of PAHs on growth, photosynthetic pigments, EPS production, their effect on the biochemical composition of the EPS, and finally, the microscopic study of the biofilm.

CHAPTER 2

ASSESSMENT OF POLYCYCLIC AROMATIC HYDROCARBONS OF THE SUNDARBANS

2.1. Introduction

PAHs are persistent organic pollutants belonging to the group of POPs which are ubiquitously present in the environment. In recent years PAH contaminants have been widely studied, owing to their hazardous effect on the living system. PAHs are mainly derived from anthropogenic activities and the incomplete combustion of organic materials. The hydrophobic nature of PAHs aid in their easy accumulation in the organisms through food chains and potentially threaten aquatic and human health (Zuloaga et al., 2013). Based on the toxicity, mutagenicity, and carcinogenicity US EPA has classified 16 PAHs as priority pollutants (Potin et al., 2004).

The Hugli River nourishes the major urban, rural, agricultural and industrial areas of Bengal before flowing into the Bay of Bengal. Consequentially, the deltaic Sundarbans (Indian part) receive about 430 million L/day (~5 m^3/sec) of effluent from industries situated on the eastern and western banks of the River Hugli. Ganga also carries about 616×106 tons of suspended solids to the Hugli estuary annually (Samanta and Dalai, 2018). The problem is compounded by massive discharges of unprocessed or partially treated general waste, fast human settlement, tourism, deforestation, and growing agricultural and aqua-cultural activities (Massolo et al. 2012). Three thousand five hundred Mg of municipal solid waste is generated daily in Kolkata and released into the Sundarbans after incomplete treatment.

Furthermore, only 20% of the waste originated in 42 riverside towns is processed, while the remainder is emptied into the Hugli (Sarkar et al. 2008). The water is heavily polluted by hydrocarbon discharges from the Haldia oil refinery and the ships docking at the Haldia port (Roy et al. 2002). An oil tanker disaster in the Bangladesh Sundarbans on 9th December 2014 released 358,000 litres of heavy fuel oil into the mangrove ecosystem. Cd, Pb, Co, Zn, As, and Cu pollute the estuarine environment (Banerjee et al. 2012; Chatterjee et al. 2007; Mukherjee

et al. 2009; Massolo et al. 2012). Sediment analysis further suggested a potential risk to the sediment-dwelling organisms induced by persistent organic pollutants POPs (PAHs, PCBs, DDTs, PBDEs, HCHs, HCB) contaminants.

PAHs were considered one of the most important pollutants in the Sundarbans (Binelli et al. 2007; Dominguez et al. 2010). All pollutants have the potential to change the estuary's geochemistry, affecting the local coastal environmental quality (Chatterjee et al. 2007; Binelli et al. 2007). In the Indian Sundarbans sediments the concentration of sixteen priority PAHs varied from 208.3 to 12,993.1 ng/g dry weight. Fla, Pyr, B(a)P , B(b)F, and D(ah)A were found to be prevalent. The diagnostic ratios suggested that the PAHs in sediments were a mixed source of both petrogenic and pyrogenic origins (Zuloaga et al., 2013). Furthermore, the high PAH concentration in the intertidal bivalve mollusk of the Sundarbans, Meretrix, which has high commercial value, was of concern (Zuloaga et al. 2009). PAH concentrations in sediments have been connected with liver neoplasms and other deformities in fish. Increased PAH concentrations are a threat to aquatic organisms and potentially to those consuming fish and shellfish (UKMPA, 2001). Previous reports have already identified PAHs at elevated levels sufficient to be toxic to flora and fauna of different regions of the Sundarbans, such as Lot 8 (Zuloaga et al. 2013), Lothian Island (Dominguez et al. 2010), Canning and Chemagari (Zuloaga et al. 2009). No further appraisal of the Indian Sundarbans PAH contamination has been done since the report of Zuloaga et al. (2013).

2.2. Materials and methods

2.2.1. Sample collection

Water and sediment samples from Indian Sundarbans estuaries were collected during November 2018 (Figure 7), covering five various sampling sites in the Indian Sundarbans, namely Purba Gurguria, Maipit , Patharpratima , Namkhana and Kakdwip with 6, 3, 5, 6, and

5 number of samples respectively (Figure 8). The geographical locations of each sampling station were recorded by the Global Positioning System (GPS). Surface water (1L) was collected in amber-colored glass bottles to prevent the photodegradation of PAHs. At the same time, sediment samples were taken at 0-4 cm depth using trowels and were collected in amber-colored glass bottles.

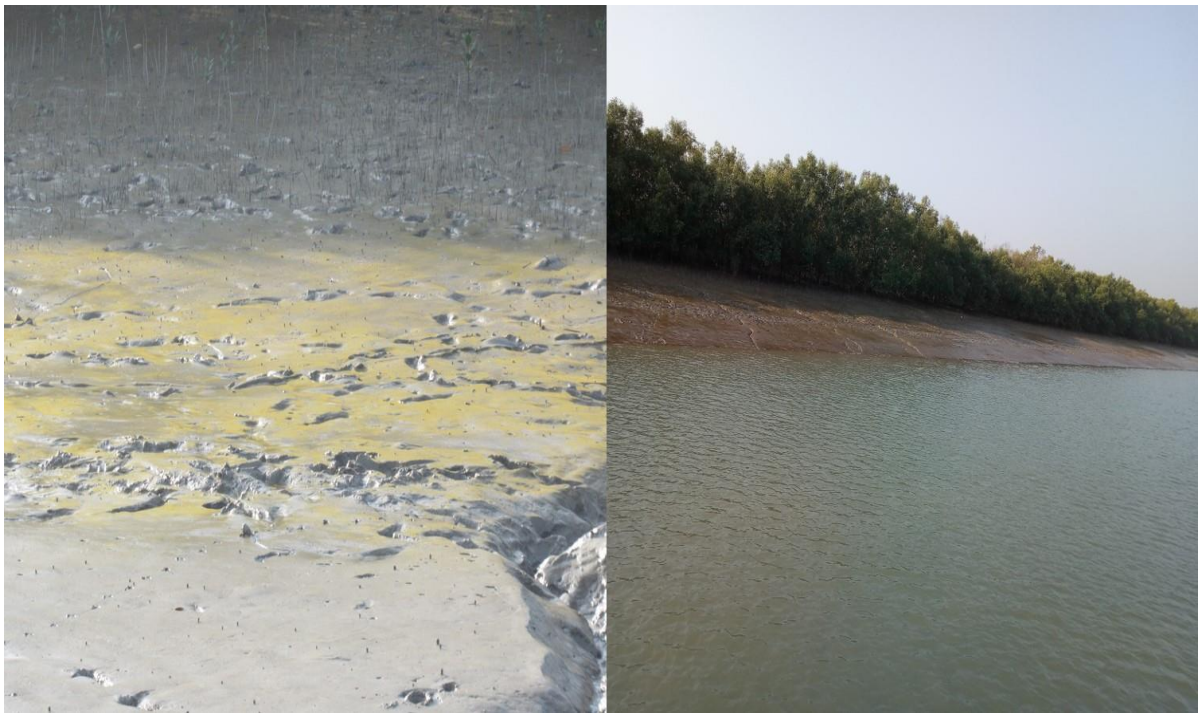

Figure 7: Water and sediment collection regions from the Indian Sundarbans mangroves.

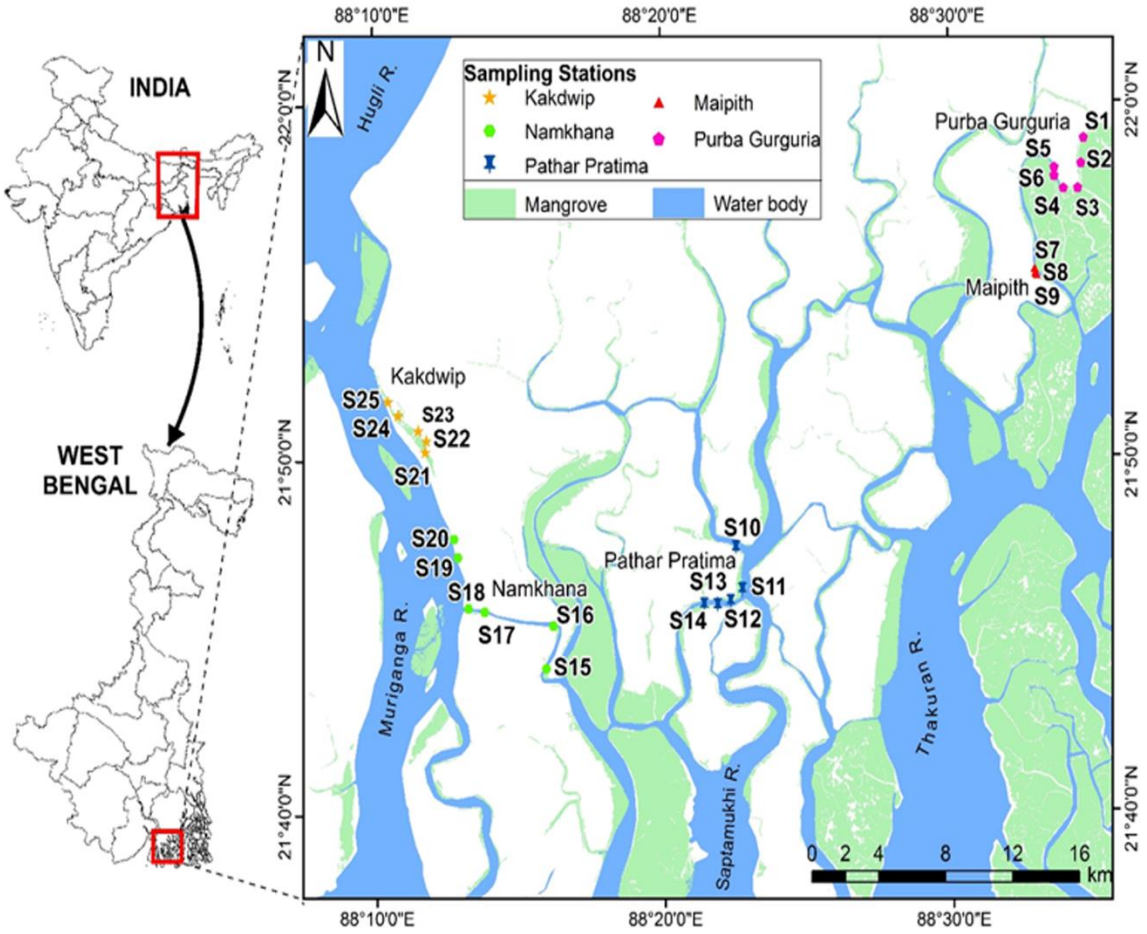

Figure 8: Geographic locations of Indian Sundarbans showing the sampling points.

2.2.2. Physico-chemical analysis of water and sediments

Physico-chemical variable such as turbidity and conductivity-salinity of water and the organic carbon content of the sediments were determined. The turbidity of the water was analyzed using a digital turbidity meter (Model 331 E, Electronic India Pvt. Ltd. (India). The turbidity meter was calibrated to 400 NTU using a standard hydrazine sulfate solution and hexamethylenetetramine solution. The turbidity meter was calibrated to 0 NTU using turbidity-free distilled water, and the sample reading was noted. The water conductivity determined the salinity of the water. The conductivity was measured using Conductivity Meter 36 (Systronics India Ltd., India), calibrated using 0.1, 0.01, and 0.001N KCl.

The organic carbon content (OC) of sediments was measured based on the Walkley-Black chromic acid wet oxidation method (Walkley and Black, 1934). First, 10 mL of the standard $K_2Cr_20_7$ solution was added to a conical refluxing flask consisting of 0.5 g of air-dried homogenized and sieved sediment, and contents were mixed thoroughly by swirling. Next, carefully 15 mL concentrated H_2SO_4 was added; the acid was dispensed a little at a time since it generated heat and swirled gently to mix. The flasks were connected to the condenser with a cold water supply, then placed in the hot plates and refluxed for 1 hr. Next, 100 mL of water was added and swirled to mix. Next, five drops of ferroin indicator was added and titrated with ferrous ammonium sulfate till the endpoint, where the colour changes from blue-green to violet-red. Finally, a blank consisting of all the same reagents but without the soil was treated similarly. OC was calculated from:

$$OC\ (mg/g) = \frac{18 \times C \times V}{M} \times (1\text{-}V1/V2)$$

Where C = concentration in mol/L of $K_2Cr_20_7$ solution (0.166 M), V= the volume of dichromate solution used (10 mL), V1= the volume of titrant used up in the sample determination (mL), V2 = the volume of titrant used up in the blank determination (mL) and M = the weight of sample used (g).

Organic carbon in % was calculated as:

$$O.C\ (\%) = O.C\ (mg/g)/\ 10$$

Organic matter (OM)concentration was quantified on the basis of OC (Radojevic and Bashkin, 1999).

$$O.M\ (\%) = 1.72 \times OC\ (\%)$$

2.2.3. Extraction of PAHs in water

PAHcontent in water samples collected from the Indian Sundarbans was extracted by liquid-liquid extraction based on USEPA method 3510C (1996a). The filtered water samples were

transferred quantitatively to a separating funnel together with 60 ml dichloromethane (DCM). The separating funnel was sealed and vigorously shaken for about 1-2 min, and the excess pressure was released by periodic venting. The organic layer separated from the water phase was compiled, and extraction was done in duplicate with a fresh portion of solvents. The pooled extract was condensed to 2 ml, the solvent exchange was required, 50 ml cyclohexane was added, and further concentrated to 2 ml.

2.2.4. Determination of PAHs in sediments

Sediment samples were air-dried in the dark to avoid photodegradation of PAHs, powdered samples were passed through a 1 mm sieve, and following the USEPA method 3540C (1996c) the PAHs were extracted. 300 ml of DCM was added to the homogenized sample to a 500 ml round-bottomed flask, and the samples extracted were carried out for 16-24 hours with 4-6 cycles/hour using a Soxhlet apparatus. Extracts were concentrated, the solvent was exchanged to cyclohexane, and further concentrated to 2 ml.

2.2.5. Silica gel clean-up

Silica gel clean-up was performed to exclude interference of sulfur compounds (USEPA method 3630C 1996a). Before the silica clean-up technique, the extracted solvent must be exchanged for cyclohexane. The slurry was prepared using 10g activated silica gel (100/200 mesh activated for at least 16 hr. at 130°C) with DCM. 1 to 2 cm of sodium sulfate (anhydrous) was added to remove the water content (if any was present), DCM was eluted. Pre-eluted the column with 40 ml of hexane with a flow rate of 2 ml/min. The eluate was discarded and 2 ml of cyclohexane sample extract was added, followed by 25 ml of hexane. Discard the hexane eluate and the column was further eluted with DCM/hexane (2:3) (v/v) into a flask for concentration. hexane elute contains the saturated aliphatic compounds whereas aromatic compounds were eluted with DCM/hexane (2:3). All the solvent fractions were concentrated to 2 ml and used for GC FID analysis.

2.2.6. Gas chromatography

Concentrated samples (2 µl) were injected into a gas chromatograph (Agilent 7820 A, Agilent Technologies, USA) provided with a split injector, a flame ionization detector (FID), and a capillary column having dimensions 30 m × 320 µm × 0.25 µm. N_2 was acted as the carrier gas with a 1 ml/min flow rate. The column temperature was set at 120 °C for 2 min and then programmed at 7 °C/min to a final hold at 300 °C. FID temperature was set at 300 °C. 16 priority PAH standard mix (Accu Std-Z013-17, 0.2 mg/ml) was diluted to prepare stock solution at a concentration of 20 ppm using DCM: methane (1:1), (v/v).

Varying concentrations (0.55, 0.75, 1, 1.5, 2, and 5 ppm) of working standard solutions were prepared from the stock solution. GC was calibrated using the working standards prescribed in US EPA method 8000B (2004). The lowest concentration leading to a signal-to-noise ratio of 3 was measured by the limit of detection (LOD), and the limit of quantification (LOQ) assessed the concentration leading to a signal-to-noise ratio of 10. LOD and LOQ values of 16 PAHs were calculated (Table 2). Quality control (QC) for water and sediments was carried out regularly to validate extraction methods. Each of the 16 PAHs at 10 ppm concentrations was used for QC analysis and was extracted similarly to the samples, followed by a silica gel clean-up procedure described in Section 2.2.5. A method blank, i.e., reagent grade water, was also subjected to a similar extraction method along with the QC sample. The recovery percentage of the PAHs ranged between 77 and 103%, which satisfied the quality control acceptance criteria mentioned in EPA method 610 (1984) (Table 3). Method 8100 Polynuclear Aromatic Hydrocarbons (1986), described by the USEPA, recommends not using deuterated analogs of PAHS as surrogates for GC FID analysis due to co-elution problems.

Table 2: Limit of detection (LOD) and Limit of Quantitation (LOQ) of 16 PAHs for Agilent GC-FID 7820A SD: standard deviation, RSD: relative standard deviation

PAH components	LOD (ppm)	LOQ (ppm)	SD	RSD (%) (n=7)
Nap	0.01	0.02	0.002	0.401
Acy	0.02	0.06	0.006	1.124
Ace	0.01	0.04	0.004	0.832
Flu	0.003	0.01	0.001	0.140
Phe	0.003	0.01	0.001	0.140
Ant	0.01	0.02	0.002	0.350
Fla	0.01	0.02	0.002	0.350
Pyr	0.01	0.03	0.003	0.702
B(a)A	0.02	0.05	0.005	0.913
Chr	0.01	0.03	0.003	0.702
B(b)F	0.01	0.02	0.002	0.421
B(k)F	0.01	0.03	0.003	0.702
B(a)P	0.01	0.03	0.003	0.702
Ind	0.01	0.03	0.003	0.350
D(a,h)A	0.01	0.03	0.003	0.698
B(ghi)P	0.01	0.04	0.004	0.832

Table 3: Quality control tests conducted in water and sediments to assess the recovery (as a percentage) of the 16 priority pollutants as a measure of extraction efficiency (n=4).

PAHs	Recovery (%) Water	Recovery (%) Sediment
Nap	94.90±2.8	84.2±2.2
Acy	96.53±4.1	102.9±1.5
Ace	95.05±1.4	92.4±3.4
Flu	83.71±1	89.3±3.6
Phe	81.4±2.7	102.8±4.6
Ant	97.83±5.6	94.5±0.5
Fla	96.75±1.4	79±1.6
Pyr	88.82±3	86.9±3.2
B(a)A	92.3±1.6	96±3.7
Chr	94 ± 5.4	89.8±0.7
B(b)F	93.84±0.4	89.9±1.2
B(k)F	80±3.5	80±0.5
B(a)P	103.7±3.4	82.8±0.8
Ind	79.23±5.3	91.9±1.9
D(a,h)A	95.38±5.5	95.6±0.9
B(ghi)P	77.85±4.5	83.4±1.9

2.2.7. Statistical analyses

Statistical analyses such as a two-tailed Student t-test, Analysis of variance (ANOVA), and the Pearson correlation were executed using SPSS 16.0 software. The statistical significance was verified at $P \leq 0.05$.

2.3. Results and discussion

2.3.1 Physico-chemical characteristics of Sundarbans water and sediments

The physico-chemical properties such as conductivity, salinity, and turbidity of water and the percentage of both organic carbon content and organic matter present in the sediments collected from Purba Gurguria, Maipit, Patharpratima, Namkhana, and Kakdwip were evaluated to understand the general nature of water and sediments in the Sundarbans estuaries. The result of the selected physico-chemical properties of the water and sediment samples was determined and shown in Table 4 and Figure 9.

Table 4: Conductivity, salinity, turbidity, OC, and OM of surface water and sediments collected from the Indian Sundarbans. Average values and ranges were established in each cluster, considering the sampling stations. The highest values obtained are indicated in bold letters. ** - $p<0.01$, * - $p<0.05$, and - for non-significant based on ANOVA conducted between the sampling sites.

Parameters / Sampling sites		Conductivity (mS/cm)	Salinity (ppt)	Turbidity (NTU)	Organic Carbon (%)	Organic Matter (%)
Purba	**Mean**	37.23**	21.37**	34.67ns	6.87**	11.81**
Gurguria	**Range**	33-40.1	18.7-23.2	34-75	5.56-7.55	9.57-12.99
Maipit	**Mean**	44.8**	26.13**	27.67 ns	2.58**	4.45**
	Range	44.5-45.1	26.2-26.3	13-46	2.25-2.91	3.87-5.01
Patharpratima	**Mean**	**45.52****	**26.56****	72.6 ns	5.93**	10.21**
	Range	43.5-46.9	25.2-27.5	60-76	2.98-6.9	5.13-11.9
Namkhana	**Mean**	35.12**	19.93**	46.67 ns	2.49**	4.29**
	Range	29.4-43.4	15.4-23.3	44- 59	1.30-4.18	2.24-7.18
Kakdwip	**Mean**	24.32**	13.3**	**75.2 ns**	**7.42****	**12.77****
	Range	22-32.5	11.9-18.2	25-76	6.7-8.3	11.53-14.41

Conductivity was measured to determine water salinity, and the mean conductivity of water ranged between 24.3 - 45.5 mS/cm, and its respective mean salinity varied from 11.9 to 27.5 ppt. The water conductivity and salinity were higher in both Patharpratima and Maipit, and the lowest was observed in Kakdwip. Turbidity ranged from 27.7 to 75.20 NTU, and the highest was observed at Kakdwip (75.2 NTU) and Patharpratima (72.60 NTU), while the lowest was recorded in Maipit (27.67 NTU). The highest organic carbon content, with a mean of 7.42%, was observed in Kakdwip, followed by Purba Gurguria. Sediments collected from different geographical regions of Sundarbans showed significant difference in their mean organic carbon and organic matter contents.

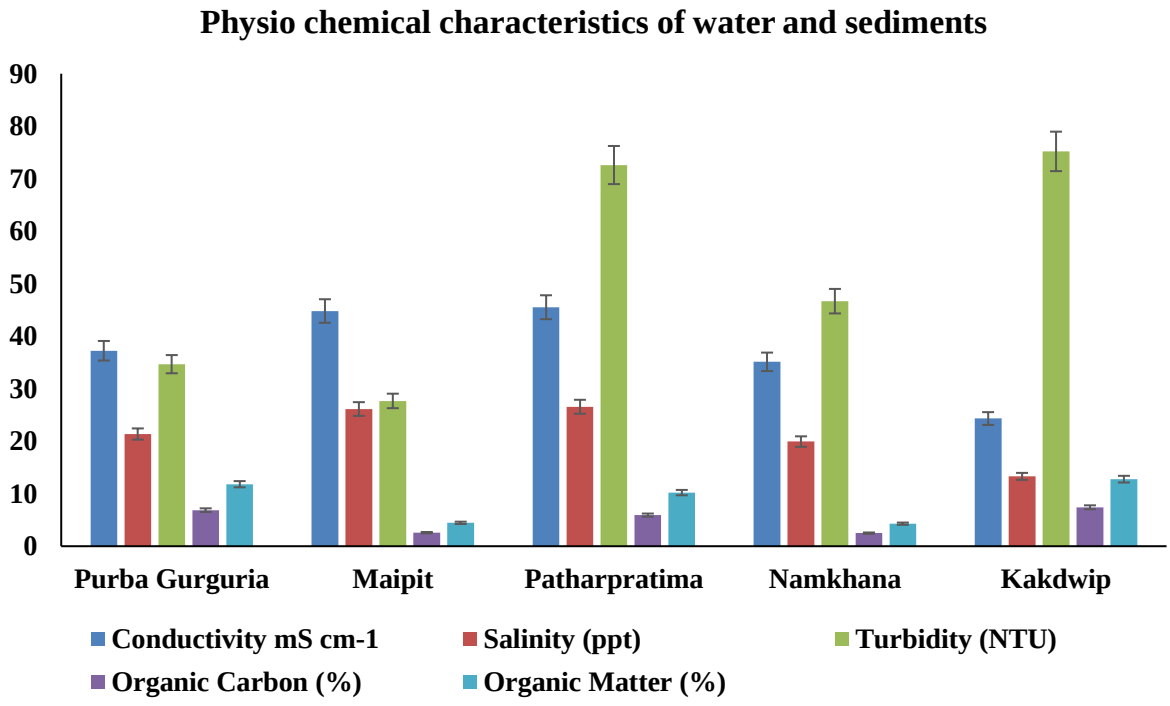

Figure 9: Graphical representation of physiochemical characteristics of water and sediments collected from various geographical locations.

Water conductivity measures a substance's ability or any solution to conduct electric current depending on the number of dissolved solids in the water. Higher conductivity implies higher the occurrence of inorganic ions Mg^{2+}, HCO^{3-}, CO_3^{2-}, NO^{3-}, Ca^{2+}, and PO_4^{3-}. Current mean salinity obtained was almost equivalent to that previously observed in Sundarbans (14-

25 ppt) (Chaudhuri et al. 2012). The continuous influx of freshwater from the Hugli River (Figure 8) is one of the primary reasons for the lower salinity in Kakdwip compared to the other sampling regions. A previous study in the Sundarbans reported high aquatic turbidity (25-125 NTU); conductivity and suspended particles were found to be high (Chaudhuri et al. 2012). A positive correlation was witnessed between salinity and PAH concentrations. Several studies found that with an increase in water salinity, the biodegradation of PAH and crude oils by indigenous microbes in the sediments decreased. Turbidity is the measure of cloudiness caused in the water by suspended or dissolved particles such as silt and clay, organic and inorganic matter, algae, and other microscopic organisms. Previous physicochemical studies in Sundarbans reported mean turbidity ranging from 25-125 NTU (Chaudhuri et al. 2012). Studies done by Chaudhuri et al. (2012) reported high aquatic turbidity, conductivity, and suspended particles in the Indian Sundarbans estuary.

2.3.2. Distribution of PAHs in Sundarban water

The PAHs concentration in the water sample is shown in Table 5. Out of 16 priority PAHs, only 6 could be detected because most of the PAHs were found to be below the LOD values (Table 2). Most of the HMW PAHs were not detected, but only some LMW PAHs with a concentration above LOD values could be detected. the most abundant PAH was Ace. The mean LMW PAHs concentration was 34.7 ng/ml, whereas HMW PAHs was 15.9 ng/ml. 64% PAHs in water were found to be 2-3 ringed while 5-6 ring PAHs encompossed 36% of total PAHs (Figure 10a). Nap was found only in Kakdwip, Purba Gurguria showed the presence of Ace, Flu as well as B(ghi)P whereas in Maipit, the presence of Ace, Flu along with Ant and B(b)F was observed. The highest values of Ace and Flu were observed in Maipit. Water collected from Patharpratima and Namkhana did not show any trace of PAHs.

B(a)P, a marker for the carcinogenic effect of PAH, was not observed in any of the water samples, studies conducted by Olayinka et al. (2018) in the deltaic river waters of Lagos,

Nigeria also showed similar results. The HMW PAHs in this study were also very low or below LOD, similar to studies done by Jaward et al. (2012) in the Mexican estuaries,. High vapor pressure and hydrophilicity of LMW PAHs contributed to the prevalence of LMW PAHs in the water. At the same time, low concentrations of HMW PAH can be attributed to their low water solubility and tendency to adsorp to solid phases (Sun et al., 2009).

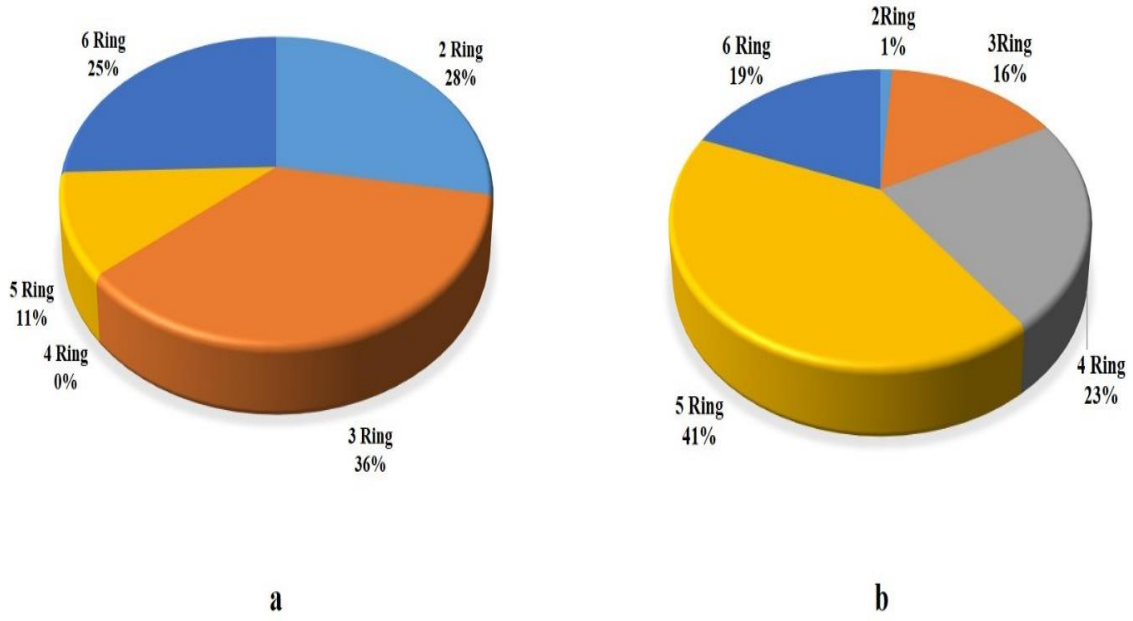

Figure 10: Distribution of the mean concentration of 2- 6-ringed PAHs in (a) water and (b) sediments samples collected from Indian Sundarbans

Generally, the occurrence of PAH in water is based on the number of aromatic rings. High molecular weight PAH comprising 4-6 ringed PAHs cannot be rapidly degraded by the indigenous microorganisms, leading to their bioaccumulation in the aquatic organisms and possessing a greater carcinogenic risk. Although the LMW PAH comprising of 2-3 aromatic rings is less carcinogenic, a high concentration of the same may have other toxic effects on many aquatic organisms (Harris et al., 2009).

Table 5: Concentrations of 16 priority PAHs (ng/ml) observed in surface water collected from Indian Sundarbans. Bold indicates the highest values of individual PAHs recorded in the sample

PAHS	Purba Gurguria		Maipit		Patharpratima		Namkhana		Kakdwip	
	Mean	Range	Mean	Range	Mean	Range	Mean	Range	Mean	Range
Nap	ND	ND	ND	ND	ND	ND	ND	ND	**23.5**	ND - 65.9
Acy	ND	ND	ND	ND	ND	ND	ND	ND	ND	ND
Ace	50.5	21.9 – 89	**53.6**	ND - 86.6	ND	ND	ND	ND	ND	ND
Flu	11	ND - 19.6	**12.8**	ND - 21.3	ND	ND-10.0	ND	ND	ND	ND
Phe	ND	ND - 19.8	ND	ND	ND	ND	ND	ND	ND	ND- 10.1
Ant	ND	ND	**22.2**	ND - 66.6	ND	ND	ND	ND	ND	ND
LMW-PAH	61.5	ND-100	88.6	84 – 108	ND	ND - 10	ND	ND	23.5	ND - 65.9
Fla	ND	ND - 26.2	ND	ND	ND	ND	ND	ND	ND	ND
Pyr	ND	ND	ND	ND	ND	ND	ND	ND	ND	ND
B(a)A	ND	ND	ND	ND	ND	ND	ND	ND	ND	ND
Chr	ND	ND	ND	ND	ND	ND	ND	ND	ND	ND
B(b)F	ND	ND	**36.4**	ND- 51.8	ND	ND	ND	ND	ND	ND- 29.4
B(k)F	ND	ND	ND	ND	ND	ND	ND	ND	ND	ND
B(a)P	ND	ND	ND	ND	ND	ND	ND	ND	ND	ND
Ind	ND	ND	ND	ND	ND	ND	ND	ND	ND	ND
D(a,h)A	ND	ND	ND	ND	ND	ND	ND	ND	ND	ND
B(ghi)P	**43.1**	ND - 85.3	ND	ND	ND	ND	ND	ND	ND	ND
HMW-PAH	43.1	ND – 134	36.4	39 – 57	ND	ND	ND	ND	ND	ND – 29.4
ΣPAH	105	58 – 109	125	123 – 165	ND	ND - 10	ND	ND	23.5	ND – 65.9

ND Not Detected

According to WHO, the concentration of individual PAHs is generally 50 ng/L or .05 ng/ml in surface and coastal water (Olayinka et al., 2018). Nevertheless, the concentrations of these PAHs were found to be much higher than the proposed WHO limit. Concentration above the WHO proposed level indicates that the source of contamination is mainly through industries, atmospheric deposition, shipyards, and urban runoff. A wide range of PAH concentrations indicates contamination was generated from different sources such as sewage outfalls, industrial waste, and oil spillage. It is difficult to differentiate the different sources of PAH contaminant inputs from the distribution of PAH in water alone. Compared to the Chinese estuaries, the contamination level in the Indian Sundarbans was lower (Table 6). Previous studies conducted in the Sundarbans by Sarkar et al.(2012) and Zuloaga et al.(2013) focused on quantifying PAHs present in the sediments, but not the PAHs in the water.

The sampling locations were situated on three of the seven primary rivers of the Sundarbans: Purba Gurguria and Maipit on Matla, Patharpratima on Saptamukhi, and Namkhana and Kakdwip on Muriganga. Purba Gurguria and Maipit recorded the highest water salinity. Concurrently, the PAH water concentration in Purba Gurguria and Maipit was relatively higher than those observed in the water collected from Saptamukhi and Muriganga rivers. Raza et al. (2013) also showed similar observations, who noted that with an increase in the salinity of seawater, the PAH concentration also increased in the Rembau–Linggi estuary, Malaysia. Furthermore, an experiment by Tam et al. (2002) showed an inverse relationship between the PAH degradation potential of bacteria isolated from the mangrove swamps and the salt concentration. The above observation suggests that with an increase in the salinity, PAHs' microbial degradation rate decreases because high salinity can lower microbial utilization rates.

Table 6: Comparison of PAH contamination in estuarine waters (ng/ml) and sediments (ng/g dry weight) around different geographical locations of the world with the present study.

Location	Reported concentration (ng/ml or ng/g dry weight)	References
Water		
San Francisco Estuary, USA	0.007–0.12	Ross and Oros, 2004
Daliaohe Estuary, China	139.2–1717.9	Men et al., 2009
Shuangtaizi River Estuary and Jinzhou Bay, China	1699.1–1307.5	Wang et al., 2016
Sundarbans, India	Undetectable-125	This study
Sediments		
Mai Po, Tolo, Sai Keng and Ho Chung, China	356–11,098	Ross and Oros, 2004
Lenga Estuary, Chile	290–6118	Pozo et al., 2011
Guan River Estuary, China	90–218	He et al., 2014
Yangtze Estuary, China	90.14–502.12	Li et al., 2012
Bahía Blanca estuary, Argentina	15–10,260	Arias et al., 2010
Klang Strait, Malaysia	100.3–3446.9	Sany et al., 2014
The Mediterranean coastal zone, Egypt	3.51–14,100	Barakat et al., 2011
Intertidal areas, Tanzania	77.9–24,600	Gaspare et al., 2009
The Mediterranean coastal zone, Spain	5.3–2627.4	Leon et al., 2014
Sundarbans, India	4880-2×10^4	This study

According to Dominguez et al. (2010) and Sarkar (2016, the hydrostatic system of Saptamukhi river represents a tidal inlet at which mixing of ebb and flood flows due to tidal asymmetry lead the re-suspension of sediments (). We assume that concentration of PAH in Patharpratima is highly influenced by such localized resuspension approach . Shipping industries along the Muriganga are comparatively more prominent than in the other rivers (Matla and Saptamukhi), which were also reflected in the high PAH concentration in the water of Kakdwip. Urban runoffs, sewage, waste discharges, and intensive boating activities might also be a reason behind an elevated PAH concentration in Kakdwip (Sarkar et al., 2012).

2.3.3. Distribution of PAHs in sediments

In the sediments, the mean concentration of PAH varies between 4880 to 2×10^4 ng/g dry weight. Contrary to the concentration of PAHs in water samples, in the sediments, HMW PAHs were more dominant than LMW PAHs (Table 7). The mean total concentrations of HMW PAHs and LMW PAHs were observed to be 1.04×10^4 and 2140 ng/g dry weight, respectively, which were significantly different ($P \leq 0.05$). The most abundant PAH was found to be B(b)F (7700 ng/g) in Namkhana and subsequently B(a)A (6590 ng/g) in Kakdwip and B(ghi)P (5460 ng/g) in Purba Gurguria. About 17% of all PAHs are 2-3 ringed aromatic PAHs, 23% are 4 ringed aromatic PAHs, and 60% are 5-6 ringed aromatic PAHs (Figure 10b). Table 7 shows that the lowest and highest concentrations of all LMW PAHs except Nap and Acy were noted in different sites. HMW PAHs like B(a)A, B(k)F, and B(a)P were recorded in different sampling locations. However, their concentrations of remaining HMW PAHs were significantly different. In contrast, the highest and lowest levels of Flu, B(b)F, Pyr, B(ghi)P, Chrysene (Chr), Indeno (1,2,3-cd) pyrene (Ind) and D(a,h)A were recorded in the exact geographical regions. Flu from Patharpratima, B(a)A from Kakdwip and Ace from all stations were found to have higher Effects Range-Median (ER-M values) than the recommended ER-M values (Table 7).

Sarkar et al. (2012) previously quantified the PAHs present in the sediment of Indian Sundarbans; according to his study Kakdwip region of Sundarbans showed a high concentration of PAH pollutants (500 ng/g) similar to the present result (2×10^4 ng/g). Studies conducted in nine locations of the Indian Sundarbans by Zuloaga et al. (2013) reported 208.3 to 12993.1 ng/g dry weight of 16 PAHs. The present study suggests that over the years, in Sundarbans, there has been an increase in the PAH contaminant concentration. Three to five-ringed PAHs, particularly Ace, B(b)F, B(a) A, and B(a)P were abundant in the Kakdwip , which was in agreement with the studies conducted by Sarkar et al. (2012) and Zuloaga et al.

(2013) in Sundarbans. Predominance of 3-5 ringed PAHs was seen in Kakdwip. The predominance of 4-6 ringed PAHs in Sundarbans sedimentswas also reported by Dominguez et al. (2010). Table 6 shows that the current sediment PAH contamination level in the Indian Sundarbans is higher than in other estuaries worldwide.. Sediment total PAH concentrations were higher than the Effects Range-Low (ER-L) threshold of 2970 ng/g. (2970 ng/g). Pyr concentration was less than the ER-L (665 ng/g) in each of the five sample stations, butthe remaining 15 PAHs were higher the ER-L values in at least one sampling station (Table 7). The greater ER-L and ER-M values of PAH imply an adverse effect of PAH contaminants on the Sundarbans biota (Kim et al., 1999; MacDonald et al., 2000). Higher Apparent Effects Threshold (AET) values were indicated by Ace from all the stations, Phe from Purba Gurguria, Fla from Namkhana, and B(a)A from Kakdwip and B(a)P from all stations apart from Namkhana (Kim et al., 1999).

Table 7: PAH concentrations (ng/g) in sediments collected at 0-4 cm depth in the Indian Sundarbans, as indicated in the Figure. 9. Bold indicates the highest values of individual PAHs recorded.

PAHs	Purba gurguria		Maipit		Patharpratima		Namkhana		Kakdwip		ERL[a]	ERM[a]	AET[b]
	Mean	Range	Mean	Range	Mean	Range	Mean	Range	Mean	Range			
Nap	158	120–828	ND	ND	25.4	ND- 27	221	79.8-504	**234**	ND - 768	160	2100	500
Acy	83.1	ND–499	ND	ND	ND	ND	104	ND–397	**207**	ND -284	16	500	
Ace	1900	939-4020	655	ND-1970	1350	92.8-3250	417	247-2020	**1920**	1140- 2950	44	640	150
Flu	470	319-1030	127	ND-381	**1210**	449-4430	83.1	ND–130	59.6	34.9- 113	19	540	350
Phe	**399**	192-1090	116	ND-192	109	97.1-291	167	66.1–307	168	20.8- 326	240	1500	260
Ant	165	ND–735	ND	ND	104	ND-318	107	ND–358	**172**	73.9- 582	85	1100	300
LMW PAH	3170	2240-5770	898	ND-2500	2800	ND-4980	1100	476–3180	2760	203- 4270	564	6380	1560
Fla	488	104-1570	117	73.7-141	172	162-528	**2420**	298-1.2×10^4	631	65.5- 2370	600	5100	1000
Pyr	**239**	ND–811	ND	ND	76.3	ND-219	ND	ND–134	ND	ND - 72	665	2600	1000
B(a)A	376	227– 696	289	ND-866	236	131-551	442	ND-1050	**6590**	1340-3.08×10^4	261	1600	550
Chr	**1150**	982-5900	411	ND-759	496	260-1500	ND	ND	122	ND- 396	384	2800	900
B (b) F	634	331-1820	207	ND-620	2790	1040-1.39×10^4	**7700**	2260-4.4×10^4	6460	3740-1.65×10^4			
B (k)F	610	277-2490	**633**	490-1410	230	263-538	112	ND– 389	306	161- 821			
B (a)P	1030	699-2380	1040	210-1700	**1560**	763-3830	609	150-1330	932	250- 1870	430	1600	700
Ind	793	635-4120	606	ND-939	387	ND-839	46.1	ND – 145	95.6	ND - 487			
D (a,h)A	**416**	454-1840	283	ND-528	169	ND-395	ND	ND	72.1	ND - 275			
B(ghi)P	**5460**	509-2.44×10^4	396	ND-673	998	504-1540	1100	602-2230	1990	644-4820			
HMW PAH	1.12×10^4	2200-4.42×10^4	3990	1440-5920	7120	2420-1.72×10^4	1.24×10^4	4870-4.6×10^4	1.72×10^4	2190-5.73×10^4	2340	1.37×10^4	4150
ΣPAH	1.44×10^4	5800-4.86×10^4	4880	3940-5920	9920	2420-2.17×10^4	1.36×10^4	7660-4.9×10^4	2.00×10^4	4110-6.13×10^4	2904	2.01×10^4	5710

2.3.4 Correlation between the total PAHs and the OC content in sediments

The present study showed a weakly positive correlation between OC concentration and PAH (r^2=0.44) and between OM and PAH (r^2=0.44) (Figure 11). The presence of high PAH contaminants in Kakdwip and Purba Gurguria may be associated to the increased OC content of the sediments. Similarly, the reduced PAH concentrations in Maipit may be linked to the decreased sediment OC. Contrary to the above observation, Namkhana was reported to have a high concentration of PAHs providing reduced sediment OC level.. Previous studies in Sundarbans showed a weak correlation between OC content and total PAH (r^2=0.014) (Sarkar et al., 2012). However, an association between high sediment PAH accumulation and high OM content was observed by Sarkar (2016), where the sampling locations differed from those reported earlier (Sarkar et al., 2012). Liu et al. (2017) suggest a positive linear relationship exists between OC content and PAH concentrations. The complex pore structure of the sediments rich in OM provides the opportunity for PAHs to be easily absorbed by the OM, serving them a repository of PAHs (Liu et al., 2017). a singmificant correlation between OC and PAH can be expected when the PAH present in the soil or sediments is entirely integrated into the soil particles, (Sojinu et al., 2010). A mild correlation suggests that fresh PAHs are continually introduced into the environment and are not fully assimilated into the soil OM. In the Rembau–Linggi estuary, Malaysia, there no correlation between sediment PAH concentrations and OC content was observed (Raza et al., 2013). The authors concluded that the association between sediment PAH levels and OC was only significant for extremely contaminated locations when the total PAH concentrations were greater than 2000 ng/g.

Zuloaga et al. (2009) also observed a relationship between low sediment OC and low PAH levels in Sundarban sediment samples. Thus, sediment OC content is one of the significant factors influencing PAH concentrations in the Sundarbans. The hydrodynamic conditions of the Sundarbans estuary, which include depositional rate of sediments, textural

composition, differential resuspension re-deposition of sedimentary PAHs, vertical mixing caused by physical or biological processes, and microbial PAH degradation,, PAH input rate, highly influences the spatial distribution of PAHs in surface sediments. In the future, to attain a comprehensive relationship between PAH contents in sediments and environmental conditions, it is crucial to integrate salinity and OC content along with the above factors.

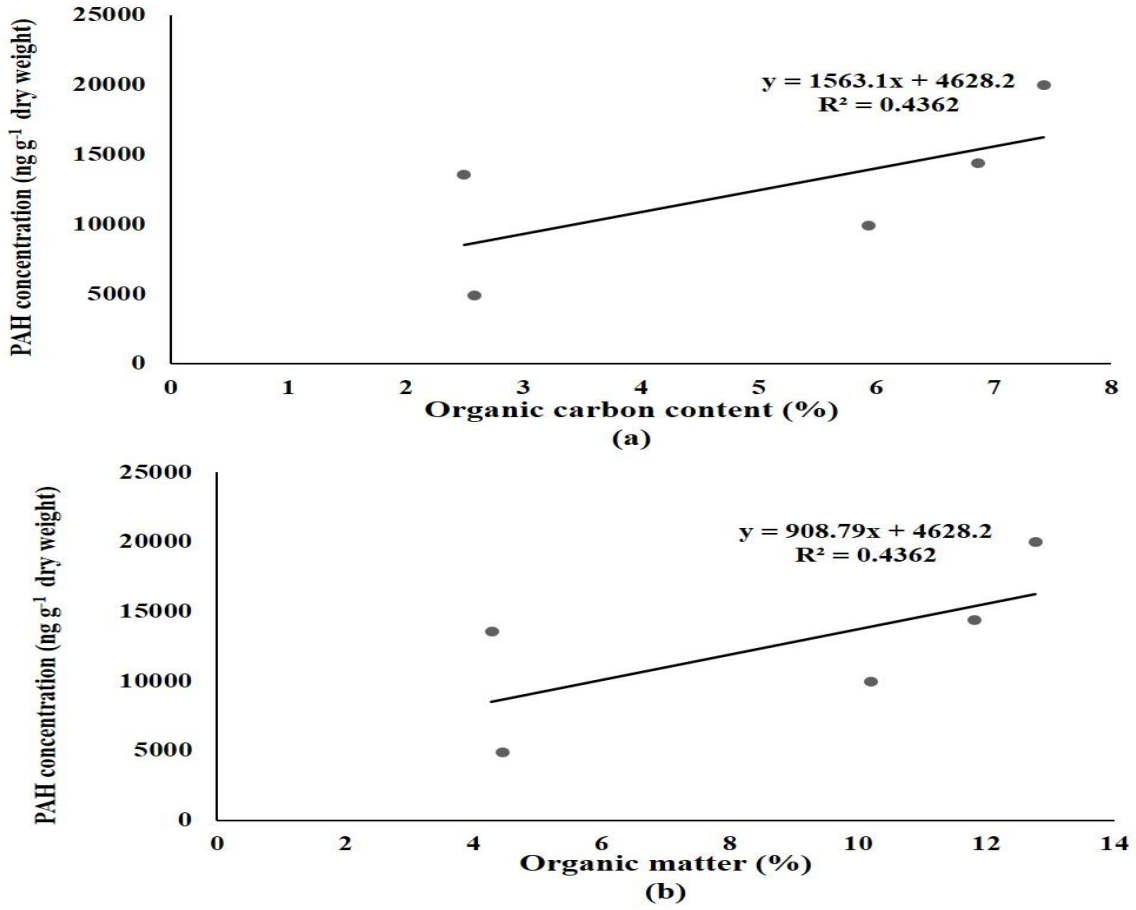

Figure 11: (a) Correlation between organic carbon and total PAHs (ng/g dry weight) in sediments and (b) Correlation betwen organic matter and total PAHs (ng/g dry weight) in sediments.

2.3.5 Identification of PAHs sources (petrogenic/pyrogenic) in the sediment

Fla/Pyr and Phe/Ant ratios in four stations showed that pyrogenic sources were the origin of PAHs like Phe, Ant, Fla, and Pyr apart from Maipit (Figure 12, Table 8). B(a)A and Chr ratios

indicate the petrogenic and the pyrogenic origin of PAHs. All the stations except Kakdwip showed Pyrogenic sources of PAH, whereas the petrogenic PAHs was identified in Kakdwip. Ind/Ind+B (ghi)P ratios in Purba Gurguria, Namkhana, and Kakdwip indicates petrogenic PAHs and pyrogenic PAHs in Maipit..

Table 8: Molecular diagnostic ratios indicating pyrogenic and petrogenic sources of PAHs found in the sediments of the Indian Sundarbans

Ratios	**Locations**					**Diagnostic ratios indicative of sources [a]**	
	Purba Gurguria	**Maipit**	**Pathar pratima**	**Namkhana**	**Kakdwip**	**Petrogenic**	**Pyrogenic**
Phe / Ant	2.41		1.05	1.57	0.98	>15	<10
Chr / B(a)A	3.05	1.42	2.10	0.00	0.02	<0.4	>0.9
Ant / Ant + Phe	0.29	0.00	0.49	0.39	0.51	<0.1	>0.1
Fla / Fla + Pyr	0.67	1.00	0.69	0.99	0.97	<0.4	≥0.5
Fla / Pyr	2.04		2.25	108.69	31.44	<1	>1
Ind / Ind +B(ghi)P	0.13	0.60	0.28	0.04	0.05	<0.2	>0.5
B(a)A / B(a)A+ Chr	0.25	0.41	0.32	1.00	0.98	<0.2	>0.35

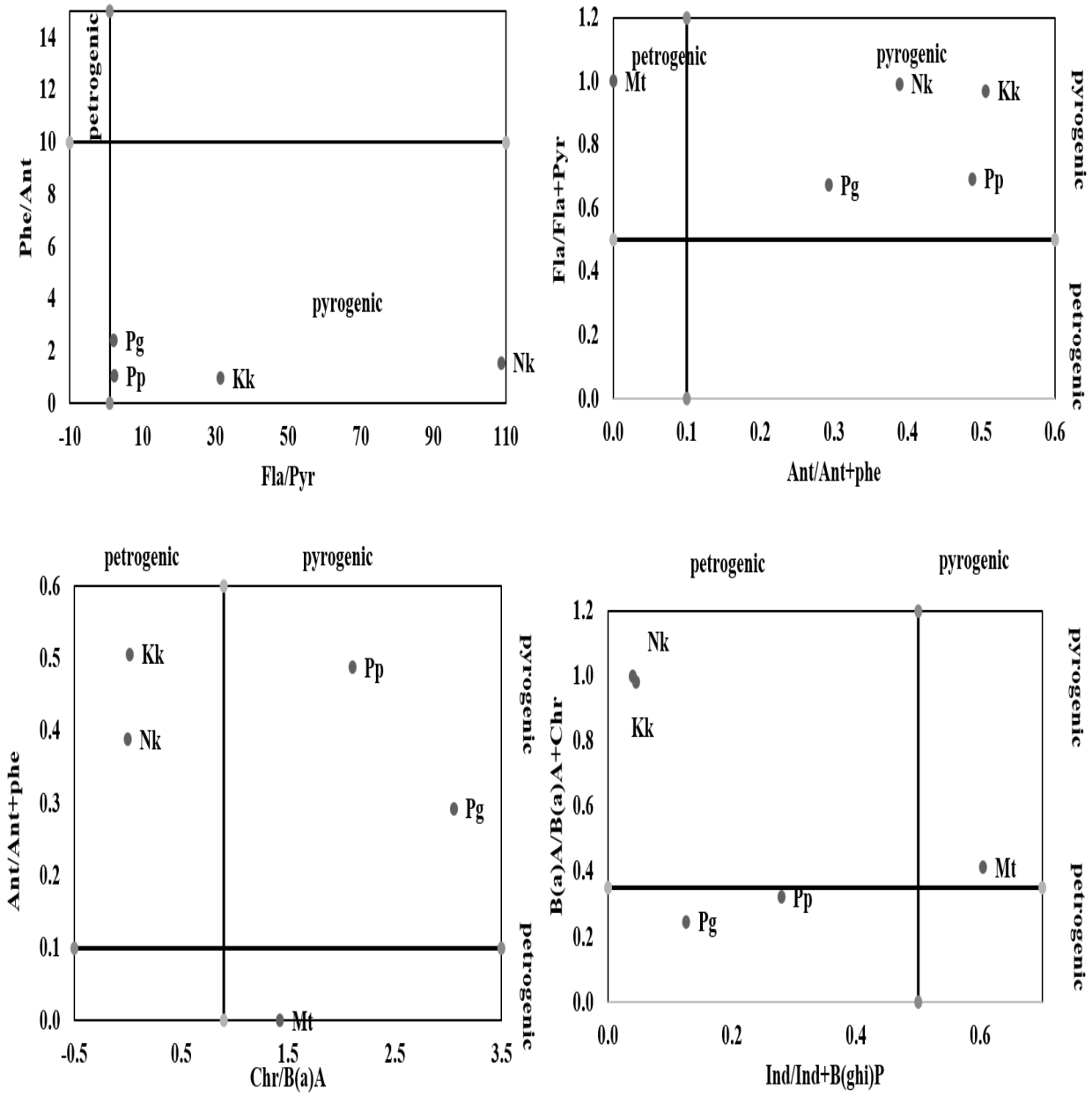

Figure 12: Identification of PAH sources using a scatterplot (Pg-Purba Gurguria, Mt-Maipit, Pp-Patharpratima, Nk- Namkhana, and Kk – Kakdwip)

Generally, two to three-ringed PAHs indicate the petrogenic source of contaminations. The pyrogenic source of PAH contamination is contributed by four to six- ringed PAHs. They are toxic and more stable thermodynamically than 2-3-ringed PAHs (Adeniji et al., 2018). The current findings are consistent with those reported by Dominguez et al. (2010) in the Sundarbans sediments and by Guzzella et al. (2005) in sediments along the Hugli river estuary. PAH in sediments mainly originated from the combustion of coal and biomass. Aside from

Maipit, all of the sampling locations showed evidence of pyrogenic and petrogenic origin of PAH contamination.. In Maipit, a pyrogenic source of contamination was identified.. Previous records also pinpoint Ind / [Ind+ B (ghi) P] isomer ratios indicate both petrogenic and pyrogenic source of PAHs. Coal power stations, rice husking, and the use of coal, charcoal, and wood for domestic cooking all contribute significantly to thePAH contamination in the Sundarbans environment (Chatterjee et al., 2009). Furthermore, Pait et al. (2008) suggested that urban runoff, automobile emissions, and river discharges are essential sources of PAHs in coastal sediments.

References

Adeniji, A.O., Okoh, O.O. and Okoh, A.I., 2018. Analytical methods for polycyclic aromatic hydrocarbons and their global trend of distribution in water and sediment: a review. Recent insights in petroleum science and engineering, 10.

Arias, A.H., Vazquez-Botello, A., Tombesi, N., Ponce-Vélez, G., Freije, H., Marcovecchio, J., 2010. Presence, distribution, and origins of polycyclic aromatic hydrocarbons (PAHs) in sediments from Bahía Blanca estuary, Argentina. Environ. Monit. Assess.160, 301–314.

Banerjee, K., Senthilkumar, B., Purvaja, R., Ramesh, R., 2012. Sedimentation and trace metal distribution in selected locations of Sundarbans mangroves and Hooghly estuary, northeast coast of India. Environ. Geochem. Health. 34(1), 27-42.

Barakat A.O., Mostafa A., Wade T.L., Sweet S.T., Sayed N.B.E, 2011. Distribution and 507 characteristics of PAHs in sediments from the Mediterranean coastal environment of Egypt. Mar. Pollut. Bull. 62, 1969-1978.

Binelli, A., Sarkar, S.K., Chatterjee, M., Riva, C., Parolini, M., Bhattacharya, B., Bhattacharya, A.K., Satpathy, K.K., 2007. Concentration of polybrominateddiphenyl ethers (PBDEs) in

sediment cores of Sundarban mangrove wetland, northeastern part of Bay of Bengal (India). Mar. Pollut. Bullet. 54(8), 1220-1229.

Chatterjee, M., Canario, J., Sarkar, S.K., Branco, V., Bhattacharya, A.K. and Satpathy, K.K., 2009. Mercury enrichments in core sediments in Hugli–Matla–Bidyadhari estuarine complex, north-eastern part of the Bay of Bengal and their ecotoxicological significance. Environ Geol, 57(5), pp.1125-1134.

Chatterjee, M.V., Silva Filho, E.V., Sarkar, S.K., Sella, S.M., Bhattacharya, A., Satpathy, K.K., Prasad, M.V., Chakraborty, S., Bhattacharya, B.D., 2007. Distribution and possible source of trace elements in the sediment cores of a tropical macrotidal estuary and their ecotoxicological significance. Environ. Int. 33(3), 346-356.

Chaudhuri, K., Manna, S., Sarma, K.S., Naskar, P., Bhattacharyya, S. and Bhattacharyya, M., 2012. Physicochemical and biological factors controlling water column metabolism in Sundarbans estuary, India. Aquat. Biosyst, 8(1), pp.1-16.

Domínguez, C., Sarkar, S.K., Bhattacharya, A., Chatterjee, M., Bhattacharya, B.D., Jover, E., Albaigés, J., Bayona, J.M., Alam, M.A. and Satpathy, K.K., 2010. Quantification and source identification of polycyclic aromatic hydrocarbons in core sediments from Sundarban Mangrove Wetland, India. Arch. Environ. Contam. Toxicol., 59(1), pp.49-61.

Gaspare L., Machiwa J.F., Mdachi S.J.M., Steck G., Brack, 2009. Polycyclic aromatic hydrocarbon (PAH) contamination of surface sediments and oysters from the inter-tidal areas of Dar es Salaam, Tanzania. Environ. Pollut. 157 , 24-34.

Guzzella, L., Roscioli, C., Vigano, L., Saha, M., Sarkar, S.K. and Bhattacharya, A., 2005. Evaluation of the concentration of HCH, DDT, HCB, PCB and PAH in the sediments along the lower stretch of Hugli estuary, West Bengal, northeast India. Environ. Int, 31(4), pp.523-534.

Harris, D.L., Huderson, A.C., Niaz, M.S., Ford, J.J., Archibong, A.E., Ramesh, A., 2009. Comparative metabolism of benzo (a) pyrene by ovarian microsomes of various species. Environ. Toxicol. 24(6), 603-609

He, X.R., Pang, Y., Song, X.J., Chen, B.L., Feng, Z.H., Ma, Y.Q., 2014. Distribution, sources and ecological risk assessment of PAHs in surface sediments from Guan River estuary, China. Mar. Pollut. Bull. 80 , 52–58.

Jaward, F.M., Alegria, H.A., Galindo Reyes, J.G. and Hoare, A., 2012. Levels of PAHs in the waters, sediments, and shrimps of Estero de Urias, an estuary in Mexico, and their toxicological effects. Sci. World J, 2012.

Kim, G.B., Maruya, K.A., Lee, R.F., Lee, J.H., Koh, C.H., Tanabe, S., 1999. Distribution and sources of polycyclic aromatic hydrocarbons in sediments from Kyeonggi Bay, Korea. Mar. Pollut. Bullet. 38, 7-15.

Leon, V.M., García, I., Martínez-Gómez, C., Campillo, J.A., Benedicto, J., 2014. Heterogeneous distribution of polycyclic aromatic hydrocarbons in surface sediments and red mullet along the Spanish Mediterranean coast. Mar. Pollut. Bull. 87, 352-363.

Li, B.H., Feng, C.H., Li, X., Chen, Y.X., Niu, J.F., Shen, Z.Y., 2012. Spatial distribution and source apportionment of PAHs in surficial sediments of the Yangtze estuary, China. Mar. Pollut. Bull. 64, 636–643.

Liu, Y.P., Wang, Y.H., Ye, C., Xie, B. and Yang, H., 2017. Sedimentary record of polycyclic aromatic hydrocarbons from the Shuanglong Catchment, southwest China. J. Chem, 2017.

MacDonald, D.D., Ingersoll, C.G. and Berger, T.A., 2000. Development and evaluation of consensus-based sediment quality guidelines for freshwater ecosystems. Arch. Environ. Contam. Toxicol., 39(1), pp.20-31.

Massolo, S., Bignasca, A., Sarkar, S.K., Chatterjee, M., Bhattacharya, B.D., Alam, A., 2012. Geochemical fractionation of trace elements in sediments of Hugli River (Ganges) and Sundarban wetland (West Bengal, India). Environ. Monit. Asses. 184(12), 7561-7577.

Men, B., He, M., Tan, L., Lin, C., Quan, X., 2009. Distributions of polycyclic aromatic hydrocarbons in the Daliao River estuary of Liaodong Bay, Bohai Sea (China). Mar. Pollut. Bullet. 58, 818-826.

Mukherjee, D., Mukherjee, A., Kumar, B., 2009. Chemical fractionation of metals in freshly deposited marine estuarine sediments of Sundarban ecosystem, India. Environ. Geol. 58(8), 1757-1767.

Olayinka, O.O., Adewusi, A.A., Olarenwaju, O.O. and Aladesida, A.A., 2018. Concentration of polycyclic aromatic hydrocarbons and estimated human health risk of water samples around Atlas Cove, Lagos, Nigeria. J. Health Pollut, 8(20).

Pait, A.S., Whitall, D.R., Jeffrey, C.F., Caldow, C., Mason, A.L., Lauenstein, G.G., Christensen, J.D., 2008. Chemical contamination in southwest Puerto Rico: an assessment of organic contaminants in near shore sediments. Mar. Pollut. Bull. 56, 580-587.

Potin, O., Veignie, E. and Rafin, C., 2004. Biodegradation of polycyclic aromatic hydrocarbons (PAHs) by Cladosporium sphaerospermum isolated from an aged PAH contaminated soil. FEMS Microbiol. Ecol, 51(1), pp.71-78.

Pozo, K., Perra, G., Menchi, V., Urrutia, R., Parra, O., Rudolph, A., Focardi, S., 2011. Levels and spatial distribution of polycyclic aromatic hydrocarbons (PAHs) in sediments from Lenga estuary, central Chile. Mar. Pollut. Bull. 62, 1572–1576.

Radojevic, M., Bashkin, V. and Bashkin, V.N., 1999. Practical environmental analysis. Royal society of chemistry.

Raza, M., Zakaria, M.P., Hashim, N.R., Yim, U.H., Kannan, N. and Ha, SY, 2013. Composition and source identification of polycyclic aromatic hydrocarbons in mangrove sediments of Peninsular Malaysia: indication of anthropogenic input. Environ. Earth Sci., 70(6), pp.2425-2436.

Ross, J.R., Oros, D.R., 2004. Polycyclic aromatic hydrocarbons in the San Francisco Estuary water column: sources, spatial distributions, and temporal trends (1993-2001). Chemosphere. 57, 909-920.

Roy, S., Hens, D., Biswas, D., Biswas, D., Kumar, R., 2002. Survey of petroleum-degrading bacteria in coastal waters of Sunderban Biosphere Reserve. World J. Microbiol. Biotechnol. 18(6), 575-581.

Samanta, S., Dalai, T.K., 2018. Massive production of heavy metals in the Ganga (Hooghly) River estuary, India: Global importance of solute-particle interaction and enhanced metal fluxes to the oceans. Geochim. Cosmochim. Ac. 228, 243-258.

Sany, S.B.T., Hashim, R., Salleh, A., Rezayi, M., Mehdinia, A., Safari, O., 2014. Polycyclic aromatic hydrocarbons in coastal sediment of Klang Strait, Malaysia: distribution pattern, risk assessment and sources. PLoS One. 9, 1-14.

Sarkar, S.K., 2016. Polycyclic aromatic hydrocarbons (PAHs) in sediment cores from Sundarban wetland. In: Sarkar, S.K. (Ed.), Marine Organic Micropollutants. Springer International Publishing, Switzerland, pp. 49-68.

Sarkar, S.K., Binelli, A., Chatterjee, M., Bhattacharya, B.D., Parolini, M., Riva, C. and Jonathan, M.P., 2012. Distribution and ecosystem risk assessment of polycyclic aromatic hydrocarbons (PAHs) in core sediments of Sundarban mangrove wetland, India. Polycycl. Aromat. Compd, 32(1), pp.1-26.

Sarkar, S.K., Binelli, A., Riva, C., Parolini, M., Chatterjee, M., Bhattacharya, A.K., Bhattacharya, B.D., Satpathy, K.K., 2008. Organochlorine pesticide residues in sediment cores of Sunderban wetland, northeastern part of Bay of Bengal, India, and their ecotoxicological significance. Arch. Environ. Contam Toxicol. 55(3), 358-371.

Sojinu, O.S., Wang, J.Z., Sonibare, O.O. and Zeng, E.Y., 2010. Polycyclic aromatic hydrocarbons in sediments and soils from oil exploration areas of the Niger Delta, Nigeria. J. Hazard. Mater., 174(1-3), pp.641-647.

Sun, J.H., Wang, G.L., Chai, Y., Zhang, G., Li, J. and Feng, J., 2009. Distribution of polycyclic aromatic hydrocarbons (PAHs) in Henan reach of the Yellow River, Middle China. Ecotoxicol. Environ. Saf, 72(5), pp.1614-1624.

UKMA: The UK Marine Special Areas Conservation Project, www.ukmarinesac.org.uk/index, 2001

United States Environmental Protection Agency (US EPA), 1984. Method 610 Polynuclear Aromatic Hydrocarbons. Federal Register, Rules and Regulations, Washington, DC. Vol. 49, No.112,

United States Environmental Protection Agency 1996a. Method 3540C: Soxhlet extraction, Washington, DC.

United States Environmental Protection Agency, 1986. Method 8100 Polynuclear Aromatic Hydrocarbons

United States Environmental Protection Agency, 1996b. EPA-Method 3630C, Silica gel clean-up.

United States Environmental Protection Agency, 1996c. Test Method 3510c: Separatory funnel liquid-liquid extraction.

United States Environmental Protection Agency, 2004. Method 8000B, Determinative chromatographic separations.

Walkley, A. and Black, I.A., 1934. An examination of the Degtjareff method for determining soil organic matter, and a proposed modification of the chromic acid titration method. Soil Sci., 37(1), pp.29-38.

Wang, Y., Wang, J., Mu, J., Wang, Z., Cong, Y., Yao, Z., Lin, Z., 2016. Aquatic predicted no effect concentrations of 16 polycyclic aromatic hydrocarbons and their ecological risks in surface seawater of Liaodong Bay, China. Environ. Toxicol. Chem. 35, 1587-1593.

Yan, N., Marschner, P., Cao, W., Zuo, C., Qin, W., 2015. Influence of salinity and water content on soil microorganisms. Int Soil Water Conser. Res. 3, 316-323. https:// doi.org/10.1016/j.iswcr.2015.11.003.

Zuloaga, O., Prieto, A., Ahmed, K., Sarkar, S.K., Bhattacharya, A., Chatterjee, M., Bhattacharya, B.D. and Satpathy, K.K., 2013. Distribution of polycyclic aromatic hydrocarbons in recent sediments of Sundarban mangrove wetland of India and Bangladesh: a comparative approach. Environ. Earth Sci, 68(2), pp.355-367.

Zuloaga, O., Prieto, A., Usobiaga, A., Sarkar, S.K., Chatterjee, M., Bhattacharya, B.D., Bhattacharya, A., Alam, M.A., Satpathy, K.K., 2009. Polycyclic aromatic hydrocarbons in intertidal marine bivalves of Sunderban mangrove wetland, India: an approach to bioindicator species. Water Air Soil Poll. 201, 305-318

CHAPTER 3

HETEROTROPHIC MIXED BIOFILM-BASED DEGRADATION OF PAHS IN A PATENTED BIOFILM-PROMOTING CULTURE VESSEL

3.1. Introduction

Bioremediation involves the complete breakdown of organic contaminants to their natural elements, such as carbon, hydrogen, nitrogen, and oxygen, then transforming these into other nontoxic chemical compounds (Othman et al., 2011). The knowledge of bioremediation has been known for several decades; however, its effectiveness gained public attention following a major oil spill in 1989 by Exxon Oil on the shorelines of Prince William Sound, Alaska (Mitra and Mukhopadhyay 2016). An era of development in bioremediation started, followed by this incident making the field one of the largest growing sectors in the waste management industry.

Some microbes are extremely efficient in breaking down natural organic compounds and organic pollutants via several complex and diverse metabolic pathways. Although the efficiency of bioremediation by microorganisms hinges on several conditions or factors, the enzymatic activities of microbes are the key factor involved in the transformation and degradation of organic pollutants into less toxic or harmless metabolic products (Das and Dash, 2014). Microbial species collected from several PAH-polluted sites are observed to becapable for PAH degradation. However, pure cultures of microbes cannot degrade different classes of PAHs with complex structures (Gieg et al., 2014). Periodic studies show that certain microorganism lacks the specific genes required for the enzyme synthesis involved in the complete mineralization of PAHs, which led the researchers to focus on developing microbial consortia for the complete degradation of pollutants. It is anticipated that different microbial species found in biofilm consortia, each with diverse catabolic pathways, are capable of degrading several pollutants synergistically (Horemans et al., 2013 Zuloaga et al., 2009), and some of them are capable of removing PAHs collectively or individually (Ghosal et al., 2016).

The term "biofilm" represents the surface-associated microbial populations in which cells are embedded in extracellular polymeric substances produced by themselves.. Biofilms demonstrate enhanced tolerance to physical, chemical, and biological stresses and are thus

resilient to various environmental stresses (Shukla et al. 2014). We propose using an entire microbial community rather than a single strain, which allows for the simultaneous biodegradation of a wide range of PAHs by a diverse array of prokaryotes operating together. (MATBIOPOL 2003). Biofilm-mediated degradation of PAHs is more efficient than singlet microbial degradation since they have a high tolerance toward hazardous pollutants. To date, few investigations have focused on applying biofilms for PAH bioremediation, and more research is required to utilize the capability of microbial biofilm communities to metabolize PAHs in suboptimal conditions (Shukla et al., 2014). It is anticipated that different microbial species found in the biofilm consortia, each with diverse catabolic pathways, can synergistically degrade several pollutants (Horemans et al., 2013).

In order to effectively manage and maintain pristine coastal environments like estuaries, deltas, and sandy beaches, it is crucial to be able to harness naturally occurring microbial communities, such as those in the biofilms to degrade pollutants like (MATBIOPOL 2003). For example, Mitra et al. (2013) demonstrated the Fla biotransformation potential of *Cunninghamella elegans*, isolated from the estuarine mud, in North Carolina in a designed enhanced surface area conico-cylindrical flask and niche mimicking bioreactor. Therefore, it is important to study biofilms developed at the Sundarbans sediment surfaces and how these interactions can be utilized for the bioremediation of PAH-contaminated sediments.

3.2. Materials and methods

3.2.1. Biofilm sampling

Biofilms were collected from the widespread microbial mats present on the surface of the sediments, which are exposed during low tide (Figure 13) and were scrapped from the five different sampling regions (Figure 8.) mentioned in section 2.2.1.

Figure 13: Biofilms scraped off from the sediment surfaces using trowels. Black arrows indicate the underlying soil exposed after the removal of the biofilms

3.2.2. In-vitro heterotrophic biofilm culturing

Twenty five biofilm samples collected were transferred to an Erlenmeyer flask consisting of 200 ml of a modified sterile mixed media with glucose yeast maltose (GYM) for the enrichment of all the heterotrophic bacteria, Czapek Dox (CD) broth for the enrichment of fungi, Bold's basal media (BBM) fortified with vitamins for preferential growth of eukaryotic microalgae, and Artificial seawater medium (ASN III) as well as blue-green algal media (BG 11) for enriched growth of phototrophic microorganisms (GYM:BBM:CD: ASN III: BG11=1:1:1:1:1) (Zammit et al., 2011) (Figure 14). Biofilms were cultivated in fluorescent irradiance (50 µmol photons/m^2/s) with 14:10 hrs light: dark photoperiod at 25±1 °C.

Figure 14: Heterotrophic biofilm cultured in an Erlenmeyer flask with modified sterile mixed media (GYM: BBM: CD: ASN III: BG11=1:1:1:1:1:1)

3.2.3. Cultivation of heterotrophic biofilms in the patented Enhanced Surface Area ES CCF

Six heterotrophic, stably-growing, robust, and well-formed heterotrophic biofilms were selected for the removal of the PAHs, each representing the different geographical locations: Pg (Purba Gurguria), Mt (Maipit), Pp1, and Pp2 (Patharpratima), Nk (Namkhana) and Kk (Kakdwip). These selected biofilms were cultured in two sets of the patented ES-CCF possessing hydrophilic glass (Set 1) and hydrophobic polymethyl methacrylate (PMMA) surfaces (Set 2) (US patent 8,945,917 B2, Sarkar et al. 2015, Figure 15.).

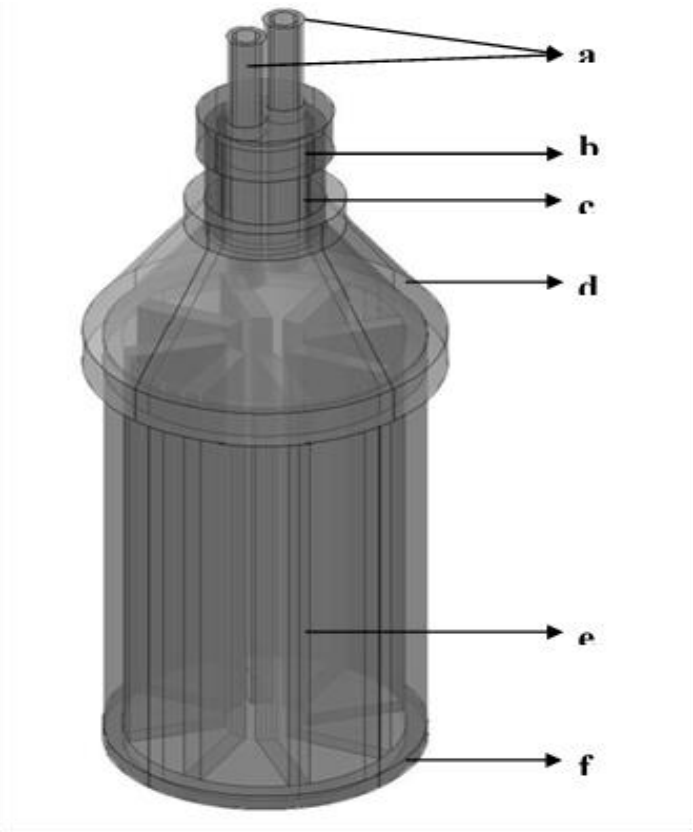

Figure 15: The enhanced surface area conico cylindrical flask (ES-CCF, US patent 8,945,917 B2, Sarkar et al. 2015) comprising of **(a)** ports for entry and exit of air, **(b)** screw cap, **(c)** neck, **(d)** funnel portion, **(e)** inner arrangement consisting of eight equally spaced rectangular strips mounted on a circular disk (surface area of the inner arrangement is 706.4 cm^2) and **(f)** lower cylindrical portion

About 200 mg of heterotrophic biofilm was inoculated into the sterile modified mixed medium (section 3.2.2). Once growth was established, PAHs were spiked to both sets of ES-CCF with varying concentrations, such as 5 ppm for Pg and Mt, 15 ppm for Pp1, 10 ppm for Pp2, and Nk and 25ppm for Kk. A control set of biofilms were cultured in the ES-CCFs without the spiked PAHs. Sterile media without PAHs and flasks containing sterile media spiked with 5, 10, 15, and 25 ppm of PAHs alone were also incubated. The PAH removal in the liquid medium was determined (n=2) and represented as percent residual PAH. The PAH removal efficiency (%) was measured using the formula, $R = (C_i - C_f) / C_i \times 100\%$

R represents the removal efficiency (%), C_i is the initial, and C_f is the final PAH concentration.

3.2.4. PAH extraction from the liquid media

The PAHs were extracted from the media after 30 days of incubation. The extraction of PAH was done using the liquid-liquid extraction method prescribed by US EPA (1996), as described in sections 2.2.3, 2.2.5, and 2.2.6.

3.2.5. Estimation of PAH present in biofilms

After 30 days of incubation, biofilms were collected and freeze-dried using the lyophilization technique (Eyela FDU-1200, Tokyo Rikakikai Co. Ltd, Japan). PAH extraction was carried out using the method described by Froehner et al. (2012). Extraction by ultrasound sonication was carried out using the solvents DCM: methanol (2:1) followed by twice the volume of DCM. Extracts were pooled, concentrated to 2 ml, and then subjected to silica gel clean-up and GC analysis as described previously (sections 2.2.5 and 2.2.6).

3.2.6. Metagenomic analysis of biofilms showing effective removal of PAHs

Metagenomic DNA from the selected heterotrophic biofilms was extracted in triplicate using Nucleospin Soil Kit (TaKaRa Bio Ltd., Japan). The isolated metagenomic DNA was quantified using Thermo Scientific ND-2000 UV-VIS Spectrophotometer. Variable region V3-V4 of 16S rRNA bacterial gene was amplified using 16S rRNA forward (5'-GCCTACGGNGGCWGCAG–3') primer and 16S rRNA reverse (5'–ACTACHVGGGTATCTAATCC-3') primer. In parallel, amplification of the fungal genome was carried out using Intergenic Transcribed Spacer (ITS) forward (5'-GCATCGATGAAGAACGCAGC-3') and ITS reverse (5'-TCCTCCGCTTATTGATATGC-3') primers. Three microliters PCR amplified solution was resolved on 1.2% agarose gel for 60 minutes at 120 V in Tris /Borate/EDTA (TBE) buffer. Using Nextera XT Index Kit (Illumina Inc., USA), amplicon libraries were developed following the standard 16S Metagenomic Sequencing Library preparation method (Part # 15044223 Rev. B). Amplicons were purified and quantified by molecular exclusion applying AMPure XP beads (Beckman

Coulter, USA) and Qubit Fluorometer (Thermo Fischer Scientific, USA). The Illumina sequencing was performed on MiSeq using 2×300 bp chemistry (~100,000 read per library) after analyzing with 4200 Tape Station System (Agilent Technologies, USA) using D1000 Screen tape.

The Quantitative Insights into Microbial Ecology (QIIME) bioinformatics pipeline (Caporaso et al., 2010) was used for the Bacterial and fungal sequence analysis. All the chimeric sequences were removed using Trimmomaticv.0.38 representative sequences with ≥3% dissimilarity were clustered into operational taxonomic units (OTUs) using UCLUST (Edgar, 2010) and classified by a naive Bayesian RDP classifier (Wang et al., 2007). Greengenes database v.13_8 (16S/Archaea database; De Santis, 2006) and UNITE database v.7.2 (ITS fungal database) following Nilsson et al. (2018) were used for identifying the OTUs

3.2.7. Statistical analyses

Analysis of variance (ANOVA), a two-tailed Student *t*-test, and the coefficient of variation were performed using SPSS software (version 16). The statistical significance of the data was verified at the significance level of $P \leq 0.05$.

3.3. Results and discussion

3.3.1. PAH removal efficiency of heterotrophic biofilms

Six efficiently growing heterotrophic biofilms were cultivated in hydrophilic glass flasks (Glass-ES-CCF) and hydrophobic PMMA flasks (PMMA-ES-CCF) (Figure 16). Concentrations of spiked PAHs in the media correspond to the total PAHs observed in their respective geographical sampling locations. Our result did not show any significant differences in the mean residual PAHs between the PAH spiked media cultured with heterotrophic biofilms isolated from different geographical locations (Table 9 and Figure 17), and also no significant

difference in the mean residual PAHs from the liquid media between hydrophobic and hydrophilic ES-CCFs of each sample (P≤0.5).

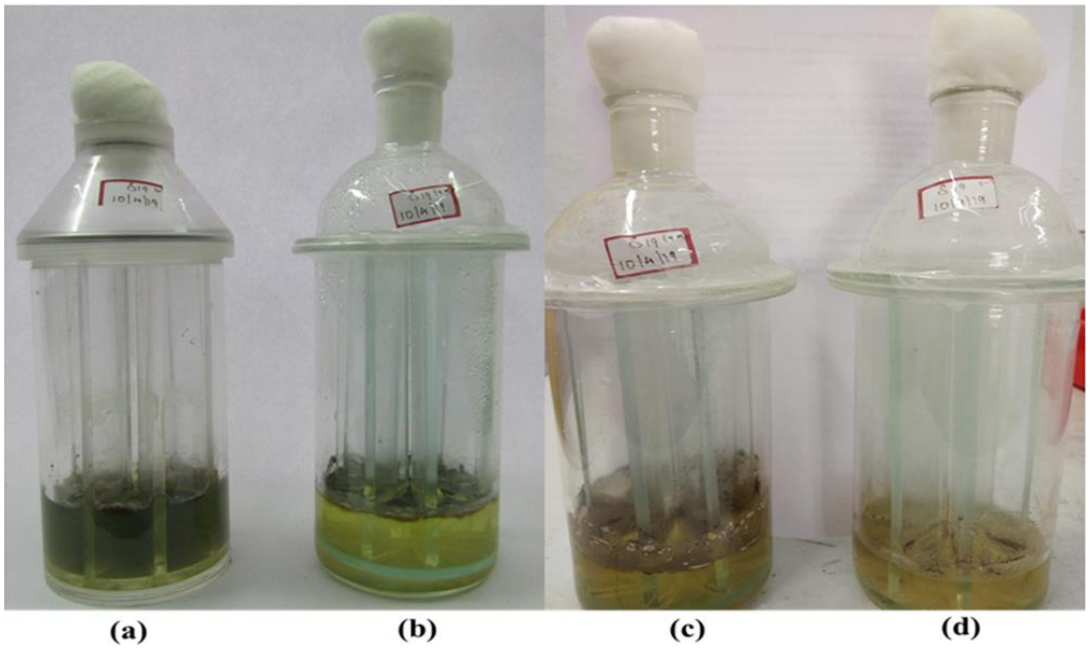

Figure 16: Microbial biofilm cultured with (a) hydrophobic PMMA surface enriched with PAHs), (b) in hydrophilic glass surface ES-CCF enriched with PAHs, (c) biofilm formation in glass ES-CCF without PAH, (d) biofilm formation in glass ES-CCF without PAH after 30 days of incubation.

Also, we could not observe any significant differences (P≤0.5) between all 6 sample media. Differences in the sequestration of certain PAHs such as Ace, Ant, B(b)F, B(a)P, and B(ghi)P were observed when cultured in flasks with hydrophobic and hydrophilic surfaces.. When compared to the hydrophilic surface flask, the hydrophobic PMMA flask showed better Ace (Kk biofilm) and Ant (Mt biofilm) sequestration.. Compared to Pg biofilm cultured in glass-ES-CCF, Pg biofilm in PMMA-ES-CCF showed a greater extent of B(b)F sequestration, in the case of Pp1 biofilms glass -ES-CCF has higher B(b)F removal potential in comparison with PMMA-ES-CCF

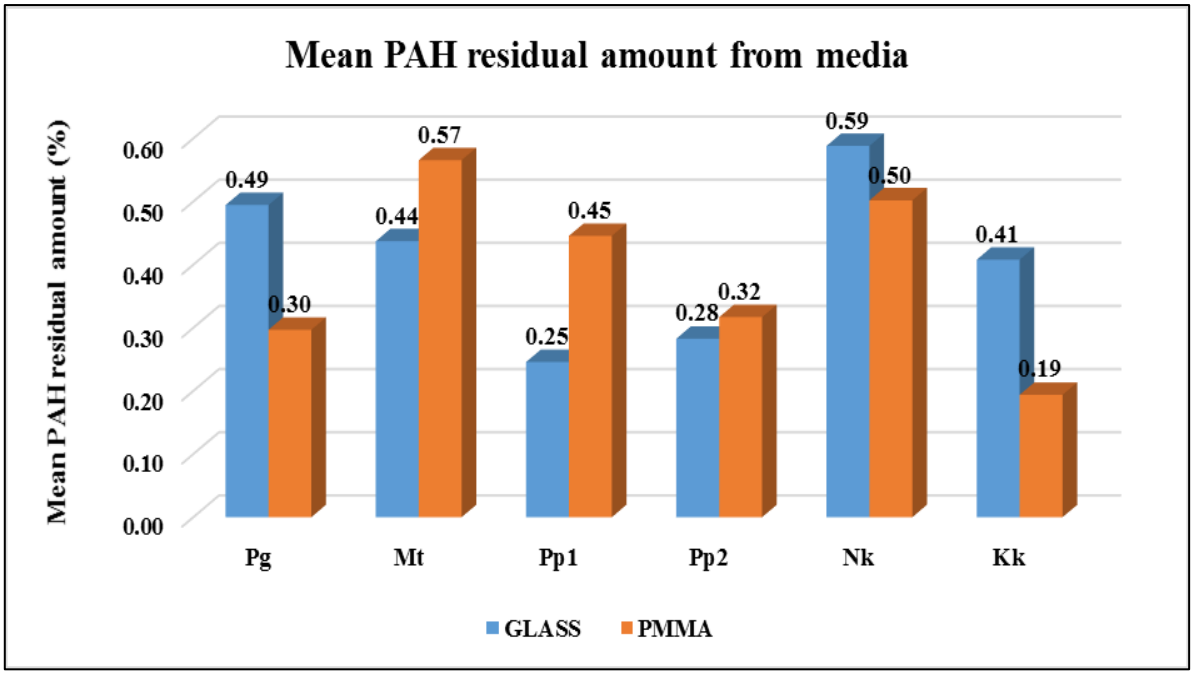

Figure 17: Mean residual amounts (percentage) of 16 priority spiked PAHs from the liquid media in glass and PMMA ES-CCF after incubation.

Pg biofilm was observed to be more prominent for the sequestration of B(ghi)P in hydrophobic ES-CCF, whereas the extent of sequestration of the same PAH by Mt, Pp1 Pp2, and Nk biofilms was greater in glass-ES-CCFcompared to PMMA-ES-CCF. Compared to the hydrophobic vessel, B(a)P was eliminated efficaciously in the hydrophilic flask with Pg biofilms. Experiments conducted using the quality control standard showed a loss of 30% PAH during the incubation and extraction procedure. In all the media, 97-100% removal efficiency of individual PAHs was observed.

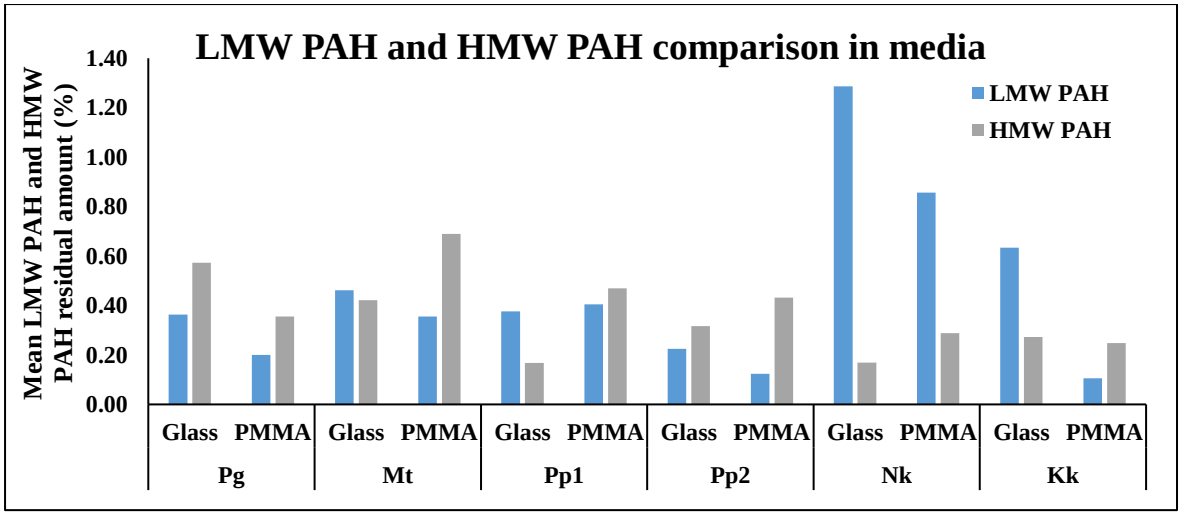

Figure 18: Comparison of LMW PAH and HMW PAH recovered from the media in glass and PMMA ES-CCF after incubation.

A comparison of LMW PAH and HMW PAH residual amounts in each liquid media collected from glass and PMMA ES-CCF after incubation can be observed in Figure 18. Mean LMW PAH and HMW PAH showed differences in glass and PMMA ES-CCF within and between the samples. In Pg media, HMW PAH was higher than LMW PAHs in both glass and PMMA ES-CCFs. Glass CCF showed higher concentrations of both LMW PAHs and HMW PAHs compared with the PMMA ES-CCF. Mt and Pp1 media showed more LMW PAH than HMW PAH in the glass CCF, whereas PMMA ES-CCF showed higher concentrations of HMW PAHs. Higher concentrations of HMW PAHs were observed in glass and PMMA CCF compared to LMW PAHs in the case of Pp2 media, whereas Nk showed higher concentrations of LMW PAHS in glass as well PMMA ES-CCF. The concentration of HMW PAHs and LMW PAHs in Kk media was similar to the Mt and Pp1 samples.

Table 9: Residual amounts (as a percentage) of 16 priority spiked PAHs from the liquid media after treatment with microbial biofilms in glass and PMMA ES-CCF after 30 days of incubation. Bold letters indicates the residual amounts that are at least double each other (PMMA ES-CCF versus glass ES-CCF or vice versa) are shown in. Values are the mean of two measurement, with the mean absolute deviations were ranging from 0.01-4.94. The coefficient of variation of duplicate data was 3.86 (n=192), following Hyslop and White (2009) and Jones and Payne (1997)

	Pg		**Mt**		**Pp1**		**Pp2**		**Nk**		**Kk**	
PAHs	**Glass**	**PMMA**	**Glass**	**PMMA**	**Glass**	**PMMA**	**Glass**	**PMMA**	**Glass**	**PMMA**	**Glass**	**PMMA**
Nap	0.14	0.12	0.25	0.13	0.00	0.11	0.20	0.22	0.13	0.05	0.10	0.15
Acy	0.31	0.42	0.81	0.94	0.04	0.05	0.00	0.04	0.17	0.07	0.05	0.03
Ace	0.11	0.06	0.07	0.13	1.83	1.76	0.10	0.00	6.66	4.52	**3.38**	**0.21**
Flu	0.23	0.13	0.20	0.19	0.07	0.09	0.17	0.07	0.07	0.08	0.04	0.03
Phe	0.60	0.09	0.16	0.15	0.23	0.28	0.44	0.19	0.17	0.32	0.15	0.14
Ant	0.79	0.38	**1.28**	**0.59**	0.09	0.14	0.44	0.22	0.52	0.10	0.08	0.07
Fla	0.09	0.08	0.14	0.15	0.07	0.10	0.05	0.07	0.04	0.10	0.04	0.00
Pyr	0.00	0.00	0.28	0.37	0.00	0.00	0.11	0.00	0.00	0.00	0.02	0.05
B(a)A	0.37	0.51	0.47	0.44	0.00	0.00	0.12	0.19	0.26	0.22	0.06	0.02
Chr	0.00	0.00	0.00	0.00	0.00	0.00	0.00	0.00	0.04	0.00	0.00	0.00
B(b)F	**1.27**	**0.27**	0.31	0.24	**0.30**	**2.57**	1.33	0.09	0.18	0.08	1.54	1.49
B(k)F	0.00	0.00	0.00	0.00	0.00	0.00	0.08	0.00	0.00	0.00	0.00	0.00
B(a)P	**0.66**	**1.57**	1.40	1.47	0.34	0.45	0.60	0.75	0.61	0.49	0.18	0.14
Ind	0.23	0.00	0.00	0.00	0.00	0.00	0.16	0.10	0.00	0.00	0.03	0.02
D(a,h)A	0.15	0.00	0.00	0.00	0.00	0.00	0.00	0.00	0.00	0.00	0.00	0.04
B(ghi)P	**2.96**	**1.12**	**1.61**	**4.23**	**0.97**	**1.58**	**0.72**	**3.12**	**0.56**	**1.99**	0.86	0.72
Mean PAH residual amounts	0.49	0.30	0.44	0.57	0.25	0.45	0.28	0.32	0.59	0.50	0.41	0.19

The mean residual amounts of PAHs obtained from heterotrophic biofilm biomass ranged between 0-106 percent (Table 10 and Figure 19). Unlike the residual amounts in the liquid medium, the mean residual amounts of PAHs obtained from biofilm biomass showed a greater significant difference at $P \leq 0.05$. In heterotrophic biofilms, the order of the mean residual amounts of 16 PAHs was Pp1<Kk<Nk<Pp2<Mt<Pg. Compared to the removal achieved in the hydrophilic glass-ES-CCF, hydrophobic PMMA-ES-CCF with Mt biofilm showed higher PAH sequestration, and Mt biofilms showed a lower residual amount of each PAHs in hydrophobic PMMA ES CCF compared to the PAH sequestrations in the glass ES CCF. All the other biofilms, such as Pg, Pp1, Pp2, Nk, and Kk, showed consistent variation in PAH sequestration between glass and PMMA –ES-CCFs (Table 10).

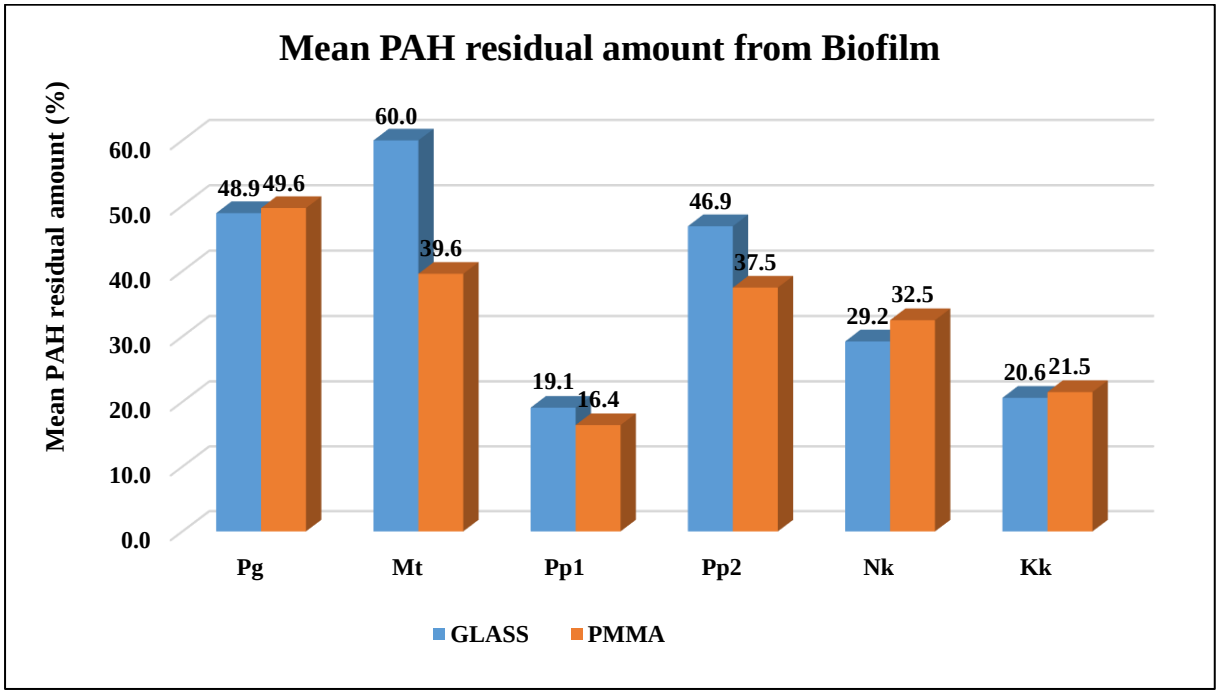

Figure 19: Mean residual amounts (percentage) of 16 priority spiked PAHs extracted from heterotrophic biofilm biomass cultured in glass and PMMA ES-CCF after 30 days of incubation.

LMW PAH and HMW PAH comparative study has been conducted in the heterotrophic biofilm biomass cultured in hydrophobic and hydrophilic ES-CCF vessels after incubation with 16 priority spiked PAHs similar to the media (Figure 20**)**. Pg biofilm showed a high concentration of HMW PAHs in both glass and PMMA ES-CCF than LMW PAHs, whereas Mt biofilms showed higher LMW PAHs in glass CCF and lower LMW PAHs in PMMA ES-CCF. The concentration of HMW PAHs in Pp1, Pp2, and Nk biofilms was similar to the Pg biofilms. Higher LMW PAHs were observed in glass and PMMA ES-CCF than HMW PAHs in the case of Kk biofilms.

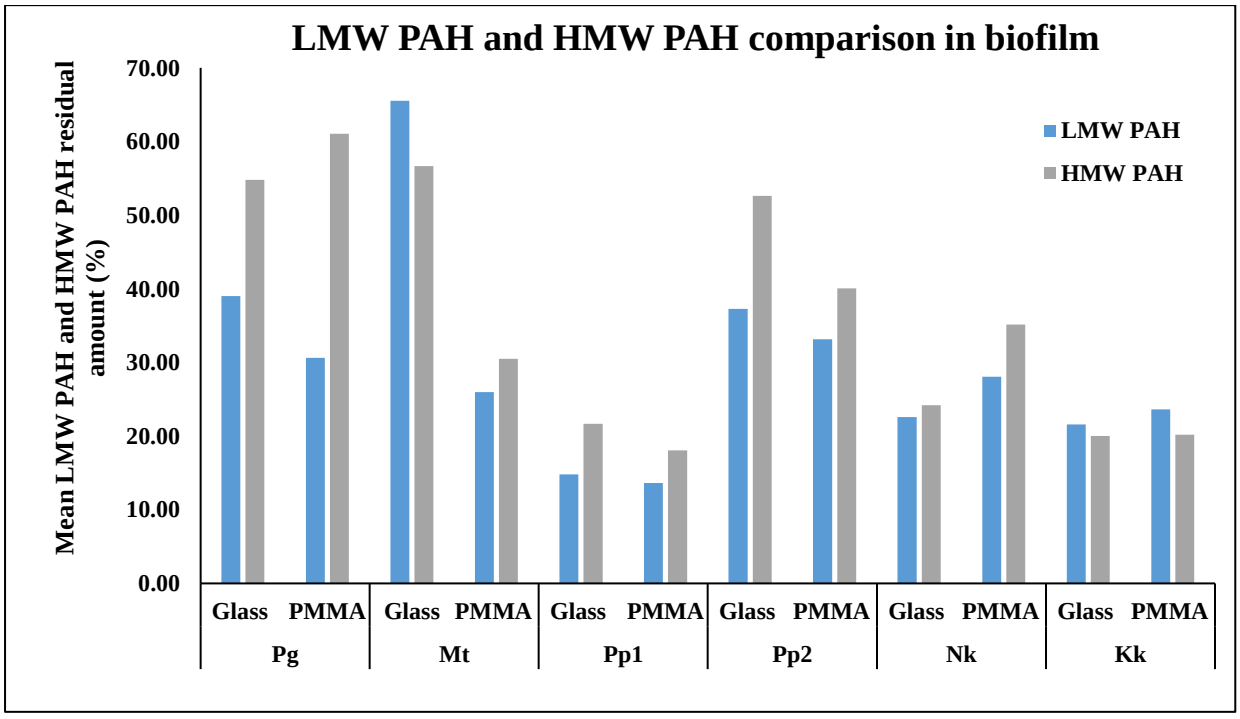

Figure 20: Comparison of LMW PAH and HMW PAH recovered from the biofilm in glass and PMMA ES-CCF after incubation.

Table 10: Residual amounts (as a percentage) of spiked 16 priority PAHs from biofilm biomass cultured in glass and PMMA flasks after 30 days incubation. Bold letters indicates the residual amounts that are at least double each other (PMMA ES-CCF versus glass ES-CCF or vice versa) are shown in. Values are the mean of two measurement, with the mean absolute deviations were ranging from 0.01-4.58. The coefficient of variation of duplicate data was 8.70 (n=192), following Hyslop and White (2009) and Jones and Payne (1997).

PAHs	Biofilm Pg		Biofilm Mt		Biofilm Pp1		Biofilm Pp2		Biofilm Nk		Biofilm Kk	
	Glass	PMMA	Glass	PMMA	Glass	PMMA	Glass	PMMA	Glass	PMMA	Glass	PMMA
Nap	64.1	50.7	**78.5**	**30.9**	10.8	9.1	34.8	47.3	17.6	33.3	7.9	9.7
Acy	43.8	28.1	**62.3**	**18.9**	10.8	6.7	21.7	41.1	**14.9**	**31.1**	12.7	21.4
Ace	**12.5**	**27.9**	79.6	43.2	**17.8**	**36.5**	**62.6**	**28.1**	63.9	42.4	72.7	73.6
Flu	20.7	18.3	**29.2**	**9.7**	8.0	5.6	7.0	6.9	9.4	17.3	5.7	10.1
Phe	**18.1**	**9.2**	**37.7**	**15.5**	16.0	13.9	27.2	35.1	14.9	9.0	9.2	9.0
Ant	74.9	49.5	**106**	**37.8**	**25.6**	**10.1**	**70.4**	**40.4**	**14.8**	**35.4**	21.2	17.9
Fla	**26.1**	**76.7**	32.7	27.5	**23.1**	**11.1**	34.6	40.1	17.1	29.8	**5.7**	**18.6**
Pyr	**58.9**	**12.7**	29.2	28.3	6.4	0.0	**55.1**	**20.5**	14.4	24.2	**4.0**	**13.5**
B(a)A	99.9	94.5	**57.3**	**27.0**	**27.1**	**12.1**	58.9	39.0	**21.0**	**59.4**	26.4	26.0
Chr	80.0	56.5	**53.4**	**6.3**	12.1	0.0	8.9	9.6	18.0	16.6	14.1	12.1
B(b)F	66.8	89.8	66.7	56.9	**56.5**	**22.7**	**52.7**	**22.5**	**15.9**	**33.1**	23.6	14.0
B(k)F	**0.0**	**21.9**	**49.3**	**0.0**	0.0	6.9	36.3	46.6	0.0	0.0	0.0	0.0
B(a)P	58.0	56.3	63.8	44.5	**6.4**	**32.2**	75.1	53.6	**81.5**	**18.2**	**5.1**	**20.2**
Ind	88.9	59.9	85.4	66.3	**36.2**	**9.0**	74.7	59.0	**36.3**	**74.4**	26.5	32.4
D(a,h)A	**11.7**	**54.4**	**49.2**	**25.7**	**27.7**	**7.1**	57.1	56.8	**15.6**	**43.8**	31.6	37.7
B(ghi)P	57.4	87.9	**79.6**	**22.6**	**21.4**	**79.6**	72.7	52.9	**22.4**	**52.0**	**63.2**	**27.6**
Mean PAH residual amounts	48.9	49.6	60.0	39.6	19.1	16.4	46.9	37.5	29.2	32.5	20.6	21.5

Irrespective of the physicochemical properties of the PAHs, compared to a biofilm cultured on a hydrophilic surface, the Mt biofilm grown on the hydrophobic PMMA surface demonstrated more efficient sequestration.. According to the previous studies conducted using ES–CCF, it can be assumed that various microbial members of the Mt biofilm with inherent hydrophobic cell surface character may have supported the better attachment and biofilm formation on the PMMA ES-CCF compared to hydrophilic surface. However, experimental validation was not within the scope of this work. For further understanding, detailed studies on the changes in the biofilm biomass, EPS content and its composition, hydrophobicity of cell surface, and gene expression are required (Mitra et al., 2013; Mitra et al., 2015).

Nearly 100% removal of all 16 priority pollutants was observed in the liquid medium. Results also suggest that some of the PAHs may have adsorbed onto the biofilm surfaces because, from Table 10, it is evident that the different microbial members of the biofilm could only remove only 40-80% of the PAHs. After initial sequestration, the microbial biofilm act as a repository for the PAHs that has not been removed while the surrounding media will remain contaminant-free (Figure 21). Further analysis is essential to validate the assumptions such as diffusion coefficients of the individual PAHs andwater/biomass OC distribution coefficients (Wicke et al., 2007), the composition of the biofilm, and the transformation of the individual PAHs such as enzymatically catalyzed inclusion of hydroxyl or carboxyl moieties by different microbial members of the biofilms and the role of external effects on the partitioning of the individual PAHs inside the biofilm (Wicke et al., 2008).

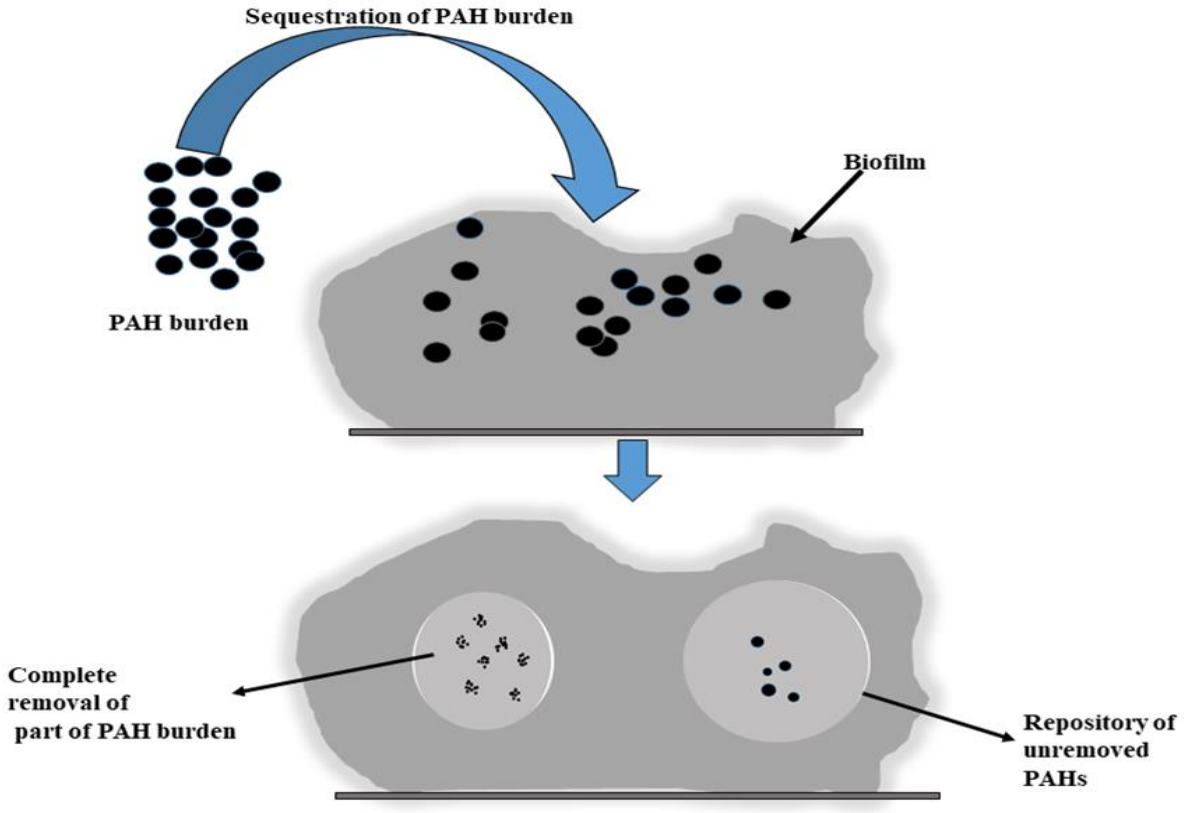

Figure 21: Fate of the PAH burden present in the media after interaction with the microbial biofilm. The biofilm biomass completely sequestered PAHs because nearly The removal rate in the liquid media was 100%. On the biofilm surface, some PAHs might have been adsorbedthe different microbial members of the biofilm then partially eliminated the PAHs. After initial sequestration, the microbial biofilm acted as a repository, storing the unremoved PAHs within its structure while the surrounding water was kept free of the contamination..

The PAH removal by the biofilms cultured in glass and PMMA-ES CCF depends on the quality and microbial composition of biofilms and the type of PAH . The hydrophobicity/hydrophilicity of the biofilm-forming surface and the hydrophobicity of biofilm cell surface regulate the quality and composition of the biofilm (Mitra et al., 2013; Mitra et al., 2015). According to Wicke et al. (2007), diffusion coefficients and the water/biomass OC distribution coefficients of Phe and Pyr were significantly dissimilar. The author (2008) also suggests that the accessibility of a specific PAH depends mainly on biofilm

water content and the hydrophilicity of PAHs. Al-Bader et al. (2013) suggest that using hydrophobic surfaces may guide the attachment of additional indigenous marine oil-utilizing bacteria. Our results agree with Al-Bader et al. (2013); from Tables 9 and 10, the differences in the removal of specific PAHs were evident.

3.3.2. PAH-sequestering microbial community composition, its abundance and diversity study

The 16S rRNA and ITS gene sequencing were performed for selected biofilms (Pp1, Nk, and Kk) which showed greater PAH removal efficiency. Figure 22 shows the specific bands which co-migrated on the agarose gels when gel electrophoresis of the amplified PCR products was performed. From 16S rRNA V3-V4 sequencing, about 120,840-145,556 high-quality reads per sample, and from ITS sequencing, 183,515-235,377 valid reads per sample were obtained. It is evident from Table 11 showing Shannon indices suggest that more diverse bacterial as well as fungal communities were present in the Kk biofilm compared to Pp1 and Nk biofilms. An ample number of species in each biofilm were unclassified, 25.82%, 47.5%, and 42.31% in Pp1, Nk, and Kk biofilms, respectively. The bacterial and fungal species richness was indicated by the rarefaction curves (Figure 23). Pp1 and Kk biofilms showed higher species richness than the Nk biofilm. The sequences are available at the NCBI Sequence Read Archive under the accession number PRJNA596375.

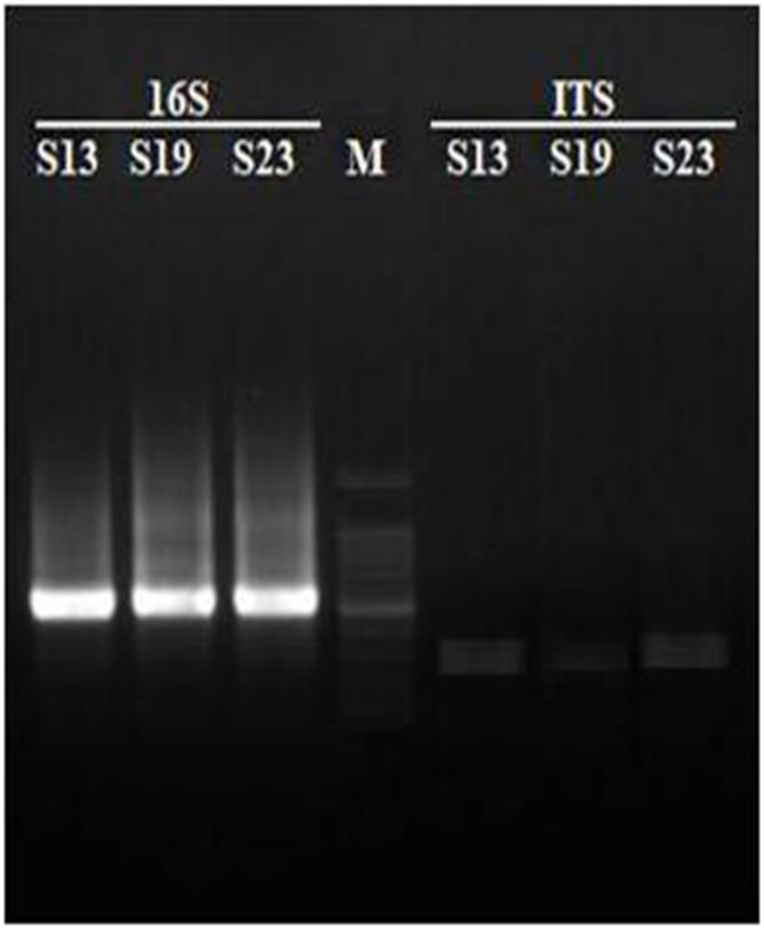

Figure 22: 1.2% agarose gel electrophoresis of the PCR products obtained after amplifying 16S rRNA and Intergenic Transcribed Spacer (ITS) genes showing specific bands that appeared to co-migrate on the gels. Lane M: DNA marker (500 bp), Lanes S13: Biofilm Pp1, Lanes S19: Biofilm Nk, and Lanes S23: Biofilm Kk.

Table 11: Alpha diversity of bacteria and fungi present in PAH-sequestering biofilms calculated using Quantitative Insights into Microbial Ecology (QIIME) bioinformatics pipeline

Biofilm	**Alpha diversity of Bacteria**		**Alpha diversity of Fungal**	
	[a] OTUs	**[b] Shannon alpha diversity**	**[a] OTUs**	**[b] Shannon alpha diversity**
Pp1	366	4.557	5	0.049
Nk	319	4.314	3	0.006
Kk	362	4.912	4	0.932

[a] OTUs: Operational Taxonomic Units, [b] Shannon: Shannon diversity index (>0, higher, more diverse)

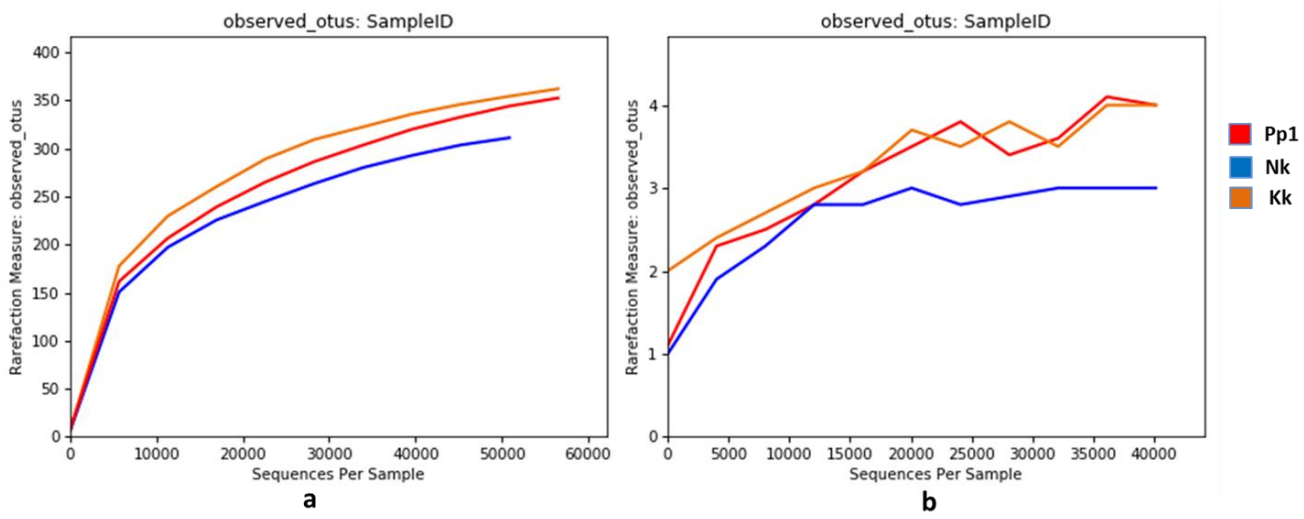

Figure 23: Rarefaction curve for estimation of (a) bacterial and (b) fungal species richness using Quantitative Insights into Microbial Ecology (QIIME) bioinformatics pipeline. The vertical axis represents the diversity of communities using the number of operational taxonomic units (OTUs). In contrast, the number of sequences considered for the diversity estimation is displayed on the horizontal axis. The rarefaction curves indicated that the Pp1 and Kk biofilms had more bacterial and fungal species diversity than the Nk biofilm..

Relative abundances of various microbial populations in PAH-sequestering biofilms of Pp1, Nk, and Kk (Table 12) showed six bacterial phyla such as *Proteobacteria* (26.3-34.1%), *Bacteroidetes* (24.3-32.9%), *Firmicutes* (19.9-38.6%), *Actinobacteria* (1.3-2.1%), *Chloroflexi* (0.8-2.3%) and *Planctomycetes* (0-15.3%) together with members of *Ascomycota* (100%) phylum of fungi (Figure 24a and Figure 24b). *Firmicutes* (38.6%) were the most abundant bacterial phylum in the Pp1 biofilm, followed by *Bacteroidetes* (32.9%), whereas, in Nk and Kk, *Proteobacteria* showed 34.1% and 31.7% dominance respectively, and followed by *Bacteroidetes* (26.2%) in Nk and *Firmicutes* (31%) in Kk biofilm. Nine PAH-sequestering groups of bacteria were detected in Pp1, Nk, and Kk biofilms, including *Sphingobacteria*

(24.1-26.2%), *Clostridium* (18.3-38.5%), *Gammaproteobacteria* (14.1-16%), *Alphaproteobacteria* (10.4-11.9%), *Betaproteobacteria* (1.8-4.5%), *Actinobacteria* (1.3-2.1%), *Bacilli* (0.1-11.8%), *Bacteroidia* (0-8.8%) and *Phycisphaerae* (0-15.3%) (Figure 25a). The most prevalent fungus class was determined to be *Saccharomycetes* (99.5% in Pp1, 100% in Nk, and 65.40% in Kk), and Kk biofilm had 34.5% of class *Sordariomycetes* along with *Saccharomycetes* (Figure 25b). The most abundant bacterial taxa in Pp1 were *Clostridium butyricum* (47%) and *Sphingobacterium multivorum* (38%), whereas Nk and Kk biofilms showed the dominance of *Sphingobacterium multivorum* (66% and 53%) (Figure 26a).

.

Table 12: Relative abundance of bacterial and fungal species in biofilms Pp1, Nk, and Kk as evidenced by 16S rRNA gene sequencing (bacterial members) and ITS gene sequencing (fungal members)

Taxonomy	Pp1 (%)	Nk (%)	Kk (%)
Bacterial			
k_Bacteria;p_Firmicutes;c_Clostridia;o_Clostridiales;f_Clostridiaceae;g_*Clostridium*;s_*butyricum*	30.1	1.9	11.8
k_Bacteria;p_Bacteroidetes;c_Sphingobacteriia;o_Sphingobacteriales;f_Sphingobacteriaceae;g_*Sphingobacterium*;s_*multivorum*	24	26.1	23.5
k_Bacteria;p_Proteobacteria;c_Gammaproteobacteria;o_Pseudomonadales;f_Pseudomonadaceae;g_*Pseudomonas*;s_*alcaligenes*	6.9	7.9	3.8
k_Bacteria;p_Firmicutes;c_Clostridia;o_Clostridiales;f_Clostridiaceae;g__;s__	5.1	13.3	2.3
k_Bacteria;p_Bacteroidetes;c_Bacteroidia;o_Bacteroidales;f_Porphyromonadaceae;g_;s_	4.7	0	0
k_Bacteria;p_Bacteroidetes;c_Bacteroidia;o_Bacteroidales;f_Porphyromonadaceae;g_*Dysgonomonas*;s__	4	0	0.1
k_Bacteria;p_Proteobacteria;c_Alphaproteobacteria;o_Caulobacterales;f_Caulobacteraceae;g_*Brevundimonas*;s_*diminuta*	2.9	3.4	5.1
k_Bacteria;p_Firmicutes;c_Clostridia;o_Clostridiales;f_Clostridiaceae;g_*Clostridium*;s_	2.7	0.7	1
k_Bacteria;p_Proteobacteria;c_Gammaproteobacteria;o_Pseudomonadales;f_Pseudomonadaceae;g_*Pseudomonas*;s_	2.6	1.9	1.8
k_Bacteria;p_Proteobacteria;c_Gammaproteobacteria;o_Pseudomonadales;f_Moraxellaceae;g_;s_	2.2	0.2	3.9
k_Bacteria;p_Proteobacteria;c_Alphaproteobacteria;o_Rhizobiales;f_;g_;s_	2.1	1.7	1.8
k_Bacteria;p_Proteobacteria;c_Betaproteobacteria;o_Burkholderiales;f_Alcaligenaceae;g_*Achromobacter*;s_	1.7	3.3	4.4
k_Bacteria;p_Proteobacteria;c_Alphaproteobacteria;o_Rhizobiales;f_Rhizobiaceae;g_;s_	1.5	1.7	1.4
k_Bacteria;p_Proteobacteria;c_Gammaproteobacteria;o_Alteromonadales;f_Alteromonadaceae;g_*Marinobacter*;s__	1.5	0	0

k__Bacteria;p__Proteobacteria;c__Alphaproteobacteria;o__Rhizobiales;f__Brucellaceae;g__*Paenochrobactrum*;s__*glaciei*	1.3	1.9	0.1
k__Bacteria;p__Proteobacteria;c__Alphaproteobacteria;o__Rhizobiales;f__Brucellaceae;g__*Ochrobactrum*;s__	0.9	1.5	0.9
k__Bacteria;p__Chloroflexi;c__Thermomicrobia;o__JG30-KF-CM45;f__;g__;s__	0.6	0.8	0.6
k__Bacteria;p__Actinobacteria;c__Actinobacteria;o__Actinomycetales;f__Micromonosporaceae;g__;s__	0.4	0.1	0.6
k__Bacteria;p__Proteobacteria;c__Gammaproteobacteria;o__Pseudomonadales;f__Pseudomonadaceae;g__;s__	0.4	0.1	0.6
k__Bacteria;p__Proteobacteria;c__Gammaproteobacteria;o__Xanthomonadales;f__Xanthomonadaceae;g__*Stenotrophomonas*;s__*geniculata*	0.3	5	1.9
k__Bacteria;p__Chloroflexi;c__Thermomicrobia;o__AKYG1722;f__;g__;s__	0.2	1.4	0.5
k__Bacteria;p__Actinobacteria;c__Actinobacteria;o__Actinomycetales;f__Nocardiaceae;g__*Rhodococcus*;s__*equi*	0.1	1.8	0
k__Bacteria;p__Firmicutes;c__Clostridia;o__Clostridiales;f__Clostridiaceae;g__*Clostridium*;s__*intestinale*	0.1	1	2.9
k__Bacteria;p__Bacteroidetes;c__Sphingobacteriia;o__Sphingobacteriales;f__Sphingobacteriaceae;g__*Pedobacter*;s__	0	0.1	0.6
k__Bacteria;p__Firmicutes;c__Bacilli;o__Bacillales;f__Bacillaceae;g__*Bacillus*;s__	0	0	4.6
k__Bacteria;p__Firmicutes;c__Bacilli;o__Bacillales;f__Sporolactobacillaceae;g__*Sporolactobacillus*;s__	0	1.3	5.4
k__Bacteria;p_Firmicutes;c_Clostridia;o__Clostridiales;f__Lachnospiraceae;g__;s_	0	0.9	0.6
k__Bacteria;p__Planctomycetes;c__Phycisphaerae;o__Phycisphaerales;f__;g__;s__	0	15.3	10.6
k__Bacteria;p__Proteobacteria;c__Gammaproteobacteria;o__Xanthomonadales;f__Xanthomonadaceae;g__*Stenotrophomonas*;s__	0	3.5	3.6
Fungal taxonomy			
k__Fungi;p__Ascomycota;c__Saccharomycetes;o__Saccharomycetales;f__Saccharomycetales_fam_Incertae_sedis;g__*Candida*;s__*Candida_tropicalis*	99.5	100	65.4
k__Fungi;p__Ascomycota;c__Sordariomycetes;o__Hypocreales;f__Clavicipitaceae;g__*Paecilomyces*;s__*Paecilomyces_fulvus*	0.5	0	34.5

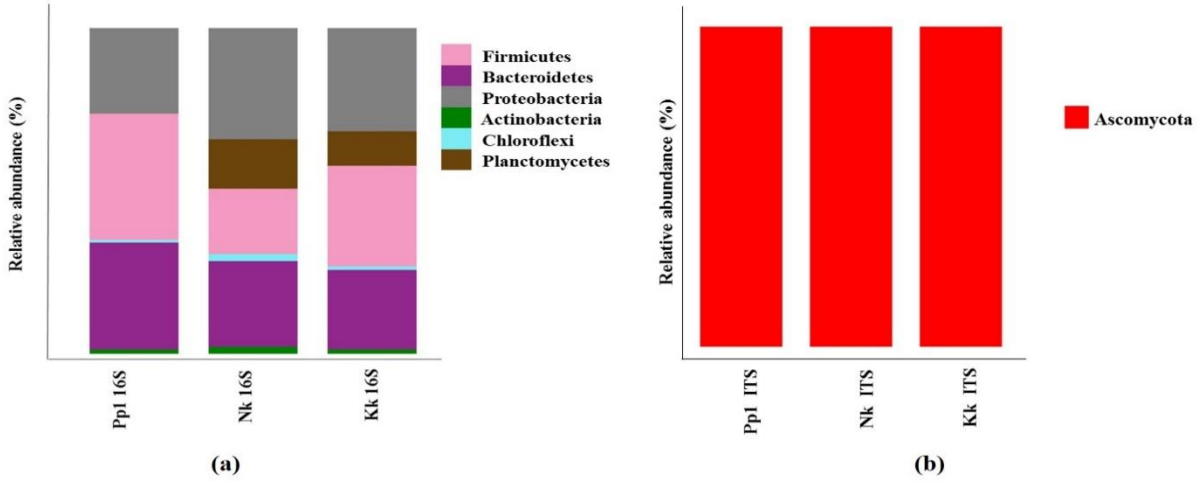

Figure 24: Relative abundance of (a) bacterial phyla that sequester PAHs was determined using 16S rRNA gene sequencing and (b) fungal phyla that sequester PAHs was determined using Intergenic Transcribed Spacer (ITS) gene sequencing in three biofilms (Pp1, Nk and Kk).

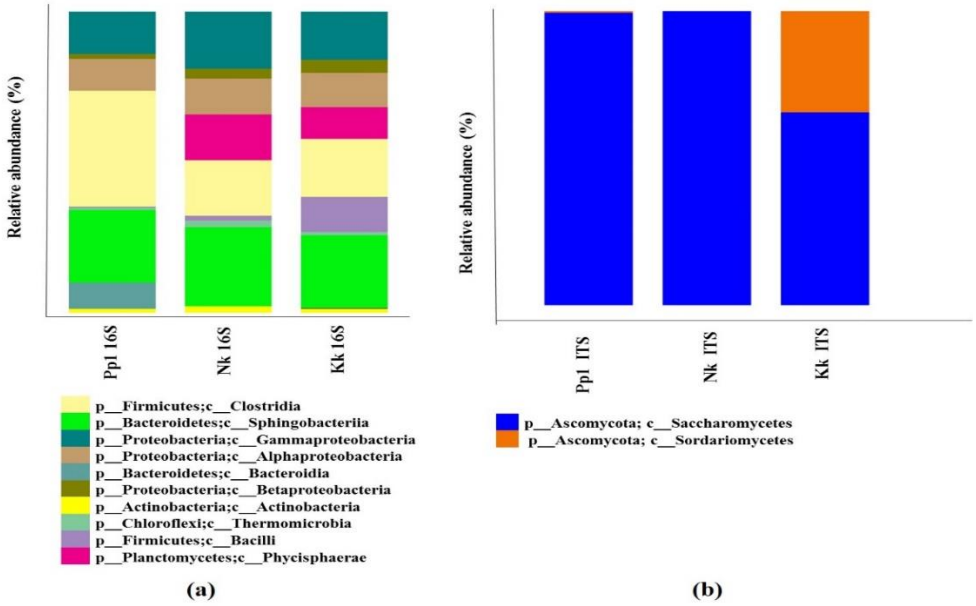

Figure 25: Relative abundance of **(a)** PAH sequestering bacteria and **(b)** PAH sequestering fungi in three biofilms (Pp1, Nk, and Kk) at the class level.

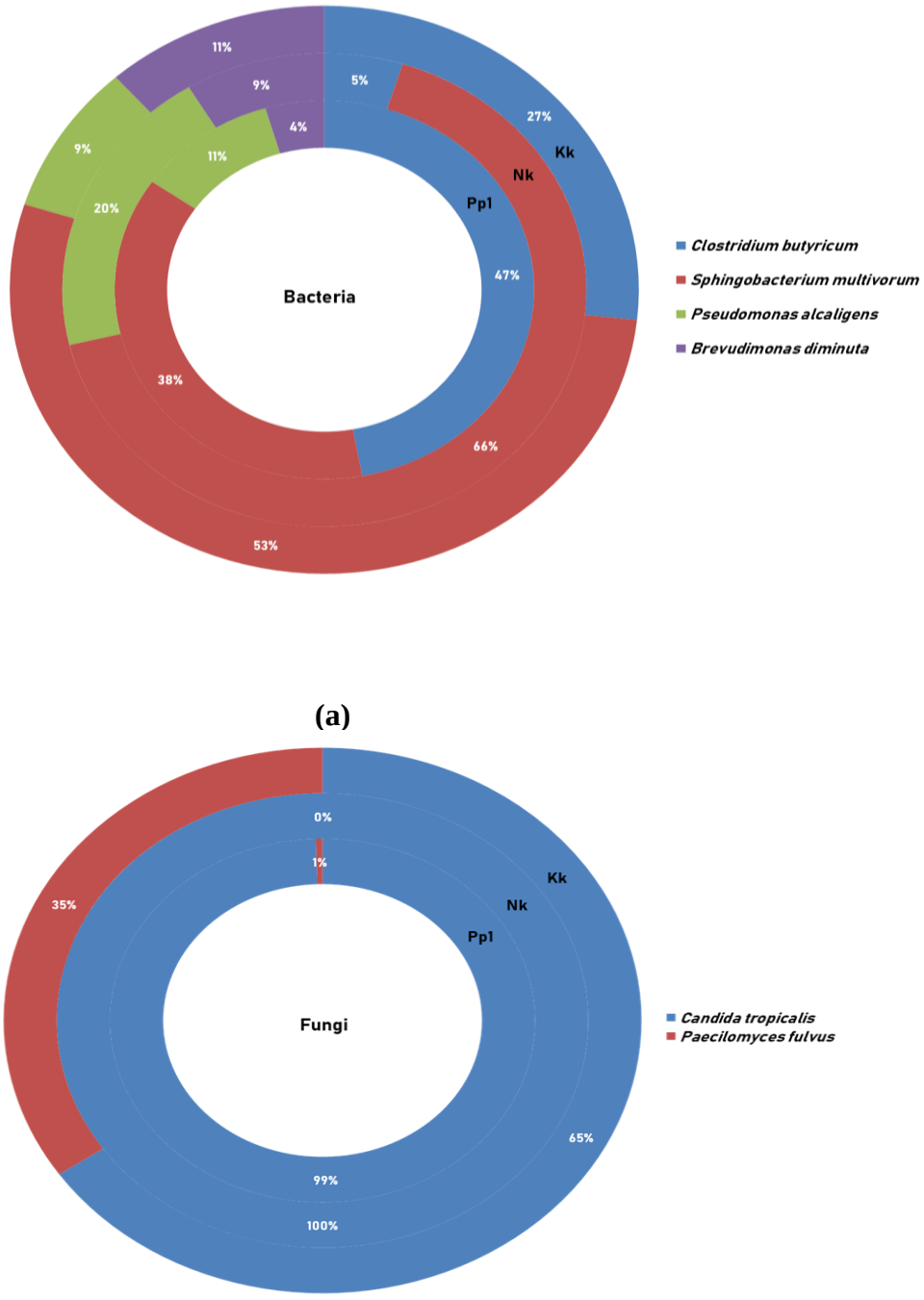

Figure 26: Relative abundances of major PAH sequestering (a) bacterial and (b) fungal communities identified through 16S rRNA gene (for bacterial) and Intergenic Transcribed Spacer or ITS gene (for fungal) in three biofilms (Pp1, Nk, and Kk).

Candida tropicalis was identified as the most abundant fungal species in all three biofilms: 99% in Pp1, 100% in Nk, and 65% in Kk and Kk biofilm also showed the presence of *Paecilomyces fulvus* (35%) (Figure 26b). Figure 27 implies that Pp1 and Nk biofilms shared more bacterial OTUs than Nk and Kk and Kk and Pp1 biofilms. Only 14 out of 1047 OTUs were common among the three biofilms.

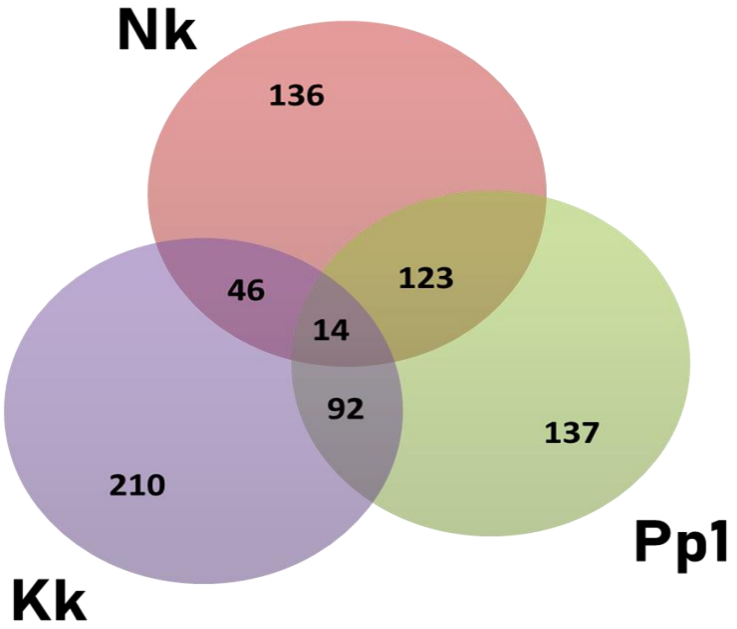

Figure 27: Venn diagram showing the abundance and distribution of specific and common bacterial operational taxonomic units (OTUs) among three biofilms Pp1, Nk, and Kk. OTUs were generated using UCLUST, classified by a naive Bayesian RDP classifier, and identified using the Greengenes database.

Microbial strains isolated from the hydrocarbon-contaminated regions showed higher biodegradation potential than those obtained from the non-contaminated environments might be because the microbes have acclimatized and adapted themselves to the contaminants present in the

environment (Tam et al., 2002). In our study, PAHs spiked to the media act as the sole carbon source for biofilm growth. Not all bacterial and fungal species can sequester the PAH compounds. Studies conducted on the PAH-contaminated Sinduri beach in Korea showed the predominance of three bacterial phyla: *Proteobacteria, Firmicutes,* and *Bacteroidetes* (Lee et al., 2018). The present study indicated the dominance of six bacterial phyla in the biofilms. Similar to the present study, Brazilian oil fields show the abundance of *Firmicutes* and *Proteobacteria* (Silva et al., 2013), while *Proteobacteria* and *Chloroflexi* predominate in water-flooded oil reservoirs, China (Grula et al., 1982).

The degradation of naphthenic acid and other PAHs by *Clostridium* was confirmed by Oko et al. (2017). Abercron et al. (2016) confirmed that in the presence of Nap, *Clostridia*, which belongs to gram-positive and endospore-forming *Firmicutes,* could multiply at a greater speed. Yuan and Chang (2007) reported a 90% degradation of Ace, Ant, Flu, Phe, and Pyr in the *Clostridium*-dominant river sediments from Taiwan. Similarly, the degradation of Nap by *Sphingobacterium multivorum* from PAH-contaminated sites in Iran was reported by Abarian et al. (2018). Ji et al. (2015) demonstrated that *Sphingobacterium* collected from contaminated municipal sludge was effective at degrading Phe.. The role of Bacteroidetes isolated from virgin soil in the degradation of HMW PAHs was confirmed by Lafortune et al. (2009). In the Sundarbans, a higher abundance of fast-growing copiotrophs such as *Proteobacteria, Bacteroidetes, Firmicutes,* and *Planctomycetes* indicated a high organic load. At the same time,

low nutrient concentrations tended to promote the abundance of slow-growing *Actinobacteria* and *Chloroflexi*. (Dai et al., 2016). The abundance of *Gammaproteobacteria* in the oil and hydrocarbon-contaminated regions of Sundarbans was reported by Ghosh et al. (2010).

Aranda (2016) identified the presence of the representative of the *Ascomycota* phylum in the anthropogenically contaminated environment, and Zafra et al. (2014) demonstrated these fungi's ability to enhance the bioavailability and degradability of PAHs. According to Hagler et al. (1979), *Candida* was one of the most prevalent genera isolated from the contaminated Brazilian estuary. *Candida* is also reported to be the most abundant taxon in a Swedish estuary and coastal sediments in Massachusetts. (Norkrans, 1996; MacGillivray and Shiaris, 1993). Furthermore, 97% of the total petroleum hydrocarbons were degraded by *Candida tropicalis* within 20 days of incubation (Gargouri et al., 2015). *Paecilomyces* genera isolated from the Red Sea Coast mangroves in Saudi Arabia, the Gulf of Mexico, and crude oil-contaminated site of Iran showed the ability to utilize and degrade hydrocarbons (Ameen et al., 2016, Dawoodi et al., 2015; Al-Nasrawi 2012;).

References

Abarian, M., Hassanshahian, M. and Badoei-Dalfard, A., 2018. Isolation, screening, and characterization of naphthalene-degrading bacteria from Zarand Mine, Iran. Polycycl Aromat Compd, 38(5), pp.410-419.

Abercron, M.V., Pacheco, D., Benito-Santano, P., Marín, P. and Marqués, S., 2016. Polycyclic aromatic hydrocarbon-induced changes in bacterial community structure under anoxic nitrate reducing conditions. Front Microbiol, 7, p.1775.

Al-Nasrawi, H., 2012. Biodegradation of crude oil by fungi isolated from Gulf of Mexico. J Bioremed Biodegrad, 3(4), pp.147-52.

Ameen, F., Moslem, M., Hadi, S. and Al-Sabri, A.E., 2016. Biodegradation of diesel fuel hydrocarbons by mangrove fungi from Red Sea Coast of Saudi Arabia. Saudi J. Biol. Sci, 23(2), pp.211-218.

Aranda, E., 2016. Promising approaches towards biotransformation of polycyclic aromatic hydrocarbons with Ascomycota fungi. Curr. Opin. Biotechnol., 38, pp.1-8.

Caporaso, J.G., Kuczynski, J., Stombaugh, J., Bittinger, K., Bushman, F.D., Costello, E.K., Fierer, N., Peña, A.G., Goodrich, J.K., Gordon, J.I. and Huttley, G.A., 2010. QIIME allows analysis of high-throughput community sequencing data. Nature methods, 7(5), pp.335-336.

Dai, Z., Hu, J., Xu, X., Zhang, L., Brookes, P.C., He, Y. and Xu, J., 2016. Sensitive responders among bacterial and fungal microbiome to pyrogenic organic matter (biochar) addition differed greatly between rhizosphere and bulk soils. Sci. Rep, 6(1), pp.1-11.

Das, S. and Dash, HR, 2014. Microbial bioremediation: A potential tool for restoration of contaminated areas. In Micro. Biodegrade. bioremed. (pp. 1-21). Elsevier.

Dawoodi, V., Madani, M., Tahmourespour, A. and Golshani, Z., 2015. The study of heterotrophic and crude oil-utilizing soil fungi in crude oil contaminated regions. J. bioremediat. biodegrad, 6(2), pp.12-26.

DeSantis, T.Z., Hugenholtz, P., Larsen, N., Rojas, M., Brodie, E.L., Keller, K., Huber, T., Dalevi, D., Hu, P. and Andersen, G.L., 2006. Greengenes, a chimera-checked 16S rRNA gene database and workbench compatible with ARB. Appl. Environ. Microbiol, 72(7), pp.5069-5072.

Edgar, R.C., 2010. Search and clustering orders of magnitude faster than BLAST. Bioinformatics, 26(19), pp.2460-2461.

Froehner, S., Machado, K.S., Dombroski, L.F., Nunes, A.C., Kishi, R.T., Bleninger, T. and Sanez, J., 2012. Natural biofilms in freshwater ecosystem: indicators of the presence of polycyclic aromatic hydrocarbons. Water Air Soil Pollu., 223(7), pp.3965-3973.

Gargouri, B., Mhiri, N., Karray, F., Aloui, F. and Sayadi, S., 2015. Isolation and characterization of hydrocarbon-degrading yeast strains from petroleum contaminated industrial wastewater. BioMed research international, 2015.

Ghosal, D., Ghosh, S., Dutta, T.K. and Ahn, Y., 2016. Current state of knowledge in microbial degradation of polycyclic aromatic hydrocarbons (PAHs): a review. Front. Microbiol., p.1369.

Ghosh, A., Dey, N., Bera, A., Tiwari, A., Sathyaniranjan, K.B., Chakrabarti, K. and Chattopadhyay, D., 2010. Culture independent molecular analysis of bacterial communities in the mangrove sediment of Sundarban, India. Saline systems, 6(1), pp.1-11.

Gieg, L.M., Fowler, S.J., Berdugo-Clavijo, C., 2014. Syntrophic biodegradation of hydrocarbon contaminants. Curr. Opin. Biotech. 27, 21-29.

Grula, E.A., Russell, H.H., Bryant, D., Kenaga, M., Hart, M., Donaldson, E. and Clark, J., 1982. Isolation and screening of clostridia for possible use in microbially enhanced oil recovery. Proceedings of the microbial enhanced oil recovery, Afton, Okla, USA, 1982.

Hagler, A.N., Santos, S.S. and Mendonca-Hagler, L.C., 1979. Yeasts of a polluted Brazilian estuary. Revista de microbiologia.

Horemans, B., Breugelmans, P., Hofkens, J., Smolders, E., Springael, D., 2013. Environmental dissolved organic matter governs biofilm formation and subsequent linuron degradation activity of a linuron-degrading bacterial consortium. Appl. Environ. Microbiol. 79(15), 4534-4542.

Hyslop, N.P. and White, W.H., 2009. Estimating precision using duplicate measurements. J Air Waste Manag Assoc. 59(9), pp.1032-1039.

Ji, D., Yang, Q., Wang, Y. and Xi, H., 2015. Estimation of phenanthrene degradation model by Sphingobacterium multivorum isolated from municipal sludge. Fresenius Environmental Bulletin, 24, pp.48-55.

Jones, R. and Payne, R., 1997. Clinical investigation and statistics in laboratory medicine. ACB Venture Publications London, pp.53-64.

Lafortune, I., Juteau, P., Déziel, E., Lépine, F., Beaudet, R. and Villemur, R., 2009. Bacterial diversity of a consortium degrading high-molecular-weight polycyclic aromatic hydrocarbons in a two-liquid phase biosystem. Microb. Ecol, 57(3), pp.455-468.

Lee, D.W., Lee, H., Lee, A.H., Kwon, B.O., Khim, J.S., Yim, U.H., Kim, B.S. and Kim, J.J., 2018. Microbial community composition and PAHs removal potential of indigenous bacteria in oil contaminated sediment of Taean coast, Korea. Environ. Pollut, 234, pp.503-512.

MacGillivray, A.R. and Shiaris, M.P., 1993. Biotransformation of polycyclic aromatic hydrocarbons by yeasts isolated from coastal sediments. Appl. Environ. Microbiol., 59(5), pp.1613-1618.

MATBIOPOL Role of microbial mats in bioremediation of hydrocarbon polluted coastal zones, funded under 5th FWP (Fifth Framework Programme) 2003, Research Area: 1.1.4.-3. Key action Sustainable Marine Ecosystems.

Mitra, A. and Mukhopadhyay, S., 2016. Biofilm mediated decontamination of pollutants from the environment. AIMS Bioeng. 3(1), pp.44-59.

Mitra, S., Gachhui, R. and Mukherjee, J., 2015. Enhanced biofilm formation and melanin synthesis by the oyster settlement-promoting Shewanella colwelliana is related to hydrophobic surface and simulated intertidal environment. Biofouling, 31(3), pp.283-296.

Mitra, S., Pramanik, A., Banerjee, S., Haldar, S., Gachhui, R. and Mukherjee, J., 2013. Enhanced biotransformation of fluoranthene by intertidally derived Cunninghamella elegans under biofilm-based and niche-mimicking conditions. Appl. Environ. Microbiol, 79(24), pp.7922-7930.

Nilsson, R.H., Larsson, K.H., Taylor, A.F.S., Bengtsson-Palme, J., Jeppesen, T.S., Schigel, D., Kennedy, P., Picard, K., Glöckner, F.O., Tedersoo, L. and Saar, I., 2019. The UNITE database for molecular identification of fungi: handling dark taxa and parallel taxonomic classifications. Nucleic acids research, 47(D1), pp.D259-D264.

Norkrans, B., 1966. On the occurrence of yeasts in an estuary off the Swedish westcoast. Svenska botaniska foreningen.

Oko, B.J., Tao, Y. and Stuckey, D.C., 2017. Dynamics of two methanogenic microbiomes incubated in polycyclic aromatic hydrocarbons, naphthenic acids, and oil field produced water. Biotechnology for biofuels, 10(1), pp.1-13.

Othman, N., Juki, M.I., Hussain, N. and Talib, S.A., 2011. Bioremediation a potential approach for soil contaminated with polycyclic aromatic hydrocarbons: an overview. Int. J. Sustain. Constr. Eng., 2(2).

Shukla, S.K., Mangwani, N., Rao, T.S., Das, S., 2014. Biofilm-mediated bioremediation of polycyclic aromatic hydrocarbons. Microbial Biodegradation and Bioremediation. Elsevier Inc., Oxford, United Kingdom, pp. 203-232.

Silva, T.R., Verde, L.C.L., Neto, E.S. and Oliveira, V.M., 2013. Diversity analyses of microbial communities in petroleum samples from Brazilian oil fields. Int. Biodeterior. Biodegrad., 81, pp.57-70.

Tam, N.F.Y., Guo, C.L., Yau, W.Y. and Wong, Y.S., 2002. Preliminary study on biodegradation of phenanthrene by bacteria isolated from mangrove sediments in Hong Kong. Mar. Pollut. Bull., 45(1-12), pp.316-324.

United States Environmental Protection Agency, 1996c. Test Method 3510C Separatory Funnel Liquid-Liquid Extraction.

Wang, Q., Garrity, G.M., Tiedje, J.M. and Cole, J.R., 2007. Naive Bayesian classifier for rapid assignment of rRNA sequences into the new bacterial taxonomy. Appl. Environ. Microbiol, 73(16), pp.5261-5267.

Wicke, D., Böckelmann, U. and Reemtsma, T., 2007. Experimental and modeling approach to study sorption of dissolved hydrophobic organic contaminants to microbial biofilms. Water Res., 41(10), pp.2202-2210.

Wicke, D., Böckelmann, U. and Reemtsma, T., 2008. Environmental influences on the partitioning and diffusion of hydrophobic organic contaminants in microbial biofilms. Environ. Sci. Technol, 42(6), pp.1990-1996.

Yuan, S.Y. and Chang, B.V., 2007. Anaerobic degradation of five polycyclic aromatic hydrocarbons from river sediment in Taiwan. J. Environ. Sci. Health B, 42(1), pp.63-69.

Zammit, G., Billi, D., Shubert, E., Kasstovskyy, J., Albertano, P., 2011. The biodiversity of subaerophytic phototrophic biofilms from Maltese hypogea. Fottea 11, 187-201.

Zafra, G., Absalón, Á.E., Cuevas, M., Carmen, D. and Cortés-Espinosa, D.V., 2014. Isolation and selection of a highly tolerant microbial consortium with potential for PAH biodegradation from heavy crude oil-contaminated soils. Water Air Soil Pollut, 225(2), pp.1-18.

CHAPTER 4

PAH DEGRADATION USING PHOTOTROPHIC BIOFILM IN A PATENTED BIOFILM-PROMOTING CULTURE VESSEL

4.1 Introduction

Phototrophic biofilms are unique arrangements of laminated, unified microbial communities composed of a consortium of microbes, predominantly photoautotrophic cyanobacteria. Phototrophic biofilms are the ubiquitous and dominant primary producers in aquatic food webs. The EPS produced by the microorganisms holds the biofilm together. Thick multi-layered phototrophic biofilms are referred to as phototrophic mats or microbial mats. Oxygenic phototrophs such as cyanobacteria and diatoms dominate the mat's top layer, followed by the anoxygenic phototrophs (green and purple sulfur bacteria) and chloroflexi-like bacteria (Roeselers et al., 2008). Oxygenic phototrophs such as unicellular and filamentous cyanobacteria, green algae, and diatoms can reduce carbon dioxide and generate energy by providing oxygen and organic substrates to the system. Phototrophic mats can execute an array of ecological functions, including primary production, nutrient cycling, organic matter decomposition, pollutant detoxification, hydrocarbon degradation, and biogeochemical cycling (Kumar and Venugopalan, 2015). Researchers are focused on the capability of these mats in the sequestration of radionuclides and heavy metals, including the degradation of persistent organic contaminants.

Studies suggest that phototrophic biofilms are involved in the degradation of oils. Dense mats of cyanobacteria formation were observed in the beaches contaminated with oil spills during the first Gulf war of 1991 (Sorkhoh et al., 1992). Compared with bacteria and fungi, relatively less attention has been given to the PAH degradation potential of phototrophic biofilms. Physiological association between the microbes of intertidal populations enhances the ability of PAH pollutants consumption by biofilm-dwelling microorganisms compared to single species populations. Thus, phototrophic biofilm-based remediation in intertidal regions can successfully remove PAHs (Mandal et al. 2021). Bacteria-driven carrier systems holding purple phototrophic

bacterial biofilm degraded substantial amounts of PAHs such as Phe, Nap, Ant, and Pyr (Nhi-Cong et al., 2021). However, PAH removal from the encircling water by laboratory-grown multispecies phototrophic biofilms isolated from the intertidal regions has not been demonstrated before.

Research on biofilm-based algal culture has strengthened because of its implication in nutrient removal of wastewater, algal production (Haripriyan et al. 2022), and a potential route to provide feedstock for bio-refinery based on microalgae. The researchers observed a positive relation between biofilm formation and growth and surface hydrophobicity. Similarly, PAHs showed positive and negative effects on the photosynthetic pigments of phototrophic microalgae. An enhancement of Chl *a* contents was reported upon PAH exposure by Luo et al. (2015), Chen et al. (2020), and Zyszka-Haberecht et al. (2019). In contrast, Panah et al. (2015) and Patel et al. (2015) confirmed a substantial reduction in the photosynthetic and its accessory pigment contents in increased PAH concentrations. Then again, EPS supports the successful survival of complex phototrophic biofilms in restricted environments. The presence of xenobiotic compounds in the environment affects the EPS secretion and controls the physico-chemical properties of the secreted polymer, thereby helping the cells adapt to harsh environmental conditions. Reports are available on the removal of PAH pollutants by mono-species microalgae and the effect of these toxicants on their photosynthetic pigment synthesis. However, phototrophic microorganisms in nature occur in a biofilm consortium, not as individual cells. The efficiency of the intertidal phototrophic biofilms to sequester the PAHs contaminants and the effect of these contaminants on the physico-chemical characteristics of these intertidal phototrophic biofilms were not evaluated previously.

4.2 Materials and methods

4.2.1 Sample collection and culturing of phototrophic biofilms

Figure 28: Phototrophic biofilm cultured in an Erlenmeyer flask with modified sterile mixed media (ASN III: BG11=1:1)

Estuarine phototrophic biofilm samples were gathered by scrapping green and brown-colored biomass on sediment surfaces in five different geographical regions of the Indian Sundarbans, namely Purba Gurguria, Maipit, Patharpratima, Namkhana, and Kakdwip. The biofilm samples were transferred immediately to an Erlenmeyer flask consisting of 200 ml of enriched growth media with ASN III and BG 11 media, specific for phototrophic microorganisms; the media were mixed in equal proportions (Figure 28). Biofilms were maintained in 14:10 h light: dark photoperiod at 25±1 °C in fluorescent irradiance (50 µmol photons m^2 s^{1}).

4.2.2 Laboratory setup and experimental design

For studying the PAH sequestration using phototrophic biofilms, out of 25 phototrophic biofilm samples cultivated in the mixed media, six stably growing and well-formed phototrophic biofilms were selected. Each biofilm represented one of the five different geographical locations of Sundarbans: Pg_P (Purba Gurguria), Mt_P (Maipit), $Pp1_P$ and $Pp2_P$ (Patharpratima), Nk_P (Namkhana), and Kk_P (Kakdwip), where $_P$ – indicates the phototrophic biofilms. These biofilms were cultured in two sets of the patented ES-CCF flasks (details mentioned in section 3.2.3) with two different surface configurations: hydrophilic glass surface (Set 1) and hydrophobic PMMA (Set 2) surface and further employed for the removal of the PAHs.

Approximately 200 mg of phototrophic biofilm was inoculated into the sterile ASN III: BG11 enriched medium. After the growth of the biofilms, different concentrations of the 16 priority PAHs were spiked into the glass and PMMA ES-CCFs: 5 ppm for Pg_P and Mt_P, 15 ppm for $Pp1_P$, 10 ppm for $Pp2_P$ and Nk_P, 25 ppm for Kk_P biofilms. Concentrations for spiking were determined based on the concentrations of the PAHs quantified from the sediments of their corresponding geographical locations, as mentioned in section 2.3.2. An additional set of biofilms were cultured in the ES-CCFs without the PAHs serving as experimental blank. Sterile media void of PAHs and control flasks with sterile media spiked with 5, 10, 15, and 25 ppm of PAHs each were also incubated. The extent of PAH removed from the liquid medium was determined after 21 days in duplicate (n = 2) and represented as percent residual PAH.

The PAH removal efficiency (%) was: $R= (C_i – C_f)/C_i \times 100$,

R represents the removal efficiency (%), C_i is the initial, and C_f is the final PAH concentration.

4.2.3 PAHs extraction from phototrophic biofilm liquid culture media

After 21 days, the extent of PAH sequestered from the liquid media was determined by extracting PAHs from the media. PAHs were extracted using a separating funnel by applying the USEPA method 3510C liquid-liquid extraction (1996), followed by silica gel clean-up and quantification using GC FID as described in sections 2.2.3, 2.2.5, and 2.2.6.

4.2.4 Estimation of PAH sequestrated in biofilms

Phototrophic biofilms were collected after 21 days and dried by lyophilization (Eyela FDU-1200, Tokyo Rikakikai Co. Ltd, Japan), weighed, and biofilm biomasses were recorded. PAHs from dried biofilm samples were extracted using the method described by Froehner et al. (2012) and processed similarly to PAH extracted from the heterotrophic biofilm, as mentioned in section 3.2.5

4.2.5 Quantification of photosynthetic pigments from biofilms

The overall concentration of phototrophic pigments such as chl *a*, chl *b*, chl *c*, chl *d*, total chl, and carotenoids from the biofilms cultured in PAH spiked media with the control biofilms was compared after 21 days of incubation. Reagent-grade methanol was used as the solvent for extracting photosynthetic pigments, where the extraction was carried out in triplicate. First, biofilm samples were weighed and homogenized using mortar and pestle; the homogenate extract was centrifuged at 3000 rpm (4 °C) for 15 minutes. Finally, the pellets were re-suspended in methanol until the pellets turned colorless. Then, all the supernatants were pooled and quantified spectrophotometrically at different absorbances, as described by Ritchie (2008):

Chl *a* (µg/ml) = $-2.0780 \times (A_{632} - A_{750}) - 6.5079 \times (A_{652} - A_{750}) + 16.2127 \times (A_{665} - A_{750}) - 2.1372 \times (A_{696} - A_{750})$ (±0.0070)

Chl *b* (µg/ml) = $-2.9450 \times (A_{632} - A_{750}) + 32.1228 \times (A_{652} - A_{750}) - 13.8255 \times (A_{665} - A_{750}) - 3.0097 \times (A_{696} - A_{750})$ (±0.0212)

Chl *c* (µg/ml) = 34.0115 × (A_{632} - A_{750}) - 12.7873 × (A_{652} - A_{750}) + 1.4489 × (A_{665} - A_{750}) - 2.5812 × (A_{696} - A_{750}) (±0.0120)

Chl *d* (µg/ml) = -0.3411 × (A_{632} - A_{750}) + 0.1129 × (A_{652} - A_{750}) - 0.2538 × (A_{665} - A_{750}) + 12.9508 × (A_{696} - A_{750}) (±0.0031)

Total Chl (µg/ml) = Chl *a* + Chl *b* + Chl *c* + Chl *d*

Carotenoids (µg/ml) = 4 × (A_{480} - A_{750})

4.2.6 EPS extraction from the biofilms

EPS from control and PAH-spiked vessels were extracted, quantified, and characterized. Two fractions of EPS were extracted from the biofilm samples, i.e., the released (RPS) and the capsular/bound polymeric substances (CPS). Phototrophic biofilms harvested in the ES-CCFs were centrifuged at 5000 rpm for 10 min. The supernatant consisting of the RPS was separated from the pellets containing the cells and the CPS. EPS from the pellets were incubated in 0.1 M sulfuric acid for 1 h at 95 °C. After the incubated samples were centrifuged at 3500 rpm for 5 min, the pellet was removed, and the supernatant with CPS was precipitated in 96% cold ethanol (Di Pippo et al. 2013). RPS from the cell-free culture was quantified using the method prescribed by Gacheva et al. (2013). The supernatant collected was precipitated using 99% chilled ethanol in a ratio of 1:3 (v/v) and was centrifuged at 10,000×g for 10min. 65% ethanol pellets were washed thrice to remove contaminants, freeze-dried, weighed, and stored at -20 °C for further analysis.

4.2.7 Characterization of extracted EPS

Quantification of total carbohydrate contents from RPS and CPS fractions was carried out spectrophotometrically by the phenol-sulphuric acid method (Dubois et al. 1956). The glucose standard was used for preparing the standard curve. Total protein constituents in EPS fractions

were quantified spectrophotometrically using Lowry's method (Lowry et al. 1951). The standard curve was prepared using different concentrations of bovine serum albumin. Uronic acid contents were determined using carbazole in 80% sulfuric acid with sodium borate. Galacturonic acid served as the standard (Taylor and Buchanan-Smith, 1992).

4.2.8 Hydrophobicity study of EPS and biofilm using the biphasic system

About 5 ml of each EPS was suspended in a clean test tube in 1% w/v in phosphate saline buffer. To the test tubes added, 300µl of hexadecane and OD_{550} (A_0) was obtained. All tubes were vortexed for about 1 min, and the phases were allowed to separate by keeping them still for 15 min. The lower aqueous phase was gently removed using a sterile Pasteur pipette, and OD_{550} (A_1) was quantified again. The hydrophobicity of the EPS was calculated using the following formula (Bhatnagar et al. 2014): $DH = [(A_0 - A_1) / A_0] \times 100$

Cultures at the early stationary phase (between 10-15 days of growth) were used to test the biofilm hydrophobicity (Zhang et al. 2011; Veerabadhran et al. 2018). The culture was washed twice thoroughly using the sterile culture medium. First, 3 ml of biofilm suspension was taken in a clean, sterile test tube, and 3 ml of n-hexadecane was added. The contents were mixed properly by manually agitating for about 1 min, and after a 5min pause, the contents were vortexed for 10s. For the complete separation of the two phases, the tubes were allowed to stand still for about 10-15 min. The biofilm cell surface property was assessed by observing adherence to the biphasic (aqueous-hydrocarbon) system as described by Fattom and Shilo (1984).

4.2.8 Light and scanning electron microscopy of biofilms

Freshly cultured biofilm was spread on a clean glass slide, covered with a coverslip, and observed at 100X magnification using a light microscope (Leica ICC50 HD, Leica Microsystems, Wetzlar, Germany). Biofilm communities growing in control media and media spiked with PAHs were

studied by scanning electron microscopy (SEM) using Hitachi FlexSEM 1000 II microscope (Hitachi, Ltd Tokyo, Japan). Biofilm mats were placed over carbon tape on the SEM sample stub and gold-sputtered (3-5 nm). SEM imaging was done using SEM coupled with detectors for secondary and back-scattered electrons and an ultra-variable-pressure detector for imaging non-conductive samples at low vacuum.

4.2.9 Statistical analyses

Analysis of variance (ANOVA), a two-tailed Student t-test, and the coefficient of variation was performed using SPSS software (version 16.0). The statistical significance was considered at a significance level of $P \leq 0.05$.

4.3 Results and discussion

4.3.1 PAHs removal from the liquid media by phototrophic biofilms in hydrophobic and hydrophilic patented vessels

Figure 29 illustrates the phototrophic biofilms cultivated with and without adding PAHs. From Table 13, it is evident that apart from the medium cultured with the phototrophic Pg_p biofilm, all the other phototrophic biofilms used were able to sequester 98-100% of all the individual spiked 16 priority PAHs in all liquid media. In contrast, the extent of sequestration of the different PAHs varied from a low 1% to a maximum of 100 % in Pg_p biofilm. Significant differences ($p \leq 0.05$) in the mean residual PAHs amounts in liquid media between all the six biofilm-cultured vessels with the spiked PAHs (Table 13). The mean residual PAHs obtained from the liquid media in the glass and PMMA ES-CCFs indicated that irrespective of the hydrophilic and hydrophobic nature of culture vessels, all the PAHs were similarly sequestrated from the liquid media.

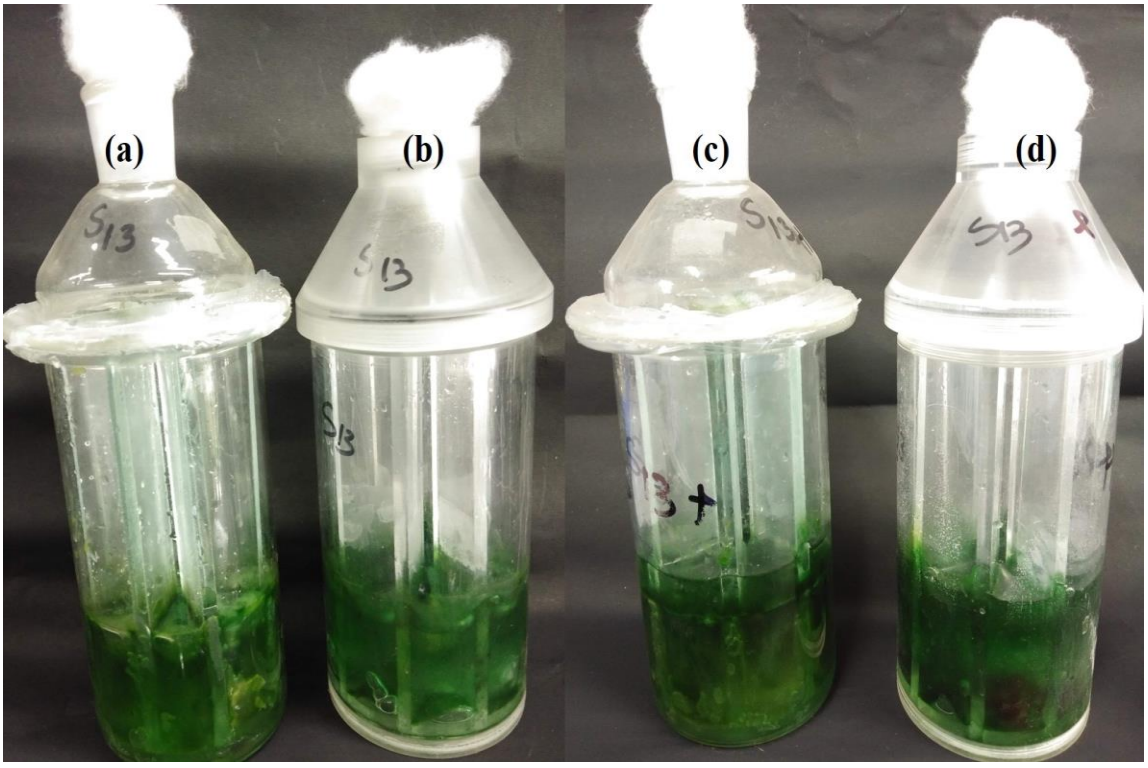

Figure 29: Phototrophic biofilm cultivated in patented ES-CCF with (a) biofilm formation in glass ES-CCF without PAH, (b) biofilm formation in PMMA ES-CCF without PAH, (c) in hydrophilic glass surface ES-CCF enriched with PAHs (d) hydrophobic polymethyl methacrylate (PMMA) surface enriched with PAHs after 21days of incubation.

Table 13: Residual amounts (as a percent of initial concentrations) of 16 priority spiked PAHs in liquid media after treatment with phototrophic biofilms in glass and PMMA ES-CCF for 21 days. The residual amounts at least double each other (PMMA ES-CCF compared to glass ES-CCF or vice versa) are shown in bold letters. The coefficient of variation of duplicate data was 2.89% (n=192), following Hyslop and White (2009) and Jones and Payne (1997)

PAHs	Pg_p		Mt_p		$Pp1_p$		$Pp2_p$		Nk_p		Kk_p	
	Glass	**PMMA**	**Glass**	**PMMA**	**Glass**	**PMMA**	**Glass**	**PMMA**	**Glass**	**PMMA**	**Glass**	**PMMA**
Nap	77.81	47.09	0.58	0.33	0.16	0.41	0.00	0.00	0.44	0.55	0.00	0.01
Acy	19.42	11.50	0.19	0.00	0.40	0.09	0.00	0.00	0.08	0.09	0.00	0.00
Ace	15.13	98.98	0.98	0.06	0.33	0.00	0.54	0.54	0.11	0.14	2.06	0.08
Flu	28.30	24.85	0.00	0.10	0.05	0.13	0.03	0.03	0.15	0.14	0.04	0.06
Phe	78.47	62.09	0.00	0.01	0.04	0.12	0.10	0.10	0.12	0.11	0.02	0.04
Ant	89.66	71.26	0.00	0.21	0.16	0.56	0.00	0.00	0.61	0.67	0.05	0.04
Fla	24.71	18.20	0.00	0.18	0.08	0.33	0.00	0.20	0.09	0.09	0.00	0.01
Pyr	0.00	0.00	0.00	0.00	0.00	0.00	0.00	0.00	0.06	0.54	0.11	0.24
B (a) A	57.97	38.39	0.23	0.49	0.00	0.14	0.10	0.10	0.16	0.13	0.05	0.06
Chr	0.00	0.00	0.00	0.00	0.13	0.11	0.00	0.00	0.12	0.11	0.00	0.05
B (b) F	0.00	0.00	0.00	0.00	0.00	0.22	0.00	0.00	0.20	0.19	0.07	0.19
B (k) F	23.65	0.00	0.00	0.31	0.00	0.00	0.00	0.00	0.00	0.00	0.00	0.00
B (a) P	83.61	44.29	0.35	0.68	0.29	0.12	0.16	0.16	0.26	1.43	0.27	0.09
Ind	0.00	0.00	0.00	0.00	0.00	0.11	0.00	0.00	0.16	0.19	0.00	0.14
D (a,h) A	0.00	0.00	0.00	0.00	0.09	0.14	0.00	0.00	0.00	0.00	0.00	0.00
B (ghi) P	95.62	20.74	0.06	0.73	0.84	0.19	2.79	1.57	0.12	0.25	0.79	0.12
Mean PAH residual amounts	37.15	27.34	0.15	0.19	0.16	0.17	0.23	0.17	0.17	0.29	0.22	0.07

The mean residual amounts of PAHs within the phototrophic biofilms after 21 days of exposure to the PAHs ranges between 0-100% (Table 14). Significant differences ($p \leq 0.05$) in the mean residual PAHs between the six biofilm-cultured vessels with the spiked PAHs were noticed. Based on the mean residual amount of PAHs, the ability to remove the 16 PAH contaminants by the phototrophic biofilms after 21 days of incubation was in the order $\mathbf{Pp1_p}$ >$\mathbf{Kk_p}$ >$\mathbf{Nk_p}$ >$\mathbf{Mt_p}$ >$\mathbf{Pp2_p}$ >$\mathbf{Pg_p}$. The $\mathbf{Pg_p}$ biofilm cultured in the hydrophobic PMMA ES-CCF has the highest mean residual PAH compared to other biofilms cultured in hydrophobic and hydrophilic vessels, which implies the low PAH sequestration potential of the $\mathbf{Pg_p}$ biofilm. On the other hand, the hydrophilic culture of the $\mathbf{Pp1_p}$ biofilm and hydrophobic culture of the $\mathbf{Kk_p}$ biofilm showed the lowest mean residual amount of PAHs, indicating high PAHs sequestration potential of $\mathbf{Pp1_p}$ and $\mathbf{Kk_p}$ biofilms (Table 14). Compared to liquid media, differences in PAHs sequestration arising due to the nature of hydrophobic/hydrophilic surface were more pronounced inside the biofilms. All the other PAHs, except for Ind and Chr, showed differences in the extent of removal between the hydrophobic PMMA and hydrophilic glass ES-CCFs for all the biofilms (indicated in bold in Table 14). Ace in PMMA ES-CCF and B(ghi)P in glass ES-CCF were the only PAHs removed from $\mathbf{Pg_p}$ biofilms, while the remaining 14 priority PAHs were extracted from the biofilms cultured in both types of flasks. Summing up the mean residual PAHs in the PAH-spiked (5 ppm) liquid media treated with $\mathbf{Pg_p}$ biofilm (Table 13) and the mean residual PAHs obtained from Pg biofilms (Table 14), we recorded a combined 92% (4.6 ppm) mean residual PAHs and a summative 89% (4.4 ppm) mean residual PAHs in the hydrophilic and hydrophobic vessels respectively. In contrast, this additive value ranged from 10-20% in the other biofilms, indicating the potency of these biofilms to sequester the PAHs in comparison to the Pgp biofilm efficiently. Hence, $\mathbf{Pp1_p}$, $\mathbf{Nk_p}$, and $\mathbf{Kk_p}$ biofilms were selected for further investigations.

Table 14: Residual amounts (as a percent of initial concentrations) of 16 priority spiked PAHs inside the biofilms after treatment with phototrophic biofilms in glass and PMMA ES-CCF for 21 days. The residual amounts at least double each other (PMMA ES-CCF compared to glass ES-CCF or vice versa) are shown in bold letters. The coefficient of variation of duplicate data was 5.77% (n=192), following Hyslop and White (2009) and Jones and Payne (1997)

PAHs	**Pg_p**		**Mt_p**		**$Pp1_p$**		**$Pp2_p$**		**Nk_p**		**Kk_p**	
	Glass	**PMMA**	**Glass**	**PMMA**	**Glass**	**PMMA**	**Glass**	**PMMA**	**Glass**	**PMMA**	**Glass**	**PMMA**
Nap	22.2	**52.9**	13.7	**23.5**	16.5	10.7	10.5	12.5	10.9	18.7	**10.1**	0.0
Acy	77.6	88.5	28.2	24.7	5.6	**18.1**	13.4	15.4	35.6	29.0	3.9	**16.4**
Ace	**74.9**	0.0	**19.6**	0.0	22.7	**83.2**	33.7	33.7	9.9	**21.8**	98.8	64.4
Flu	61.7	65.1	**60.0**	18.0	**14.6**	7.5	7.8	7.8	**13.7**	6.2	4.3	2.9
Phe	21.5	27.9	5.3	**30.1**	3.5	**10.6**	21.2	19.3	**18.9**	6.1	2.8	3.7
Ant	8.3	**18.7**	**83.5**	49.9	10.3	**20.9**	20.0	23.0	27.8	24.7	4.9	10.0
Fla	65.3	71.8	29.8	24.3	4.4	4.6	29.1	29.1	8.9	**20.3**	**7.0**	0.0
Pyr	85.4	89.3	0.0	0.0	**12.7**	0.0	0.0	0.0	0.0	**20.2**	13.6	15.5
B (a) A	32.0	41.6	32.0	40.3	0.0	0.0	57.8	57.8	**28.1**	0.0	**6.5**	0.0
Chr	89.9	95.0	0.0	0.0	0.0	0.0	0.0	0.0	0.0	0.0	3.2	0.0
B (b) F	**81.5**	34.2	0.0	0.0	0.0	**7.1**	0.0	0.0	0.0	**12.0**	8.7	10.5
B (k) F	66.4	85.3	0.0	**37.0**	0.0	0.0	14.5	14.5	0.0	0.0	0.0	0.0
B (a) P	16.4	**45.7**	13.4	19.2	**37.9**	10.8	52.2	65.6	55.5	45.3	14.8	12.4
Ind	99.0	100.0	0.0	0.0	0.0	0.0	0.0	0.0	0.0	0.0	0.0	0.0
D (a,h) A	75.0	86.0	0.0	0.0	0.0	**5.5**	0.0	0.0	9.7	**17.0**	11.3	11.0
B (ghi) P	0.0	**79.3**	0.0	0.0	30.5	26.1	11.5	15.5	**67.4**	23.6	**38.0**	5.4
Mean PAH residual amounts	54.8	61.4	17.8	16.7	9.9	12.8	17.0	18.4	17.9	15.3	14.2	9.5

The hydrophobicity test using n-hexadecane was conducted to establish the biofilm surface properties (hydrophobic/hydrophilic). $Pp1_p$, Nk_p, and Kk_p biofilms demonstrated hydrophobic characteristics. Biofilms migrated toward the upper hydrocarbon layer in preference to the lower aqueous layer (Figure 30).

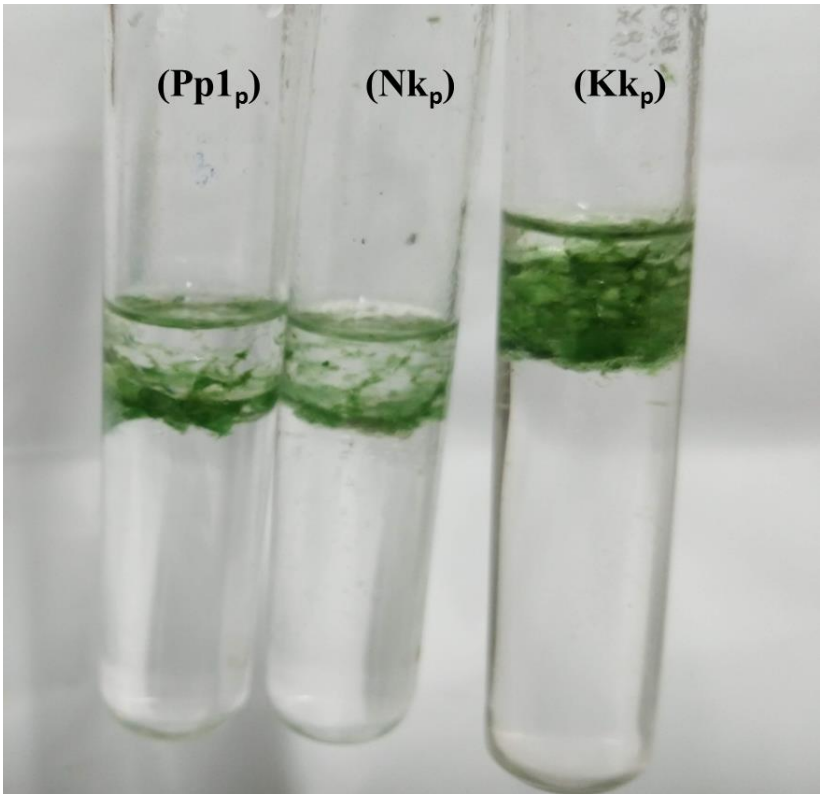

Figure 30: Partitioning of phototrophic biofilms in the biphasic system. $Pp1_p$, Nk_p, and Kk_p biofilms preferentially adhered to the hydrocarbon layer indicating the hydrophobicity of biofilms.

Morphological studies using a light microscope revealed cyanobacteria such as *Gloeocapsa* sp., *Chloroidium* sp., *Closterium* sp. like green algae, and pennate diatoms, and purple sulfur bacteria in $Pp1_p$ biofilms. Again, purple sulfur bacteria and cyanobacteria such as *Gloeocapsa* sp. and *Microcystis* sp. were observed in Nk_p biofilms, whereas Kk_p biofilms showed the occurrence of purple sulfur bacteria, cyanobacteria such as *Gleocapsa* sp. *Microcystis* sp. and, *Phormidium* sp., *Closterium* sp. like green algae as well as pennate diatoms

(Figure 31). PAH-treated biofilms also showed the presence of similar phototrophic microorganisms.

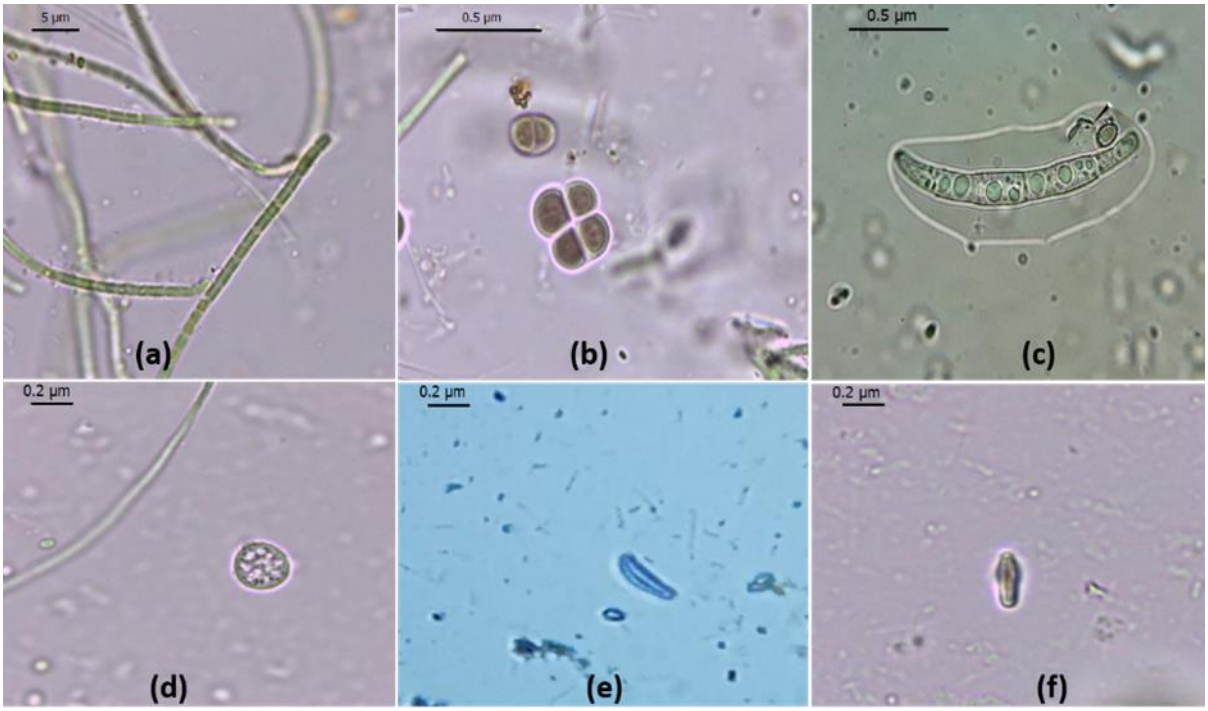

Figure 31: Morphological analyses of PAH degrading phototrophic biofilms employing a light microscope at a magnification of 100×10 X showed the presence of **(a)** *Phormidium* sp. **(b)** *Gloeocapsa* sp. **(c)** *Closterium* sp. **(d)** *Microcystis* sp. **(e)** and **(f)** pennate diatoms.

SEM observations (Figure 32) and comparisons with similar published images (Boelee, 2013; Cole et al., 2014) suggest the biofilm is composed predominantly of filamentous cyanobacteria where the algal cells occurred in clusters embedded in the EPS matrix. Filaments with the associated EPS were observed in the control biofilms. Heterotrophic bacteria formed a close association with filamentous phototrophic microorganisms (Figure. 33b). In the PAH-treated biofilms, cells were found as clusters and embedded firmly within the produced EPS in response to the xenobiotic challenge. Biofilm structures were largely unchanged after 21 days of incubation with PAHs. Salt crystals appeared as cube-like structures in SEM images.

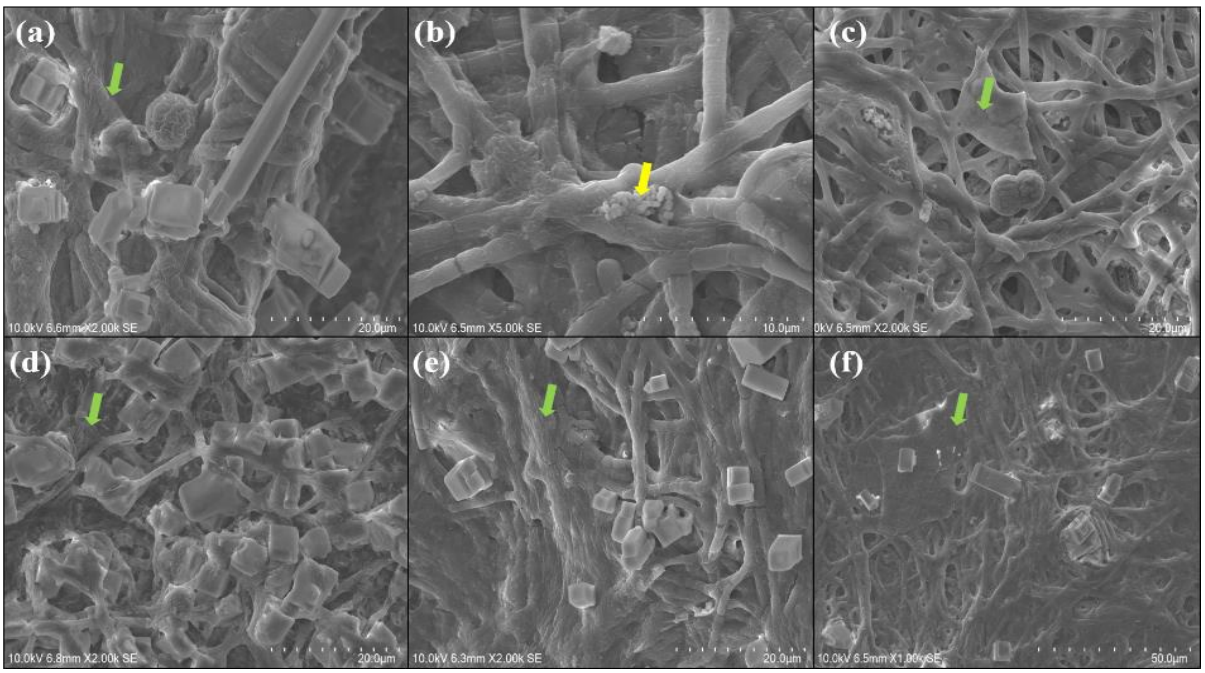

Figure 32: Scanning electronic microscope (SEM) micrographs of **(a)** $Pp1_p$ **(b)** Nk_p **(c)** Kk_p phototrophic biofilms without PAHs and **(d)** $Pp1_p$ **(e)** Nk_p **(f)** Kk_p phototrophic biofilms treated with PAHs. The yellow arrow indicates bacteria associated with the biofilm, and the green arrows denote the EPS matrix

Phototrophic biofilms isolated from Patharpratima, followed by Kakdwip and Namkhana, showed the lowest mean PAH recoveries, which, interestingly, were the same geographical locations of the Indian Sundarbans from where the isolated heterotrophic biofilms also demonstrated maximum PAH sequestration activity. Similar to observations from heterotrophic biofilms, there was no substantial deviation between the mean residual PAHs persisting in the liquid media between hydrophobic and hydrophilic vessels. However, residual amounts of certain PAHs showed divergences in their sequestration when heterotrophic biofilms cultivated in flasks had distinct surface properties. Initial layers of microalgal cells are more likely to adhere to hydrophobic surfaces than hydrophilic surfaces (Wang et al. 2018). Mantzorou and Ververidis (2019) showed that hydrophobic materials favored cell adhesion, although arguments disapproved of the role of surface hydrophobicity in microalgae adhesion. For example, Zhuang et al. (2018) noted that hydrophilic support media was more inclined to

form the initial conditioning algal biofilm. The extent of PAH removal from the culture media and formation of phototrophic biofilm biomass in hydrophobic/hydrophilic vessels indicated that no generalizations could be made on the preference of surface hydrophobicity/hydrophilicity towards biofilm growth and PAH sequestration. The physico-chemical characteristics of the individual PAHs and the presence of PAHs in the liquid medium play a significant role in determining the effect of surface hydrophobicity/hydrophilicity in biofilm biomass formation and pollutant sequestration.

According to Hong et al. (2008), the accumulation and biodegradation of Phe and Fla by diatoms collected from mangroves of the Jiulong river estuary (China) showed higher biomass provided more cell surface area and cell volume for absorption and adsorption of the PAHs, indicating enhanced removal in a shorter period. Studies conducted by Chan et al. (2006) and Lei et al. (2007) showed similar results that align with our study because a correlation between the highest biofilm biomass and the lowest mean residual PAHs can be observed. Generally, biological environments are polluted by multiple PAHs. Hong et al. (2008) indicated that in the presence of two or more PAHs, individual PAH could influence the rate and extent of biodegradation of another, and this positive interaction was again validated by Lei et al. (2007) and Chan et al. (2006). Such positive influences presumably occurred amongst the 16 PAHs in the present investigation as well, which led to their enhanced extent of sequestration.

In the natural environment, finding a single microorganism that can metabolize or completely remove the xenobiotic compound under various environmental conditions is extremely unusual; therefore, the combined action of microalgae and other phototrophic microbes plays an important role in the elimination of these contaminants (Semple et al. 1999). Consortia of the microbial population can exhibit roles that are challenging and require numerous steps to carry out for single species. Furthermore, mixotrophs can assimilate both

organic carbon and CO_2 simultaneously, and autotrophic biofilms of the present investigation favored mixotrophic metabolism by assimilating PAHs with concomitant photosynthetic activity. Given their tolerance towards extreme environmental conditions, the mixotrophic culture of algae/cyanobacteria was found to have an advantage over heterotrophic culture when cultivated at a low nutrient concentration (Hamouda et al. 2016). Phototrophic biofilms of this study can actively sequester PAHs compared to the equivalent heterotrophic biofilms of our previous study. The average mean residual PAH amounts in the phototrophic biofilms of this study were 22%, while the same in heterotrophic biofilms was 35%.

Photosynthetic organisms such as *Phormidium* sp., *Gloeocapsa* sp., *Closterium* sp., *Microcystis* sp., and diatoms were identified in these biofilms. Several studies using these organisms showed their PAH degradation capability and the potential to degrade other pollutants, including metals. For example, hypersaline *Phormidium tenue* can degrade Ant (Zyszka-Haberecht et al. 2019). Abed et al. (2002) identified *Phormidium* sp. as the predominant cyanobacterium in indigenous microbial communities isolated from a heavily polluted site in a coastal stream (Wadi Gaza) also the PAH degradation potential of the same organism, especially Phe. Phe, Ant, and Nap degradation potential of *Phormidium* sp. were demonstrated by Ibraheem (2010) and Kumar et al. (2009). PAH degradation efficiency of *Gloeocapsa* sp. has not yet been identified, but it is widely applied in removing lead (Pb2+) (Raungsomboon et al. 2006). The capacity to adsorb cadmium and manganese by *Gloeocapsa* sp. was demonstrated by Mohamed (2001). Rath (2012) demonstrated the Nap, Phe, and Pyr degradation by the cyanobacterium *Microcystis aeruginosa*. The biosorption of Phe by the EPS of *Microcystis aeruginosa* was studied by Bai et al. (2016). The Phe degrading capability of *Phormidium* sp. and *Microcystis* sp. was reported by Ichor et al. (2016). PAH degradation capacity of *Closterium* sp. is not yet reported, whereas degradation of the crude oil in a polluted environment, especially in the dark (Uzoh et al., 2015), was reported.

4.3.2 Effect of PAHs on the phototrophic biofilm biomass and photosynthetic pigments in hydrophobic and hydrophilic vessels

Table 15 represents the phototrophic biofilm biomass estimated at the end of the investigation. Results suggest that the presence of PAHs in the phototrophic growth media enhanced phototrophic biofilm biomass in hydrophobic and hydrophilic flasks. A significant increase ($P \leq 0.05$) of biomass cultured in glass and PMMA ES-CCF spiked with and without PAHs was recorded in all the samples except the $Kk_{\mathbf{p}}$ cultured in glass ES-CCF (Figure 33). $Pp1_{\mathbf{p}}$ control biofilm showed higher biomass in the hydrophobic PMMA flask compared to the hydrophilic glass flask. In contrast, in the presence of PAHs, $Pp1_{\mathbf{p}}$ biofilm biomass was higher in the glass flask than in the PMMA flask. $Pp1_{\mathbf{p}}$ biofilm in the presence of PAHs showed a 100% increase in biomass in glass CCF and 58% in the PMMA flask. $Nk_{\mathbf{p}}$ and $Kk_{\mathbf{p}}$ biofilms showed fairly high biomass in the hydrophilic glass control flask. Biomass increased marginally compared to the controls upon adding PAHs and did not display any differences concerning the nature of the vessel surface. Compared to control biofilms, 19% and 22 % increases in biomass were noted in the hydrophobic and hydrophilic flasks cultured with $Nk_{\mathbf{p}}$ biofilms, respectively. The Kk biofilms increase in biofilm biomass was 12% and 33% in glass and PMMA CCF, respectively. The mean residual PAH amounts were lowest in the liquid medium and biofilm biomass in the hydrophobic flask where the $Kk_{\mathbf{p}}$ biofilm was cultivated. Interestingly, the highest biofilm biomass was recorded in this cultivation (Table 15, indicated in bold).

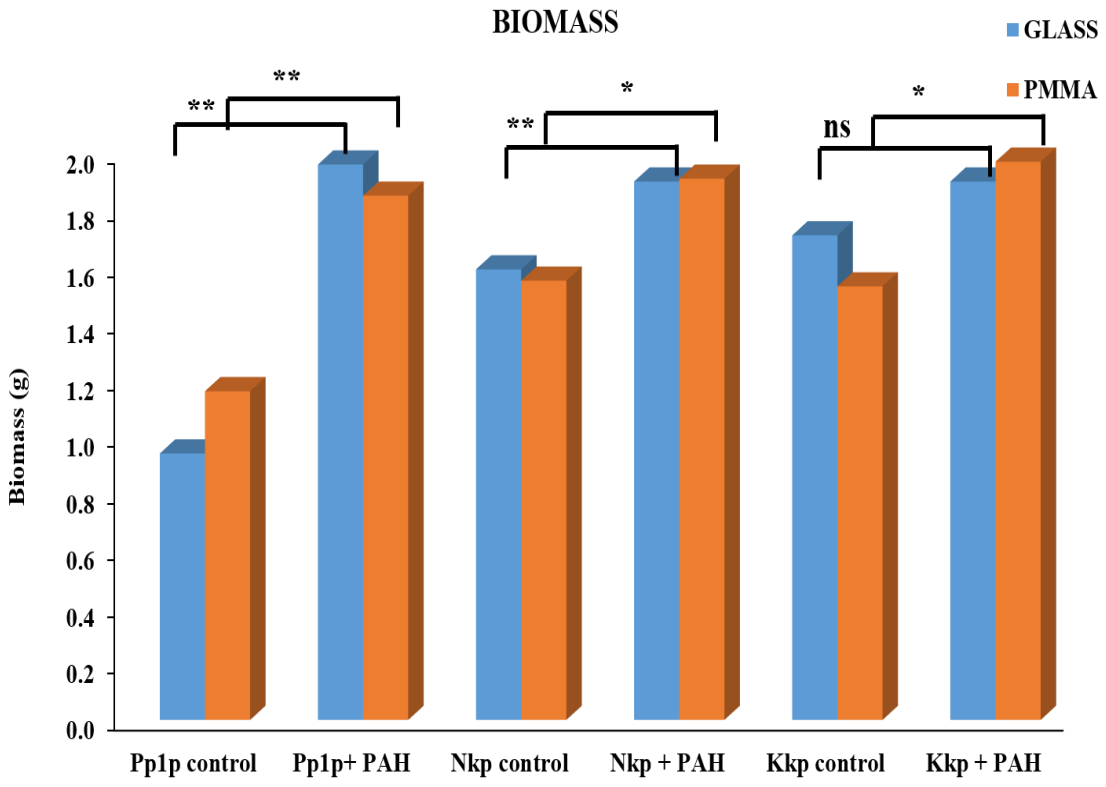

Figure 33: Biomass (g) of selected phototrophic biofilm ($Pp1_p$, Nk_p, and Kkp) having high PAH degradation potential cultured with and without spiked 16 priority PAHs in hydrophobic and hydrophilic ES-CCFs.

Table 15: Biomass (g), the concentration of Chl *a*, Chl *b*, Chl *c*, Chl *d*, total Chl and carotenoid pigments (µg/g) extracted from biofilm biomass cultured with and without 16 priority PAH contaminants after 21 days of incubation (values are means ± SD; n=3). Bold figures indicate the highest values obtained. ** represents p<0.01, * denotes p<0.05, and ns stands for non-significant based on paired *t*-test.

Biofilm sample \ Parameters		Biomass	Total Chl	Chl *a*	Chl *b*	Chl *c*	Chl *d*	Carotenoids
$Pp1_p$	**GLASS**	0.94±0.01	1374.4±13.2	868.4±10.1	181.5±9.8	284.7±5.7	19.9±2.2	344.3±5.6
control	**PMMA**	1.16±0.02	965.9±14.0	709.1±3.6	68.3±8.2	176.4±15.3	12.1±0.7	275.1±4.9
$Pp1_p$+ PAH	**GLASS**	1.96±0.04**	1495.0±9.7*	903.2±9.9*	247.2±6.2*	**338.5±6.5***	**22.8±3.4^{ns}**	351.0±14.6^{ns}
	PMMA	1.85±0.01**	1397.7±10.5**	889.2±4.7**	194.2±5.6**	295.7±4.3*	18.5±3.1^{ns}	**355.9±10.1***
Nk_p	**GLASS**	1.59±0.03	897.8±6.1	658.2±10.4	47.0±2.9	188.0±0.4	4.6±1.9	231.3±2.4
control	**PMMA**	1.55±0.06	1024.2±13.7	722.4±11.8	78.1±8.4	217.0±2.4	6.7±1.7	252.6±1.4
Nk_p + PAH	**GLASS**	1.90±0.00**	1323.9±6.7**	846.8±2.7**	181.9±7.9**	268.5±9.6**	11.5±1.1^{ns}	289.4±5.7**
	PMMA	1.91±0.01*	1408.3±6.4**	898.3±8.2**	221.2±20.2**	301.4±6.0**	17.1±1.7**	293.4±8.3^{ns}
Kk_p	**GLASS**	1.71±0.04	1221.2±14.7	842.4±8.2	88.4±3.7	280.6±6.1	9.8±1.2	315.5±2.2
control	**PMMA**	1.53±0.13	1153.6±3.5	789.5±2.8	112.2±7.3	240.8±3.5	11.1±1.7	283.4±8.6
Kk_p + PAH	**GLASS**	1.90±0.06^{ns}	1381.7±13.3*	896.2±3.2*	172.5±7.3**	299.3±1.3^{ns}	13.6±1.6*	315.5±12.7^{ns}
	PMMA	**1.97±0.02***	**1568.5±8.3****	**933.4±9.4****	**268.2±7.9****	332.7±10.6**	17.6±1.6*	344.7±6.2*

Total chl contents in the biofilms cultured with and without PAHs were analyzed (Table 15 and Figure 34). A significant increase ($P \leq 0.05$) in their chl contents between all the biofilms was noted. The hydrophilic culture of $Pp1_p$ biofilm and hydrophobic culture of Kk_p biofilm measured the highest total chl content in PAH-spiked media. Increased total chl content in these two flasks correlated with the lowest mean residual amount of PAHs recovered in the hydrophilic culture of the $Pp1_p$ biofilm and the hydrophobic culture of the Kk_p biofilm. Thus, elevated chl concentrations in PAH-treated biofilms indicated an increased photosynthetic efficiency compared to control biofilms, significantly reducing PAH pollutant levels. Total chl amounts in control and PAH-treated Nk_p biofilms were higher in hydrophobic PMMA ES-CCF compared to hydrophilic glass flasks.

Chl *a*, chl *b*, chl *c*, chl *d*, and carotenoid contents were measured and compared statistically in the control biofilms and PAH-treated biofilms. Concentrations of all the photosynthetic pigments in $Pp1_p$, Nk_p, and Kk_p biofilms indicated significant differences at $P \leq 0.05$ between the control and treated biofilms (Figure 34). Individual chl contents in $Pp1_p$ biofilm samples were higher in the hydrophilic glass flasks than in the hydrophobic PMMA vessels for control and PAH-spiked biofilms. However, in $Pp1_p$ biofilm, carotenoid concentration was slightly higher with PAHs in the hydrophobic PMMA ES-CCF compared to hydrophilic glass ES-CCF. In contrast, carotenoids were higher in hydrophilic glass ES-CCF than the PMMA ES-CCF in the control experiments. In the case of Nk_p biofilms, both controls, and PAH-treated biofilms in hydrophobic PMMA ES-CCFs, displayed higher levels of all pigments compared to similar cultivation in the hydrophilic glass ES-CCFs. On the other hand, Kk_p biofilms showed deviations from both $Pp1_p$ and Nk_p biofilms. In the control flasks, elevated concentrations of chl *a*, *c*, and carotenoids were measured in hydrophilic glass ES-CCF compared with PMMA ES-CCF, but chl *b* and *d* contents were higher in the PMMA CCF compared to glass ES-CCFs.

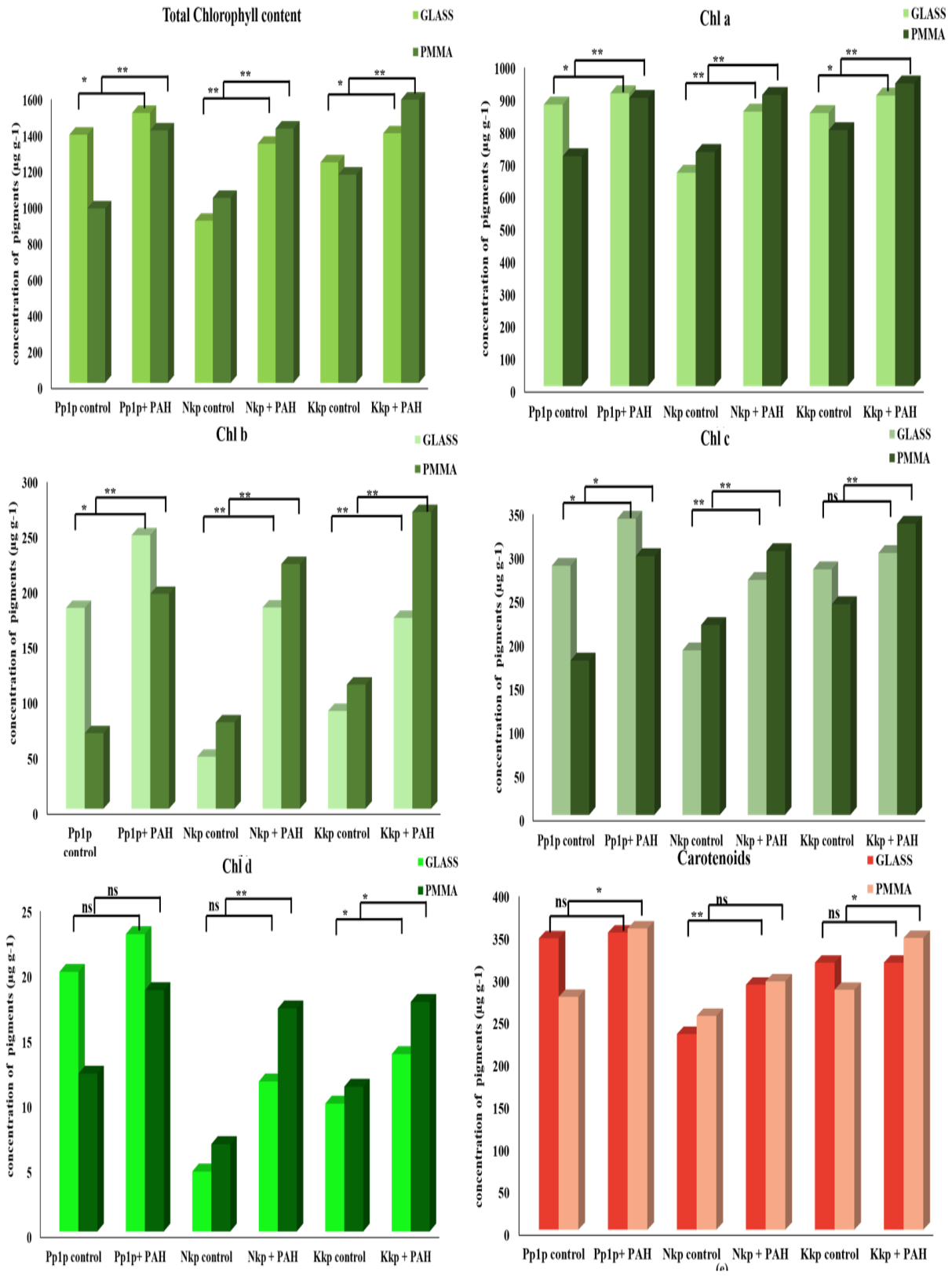

Figure 34: Total chl contents, chl *a*, chl *b*, chl *c*, chl *d*, and carotenoid contents (µg/g) of phototrophic biofilm ($Pp1_p$, Nk_p, Kk_p) cultured with and without spiked 16 priority PAHs in hydrophobic and hydrophilic ES-CCFs.

All photosynthetic pigment concentrations were higher in the hydrophobic PMMA ES-CCF than in the hydrophilic glass ES-CCF when the Kkp biofilms spiked with PAHs.

$Pp1_{\mathbf{p}}$ biofilm in the hydrophobic PMMA ES-CCF (25–100% increase) showed a significant increase in concentrations of all pigments compared to biofilms cultivated in hydrophilic glass ES-CCF (1–38%) after spiking with PAHs. Enhancement of all pigment concentrations except chl *d* was noticeably higher in the hydrophilic vessels cultured with the $Nk_{\mathbf{p}}$ biofilms spiked with the PAH contaminants compared with the hydrophobic flasks. On the contrary, the hydrophobic PMMA ES-CCF where $Kk_{\mathbf{p}}$ biofilms were cultivated showed enhanced concentrations of all photosynthetic pigments compared to its hydrophilic flasks. Among all the pigments, carotenoids showed a relatively lower increase in their contents in the biofilm samples spiked with PAHs compared to their respective controls. When $Pp1_{\mathbf{p}}$ and $Kk_{\mathbf{p}}$ biofilms were tested, enhancement of carotenoid pigment concentration in the glass ES-CCF with the spiked PAHs compared to its equivalent control was negligible (1.9% and 0.02%), whereas hydrophobic ES-CCF showed 29.4% increase in $Pp1_{\mathbf{p}}$ biofilm and 21.7% increase in $Kk_{\mathbf{p}}$ biofilm. $Nk_{\mathbf{p}}$ biofilm cultured in the hydrophilic glass ES-CCF recorded about 25% enhancement in carotenoid content spiked with PAH pollutants, whereas the biofilm grown in the hydrophobic PMMA ES-CCF showed a 16.2 % increase in carotenoid content.

An increase in biomass accompanied by higher PAH degradation can be observed in the present study. Our results are in agreement with the studies conducted by Lei et al.(2007), who reported the removal of the PAH (Pyr) depends on the algal biomass content; authors also suggested higher PAH removal if more biomass was formed. The relationship between biomass and PAH removal was yet again proved by Lei et al. (2007) using Flu, Pyr, and a mixture of Flu-Pyr as substrates for four microalgal species and demonstrated an increase in the PAH removal efficiency with an increase in the concentration of the biofilm biomass. Aldaby and Mawad (2019) also reported an increase in chl content accompanied by an increase

in biomass concentration during Pyr degradation, which also supports our findings since an increase in photosynthetic activity was also observed in this experiment. Along with the biofilm biomass, cell wall composition, and cell density during the addition of PAHs, enzymes and the species-species interaction play an important role in removing the contaminants.

The present study shows an increase in the photosynthetic pigment concentrations in all three biofilm samples after growing in media spiked with 16 priority pollutants for 21 days. Luo et al. (2014) demonstrated the removal and transformation of HMW PAHs like B(a)A, B(b)F, B(k)F, B(a)P, D(a,h)A, B(g,h, i)P and Ind by *S. capricornutum* and *Chlorella* sp. and the effect of these PAHs in the chl *a* content in these algal cells. PAH degradation by the algal cells correlated with the algal growth and the chl *a* content. They also demonstrated an increase in chl *a* content in the algal cells in the presence of mixed PAHs under irradiation and their tolerance toward the toxic HMW PAHs since the mixed pollutants do not affect the growth of the algal biomass. Application of the microalgal species *S. capricornutum* on the two most biologically active LMW PAH pollutants of aquatic ecosystems, Ant and Phe, showed their influence in the microalgal growth stimulation and also an increase in the chl *a* content by the biodegradation metabolites of Ant and Phe (Traczewska et al., 1999).

The studies conducted by Luo et al. (2015) elucidated microalgal chl (especially chl *a* and *b*) as the major active component accelerating B(a)P photo-transformation under irradiation. Porphyrin's core structure in the chls represents an effective photosensitizer that helps in the photo-transformation of other organic compounds, like pesticides, 4-nitrophenol, and dye. Biodegradation potential studies conducted with different concentrations of Pyr using different species of cyanobacteria *Chlorella* and *Oscillatoria* showed that the concentration of PAH used and type of microalgal sp. play a major role in the chl concentration accompanied by the dry weight concentration (Aldaby and Mawad, 2019). At lower concentrations of Pyr (10-30ppm), *Oscillatoria* sp. showed a significant increase in the total chl content accompanied

by its dry weight, whereas *Chlorella* sp. exhibited enhanced total chl content and carotenoid concentrations at a higher concentration of Pyr (50ppm). An increase in photosynthesis implies the increase in the chl concentrations correlated with the increase in dry weight. A mixotrophic study using *A. oryzae*, *C. kessleri*, and its consortium indicated the increase in chl *a* content from the day of cultivation with 0.5 and 1% crude oil up to 14 days while a decline in the chl *b* contents where observed. The carotenoid content was observed to increase at 0.5% crude oil concentration, whereas at 1% crude oil concentration, the carotenoid contents were reduced after 14 days of incubation (Hamouda et al., 2016). Biodegradation study of crude oil under heterotrophic conditions by cyanobacteria *Nostoc punctiforme* demonstrated an increase in both chl *a* and carotenoid contents after incubation (El-Sheekh and Hamouda, 2014). Carotenoids prevent the chls from photo-oxidative destruction due to increased ROS formation at various steps in the photosynthetic system. An increase in the carotenoid contents in the biofilms simultaneously with the increase in other photosynthetic pigments in this study suggested that the increase in carotenoid contents may prevent the toxicity of the PAH on the thylakoid compartment of a chloroplast.

Contrary to all these reports, some phototrophic microalgae do not positively correlate with the increase in PAH concentrations. *Leptolyngbya* sp. in the presence of the LMW Nap showed the negative effect of Nap in the photosynthetic activity, thereby reducing the oxygen release and decreasing their photosynthetic pigment contents, but they can effectively degrade Nap (Panah et al., 2015). Patel et al. (2015) demonstrated a substantial reduction in the photosynthetic and its accessory pigment contents with the increase in the LMW Ant in three different phototrophic species like *Synechocystis* sp., *A. fertilissima*, and *N. muscorum*. They also suggest that the reduction in the pigment contents might be ascribed due to PAH-thylakoid membrane interaction, lipoprotein membrane dispersion, and an increase in the active oxygen

species (AOS) in the living cells. Microalgae cultured with HMW PAH showed relatively increased pigment concentration compared to the LMW PAH.

Although these authors reported enhancement of chl levels in photoautotrophs upon PAH exposure, the reasons for such an increase were not discussed. Studies conducted by Jajoo et al. (2014) suggest that PAHs inhibited photosystem II (PS II) in wild-type *Arabidopsis thaliana* plants. However, the mechanism of PAHs' action on the microalgae's photosynthetic system has not been explored. On the other hand, Ricart et al. (2009) reported that herbicide diuron exposure enhanced chl *a* content of a riverine biofilm community. Chl *a* increased with high diuron concentrations, which were similar to our findings. The disruption of electron flow in PSII during the light reaction of photosynthesis occurs at low concentrations and induces the formation of shade-type chloroplasts. Microalgae may regulate the intracellular concentration of photosynthetic pigments in response to changing environmental situations. "Shade-adaptation" response involves an increase in photosynthetic pigments in response to decreased light intensity. This adaptation may compensate for the reduction in photosynthetic efficiency. Even higher diuron concentrations inhibit PSI and can lead to the photo destruction of pigments. However, a reduction in pigment concentration was not detected in our study. In consonance with the mechanism proposed by Ricart et al. (2009), our results indicate the formation of shade-type chloroplasts in tune with the associated increase in chl *a* in response to PAH exposure.

Additionally, the accessory light-harvesting pigment (chl *b*) content of *Nephroselmis pyriformis* increased significantly when exposed to three PSII–inhibiting herbicides. In contrast, another accessory pigment (chl *c*) enhanced marginally in the presence of these herbicides (Magnusson et al. 2008) supports our contemplated PSII disruption hypothesis. Carotenoids play a key role in light-protection reactions and contribute towards cell wall stabilization. Therefore, enhanced synthesis of carotenoids in phototrophic biofilms, as

observed in the presence of PAHs in this study, indicates suboptimal cultivation conditions (Stiefelmaier et al. 2020).

Our studies emphasized the difference in the pigment contents when biofilms were cultured in flasks with hydrophobic/hydrophilic surfaces and the change in the concentration of the contents in these flasks after incubating with 16 PAHs. The above results also highlight that the hydrophobicity of the pollutants also plays a role in the increase in the pigment contents irrespective of the hydrophobic /hydrophilic properties of both flasks and biofilms cultured. The chl content investigation of five different microalgal species (*Amphora coffeaeformis, Navicula incerta, Cylindrotheca fusiformis, Chaetoceroups* sp. and *Nannochloropsis* sp.) based on adherence to the hydrophobic/hydrophilic membrane indicates the preference of all the species towards the hydrophilic membrane over the hydrophobic membrane and also increased production of chl contents in the biofilms attached to the hydrophilic membranes (Poad and Derek, 2019). The current results show a complex relationship between the species, PAH, and the properties of the surface to which it was exposed. Most previous reports show the effect of individual PAHs in either pure or mixotrophic algal culture rather than the effect of mixed pollutants on mixed microbial populations, similar to the environmental conditions. Concomitant chl concentrations were higher in the microalgae attached to hydrophilic membranes compared to the hydrophobic membrane. Similarly, biofilm's wet weight and chl *a* contents of *Synechocystis salina* and *Cyanobium* sp. were higher on hydrophilic glass than on hydrophobic epoxy-coated glass (Faria et al. 2020). Variability in the concentration of each type of pigment (Chl *a*, *b*, *c*, *d*, and carotenoids) depended on the geographical location from where the biofilm was sourced ($Pp1_{\mathbf{p}}$, $Nk_{\mathbf{p}}$, and $Kk_{\mathbf{p}}$) as well as surface hydrophobicity/hydrophilicity of the culture flask.

4.3.3 Effect of PAHs on the production of exopolymeric substances (EPS) in hydrophobic and hydrophilic vessels

To evaluate EPS production by the phototrophic biofilms when challenged with the 16 PAHs after 21 days of incubation, the RPS and CPS were extracted separately from the PAH-spiked and control experiments (Table 16). Biofilms spiked with different concentrations of PAHs showed an increased production of the RPS and CPS. In the presence of PAHs, the highest production of RPS was observed in Nk biofilms cultured in glass ES-CCF and PMMA ES-CCF compared to $Pp1_p$ and Kk_p biofilms. RPS production in Nk control biofilm was also higher than in $Pp1_p$ and Kk_p control biofilms. When cultivated with PAHs, the mean RPS production by the phototrophic biofilms was in the order $Pp1_p < Kk_p < Nk_p$. RPS formation was higher in the PMMA ESCCF cultured with $Pp1_p$ and Kk_p biofilms (control as well as their tests) compared to the glass CCFs, but the reverse was observed in Nk_p biofilms. After 21 days of incubation, $Pp1_p$, Nk_p, and Kk_p biofilms cultured in the hydrophilic flasks showed enhancement of RPS by 42.3%, 43.2%, and 46%, respectively, in comparison with their respective controls, whereas in the PMMA ESCCF 22.9%, 30.8% and 17.4% enhancements in RPS production were recorded in $Pp1_p$, Nk_p, and Kk_p biofilms.

Similar to RPS, the CPS production by the biofilms also increased but to a relatively lesser extent than RPS production after 21 days of incubation with PAH contaminants (Table 16). In the presence of PAHs, the mean CPS production by the phototrophic biofilms was in the order $Kk_p > Pp1_p > Nk_p$ biofilms. Greater CPS production in $Pp1_p$ and Kk_p biofilms was observed in hydrophilic flasks spiked with PAHs compared to their hydrophobic flask cultures, whereas CPS production in Nk_p biofilms was higher in hydrophobic flask compared to glass ES-CCF vessel. In $Pp1_p$ and Kk_p biofilms, the increase in CPS production in the presence of PAHs compared to the control was less in the hydrophilic CCF, i.e.3.9 % and 4.9 %. In contrast, the increase in the CPS production in the hydrophobic vessel was 50.9 % ($Pp1_p$

biofilm) and 20.6 % (Kk_p biofilm). Compared to the Nk_p control biofilms, CPS production in the glass CCF incubated with PAHs was enhanced negligibly (0.84 %). On the other hand, a 12.3 % enhancement of CPS production in the PMMA CCF was recorded. A statistically significant difference ($P< 0.05$) in their RPS, and CPS production, was observed in all the biofilms.

4.3.3.1 EPS total carbohydrates content

EPS total carbohydrates, proteins, and uronic acid contents play distinct roles in biofilm growth and attachment (Table 16). The total protein content was rather low, less than 15 mg/g of EPS on average, which accounted for only a small fraction of the EPS constituents (less than 9 % in RPS and 5% in CPS), while uronic acid and carbohydrates were the major biochemical components of the EPS, having proportions of above 91% in RPS and over 95% in CPS. In the presence of PAHs, protein, carbohydrates, and uronic acid contents increased in RPS and CPS. A significant increase ($P\leq0.05$) in the RPS and CPS carbohydrates in biofilms when spiked with PAHs (Table 16). Additionally, the highest concentration of carbohydrates was recorded in the RPS and CPS extracted from Kk_p biofilms cultured in the hydrophobic flask. After 21 days of incubation with PAHs, CPS carbohydrate was in the order $Kk_p > Pp1_p > Nk_p$, whereas RPS carbohydrates were formed in the order $Kk_p > Nk_p > Pp1_p$. In every biofilm, EPS carbohydrates concentrations differed when extracted from hydrophilic/hydrophobic vessels. The carbohydrate concentrations were higher in the EPS extracted from the PMMA flask in the presence of PAHs, whereas in control, carbohydrates were higher in glass vessels. RPS and CPS carbohydrate content from the Nk_p biofilms was higher in EPS extracted from the control PMMA ESCCF and in the test PMMA ESCCF than the corresponding glass ESCCFs. RPS carbohydrate contents extracted from the Kk_p biofilms were similar to that obtained from Nk_p biofilms.

Table 16: RPS and CPS (mg/g of dry weight of biomass); carbohydrate, protein, and uronic acid contents (mg/g of dry weight of RPS/CPS) and protein/polysaccharide ratio as a percentage (%) in control and experimental biofilms cultured in hydrophilic glass and hydrophobic PMMA ES-CCFs (values are means ± SD; n=3). Protein/ polysaccharide ratios of RPS and CPS were estimated by summing up the carbohydrate and uronic acid contents as total polysaccharides. Bold figures indicate the highest values obtained. ** represents $p<0.01$, * denotes $p<0.05$ and ns stands for non-significant. Differences made on paired *t*-test.

Parameters	$Pp1_p$ control		$Pp1_p$ +PAH		Nk_p control		Nk_p +PAH		Kk_p control		Kk_p +PAH	
	GLASS	**PMMA**	**GLASS**	**PMMA**	**GLASS**	**PMMA**	**GLASS**	**PMMA**	**GLASS**	**PMMA**	**GLASS**	**PMMA**
RPS	55.9 ± 0.2	63.1 ± 8.7	78.7± 2.5**	82.3 ± 3.0^{ns}	83.9 ± 6.0	85.7 ± 1.3	**122.0±3.5****	111.4 ±7.3*	59.0 ± 3.7	81.2 ± 3.4	90.6 ± 7.4^{ns}	96.6 ± 8.4*
Carbohydrate	47.6 ± 0.9	50.9 ± 1.8	63.7 ± 2.3*	52.6 ± 2.6^{ns}	77.8 ±2.3	84.7 ± 1.9	92.5±11.4^{ns}	100.3±2.3*	78.6 ± 6.2	88.3 ± 3.1	90.8 ± 2.8^{ns}	**128.2±3.2***
Protein	6.6 ± 0.1	7.4 ± .2	**11.4± 0.3****	9.4 ± 0.6^{ns}	5.7 ± 0.1	5.9 ± 0.1	9.2 ± 0.6**	10 ± 0.6*	5.5 ± 0.0	5.6 ± 0.0	9.8 ± 0.2**	10.4± 0.2**
Uronic acid	43.1 ± 2.8	33.7 ± 3.4	54.8± 2.0**	48.8 ± 0.9*	36.2±1.8	43.1 ± 2.0	64.1 ± 3.7**	68.5 ± 5.9*	31.9 ± 1.6	37.3 ± 0.8	63.7 ± 2.2**	**90.2± 7.4****
Protein/ polysaccharide	7.2	8.7	**9.6****	9.3^{ns}	5.0	4.6	5.9^{ns}	5.8^{ns}	4.8	4.5	6.3*	5.0^{ns}
CPS	51.2 ± 0.9	27.9± 1.4	53.2 ± 3.1^{ns}	42.2 ± 6.2^{ns}	22.5±1.2	31.6 ± 1.2	25.2 ± 2.1^{ns}	31.8 ± 6.2^{ns}	65.1± 2.2	44.2 ± 4.3	**68.3 ± 6.0^{ns}**	53.3±10^{ns}
Carbohydrate	148.3±5.9	169.6±3.2	297.8±4.7**	274.6±4.8**	126.0±4	136.2±1.9	232.6±5.2**	294.6±2.2**	208.0±10.1	178.7±3.0	325.1 ± .5*	**398.4 ± 9****
Protein	5.5 ± 0.8	5 .0 ± 0.1	11.1 ± 0.7**	8.1 ± 0.6*	4.7±0.5	4.9 ± 0.9	8.8 ± 0.9**	10.7 ± 0.3*	5.8 ± 3.3	6.2 ± 0.4	9.1 ± 1.0*	**14.1±3.5****
Uronic acid	30.1 ± 2.8	32.2 ± 0.3	40.9 ± 3.5*	55.0 ± 8.6*	54.1±4.5	56.3 ± 2.6	59.0 ± 0.9**	61.6 ± 5.6^{ns}	34.6 ± 2.4	55.2 ± 4.2	66.1± 4.9**	**90.2 ±8.4****
Protein/ Polysaccharide	3.0	2.5	3.3^{ns}	2.5^{ns}	2.6	2.6	3.0^{ns}	3.0^{ns}	2.4	2.7	2.4^{ns}	2.9^{ns}

CPS carbohydrate contents obtained from Kk_p biofilms were higher in hydrophobic vessels than in the hydrophilic vessel for the control. However, after incubating with 16 priority PAHs, CPS carbohydrates were lower in hydrophilic vessels compared to hydrophobic vessels.

4.3.3.2 EPS total protein content

EPS protein contents were low compared to the corresponding carbohydrates and uronic acids. Despite their lower concentration, proteins are important because they comprise the enzymes required for metabolism, photosynthesis, and CO_2 fixation. Similar to carbohydrates (RPS and CPS), both the RPS as well as CPS proteins increased significantly in hydrophilic/hydrophobic vessels spiked with PAHs ($P<0.05$), as evident from Table 16. Protein (RPS and CPS) concentrations also showed differences from vessels of hydrophilic/hydrophobic surface properties, similar to RPS and CPS carbohydrates. In the presence of PAHs, the RPS protein content in $Pp1_p$ biofilms was higher in the glass ESCCF compared to PMMA CCF, whereas in control, protein content was higher in the PMMA CCF than glass ESCCF. Furthermore, CPS protein contents in the control and test were higher in the glass hydrophilic flask compared to hydrophobic vessels. In Nk_p and Kkp biofilms (control and test), the PMMA flask showed higher RPS and CPS protein concentrations compared to glass CCFs. Protein concentration in the RPS was measured in the order $Pp1_p > Kk_p > Nk_p$, whereas for the CPS protein, the series was $Kk_p > Nk_p > Pp1_p$. Moreover, the ratio of protein to polysaccharides (as a percentage) upon exposure to PAHs pollutants was evaluated to decipher the specific character of EPS excretion (Table 16). In general, in the presence of PAHs, CPS protein to polysaccharides ratios showed no significant difference ($P>0.05$) for all the biofilms after 21 days of incubation. However, the ratios of RPS protein to polysaccharides for all the biofilms incubated with PAHs increased significantly.

4.3.3.3 EPS total uronic acid content

Kk_p biofilms cultured in the hydrophobic flasks showed the highest concentrations of CPS carbohydrates, uronic acid and RPS carbohydrates, proteins, and uronic acids when treated with PAHs, which correlates with the lowest mean residual amount of PAHs in the hydrophobic culture of the Kk_p biofilm. In the presence of PAH pollutants, a significant increase ($P \leq 0.05$) in the uronic acid contents in RPS, and CPS in all the biofilms, could be observed. RPS uronic acids extracted from Nk_p and Kk_p biofilms and CPS uronic acids obtained from all three biofilms showed enhanced uronic acid content in the hydrophobic vessel for control and test experiments, except for the RPS uronic acids obtained from the $Pp1_p$ biofilms. The order of RPS and CPS uronic acid was $Kk_p > Nk_p > Pp1_p$.

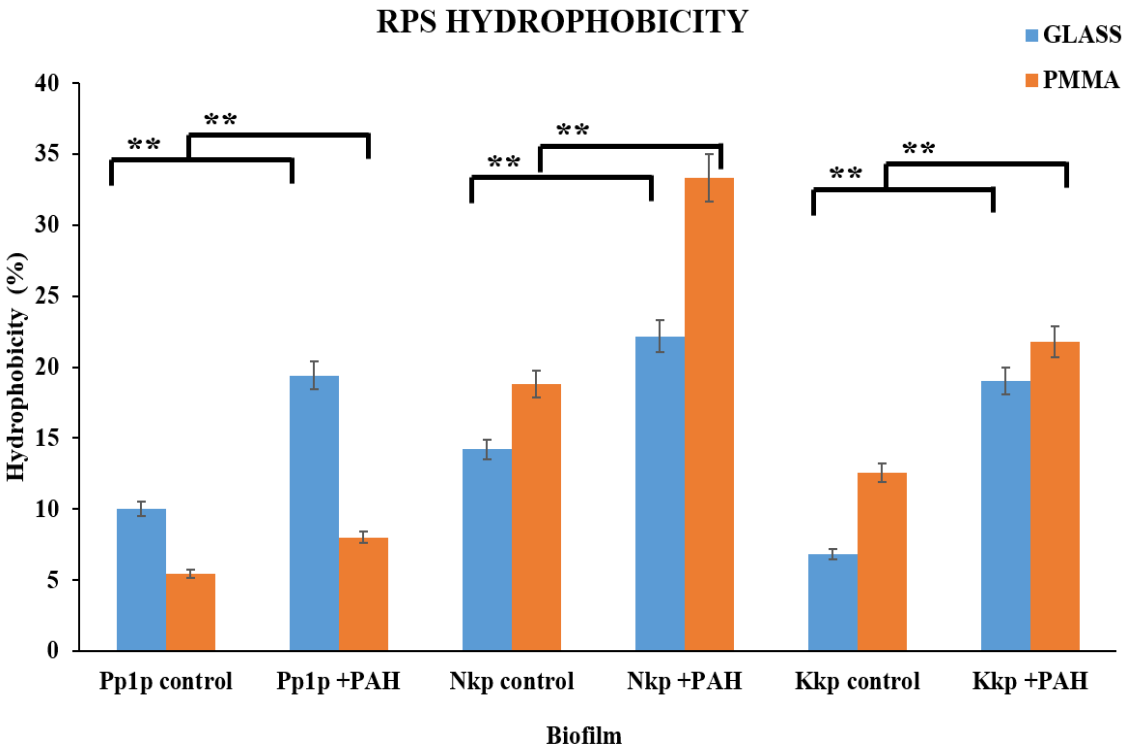

(a)

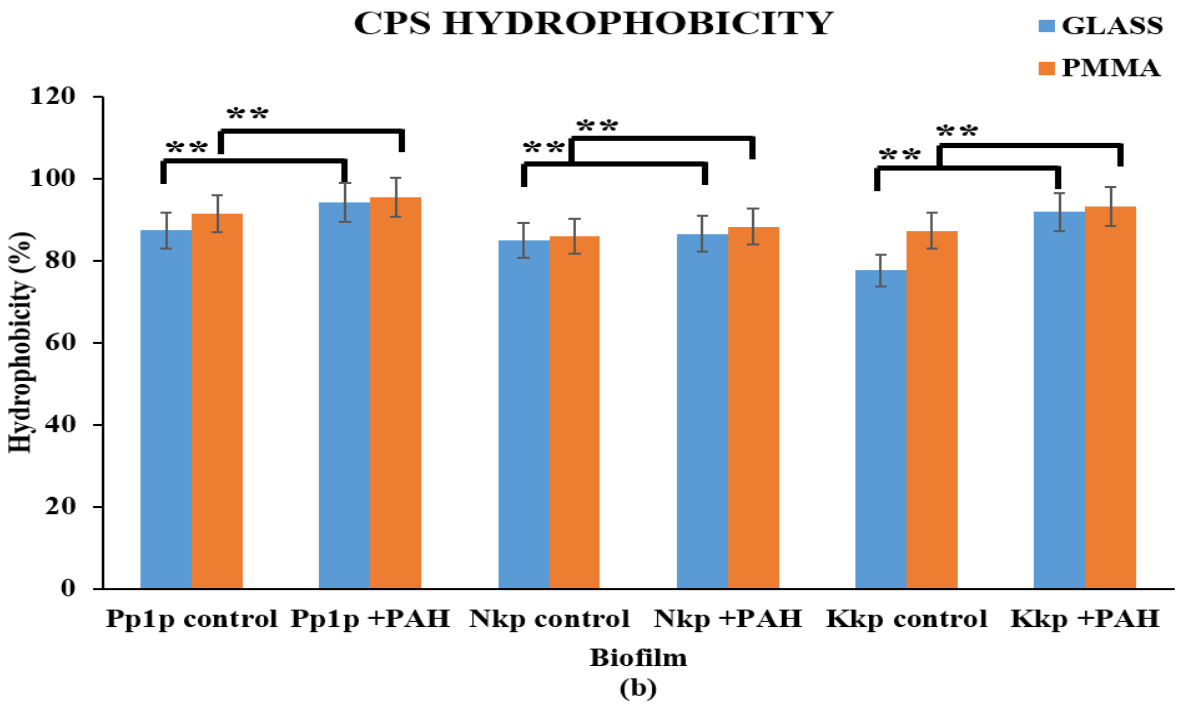

Figure 35: Hydrophobicity of released (RPS) **(a)** as well as capsular (CPS) **(b)** extracellular polymeric substances. While RPS hydrophobicity is altered in response to PAH exposure, CPS hydrophobicity remains constant. Significance was determined through paired t-test at $p < 0.01$.

The uronic acid content of EPS (comprising of RPS and CPS) corroborated with the hydrophobicity of the EPS. The hydrophobicity of the EPS increased significantly after spiking with PAHs. Like uronic acid contents, the hydrophobicity of RPS extracted from the $Pp1_p$ biofilms, hydrophobicity of RPS from Nk_p and Kk_p biofilms, and CPS hydrophobicity from all three biofilms was higher in the hydrophobic vessel for control and test biofilms (Figure 35).

In phototrophic biofilms, the major producers of the EPS are cyanobacteria, whereas diatoms and microalgae participate in the biosynthetic process. The cyanobacterial EPS plays an important role in protecting biofilms from drought, UV radiation, and other unfavorable environmental conditions. More condensed fractions of the EPS are usually embodied under the terms of sheaths and capsules [capsular polysaccharides (CPSs)] surrounding cells or cell groups. The CPS enhanced the microbial adhesion to solid substrates and the accumulation of

coarse substrates. The hydrophobic characteristics of the EPSs play a major role in the adhesion of cyanobacterial cells to solid surfaces. Less condensed EPS fractions, loosely attached to cells, are usually incorporated under the term "slime" and do not reflect the shape of the cells. Released polysaccharides (RPSs) represent the polysaccharides external layers that can be partly released in the surrounding medium. The RPS and CPS content produced by the biofilm depends on the microorganism and growing conditions. Although all microbes can produce EPS, cyanobacterial EPS exudates some characteristics that make them different from other microbial EPS. The presence of sulfate groups (also present in some eukaryotes and archaea) and uronic acids play a key role in determining the hydrophobicity, anionic and sticky nature of EPS to the macromolecules. Hydrophobic characteristics of EPS are determined mainly by the presence of peptides, deoxy-sugars (rhamnose and fucose), and ester-linked acetyl groups, which significantly affect the rheological and emulsifying properties, and also the capability to adhere to solid surfaces (Rossi and De Philippis, 2015).

High EPS production is generally considered a protective mechanism against stress factors (Stiefelmaier et al., 2020). Environmental stressors, i.e., the presence of PAHs, affect not only EPS production, but can also affect the physical and chemical characteristics of the polymer secreted, thereby helping the cells adapt to harsh environmental conditions. Depending on the polymer's functions in the different species, the polymer release's timing in response to environmental factors variations occurs (Rossi and De Philippis, 2015). The high molecular weight heteropolymers of polysaccharide nature produced by the cyanobacteria in the biofilm can act as biosurfactants. During bioremediation, the EPS immobilizes the pollutants and enhances the degradation; their surfactants aid in solubilizing the hydrophobic substrates. Biosurfactants form a specific separation at the interface between hydrocarbons and water, thus forming micro-emulsion which enhance the bioavailability and desorption of hydrocarbon moiety (McGenity et al., 2012). Extracellular enzymes within EPS also promote

the decontamination of pollutants like organic compounds and heavy metals (Mitra and Mukhopadhyay. 2016).

The polysaccharide in the EPS matrix contains both hydrophobic and hydrophilic moieties. The hydrophobic moieties are mainly responsible for increasing the PAH solubility, while the hydrophilic ones are associated with cell movement in the aqueous phase. The presence of proteins in the EPS, along with polysaccharides, has specific functions and characteristics; they help to enhance the biosurfactant properties of EPS and thereby increase the PAH solubility (Zhang et al., 2011). In agreement with these findings, upon exposure to PAHs, the hydrophobicity of the RPS fraction secreted in our experiments was found to be increased (Figure 35). Irrespective of PAH, CPS hydrophobicity was maintained above 80%, which was also confirmed by the hexadecane partition test, suggesting that the tested biofilms are inherently hydrophobic. Chen et al. (2020) studied the biochemical responses of a freshwater microalga when exposed to sulfonamides, and an increase in CPS production was observed, which may contribute to the rerouting of energy production towards the synthesis of storage polysaccharides under xenobiotic stress. Similarly, enhancement in the RPS accumulation may be an adaptive response to free xenobiotics that may affect the carbon cycle, causing cells to secrete large amounts of RPS to achieve carbon balance (Chen et al. 2020). EPS polysaccharide contents increased in the presence of PAH pollutants, which is conducive to removing the toxicant through adsorption, accumulation, or degradation (Chen et al. 2020).

Microbes can regulate their EPS composition and constituents while adapting to growth with hydrophobic substrates such as PAHs. The modification of EPS composition in the presence of hydrophobic PAHs can be assessed by ascertaining the ratio of proteins to polysaccharides (Zhang et al. 2011). The present study shows an increase in the ratio of RPS protein to polysaccharide for all the biofilms revealing that when PAHs were used as a substrate, RPS proteins increased faster than RPS polysaccharides. However, the ratios of CPS

protein to CPS polysaccharide remained unvarying after incubation for all the biofilms, indicating no amendment in the CPS biochemical configuration. Moreover, enhancement in the RPS protein to polysaccharide ratio of $Pp1_{\mathbf{p}}$ biofilm cultured in glass and PMMA flasks was observed, signifying that $Pp1_{\mathbf{p}}$ biofilms regulate its EPS constituents more effectively than $Nk_{\mathbf{p}}$ and $Kk_{\mathbf{p}}$ biofilms during acclimatization to PAH exposure. RPS was found to be more important than CPS during the growth of $Pp1_{\mathbf{p}}$, $Nk_{\mathbf{p}}$, and $Kk_{\mathbf{p}}$ biofilms in the presence of PAHs. The hydrophobic domains of EPS, mainly consisting of proteins are known to adsorb organic petroleum hydrocarbons such as Phe and benzene. Xu et al. (2018) suggest that the relative abundance of protein to polysaccharides can also be considered a major parameter that regulates the hydrophobicity/ hydrophilicity of EPS. According to Nikolova and Gutierrez (2021), higher enzymatic activity in EPS with higher protein and polysaccharide ratios can be observed in EPS.

Studies conducted by Zhang et al. (2011) using two Phe-degrading bacteria, *Sphingobium* sp. and *Micrococcus* sp., which are capable of producing EPS, suggested that the ratios of CPS proteins to polysaccharides remained constant after incubating with Phe. There was no change in the biochemical composition of CPS, whereas the ratios of RPS proteins to polysaccharides increased for both bacteria, showing that when hydrophobic Phe was used as the substrate, RPS proteins increased faster than RPS polysaccharides. Another important chemical component of the EPS is uronic acid which can efficiently emulsify hydrocarbons. Uzoigwe et al. (2015) state that high uronic acids containing EPS contain lower carbohydrate and protein amounts. Uronic acids confer the ability of the EPS to interface with hydrophobic organic chemicals (such as PAHs). The EPS-mediated increase in the solubilization of hydrocarbons with lower log *P* values may be connected with the polarity of these compounds, allowing them to be moderately associated with the negatively-charged residues of uronic acids that are constituents of the EPS (Gutierrez et al. 2013).

In our experiments, depending on the source of the biofilm ($Pp1_{\mathbf{p}}$, $Nk_{\mathbf{p}}$, $Kk_{\mathbf{p}}$) as well as with the type of culture vessel (hydrophobic/hydrophilic) used production of CPS, RPS, carbohydrate, protein, uronic acids, protein/polysaccharide ratios also varied. No generalizations on specific reasons for such influences can be made because there is very limited knowledge of the effect of surface hydrophobicity/hydrophilicity on the synthesis of EPS. Few reports illustrated that EPS production was influenced by available nutrients and/or surface hydrophobic/hydrophilic properties of the culture vessel. For example, higher EPS concentration of *Botryococcus braunii* in a modified basal medium (MB) when cultivated on a glass fiber-reinforced plastic (hydrophilic) surface in a multilayered photo-bioreactor compared to culture on polyethylene foam (hydrophobic surface). The protein secreted from the biofilm cells was pivotal for strong biofilm adhesion on glass fiber-reinforced plastic (Cheah and Chan, 2021). In the present investigation, in addition to the surface hydrophobicity/hydrophilicity of the cultivation vessel, the adaptive response to PAH exposure was also influential in determining the EPS levels.

References

Abed, R.M., Safi, N.M., Köster, J., De Beer, D., El-Nahhal, Y., Rullkötter, J. and Garcia-Pichel, F., 2002. Microbial diversity of a heavily polluted microbial mat and its community changes following degradation of petroleum compounds. Appl. Environ. Microbiol. 68(4), pp.1674-1683.

Aldaby, E.S.E. and Mawad, A.M.M., 2019. Pyrene biodegradation capability of two different microalgal strains. Glob. Nest. J. 21(3), pp.291-296.

Bai, L., Xu, H., Wang, C., Deng, J. and Jiang, H., 2016. Extracellular polymeric substances facilitate the biosorption of phenanthrene on cyanobacteria *Microcystis aeruginosa*. Chemosphere. 162, pp.172-180.

Bhatnagar, M., Parwani, L., Sharma, V., Ganguly, J. and Bhatnagar, A., 2014. Exopolymers from *Tolypothrix tenuis* and three *Anabaena* sp. (Cyanobacteriaceae) as novel blood clotting agents for wound management. Carbohydr. Polym. 99, pp.692-699.

Boelee, N.C., 2013. Microalgal biofilms for wastewater treatment. Wageningen University and Research. ISBN: 978-94-6173-666-6

Chan, S.M.N., Luan, T., Wong, M.H. and Tam, N.F.Y., 2006. Removal and biodegradation of polycyclic aromatic hydrocarbons by *Selenastrum capricornutum*. Environ. Toxicol. Chem. 25(7), pp.1772-1779.

Cheah, Y.T. and Chan, D.J.C., 2021. Physiology of microalgal biofilm: a review on prediction of adhesion on substrates. Bioengineered. 12(1), pp.7577-7599.

Chen, S., Li, J., Feng, W., Yuan, M., Zhang, W., Xu, H., Zheng, X. and Wang, L., 2020. Biochemical responses of the freshwater microalga *Dictyosphaerium* sp. upon exposure to three sulfonamides. J. Environ. Sci. 97, pp.141-148.

Cole, J.K., Hutchison, J.R., Renslow, R.S., Kim, Y.M., Chrisler, W.B., Engelmann, H.E., Dohnalkova, A.C., Hu, D., Metz, T.O., Fredrickson, J.K. and Lindemann, S.R., 2014. Phototrophic biofilm assembly in microbial-mat-derived unicyanobacterial consortia: model systems for the study of autotroph-heterotroph interactions. Front. microbiol. 5, p.109.

Di Pippo, F., Ellwood, N.T., Gismondi, A., Bruno, L., Rossi, F., Magni, P. and De Philippis, R., 2013. Characterization of exopolysaccharides produced by seven biofilm-forming cyanobacterial strains for biotechnological applications. J. Appl. Phycol. 25(6), pp.1697-1708.

Dubois, M., Gilles, K.A., Hamilton, J.K., Rebers, P.T. and Smith, F., 1956. Colorimetric method for determination of sugars and related substances. Anal. Chem. 28(3), pp.350-356.

Faria, S.I., Teixeira-Santos, R., Romeu, M.J., Morais, J., Vasconcelos, V. and Mergulhão, F.J., 2020. The relative importance of shear forces and surface hydrophobicity on biofilm formation by coccoid cyanobacteria. Polymers. 12(3), p.653.

Fattom, A. and Shilo, M., 1984. Hydrophobicity as an adhesion mechanism of benthic cyanobacteria. Appl. Environ. Microbiol. 47, pp 135–143.

Froehner, S., Machado, K.S., Dombroski, L.F., Nunes, A.C., Kishi, R.T.,Bleninger, T., Sanez, J., 2012. Natural biofilms in freshwater ecosystem: indicators of the presence of polycyclic aromatic hydrocarbons. Water Air Soil Poll. 223(7), pp 3965-3973.

Gacheva, G., Gigova, L., Ivanova, N., Iliev, I., Toshkova, R., Gardeva, E., Kussovski, V. and Najdenski, H., 2013. Suboptimal growth temperatures enhance the biological activity of cultured cyanobacterium *Gloeocapsa* sp. J. Appl. Phycol. 25(1), pp.183-194.

Gutierrez, T., Berry, D., Yang, T., Mishamandani, S., McKay, L., Teske, A. and Aitken, M.D., 2013. Role of bacterial exopolysaccharides (EPS) in the fate of the oil released during the Deep-water Horizon oil spill. Plos one. 8(6), p.-67717.

Govarthanan, M., Mythili, R., Selvankumar, T., Kamala-Kannan, S., Choi, D., Chang, Y.C., 2017. Isolation and characterization of a biosurfactant-producing heavy metal resistant *Rahnella* sp. RM isolated from chromium-contaminated soil. Biotechnol. Bioprocess Eng. 22 (2), 186–194.

Hamouda, R.A.E.F., Sorour, N.M. and Yeheia, D.S., 2016. Biodegradation of crude oil by *Anabaena oryzae*, *Chlorella kessleri* and its consortium under mixotrophic conditions. Int. Biodeterior. Biodegrad. 112, pp.128-134.

Haripriyan, U., Gopinath, K.P., Arun, J. and Govarthanan, M., 2022. Bioremediation of organic pollutants: a mini review on current and critical strategies for wastewater treatment. Arch. Microbiol. 204(5), pp.1-9.

Hong, Y.W., Yuan, D.X., Lin, Q.M. and Yang, T.L., 2008. Accumulation and biodegradation of phenanthrene and fluoranthene by the algae enriched from a mangrove aquatic ecosystem. Mar. Pollut. Bull. 56 (8), pp 1400-1405.

Hyslop, N.P. and White, W.H., 2009. Estimating precision using duplicate measurements. J Air Waste Manag Assoc. 59(9), pp.1032-1039.

Ibraheem, IBM, 2010. Biodegradability of hydrocarbons by cyanobacteria. J. Phycol. 46(4), pp.818-824.

Ichor, T., Gberikon, G.M. and Nevkaa, D., 2016. Biodegradation of phenanthrene by a consortium of aerobic heterotrophic bacteria and cyanobacteria in petroleum hydrocarbon polluted brackish water of Bodo Creek. J. Microbiol. 6, pp.1-8.

Jajoo, A., Mekala, N.R., Tomar, R.S., Grieco, M., Tikkanen, M. and Aro, E.M., 2014. Inhibitory effects of polycyclic aromatic hydrocarbons (PAHs) on photosynthetic performance are not related to their aromaticity. J. Photochem. Photobiol. B: Biol., 137, pp.151-155.

Kumar, R. and Venugopalan, V.P., 2015. Development of self-sustaining phototrophic granular biomass for bioremediation applications. Curr.Sci. pp.1653-1661.

Kumar, M.S., Muralitharan, G. and Thajuddin, N., 2009. Screening of a hypersaline cyanobacterium, *Phormidium tenue*, for the degradation of aromatic hydrocarbons: naphthalene and anthracene. Biotechnol. Lett. 31(12), pp.1863-1866.

Lei, A.P., Hu, Z.L., Wong, Y.S. and Tam, N.F.Y., 2007. Removal of fluoranthene and pyrene by different microalgal species. Bioresour. Technol. 98(2), pp.273-280.

Lowry, O.H., Rosebrough, N.J., Farr, A.L. and Randall, R.J., 1951. Protein measurement with the Folin phenol reagent. J. Biol. Chem. 193, pp.265-275.

Luo, L., Lai, X., Chen, B., Lin, L., Fang, L., Tam, N.F. and Luan, T., 2015. Chlorophyll catalyse the photo-transformation of carcinogenic benzo [a] pyrene in water. Sci. Rep. 5(1), pp.1-11.

Luo, L., Wang, P., Lin, L., Luan, T., Ke, L. and Tam, N.F.Y., 2014. Removal and transformation of high molecular weight polycyclic aromatic hydrocarbons in water by live and dead microalgae. Process. Biochem. 49(10), pp.1723-1732.

Magnusson, M., Heimann, K. and Negri, A.P., 2008. Comparative effects of herbicides on photosynthesis and growth of tropical estuarine microalgae. Mar. Pollut. Bull. 56(9), pp.1545-1552.

Mandal, A., Dutta, A., Das, R. and Mukherjee, J., 2021. Role of intertidal microbial communities in carbon dioxide sequestration and pollutant removal: A review. Mar. Pollut. Bull. 170, p.112626.

Mantzorou, A. and Ververidis, F., 2019. Microalgal biofilms: A further step over current microalgal cultivation techniques. Sci. Total Environ. 651, pp.3187-3201.

McGenity, T.J., Folwell, B.D., McKew, B.A. and Sanni, GO, 2012. Marine crude-oil biodegradation: a central role for interspecies interactions. Aquat. Biosyst. 8(1), pp.1-19.

Mitra, A. and Mukhopadhyay, S., 2016. Biofilm mediated decontamination of pollutants from the environment. Aims. Bioeng. 3(1), pp.44-59.

Mohamed, Z.A., 2001. Removal of cadmium and manganese by a non-toxic strain of the freshwater cyanobacterium *Gloeothece magna*. Water Res. 35(18), pp.4405-4409.

Moreno Osorio, J.H., Pollio, A., Frunzo, L., Lens, P.N.L. and Esposito, G., 2021. A review of microalgal biofilm technologies: definition, applications, settings and analyzing. Front. Chem. Eng. pp.43.

Nhi-Cong, L. T., Lien, D. T., Mai, C. T. N., Linh, N. V., Lich, N. Q., Ha, H. P., and Show, P. L. 2021. Advanced materials for immobilization of purple phototrophic bacteria in bioremediation of oil-polluted wastewater. Chemosphere. 278, 130464.

Nikolova, C. and Gutierrez, T., 2021. Biosurfactants and their applications in the oil and gas industry: current state of knowledge and future perspectives. Front. Bioeng. Biotechnol. pp.46.

Panah, B.A., Najafi, F., Soltani, N., Nejad, R.A. and Babaei, S., 2015. Biodegradation ability and physiological responses of cyanobacterium *Leptolyngbya* sp. ISC 25 under naphthalene treatment. Algologia. 25(2), pp125-134.

Patel, J.G., Kumar, J.N. and Khan, S.R., 2015. Consequences of environmentally hazardous polycyclic aromatic hydrocarbon-anthracene treatment on Cyanobacteria. Int. J. Appl. Sci. Biotechnol. 3(3), pp.381-386.

Poad, S.M. and Derek, C.J.C., 2019. Microalgae adhesion on polymeric membrane. In AIP Conference Proceedings. AIP Publishing LLC. 2124(1), pp. 020061.

Prakash, A.A., Rajasekar, A., Sarankumar, R.K., AlSalhi, M.S., Devanesan, S., Aljaafreh, M.J., Govarthanan, M. and Sayed, S.R., 2021. Metagenomic analysis of microbial community and its role in bioelectrokinetic remediation of tannery contaminated soil. J. Hazard. Mater. 412, p.125133.

Qian, X., Liang, B., Fu, W., Liu, X. and Cui, B., 2016. Polycyclic aromatic hydrocarbons (PAHs) in surface sediments from the intertidal zone of Bohai Bay, Northeast China: Spatial

distribution, composition, sources and ecological risk assessment. Mar. Pollut. Bull. 112(1-2), pp.349-358.

Rath, B., 2012. Microalgal bioremediation: current practices and perspectives. J. Biochem. Technol. 3(3), pp.299-304.

Raungsomboon, S., Chidthaisong, A., Bunnag, B., Inthorn, D. and Harvey, N.W., 2006. Production, composition and Pb^{2+} adsorption characteristics of capsular polysaccharides extracted from a cyanobacterium *Gloeocapsa gelatinosa*. Water Res. 40(20), pp.3759-3766.

Ricart, M., Barceló, D., Geiszinger, A., Guasch, H., de Alda, M.L., Romaní, A.M., Vidal, G., Villagrasa, M. and Sabater, S., 2009. Effects of low concentrations of the phenylurea herbicide diuron on biofilm algae and bacteria. Chemosphere. 76(10), pp.1392-1401.

Ritchie, R.J., 2008. Universal chlorophyll equations for estimating chlorophylls a, b, c, and d and total chlorophylls in natural assemblages of photosynthetic organisms using acetone, methanol, or ethanol solvents. Photosynthetica. 46(1), pp.115-126.

Roeselers, G., Van Loosdrecht, M.C. and Muyzer, G., 2008. Phototrophic biofilms and their potential applications. J. Appl. Phycol. 20(3), pp.227-235.

Rossi, F. and De Philippis, R., 2015. Role of cyanobacterial exopolysaccharides in phototrophic biofilms and in complex microbial mats. Life. 5(2), pp.1218-1238.

Semple, K.T., Cain, R.B. and Schmidt, S., 1999. Biodegradation of aromatic compounds by microalgae. FEMS Microbiol. Lett. 170(2), pp.291-300.

Sorkhoh, N., Al-Hasan, R., Radwan, S. and Hopner, T., 1992. Self-cleaning of the Gulf. Nature. 359(6391), pp.109-109.

Stiefelmaier, J., Strieth, D., Di Nonno, S., Erdmann, N., Muffler, K. and Ulber, R., 2020. Characterization of terrestrial phototrophic biofilms of cyanobacterial species. Algal Res. 50, p.101996.

Taylor, K.A. and Buchanan-Smith, J.G., 1992. A colorimetric method for the quantitation of uronic acids and a specific assay for galacturonic acid. Anal. Biochem. 201(1), pp.190-196.

Traczewska, T.M., Woźniak, B. and Moskal, J., 1999. Application of bioassay with *Selenastrum capricornutum* to evaluation of toxicity of anthracene and phenanthrene in water. Environ. Prot. Eng. 25(4), pp.51-59.

United States Environmental Protection Agency, 1996. Test Method 3510C: Separatory

Uzoh, C.V., Ifeanyi, V.O., Okwuwe, C.I., Oranusi, S.U., Braide, W., Iheukwumere, I.H., Anyanwuocha, C.E. and Ntamzor, B.G., 2015. Effect of light on the biodegradation of crude oil by the algae Closterium species. J. Nat. Sci. Res. 5(22), pp.112-118.

Uzoigwe, C., Burgess, J.G., Ennis, C.J. and Rahman, P.K., 2015. Bioemulsifiers are not biosurfactants and require different screening approaches. Front. Microbiol. 6, p.245.

Vaishnavi, J., Devanesan, S., AlSalhi, M.S., Rajasekar, A., Selvi, A., Srinivasan, P. and Govarthanan, M., 2021. Biosurfactant mediated bioelectrokinetic remediation of diesel contaminated environment. Chemosphere. 264, p.128377.

Veerabadhran, M., Chakraborty, S., Mitra, S., Karmakar, S. and Mukherjee, J., 2018. Effects of flask configuration on biofilm growth and metabolites of intertidal Cyanobacteria isolated from a mangrove forest. J. Appl. Microbiol. 125(1), pp.190-202.

Wang, J.H., Zhuang, L.L., Xu, X.Q., Deantes-Espinosa, V.M., Wang, X.X. and Hu, H.Y., 2018. Microalgal attachment and attached systems for biomass production and wastewater treatment. Renew. Sustain. Energy Rev. 92, pp.331-342.

Wang, Y.S., Wu, F.X., Gu, Y.G., Huang, H.H., Gong, X.Y. and Liao, X.L., 2021. Polycyclic Aromatic Hydrocarbons (PAHs) in the intertidal sediments of Pearl River Estuary: Characterization, source diagnostics, and ecological risk assessment. Mar. Pollut. Bull. 173, p.113140.

Wicke, D., Böckelmann, U. and Reemtsma, T., 2007. Experimental and modeling approach to study sorption of dissolved hydrophobic organic contaminants to microbial biofilms. Water Res. 41(10), pp.2202-2210.

Wicke, D., Böckelmann, U. and Reemtsma, T., 2008. Environmental influences on the partitioning and diffusion of hydrophobic organic contaminants in microbial biofilms. Environ. Sci. Technol. 42(6), pp.1990-1996.

Wyatt, K.H., Seballos, R.C., Shoemaker, M.N., Brown, S.P., Chandra, S., Kuehn, K.A., Rober, A.R. and Sadro, S., 2019. Resource constraints highlight complex microbial interactions during lake biofilm development. J. Ecol. 107(6), pp.2737-2746. Xu, C., Zhang, S., Beaver, **M., Lin,** P., Sun, L., Doyle, S.M., Sylvan, J.B., Wozniak, A., Hatcher, P.G., Kaiser, K. and Yan, G., 2018. The role of microbially-mediated exopolymeric substances (EPS) in regulating Macondo oil transport in a mesocosm experiment. Mar. Chem. 206, pp.52-61.

Zhang, Y., Wang, F., Yang, X., Gu, C., Kengara, F.O., Hong, Q., Lv, Z., Jiang, X., 2011. Extracellular polymeric substances enhanced mass transfer of polycyclic aromatic hydrocarbons in the two-liquid-phase system for biodegradation. Appl. Microb. Biotechnol. 90 (3), 1063–1071.

Zhuang, L.L., Yu, D., Zhang, J., Liu, F.F., Wu, Y.H., Zhang, T.Y., Dao, G.H. and Hu, H.Y., 2018. The characteristics and influencing factors of the attached microalgae cultivation: a review. Renew. Sustain. Energy Rev. 94, pp.1110-1119.

Zyszka-Haberecht, B., Niemczyk, E. and Lipok, J., 2019. Metabolic relation of cyanobacteria to aromatic compounds. Appl. Microbiol. Biotechnol. 103(3), pp.1167-1178.

CHAPTER 5

SUMMARY AND CONCLUSION

This thesis present for the first time **(i)** an evaluation of the amount of PAH contaminants present in the mangrove ecosystem, which is the focus of global conservation efforts.. Mangrove forests and estuaries are among the pristine ecosystems existing on the planet. To compile a detailed picture of PAH pollution status of the Sundarbans, an extensive field sampling including both surface water and sediment was made **(ii)** in vitro application of a patented biofilm-promoting reaction flask to grow the heterotrophic and phototrophic biofilms that were collected from the field in a way that faithfully replicate the field conditions. **(iii)** determining the biofilms potential to remove spiked PAHs that may indicate their contribution in discovering the PAH contaminants in the sediments. In addition, the role of naturally occurring biofilms in intertidal PAH dynamics was evaluated for the first time in any estuary of the world.

This study revealed the current status of PAH contamination in surface water and sediments of the world's largest tidal mangrove ecosystem, the Indian Sundarbans. The prevalent PAH concentrations in the Sundarbans increased considerably concerning the last recorded value in 2012. Disconcertingly, the PAH concentrations exceed ER-L guidelines' values, suggesting that this mangrove forest's prevailing PAHs are likely to cause adverse biological effects. Therefore, there is an urgent necessity to monitor and take remedial actions to ensure the acceptable quality of the sediments. The current study also reveals the presence of intertidal microbial biofilms (heterotrophic and phototrophic biofilms) with remarkable potential for removing contaminants. Using indigenous microbial biofilms found effective in all the geographical locations tested in the present study may be a helpful bioremediation strategy for removing PAH contamination. Furthermore, the metagenomic study of the heterotrophic biofilms suggested that a diverse microbial population was present in the naturally occurring biofilms of the Sundarbans with PAH degradation potential, which may be utilized for the successful remediation of PAH contamination in the field.

Indigenous phototrophic biofilms of the Sundarbans presented a high potential for PAH sequestration. The lowest mean residual amounts of PAHs in the liquid medium and the biofilms were recorded in the Kk_p biofilm cultivated in the hydrophobic flask. Simultaneously, the highest values of biofilm biomass, total chl, RPS carbohydrates, RPS uronic acids, CPS carbohydrates, CPS proteins, and CPS uronic acids were obtained from the same biofilm cultured in the hydrophobic vessel. A strong association between PAH sequestration and biochemical measurements was not observed in the Kk_p biofilm grown in the hydrophilic vessel. In addition, the cultivation vessel impacted the removal of individual PAHs and the synthesis of photosynthetic pigments and EPS. Analyses of the underlying mechanisms were beyond the scope of this study. However, our observations emphasise the hydrophobic/hydrophilic property of the culture surface as a major impelling factor in research involving biofilms. Therefore, the surface property of the culture vessel will affect experimental results and inferences drawn from there. It may also be concluded that heterotrophic and phototrophic biofilm communities from the sampling sites with the highest PAH sediment contaminations (Nk and Kk) adapted themselves by developing biochemical responses to the presence of high levels of PAHs. Clean-up and conservation of contaminated sediments are really challenging, since traditional environmental dredging methods are intrusive,, costly, time consuming and occasionally unsuccessful or difficult to implement on vast and diverse regions. Phototrophic biofilms showed huge potential for field applications in sequestering PAH contaminants compared to the heterotrophic biofilms in mangrove forest intertidal sediments. These films should be propagated in preference to heterotrophic ones due to their enhanced extent of PAH removal compared to heterotrophic biofilms. For a better understanding of the PAH degradation process, the composition of the biofilms with PAH degradation potential and the involvment of external factors influencing breakdown and

transformation of specific PAHs within the biofilms are essential. The information gained from the present study will significantly advance our knowledge and understanding of environmental biofilms and help us foresee their response(s) to PAH pollution. This study should generate knowledge for future applications of biofilms for the bioremediation of various other pollutants in the estuarine waters and sediments.

CHAPTER 6

FUTURE SCOPE OF THE STUDY

In mainstream natural environments, microbes are generally associated with surfaces and interfaces in the form of biofilms, multicellular aggregates that bond together with slime secreted by the microbes within the biofilms. Microbes within a biofilm can resist shear forces, natural deprivation, pH changes, and antibiotics, more evidently due to the mechanical strength of the secreted EPS. The major future scope of this study is translating the laboratory study into the field where PAH sequestration will be assessed through two major bioremediation techniques, such as bio-augmentation and bio-stimulation. The biofilms (Phototrophic and heterotrophic), which showed maximum PAH degradation potential, should be cultivated on a large scale, and the addition of these to the sediments of the intertidal zone of the Indian Sundarbans to attain an acceptable sediment quality—assessing the physico-chemical characteristics and nutrient contents of the sediments and modifying the environment to stimulate the indigenous microbial biofilms present in the contaminated location. Concurrently, microbial diversity and metagenomic study of phototrophic and heterotrophic microbial diversity from the field before and after the bioremediation process helps to characterize the microbes involved in the bioremediation process.

PUBLICATIONS

Environmental Pollution 266 (2020) 115270

Contents lists available at ScienceDirect

Environmental Pollution

journal homepage: www.elsevier.com/locate/envpol

Assessment of polycyclic aromatic hydrocarbon contamination in the Sundarbans, the world's largest tidal mangrove forest and indigenous microbial mixed biofilm-based removal of the contaminants☆

Saranya Balu [a], Shantanu Bhunia [a], Ratan Gachhui [b], Joydeep Mukherjee [a, *]

[a] School of Environmental Studies, Jadavpur University, Kolkata, 700032, India
[b] Department of Life Science and Biotechnology, Jadavpur University, Kolkata, 700032, India

ARTICLE INFO

Article history:
Received 2 March 2020
Received in revised form
18 July 2020
Accepted 22 July 2020
Available online 6 August 2020

Keywords:
Sequestration
Polycyclic aromatic hydrocarbons
Sundarbans
Biofilm
Microbial community

ABSTRACT

The distribution of polycyclic aromatic hydrocarbons (PAHs) in the surface water and sediments in five regions of the Indian Sundarbans was assessed. The capability of microbial biofilm communities to sequester PAHs in a biofilm-promoting vessel was evaluated. The total PAH concentration of water and sediments ranged from undetectable to 125 ng ml^{-1} and 4880 to 2×10^4 ng g^{-1} dry weight respectively. The total PAHs concentration of sediments exceeded the Effects Range–Low value and the recommended Effects Range-Median values, implying the PAHs might adversely affect the biota of the Sundarbans. Pyrogenic and petrogenic sources of PAH contamination were identified in most of the sampling sites. Indigenous biofilms were cultivated in a patented biofilm-promoting culture vessel containing liquid media spiked with 16 priority PAHs. Biofilm-mediated 97–100% removal efficiency of 16 PAHs was attained in all media. There was no significant difference between the mean residual PAH from the liquid media collected from hydrophobic and hydrophilic flasks. Residual amounts of acenaphthene (Ace), anthracene (Ant), benzo(b)fluoranthene [B(b)F], benzo(a)pyrene [B(a)P] and benzo(g,h,i)perylene [B(g,h,i)P] showed differences when cultivated in hydrophobic and hydrophilic flasks. The mean residual amounts of total PAHs extracted from biofilm biomasses were variable. A biofilm obtained from a specific sampling site cultured in the hydrophobic flask showed higher PAH sequestration when compared to the removal attained in the hydrophilic flask. Relative abundances of different microbial communities in PAH-sequestering biofilms revealed bacterial phyla including *Proteobacteria*, *Bacteroidetes*, *Firmicutes*, *Actinobacteria*, *Chloroflexi* and *Planctomycetes* as well as members of *Ascomycota* phylum of fungi. The dominance of *Candida tropicalis*, *Clostridium butyricum*, *Sphingobacterium multivorum* and *Paecilomyces fulvus* were established.

1. Introduction

Sixteen polyaromatic hydrocarbons (PAHs) have been identified and classified as priority pollutants by the United States Environmental Protection Agency (USEPA) based on their toxicity, mutagenicity and carcinogenicity (Potin et al., 2004). The distribution, behavior and sources of PAHs in the different intertidal regions of Asia, Africa, South America and Europe are subjects of recent research (Qian et al., 2016; Raza et al., 2013). The immobilization and remobilization of PAHs from the intertidal sediments can be a threat to the coastal ecosystem as well as to human health (Qian et al., 2016). Therefore, it is crucial to understand the processes which influence the behavior of PAHs in these aquatic systems (Shilla and Routh, 2018). Intertidal biofilm is a ubiquitous thin layer of adhering microorganisms and abiotic community driven by physical processes occurring on intertidal mudflats. A matrix-enclosed community of microphytobenthos, bacteria and organic detritus are bound together and contained within intertidal biofilms. They are attached to the sediment surface by profuse amounts of extracellular polymeric substances secreted by microorganisms living within the biofilm (Jimenez et al., 2015). Intertidal biofilms provide various ecosystem services such as nutrient

☆ This paper has been recommended for acceptance by Eddy Y. Zeng.

* Corresponding author.
E-mail addresses: sarusaranya.balu@gmail.com (S. Balu), shanu.bhunia@gmail.com (S. Bhunia), ratangachhui@gmail.com (R. Gachhui), joydeep.mukherjee@jadavpuruniversity.in (J. Mukherjee).

https://doi.org/10.1016/j.envpol.2020.115270
0269-7491/

recycling, degradation of pollutants, sediment stabilization as well as recruitment of numerous benthic organisms (Passarelli et al., 2015). Although occurring universally in all intertidal regions of the world, the role of intertidal biofilms in the removal of the PAH contaminants was never explored before.

The Sundarbans (meaning the beautiful forest) is the largest contiguous mangrove forest on earth. The Indian Sundarbans is recognized as a UNESCO world heritage site as well as a "Wetland of International Importance" under the Ramsar Convention. This ecosystem receives international attention due to vulnerability to climate change, exploitation of natural resources, human-wildlife conflict and pollution. PAH concentrations in the Sundarbans are of concern due to their potential toxicity to the biota (Binelli et al., 2008; Dominguez et al., 2010). PAH concentrations were higher in comparison to the sediment quality guidelines (Dominguez et al., 2010). The tissue of the intertidal bivalve mollusk *Sanguilonaria (Soletellina) acuminata* accumulated PAHs at concentrations higher than that permitted by the European Commission Regulation (Zuloaga et al., 2009). Total benzo(a)pyrene [B(a)P] toxicity equivalent (TEQ) values in the Indian Sundarbans were higher than that recorded in other estuaries of the world (Zuloaga et al., 2013). PAHs concentration in sediments of the Indian Sundarbans varied from 208 to 12,993 ng g^{-1} dry weight. Fluoranthene (Flu), pyrene (Pyr), benzo(b)fluoranthene [B(b)F], B(a)P and dibenzo (a,h)anthracene [D(a,h)A] were dominant (Zuloaga et al., 2013). No further assessment of PAH contamination in the Indian Sundarbans was done since this report. Moreover, no biological-based strategies to control PAH pollution in the Sundarbans were considered.

We focused on intertidal biofilms of the Sundarbans and the manner these biofilms may be exploited for the removal of PAH polluted sediments. Previously we had described Flu biotransformation by biofilms of *Cunninghamella elegans* isolated from the estuarine mud of North Carolina in an intertidal environment-mimicking bioreactor (Mitra et al., 2013), demonstrating the potential of intertidal microbial biofilms for bioremediation. The objectives of this study are (i) quantitative determination of PAH contaminants present in the Indian Sundarbans (ii) removal of PAH contaminants by applying microbial biofilms in a biofilm-promoting vessel (iii) microbial diversity study of the biofilms capable of sequestering PAH contaminants. The novelties of the present investigation are (i) assessment of the PAH contamination level in a tidal mangrove forest which is the focus of international conservation efforts. Extensive field sampling was done covering three different rivers of the Sundarbans to obtain a comprehensive representation of the status of PAH contamination (ii) application of a patented biofilm-promoting reaction vessel to cultivate the field-collected biofilms in a way to faithfully simulate the field situation in the laboratory (iii) ascertaining the potential of these biofilms to remove spiked pollutants that may indicate their contribution in determining the PAH levels in the sediments.

2. Materials and methods

2.1. Determination of water salinity, sediment organic carbon (OC) and organic matter (OM)

Conductivity of water samples as an indicator of water salinity was determined with Conductivity Meter 36 (Systronics India Ltd., India). The OC content of sediments was determined following Walkley and Black (1934). OM content was calculated from the OC (Radojevic and Bashkin, 1999). $OM(\%) = 1.72 \times OC(\%)$

2.2. Determination of PAHs in water and sediments

PAHs present in water samples was extracted following the USEPA method 3510C liquid-liquid extraction (1996c). The filtered water samples were quantitatively transferred to a separating funnel along with 60 ml dichloromethane (DCM). The organic layer was collected and extraction repeated twice with fresh solvents. The combined extract was concentrated to 2 ml, exchanged to cyclohexane and further concentrated to 2 ml. Sediment samples were air-dried, powdered sieved and the PAHs were extracted following the USEPA method 3540C (1996a). Homogenized samples were extracted with DCM for 16 h using a Soxhlet apparatus. Extracts were concentrated to 2 ml and the solvent was exchanged to cyclohexane.

Silica gel clean-up was carried out following the USEPA method 3630C (1996b) to preclude interference of sulfur compounds. Saturated aliphatic compounds were eluted with hexane and aromatic compounds were washed with DCM/hexane (2:3). All fractions were concentrated to 2 ml. Two microliters of the concentrate was injected to a gas chromatograph equipped with a flame ionization detector (Agilent 7820 A, Agilent Technologies, USA) using nitrogen as the carrier gas following the EPA method 8000 B (1996d). Equipment details, calibration, limits of detection and quantification and quality control procedures are described in Supplementary Text and Supplementary Table 1 a, b and c.

2.3. In-vitro biofilm culturing

Twenty five field-collected biofilm samples were transferred to 200 ml of a modified mixed media consisting of glucose yeast maltose (GYM) for enrichment of all heterotrophic bacteria. Bold's basal media (BBM) fortified with vitamins was used for preferential growth of eukaryotic microalgae and Czapek Dox (CD) broth was applied for enrichment of fungi. ASN III as well as BG 11 media were utilized for enriched growth of phototrophic microorganisms (GYM:BBM:CD:ASN III:BG11 = 1:1:1:1:1) following Zammit et al. (2011). Biofilms were cultivated in fluorescent irradiance (50 μmol photons m^{-2} s^{-1}) with 14:10 h light:dark photoperiod at 25 ± 1 °C.

2.4. Cultivation of biofilms in the patented enhanced surface area conico cylindrical flask (ES-CCF)

Six primarily heterotrophic, stably-growing, robust and well-formed biofilms were selected each representing the different geographical locations: Pg (Purba Gurguria), Mt (Maipit), Pp1 and Pp2 (Patharpratima), Nk (Namkhana) and Kk (Kakdwip). These biofilms were utilized for the removal of the PAHs and were cultured in two sets of the patented ES-CCF possessing hydrophilic glass surface (Set 1) and hydrophobic polymethyl methacrylate (PMMA) surface (Set 2). Approximately 200 mg of biofilm was inoculated in to the sterile mixed medium (section 2.3). After 15 d of incubation, PAHs were spiked in to the glass-ES-CCFs and PMMA-ES-CCFs containing stable biofilms: 5 ppm for Pg and Mt, 15 ppm for Pp1, 10 ppm for Pp2 and Nk, and 25 ppm for Kk biofilms. Another set of biofilms were cultured in the ES-CCFs without the spiked PAHs. Sterile media without PAHs and control flasks containing sterile media spiked with 5, 10, 15 and 25 ppm of PAHs were also incubated. The extent of PAH removal in the liquid medium was determined after 30 d of incubation in duplicate (n = 2) and represented as percent residual PAH. The PAH removal efficiency (%) was: R=(Ci − Cf)/Ci × 100%, where R represents the removal efficiency (%), Ci is the initial and Cf is the final PAH concentration.

2.5. Estimation of PAH contents in biofilms

Biofilms were collected after 30 d and dried by lyophilization (Eyela FDU-1200, Tokyo Rikakikai Co. Ltd, Japan). PAHs were

extracted from dried biofilm samples following Froehner et al. (2012). Extraction by ultrasound sonication was carried out using DCM:methanol (2:1) and twice the volume of DCM. Extracts were combined, concentrated to 2 ml and then subjected to silica gel clean up and GC analysis as described previously (section 2.2).

2.6. Metagenomic analysis of biofilms showing effective removal of PAHs

Metagenomic DNA from biofilms was extracted in triplicate using Nucleospin Soil Kit (TaKaRa Bio Ltd., Japan). Isolated metagenomic DNA was quantified using Thermo Scientific ND-2000 UV-VIS Spectrophotometer. Amplification of the variable region V3–V4 of the 16 S rRNA bacterial gene was carried out using 16 S rRNA forward (5′-GCCTACGGNGGCWGCAG-3′) and 16 S rRNA reverse (5′-ACTACHVGGGTATCTAATCC-3′) primers, whereas the fungal intergenic transcribed spacer (ITS) region was amplified by using ITS forward (5′-GCATCGATGAAGAACGCAGC-3′) and ITS reverse (5′-TCCTCCGCTTATTGATATGC-3′) primers. Three microliters PCR amplified solution was resolved on 1.2% agarose gel for 60 min at 120 V in Tris/borate/EDTA (TBE) buffer. The amplicon libraries were developed using Nextera XT Index Kit (Illumina Inc., USA) following the standard 16 S Metagenomic Sequencing Library preparation method (Part # 15044223 Rev. B), then purified by molecular exclusion applying AMPure XP beads (Beckman Coulter, USA) and quantified using Qubit Fluorometer (Thermo Fischer Scientific, USA). Illumina sequencing was performed on MiSeq using 2 × 300 bp chemistry (~100,000 read per library) after analyzing with 4200 Tape Station System (Agilent Technologies, USA) using D1000 Screen tape.

Bacterial and fungal sequences were analyzed using the Quantitative Insights into Microbial Ecology (QIIME) bioinformatics pipeline (Caporaso et al., 2010). After removing all the chimeric sequences using Trimmomaticv.0.38, representative sequences with ≥3% dissimilarity were clustered into operational taxonomic units (OTUs) using UCLUST (Edgar, 2010) and classified by a naive Bayesian RDP classifier (Wang et al., 2007). OTUs were identified using Greengenes database v.13_8 (16S/archaea database; De Santis et al., 2006) and UNITE database v.7.2 (ITS fungal database) following Nilsson et al. (2018). Sequences are available at the NCBI Sequence Read Archive having accession number PRJNA596375.

2.7. Statistical analyses

Analysis of variance (ANOVA), a two-tailed Student *t*-test and the Pearson correlation were performed using SPSS software (version 16.0). The statistical significance of the results was verified at the significance level of $P \leq 0.05$.

3. Results and discussion

3.1. Water salinity, sediment organic carbon and organic matter

Water, sediments and biofilms from the extensive microbial mats on the surface of the sediments exposed during low tide (Supplementary Figs. 1 and 2) were collected covering five different sampling regions (Fig. 1) namely Purba Gurguria (6 samples), Maipit (3 samples), Patharpratima (5 samples), Namkhana (6 samples) and Kakdwip (5 samples). Mean conductivity varied between 24.3 and 45.5 mS cm^{-1} and the corresponding mean salinity ranged between 11.9 and 27.5 ppt. Higher values of conductivity implied the presence of inorganic ions Mg^{2+}, Ca^{2+}, CO_3^{2-}, HCO_3^-, PO_4^{3-} and NO_3^-. The mean salinity of the sampling sites was similar to previous studies (14–25 ppt) conducted in the Sundarbans by Chaudhuri et al. (2012). The salinity in Kakdwip was comparatively lower due to the continuous influx of freshwater from the Hugli river (Fig. 1). OC contents are presented in Supplementary Table 2. A significant difference in the mean OC and OM contents in the sediments collected at various locations was noted.

3.2. Distribution of PAHs in water

Most of the high molecular weight PAHs (HPAHs) could not be detected in the water samples but some low molecular weight PAHs (LPAHs) were detected (Supplementary Table 3). Ace was the most abundant PAH. The mean concentration of LPAHs was 34.7 ng ml^{-1} while that of HPAHs was 15.9 ng ml^{-1}. Two-three ringed PAHs encompassed 64% while 5–6 ring PAHs comprised 36% of total PAHs in water respectively. Naphthalene (Nap), B(b)F and B(g,h,i)P were found only in Kakdwip, Maipit and Purba Gurguria respectively. Water solubility and high vapor pressure of LPAHs contribute to the dominance of LPAHs in water while low concentration of HPAHs can be ascribed to their hydrophobicity and tendency for adsorption in solid phases (Sun et al., 2009).

Comparing other geographical regions, absence of B(a)P in the water samples was similar to the observation made in the deltaic river waters of Lagos, Nigeria (Olayinka et al., 2018). HPAHs levels were very low or below the quantification limit in this study, similar to the findings in the Mexican estuaries (Jaward et al., 2012). The present contamination level in the Indian Sundarbans was lower compared to the Chinese estuaries (Supplementary Table 4). Previous studies (Sarkar et al., 2012; Zuloaga et al., 2013) on the assessment of PAH contamination in the Sundarbans focused on the sediments and not water.

The sampling sites were located on three of the seven major rivers of the Sundarbans: Purba Gurguria and Maipit on Matla, Patharpratima on Saptamukhi and Namkhana and Kakdwip on Muriganga. Higher water salinities were recorded in Purba Gurguria and Maipit. Concomitantly, the water PAH concentrations in these two locations (Supplementary Table 3) were comparatively higher than those recorded in the water of the other two rivers (Saptamukhi and Muriganga). This observation was in concurrence with Raza et al. (2013) who observed higher PAH concentration correlated with increasing salinity of seawater in the Rembau–Linggi estuary, Malaysia. The rate of microbial biodegradation of PAHs decreases with increasing salinity because high salinity can lower microbial utilization rates. Salinity reduces microbial activity, microbial biomass and changes microbial community structure (Yan et al., 2015). Additionally, inverse relationship between ambient salt concentrations and PAH degradation ability of bacterial isolates from the mangrove swamps in Hong Kong was reported by Tam et al. (2002).

3.3. Distribution of PAHs in sediments

Contrary to the PAH levels evidenced in water samples, HPAHs were more dominant than LPAHs in the sediments (Supplementary Table 5). The mean total concentrations were 1.04 × 10^4 and 2150 ng g^{-1} dry weight for HPAHs and LPAHs respectively, which were significantly different ($P \leq 0.05$). Highest concentrations recorded were B(b)F (7700 ng g^{-1}) in Namkhana followed by benzo(a)anthracene [B(a)A] (6590 ng g^{-1}) in Kakdwip and B(g,h,i)P (5460 ng g^{-1}) in Purba Gurguria. Two-three ringed aromatic PAHs comprised 17% whereas 4 ringed PAH covered 23% while 5–6 ringed PAH constituted 60% of the total PAHs. It is evident from Supplementary Table 5 that the highest and lowest concentrations of all LPAHs were recorded in different locations except Nap and acenaphthylene (Acy). B(a)A, benzo(k)fluoranthene [B(k)F] and B(a)P were recorded in different stations, while maximum and minimum levels of Flu, B(b)F, Pyr, B(g,h,i)P, chrysene (Chr), indeno

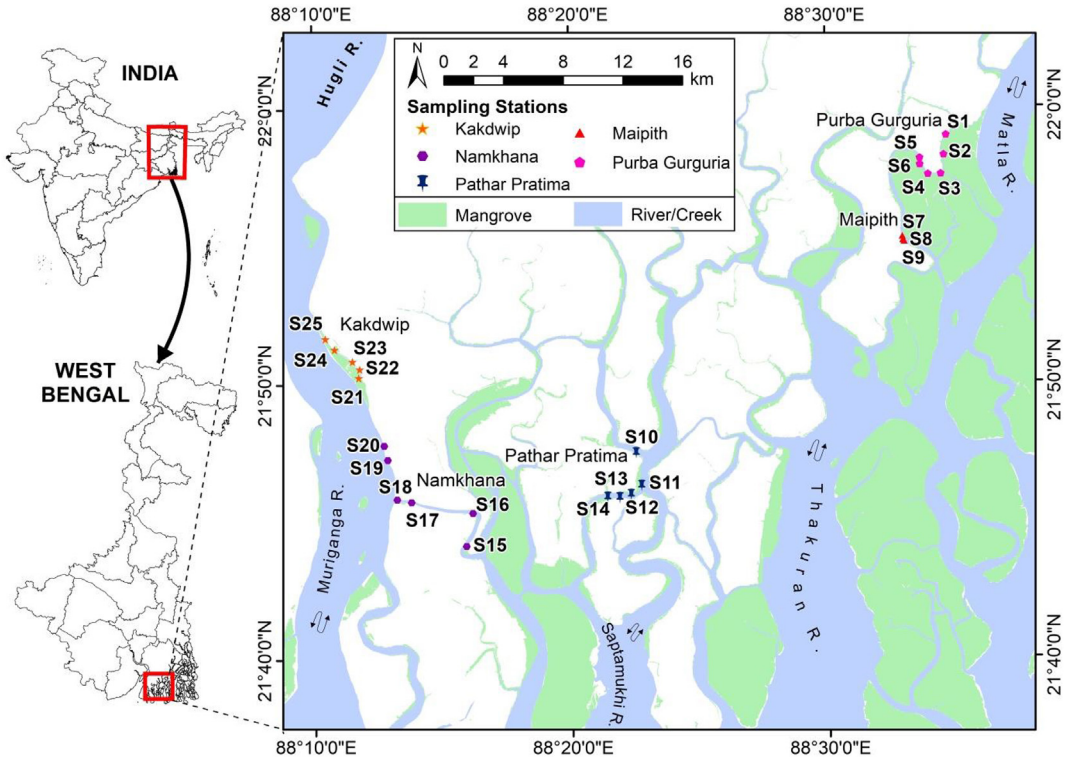

Fig. 1. Five different sampling regions in the Indian Sundarbans namely Purba Gurguria (6 samples); Maipit (3 samples); Patharpratima (5 samples); Namkhana (6 samples); Kakdwip (5 samples). Water, sediments and biofilms were collected from the extensive microbial mats on the surface of the sediments exposed during low tide.

(1,2,3-cd) pyrene (Ind) and D (a,h)A were found in the same locations although their concentrations were significantly different.

The mean concentration of PAH in sediments ranged from 4880 to 2×10^4 ng g^{-1} dry weight. Previous work on the distribution of PAH in sediments of the Sundarbans (Sarkar et al., 2012) showed high concentration of PAH contaminants in the Kakdwip region like the present study (2×10^4 ng g^{-1}), which was much higher than the value reported (500 ng g^{-1}). Zuloaga et al. (2013) reported 208.3–12993.1 ng g^{-1} dry weight of 16 PAHs from nine sampling locations of the Indian Sundarbans. Our results suggest an escalation of the contaminant concentration in the Sundarbans over these years. Higher abundance of 3–5 ringed PAHs especially Ace, B(a)A, B(b)F and B(a)P was observed in the Kakdwip region corroborating previous studies in the Sundarbans (Sarkar et al., 2012; Zuloaga et al., 2013) showing predominance of 3–5 ringed PAHs in Kakdwip. Dominguez et al. (2010) demonstrated a similar prevalence of 4–6 ringed PAHs in sediments of the Sundarbans. The hydrodynamic regime of the Saptamukhi river represents a tidal inlet where the mixing of ebb and flood flows because of tidal asymmetry resuspends the sediments (Dominguez et al., 2010; Sarkar, 2016). This local resuspension process influenced the PAH concentration recorded in Patharpratima. Shipping activities are more pronounced along the Muriganga compared to the other rivers (Matla and Saptamukhi) and the consequential contamination was reflected in the high PAH levels in sediments of Kakdwip. Sarkar et al. (2012) remarked that the high concentration of PAHs evidenced in Kakdwip may be associated with urban runoffs, sewage and waste discharges as well as intensive boating activities.

The present sediment contamination level in the Indian Sundarbans was higher compared to estuaries located in other countries (Supplementary Table 4). The total PAH concentrations of sediments exceeded the Effects Range–Low (ER-L) value (2970 ng g^{-1}). Pyr concentration was lower than the ER-L (665 ng g^{-1}) in all the stations while the other 15 PAHs exceeded the ER-L values in at least one sampling station (Supplementary Table 5). The Effects Range-Median (ER-M values) of Ace from all stations, fluorene (Flr) from Patharpratima and B(a)A from Kakdwip were found to be higher than the recommended ER-M values (Supplementary Table 5). The excessive ER-L and ER-M values of PAHs suggested that the contaminants might adversely affect the biota of the Sundarbans (Kim et al., 1999; MacDonald et al., 2000). Ace concentration recorded in all the stations, phenanthrene (Phe) detected in Purba Gurguria, Flu level found in Namkhana, B(a)A concentration recorded in Kakdwip and B(a)P detected in all stations except Namkhana showed Apparent Effects Threshold (AET) values greater than the reference values (Kim et al., 1999).

A moderately positive correlation was observed between OC content and PAH ($r^2 = 0.44$) and between OM and PAH ($r^2 = 0.44$) as shown in Fig. 2. Higher PAH concentration recorded in Kakdwip and Purba Gurguria may be related to the higher OC of the sediments. Likewise, the lower PAH level in Maipit may be associated with the lower sediment OC. However, despite low sediment OC content, the PAH concentration was high in Namkhana. OC content and PAHs showed a positive linear relationship (Liu et al., 2017). The sediments rich in OM had a complex pore structure and this complexity allowed PAHs to be absorbed easily by the OM making them a repository of PAHs (Liu et al., 2017). A strong correlation between OC and PAH can be expected only when the PAH present in the soil or sediments are fully integrated into the soil particles (Sojinu et al., 2010). A weak correlation implies a continuous influx of fresh hydrocarbon which is not fully assimilated into the soil OM. Raza et al. (2013) did not find any correlation between sediment PAH concentrations and OC content in the Rembau–Linggi estuary, Malaysia. Authors concluded that association of sediment PAH level with OC was significant only for highly contaminated sites where the total PAH concentrations were greater than 2000 ng g^{-1}. Sarkar

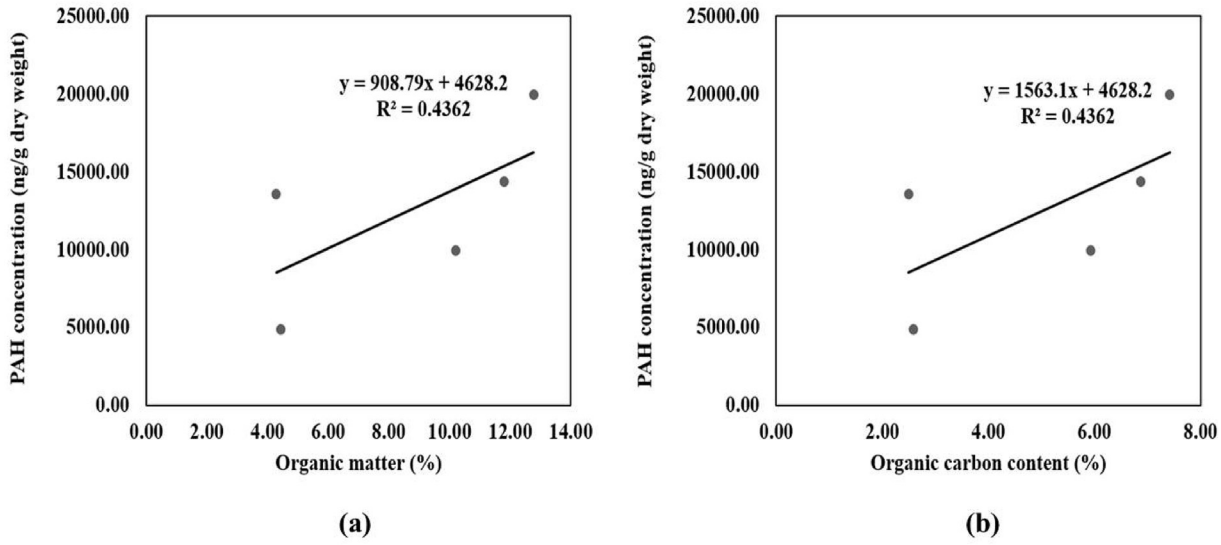

Fig. 2. **(a)** Correlation of organic matter with total PAHs (ng g^{-1} dry weight) in sediments and **(b)** correlation of organic carbon with total PAHs (ng g^{-1} dry weight) in sediments. Organic carbon content of sediments was determined following Walkley and Black (1934). Organic matter content was calculated from the organic carbon of the sediments (Radojevic and Bashkin, 1999). Organic matter (%) = 1.72 × organic carbon (%). Pearson correlation was performed using SPSS software (version 16). A moderately positive correlation was observed between OC and PAH ($r^2 = 0.44$) and between OM and PAH ($r^2 = 0.44$).

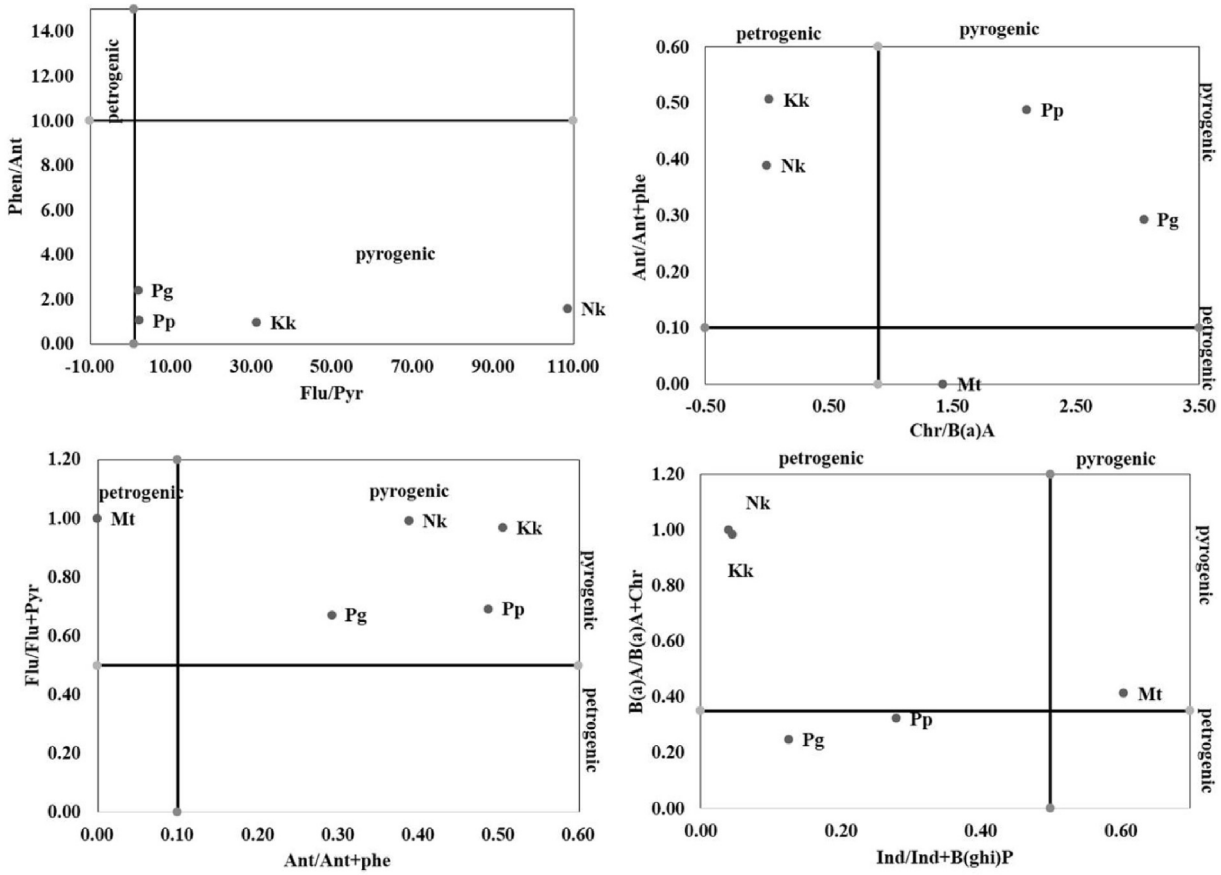

Fig. 3. Scatterplot for identification of PAH sources (pyrogenic/petrogenic) Pg-Purba Gurguria, Mt-Maipit, Pp-Patharpratima, Nk- Namkhana and Kk – Kakdwip. Phe/Ant ratio ranged from 0.98 to 2.41, Ant/Ant + Phe varied from 0.0 to 0.51, Chr/B(a)A varied from 0 to 3.05, B(a)A/B(a)A + Chr ranged from 0.25 to 1, Ind/Ind + B(g,h,i)P varied from 0.04 to 0.60, Flu/Flu + Pyr ratio ranged from 0.67 to 1 and Flu/Pyr ratio ranged from 2.04 to 108.69. Both pyrogenic and petrogenic sources of PAH contamination occurred in all the sampling sites except Maipit where pyrogenic source of contamination was indicated.

et al. (2012) reported a weak correlation ($r^2 = 0.014$) between OC and total PAH in the Sundarbans. However, Sarkar et al. (2016) while sampling locations other than those reported by them earlier (Sarkar et al., 2012) found an association between high sediment PAH accumulation and high OM content. Zuloaga et al. (2009) observed relationship between low sediment OC and low PAH concentration in sites of the Sundarbans. Thus, sediment OC content is a significant but not the only factor influencing sediment PAH levels in the Sundarbans. It should also be considered that the spatial distribution of PAHs in surface sediments is influenced by the hydrodynamic conditions of the Sundarbans estuary such as textural composition and depositional rate of sediments, input rate of PAHs, differential resuspension and redeposition of sedimentary PAHs, vertical mixing due to physical or biological processes and microbial degradation of PAHs (Sarkar et al., 2016). Future studies should integrate salinity and OC with these factors to derive a comprehensive relationship between sedimentary PAH concentration and environmental factors.

3.4. Identification of PAH sources (petrogenic/pyrogenic) from sediment data

Phe/Ant and Flu/Pyr ratios indicated pyrogenic source of PAHs namely Phe, Ant, Flu and Pyr in four stations except Maipit (Fig. 3, Supplementary Table 6). Chr and B(a)A ratios indicated pyrogenic as well as the petrogenic origin; pyrogenic sources were observed in all stations except Kakdwip where petrogenic origin was identified. Ind/Ind + B(g,h,i)P ratio implied a dominant petrogenic source of Ind and B(g,h,i)P in Purba Gurguria, Namkhana and Kakdwip; pyrogenic origin was evident only in Maipit.

Petrogenic source of contamination can be characterized by two to three-ringed PAHs. Four to six-ringed PAHs which are thermodynamically more stable and toxic than the two to three-ringed PAHs are suitable indicators of pyrogenic source of PAH contamination (Adeniji et al., 2018). Our results are in agreement with the findings of Dominguez et al. (2010) recorded in the Sundarbans sediments as well as with that measured in the sediments along the Hugli river estuary (Guzzella et al., 2005). PAHs in the sediments are introduced from coal and biomass combustion. Both pyrogenic and petrogenic sources of PAH contamination occurred in all the sampling sites except Maipit where pyrogenic source of contamination was indicated. Ind/[Ind + B(g,h,i) P] isomer ratios indicated petrogenic as well as pyrogenic origin of PAHs corroborating previous records. Use of coal, charcoal and wood for domestic cooking, rice husking and coal power stations play a major role in contributing PAHs to the Sundarbans environment (Chatterjee et al., 2009). Urban runoff, automobile emission and river discharges also act as important sources of PAHs in coastal sediments Pait et al. (2008).

3.5. Removal of PAHs from PAH-spiked media by biofilms

Biofilms were cultured in hydrophobic PMMA vessels (PMMA-ES-CCF) and hydrophilic glass vessels (Glass-ES-CCF) (US patent 8,945,917 B2, Sarkar et al., 2015; Supplementary Figs. 3 and 4). Concentrations of spiked PAH were in consistency with the total PAHs recorded in their respective geographical locations. Treatment of PAH-spiked media with microbial biofilms collected from different geographical locations did not show any significant differences in residual PAHs (Supplementary Table 7). There was no significant difference between the mean residual PAHs from the liquid media between PMMA and glass ES-CCFs ($P \leq 0.05$). However, residual amounts of certain PAHs such as Ace, Ant, B(b)F, B(a)P and B(g,h,i)P showed differences in their sequestration when cultivated in flasks with hydrophobic and hydrophilic surfaces. Sequestration of Ace (Kk biofilm) and Ant (Mt biofilm) were found to be better in hydrophobic than in hydrophilic surface flask. Extent of B(b)F sequestration with Pg biofilm cultured in PMMA-ES-CCF was higher compared to glass-ES-CCF whereas Pp1 biofilm showed higher removal of B(b)F in glass-ES-CCF compared to the PMMA-ES-CCF. Hydrophilic ES-CCF was found to be more efficient for the sequestration of B(g,h,i)P with Pg biofilm while the same PAH was removed to a greater extent by Mt, Pp1, Pp2 and Nk biofilms in glass-ES-CCF than PMMA-ES-CCF. B(a)P was eliminated more effectively in the hydrophilic vessel compared to the hydrophobic one. At most 30% PAH was lost during incubation and extraction procedure. Biofilm-mediated 97–100% removal efficiency of individual PAHs was observed in all media.

The residual amounts of PAHs from biofilms varied between 0 and 106% which showed a greater significant difference at $P \leq 0.05$ in contrast to the residual amounts in the liquid medium (Table 1). The mean residual amounts of total PAHs in biofilms were in the order Pp1<Kk < Nk < Pp2<Mt < Pg. The Mt biofilm cultured in hydrophobic PMMA-ES-CCF showed higher PAH sequestration

Table 1
Residual amounts (as percentage) of spiked 16 priority PAHs from biofilm biomass developed in glass and PMMA ES-CCF after 30 d incubation. The residual amounts that are at least double of each other (PMMA ES-CCF compared to glass ES-CCF or vice versa) are shown in bold letters. Values are the average of two determinations and the mean absolute deviations were found between 0.01 and 4.58.

COMPONENTS	Pg		Mt		Pp1		Pp2		Nk		Kk	
	Glass	PMMA	Glass	PMMA	Glass	PMMA	Glass	PMMA	Glass	PMMA	Glass	PMMA
Naphthalene	64.1	50.7	**78.5**	**30.9**	10.8	9.1	34.8	47.3	17.6	33.3	7.9	9.7
Acenaphthylene	43.8	28.1	**62.3**	**18.9**	10.8	6.7	21.7	41.1	**14.9**	**31.1**	12.7	21.4
Acenaphthene	**12.5**	**27.9**	79.6	43.2	**17.8**	**36.5**	**62.6**	**28.1**	63.9	42.4	72.7	73.6
Fluorene	20.7	18.3	**29.2**	**9.7**	8.0	5.6	7.0	6.9	9.4	17.3	5.7	10.1
Phenanthrene	**18.1**	**9.2**	**37.7**	**15.5**	16.0	13.9	27.2	35.1	14.9	9.0	9.2	9.0
Anthracene	74.9	49.5	**106**	**37.8**	**25.6**	**10.1**	**70.4**	**40.4**	**14.8**	**35.4**	21.2	17.9
Fluoranthene	**26.1**	**76.7**	32.7	27.5	**23.1**	**11.1**	34.6	40.1	17.1	29.8	**5.7**	**18.6**
Pyrene	**58.9**	**12.7**	29.2	28.3	6.4	0.0	**55.1**	**20.5**	14.4	24.2	**4.0**	**13.5**
Benzo(a)anthracene	99.9	94.5	**57.3**	**27.0**	**27.1**	**12.1**	58.9	39.0	**21.0**	**59.4**	26.4	26.0
Chrysene	80.0	56.5	**53.4**	**6.3**	12.1	0.0	8.9	9.6	18.0	16.6	14.1	12.1
Benzo(b)flouranthene	66.8	89.8	66.7	56.9	**56.5**	**22.7**	**52.7**	**22.5**	**15.9**	**33.1**	23.6	14.0
Benzo(k)fluoranthene	**0.0**	**21.9**	**49.3**	**0.0**	0.0	6.9	36.3	46.6	0.0	0.0	0.0	0.0
Benzo (a)pyrene	58.0	56.3	63.8	44.5	**6.4**	**32.2**	75.1	53.6	**81.5**	**18.2**	**5.1**	**20.2**
Indeno(1,2,3-cd) Pyrene	88.9	59.9	85.4	66.3	**36.2**	**9.0**	74.7	59.0	**36.3**	**74.4**	26.5	32.4
Dibenz(a,h) anthracene	**11.7**	**54.4**	**49.2**	**25.7**	**27.7**	**7.1**	57.1	56.8	**15.6**	**43.8**	31.6	37.7
Benzo(g,h,i)perylene	57.4	87.9	**79.6**	**22.6**	**21.4**	**79.6**	72.7	52.9	**22.4**	**52.0**	**63.2**	**27.6**
Mean PAH residual amounts	48.9	49.6	60.0	39.6	19.1	16.4	46.9	37.5	29.2	32.5	20.6	21.5

when compared to the removal attained in the hydrophilic glass-ES-CCF. Additionally, the residual amounts of all the individual PAHs were lower in the PMMA- ES-CCF in comparison to the glass-ES-CCF. Such consistent variations were not observed in the other five biofilms (Table 1). The PAHs, irrespective of their physico-chemical properties were sequestered more effectively by the Mt biofilm formed on the hydrophobic surface in comparison to the biofilm on the hydrophilic surface. Such differences may be explained by the inherently hydrophobic cell surface character of the different microbial members of the Mt biofilm that may have favored better attachment and biofilm formation on the hydrophobic surface in contrast to the hydrophilic surface. However, experimental confirmation was beyond the scope of this work. Further insights may be obtained from measurements of biofilm weight, amounts of exopolymeric substances and composition, cell surface hydrophobicity, PAH-metabolizing gene expression and multi-channel confocal laser scanning microscopy (Mitra et al., 2013, 2015).

All the 16 priority pollutants were completely sequestered by the biofilm biomass because near 100% removal was observed in the liquid medium. Some PAHs may be adsorbed on the biofilm surface. The PAHs were then partially removed by the different microbial members of the biofilm (20–60% residual amounts in Table 1). Thus, the microbial biofilm behaved as a repository holding the unremoved PAHs inside its structure after initial sequestration while the surrounding water remained free of the contaminant (Supplementary Fig. 5). However, this hypothesis requires further experimental substantiation. The determination of the water/biomass OC distribution coefficients and diffusion coefficients of the individual PAHs (Wicke et al., 2007) is essential. The composition of the biofilm and the role of external effects on the partitioning of the individual PAHs inside the biofilm and the transformation of the individual PAHs such as enzymatically catalyzed inclusion of hydroxyl or carboxyl moieties by different microbial members of the biofilms (Wicke et al., 2008) are necessary.

There are evidences to corroborate the differences in the removal of the specific PAHs recorded in Supplementary Table 7 and Table 1. However, the establishment of a regular rule to justify the observations should be the subject of separate investigations. It may be presumed the removal of the PAHs by the glass and PMMA-ES CCF was dependent on the specific PAH and the quality and composition of the biofilm. For example, the water/biomass OC distribution coefficients and diffusion coefficients of Phe and Pyr in a biofilm were substantially dissimilar (Wicke et al., 2007). The quality and composition of the biofilm was governed by the cell surface hydrophobicity of the biofilm and the hydrophobicity/hydrophilicity of the biofilm-forming surface (Mitra et al., 2013, 2015) while the accessibility of an individual PAH was dependent on its hydrophilicity and water content of the biofilm (Wicke et al., 2008). Only two hydrocarbon-utilizing γ-proteobacterial genera were found in the biofilm described by Al-Bader et al. (2013) probably due to specific cell surface properties that allowed adherence to the hydrophilic surfaces only. The use of hydrophobic surfaces may lead to the attachment of other indigenous marine oil-utilizing bacteria.

3.6. Abundance, diversity and composition of PAH-sequestering microbial communities

The 16 S rRNA and ITS gene sequencing of Pp1, Nk, and Kk biofilms which showed the highest PAH sequestration was performed. Gel electrophoresis of the PCR products showed specific bands which co-migrated on the gels (Supplementary Fig. 6). 120,840–145,556 high quality reads per sample from 16 S rRNA V3–V4 and 183,515–235,377 valid reads per sample from ITS sequencing were obtained respectively. Shannon indices (Supplementary Tables 8 and 9) showed that Kk biofilm had more diverse bacterial and fungal communities than Pp1 and Nk biofilms. A sizeable number of the total species: 25.82%, 47.5% and 42.31% in Pp1, Nk and Kk biofilms respectively were unclassified. The rarefaction curves (Supplementary Fig. 7) indicated that bacterial as well as fungal species richness were higher in the Pp1 and Kk biofilms in comparison to the Nk biofilm.

Relative abundances of different microbial communities (Supplementary Table 10 and Fig. 4 a and b) revealed the presence of bacterial phyla *Proteobacteria* (26.3–34.1%), *Bacteroidetes* (24.3–32.9%), *Firmicutes* (19.9–38.6%), *Actinobacteria* (1.3–2.1%), *Chloroflexi* (0.8–2.3%) and *Planctomycetes* (0–15.3%) as well as members of *Ascomycota* (100%) phylum of fungi in PAH-sequestering biofilms of Pp1, Nk, and Kk. The most abundant bacterial phylum was *Firmicutes* (38.6%) in Pp1 followed by *Bacteroidetes* (32.9%) and *Proteobacteria* in Nk and Kk with 34.1% and

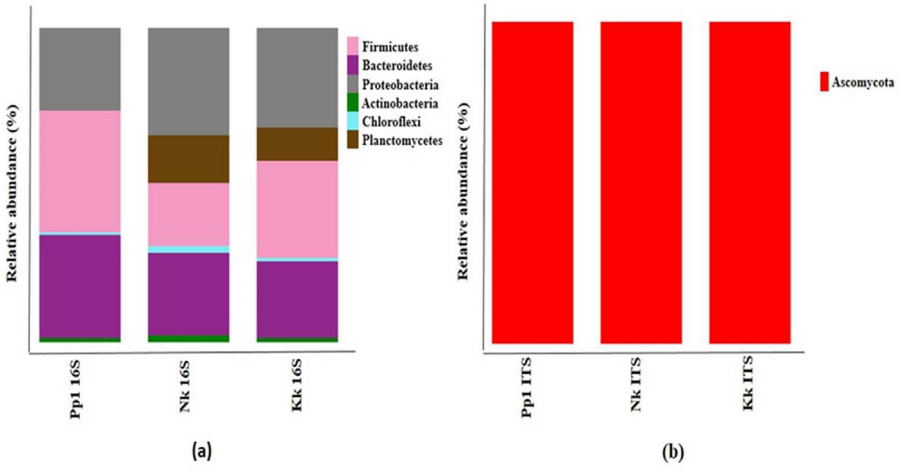

Fig. 4. Relative abundance of **(a)** PAH sequestering bacterial phyla as determined by 16 S rRNA gene sequencing and **(b)** PAH sequestering fungal phyla as determined by intergenic transcribed spacer (ITS) gene sequencing in three biofilms (Pp1, Nk and Kk). Amplification of the V3–V4 region of 16 S rRNA bacterial gene and ITS of fungal gene was carried out. High throughput Illumina sequencing was performed on MiSeq using 2 × 300 bp chemistry. Bacterial and fungal sequences were analyzed using the Quantitative Insights into Microbial Ecology (QIIME) bioinformatics pipeline. Details provided in Section 2.6.

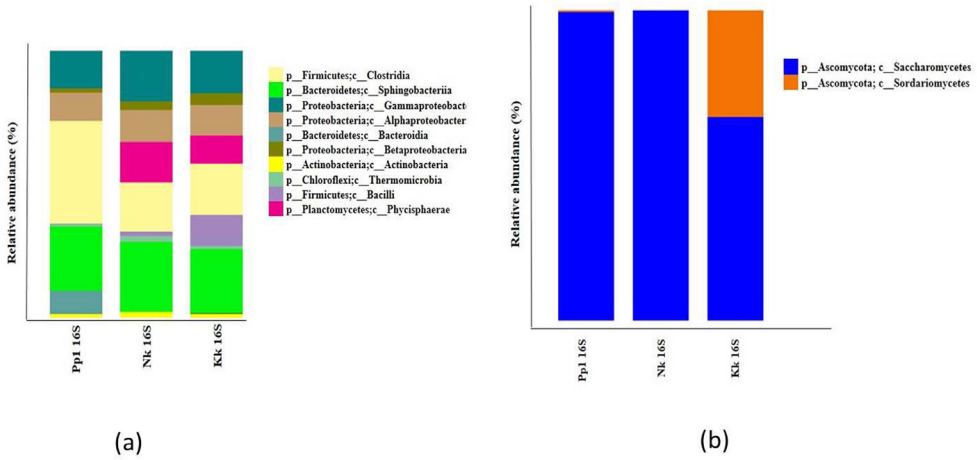

Fig. 5. Class level relative abundance of **(a)** PAH sequestering bacteria and **(b)** PAH sequestering fungi in three biofilms (Pp1, Nk and Kk). Amplification of the V3–V4 region of 16 S rRNA bacterial gene and intergenic transcribed spacer (ITS) of fungal gene was carried out. High throughput Illumina sequencing was performed on MiSeq using 2 × 300 bp chemistry. Bacterial and fungal sequences were analyzed using the Quantitative Insights into Microbial Ecology (QIIME) bioinformatics pipeline. Details provided in Section 2.6.

31.7% dominance respectively; and subsequently *Firmicutes* (31%) in Kk and *Bacteroidetes* (26.2%) in Nk. Nine PAH-sequestering classes of bacteria namely *Sphingobacteria* (24.1–26.2%), *Clostridium* (18.3–38.5%), *Gammaproteobacteria* (14.1–16%), *Alphaproteobacteria* (10.4–11.9%), *Betaproteobacteria* (1.8–4.5%), *Actinobacteria* (1.3–2.1%), *Bacilli* (0.1–11.8%), *Bacteroidia* (0–8.8%) and *Phycisphaerae* (0–15.3%) were detected from Pp1, Nk, and Kk biofilms (Fig. 5a). Fungal class *Saccharomycetes* (99.5% in Pp1, 100% in Nk, and 65.40% in Kk) were found to be dominant and Kk biofilm had 34.5% abundance of class *Sordariomycetes* (Fig. 5b). *Clostridium butyricum* (47%) and *Sphingobacterium multivorum* (38%) were the most abundant bacterial taxa in Pp1, whereas the dominance of *Sphingobacterium multivorum* was 66% in Nk and 53% in Kk respectively (Supplementary Fig. 8a). The abundance of *Candida tropicalis* was 99% in Pp1, 100% in Nk and 65% in Kk and *Paecilomyces fulvus* accounted for 35% of the total fungal sequences (Supplementary Fig. 8b). Supplementary Fig. 9 shows higher numbers of bacterial OTUs shared between Pp1 and Nk biofilms in comparison to those in common between Nk and Kk as well as Kk and Pp1 biofilms. Only 14 out of 1047 OTUs were mutual among the three biofilms.

Biodegradation capacity of strains obtained from hydrocarbon-contaminated environments was higher than those isolated from uncontaminated sediments because certain bacteria had acclimatized and adapted themselves to the contaminated environment (Tam et al., 2002). In the present study, biofilms were grown with PAHs as the sole source of carbon. Therefore, only specialized bacteria and fungi which were able to sequester the PAH compounds proliferated. Recently, Lee et al. (2018) reported only three dominant phyla (*Proteobacteria*, *Firmicutes* and *Bacteroidetes*) in the PAH-contaminated Sinduri beach in Korea. We found six phyla in the examined biofilms, higher than that obtained by Lee et al. (2018). The different bacterial as well as fungal phyla, classes, genera and species found to sequester the PAHs in the present study have also been detected by other researchers from various ecosystems. Silva et al. (2013) detected abundance of *Firmicutes* and *Proteobacteria* from the Brazilian oil fields while Grula et al. (1982) observed dominance of *Proteobacteria* and *Chloroflexi* in water-flooded oil reservoirs of China. Likewise, Oko et al. (2017) confirmed that *Clostridium* was responsible for the degradation of naphthenic acid and other PAHs. Gram-positive and endospore-forming *Firmicutes* especially members of *Clostridia* multiplied fast in presence of Nap (Abercron et al., 2016). River sediments from Taiwan which were rich in *Clostridium* showed 90% degradation of Ace, Ant, Flr, Phe and Pyr (Yuan and Chang, 2007). Similarly, degradation of Nap by *Sphingobacterium multivorum* was reported by Abarian et al. (2018) from PAH contaminated sites of Iran. The Phe degradation potential of *Sphingobacterium* isolated from contaminated municipal sludge was demonstrated by Ji et al. (2015). Lafortune et al. (2009) confirmed that *Bacteroidetes* isolated from pristine soil played a key role in the degradation of HPAHs. Higher abundance of fast-growing copiotrophs like *Proteobacteria*, *Bacteroidetes*, *Firmicutes* and *Planctomycetes* in the Sundarbans indicated a high organic load while slow-growing *Actinobacteria* and *Chloroflexi* tended to be abundant in low nutrient concentrations (Dai et al., 2016). Ghosh et al. (2010) also found *Gammaproteobacteria* to be the most abundant in hydrocarbon and oil contaminated sediments of the Sundarbans.

Most of the members of the phylum *Ascomycota* frequently grew in anthropogenically polluted sites (Aranda et al., 2016) and enhanced the bioavailability and degradability of PAHs (Zafra et al., 2014). Hagler et al. (1979) reported *Candida* as the most frequently isolated genera from a polluted Brazilian estuary. Similarly, Norkrans (1996) and MacGillivray and Shiaris (1993) found *Candida* as the most abundant taxa in a Swedish estuary and Massachusetts coastal sediments respectively. According to Gargouri et al. (2015) *Candida tropicalis* degraded 97% of the total petroleum hydrocarbons in 20 d. Dawoodi et al. (2015), Al-Nasrawi (2012) and Ameen et al. (2016) reported hydrocarbon utilization and degradation by *Paecilomyces* genera isolated from crude oil contaminated sites of Iran, Gulf of Mexico and mangroves of Red Sea Coast in Saudi Arabia respectively. Thus, specific bacteria and fungi are preferentially selected for the sequestration of PAHs and this selection process affects the community structure of a PAH-challenged microbial population.

4. Conclusion

We not only highlighted the problem of PAH contamination in the world's largest mangrove forest but also revealed the potential of intertidal microbial biofilms for the removal of the contaminants. This ability of the biofilms may be investigated in other intertidal regions of the world. There is an urgent necessity to monitor and take remedial actions to ensure acceptable quality of the sediments. This investigation provides strong evidence of the presence of bacterial and fungal species structured in well-formed biofilms that

can effectively remove PAH pollutants. The results should be the foundation for further field investigations. Field conditions such as nutrient levels, redox potential and presence of competing micro as well as macro-organisms will drastically alter the PAH sequestering community. The aim of the field study will be to maximize the activities of the PAH sequestering bacteria and fungi identified in this laboratory study in the real intertidal situation considering the prevalent field conditions.

Main finding

Laboratory grown indigenous microbial biofilms isolated from naturally occurring estuarine biofilms were found to be effective for removal of PAH contamination.

Credit author statement

Saranya Balu, Shantanu Bhunia, Ratan Gachhui, Joydeep Mukherjee, Conceptualization: Joydeep Mukherjee, Data curation, Formal analysis: Saranya Balu, Shantanu Bhunia, Funding acquisition: Joydeep Mukherjee, Ratan Gachhui, Investigation: Saranya Balu, Shantanu Bhunia, Methodology: Saranya Balu, Shantanu Bhunia, Project administration: Joydeep Mukherjee, Resources, Software, Supervision: Joydeep Mukherjee, Ratan Gachhui, Validation, Visualization: Joydeep Mukherjee, Roles/Writing - original draft: Saranya Balu, Shantanu Bhunia, Writing - review & editing: Joydeep Mukherjee

Declaration of competing interest

The authors declare that they have no known competing financial interests or personal relationships that could have appeared to influence the work reported in this paper.

Acknowledgments

Authors thank the Department of Biotechnology, Government of West Bengal, India [72 (Sanc.)-BT/P/Budget/RD-34/2017] for financial support. Technical help in preparing the map from Sourav Samanta, School of Oceanographic Studies, Jadavpur University is thankfully acknowledged. Authors thank Sanjoy Mondal (Sundarbans Safari) for organizing the field cruise.

Appendix A. Supplementary data

Supplementary data to this article can be found online at https://doi.org/10.1016/j.envpol.2020.115270.

References

Abarian, M., Hassanshahian, M., Badoei-Dalfard, A., 2018. Isolation, screening, and characterization of naphthalene-degrading bacteria from Zarand Mine, Iran. Polycycl. Aromat. Comp. 38, 410–419. https://doi.org/10.1080/10406638.2016.1224260.

Abercron, M.V., Pacheco, D., Benito-Santano, P., Marin, P., Marques, S., 2016. Polycyclic aromatic hydrocarbon-induced changes in bacterial community structure under anoxic nitrate reducing conditions. Front. Microbiol. 7, 1–16. https://doi.org/10.3389/fmicb.2016.01775.

Adeniji, A.O., Okoh, O.O., Okoh, A.I., 2018. Analytical methods for polycyclic aromatic hydrocarbons and their global trend of distribution in water and sediment: a review. In: Zoveidavianpoor, M. (Ed.), Recent Insights in Petroleum Science and Engineering. InTech Open, Croatia, pp. 393–423. https://doi.org/10.5772/intechopen.71163.

Al-Bader, D., Kansour, M.K., Rayan, R., Radwan, S.S., 2013. Biofilm comprising phototrophic, diazotrophic, and hydrocarbon-utilizing bacteria: a promising consortium in the bioremediation of aquatic hydrocarbon pollutants. Environ. Sci. Pollut. Res. 20, 3252–3262. https://doi.org/10.1007/s11356-012-1251-z.

Al-Nasrawi, H., 2012. Biodegradation of crude oil by fungi isolated from Gulf of Mexico. J. Biorem. Biodegrad. 3, 1–6. https://doi.org/10.4172/2155-6199.1000147.

Ameen, F., Moslem, M., Hadi, S., Al-Sabri, A.E., 2016. Biodegradation of diesel fuel hydrocarbons by mangrove fungi from Red Sea Coast of Saudi Arabia. Saudi J. Biol. Sci. 23, 211–218. https://doi.org/10.1016/j.sjbs.2015.04.005.

Aranda, E., 2016. Promising approaches towards biotransformation of polycyclic aromatic hydrocarbons with Ascomycota fungi. Curr. Opin. Biotechnol. 38, 1–8. https://doi.org/10.1016/j.copbio.2015.12.002.

Binelli, A., Sarkar, S.K., Chatterjee, M., Riva, C., Parolini, M., Bhattacharya, B., Bhattacharya, A.K., Satpathy, K.K., 2008. A comparison of sediment quality guidelines for toxicity assessment in the Sunderban Wetlands (Bay of Bengal, India). Chemosphere 73, 1129–1137. https://doi.org/10.1016/j.chemosphere.2008.07.019.

Caporaso, J.G., Kuczynski, J., Stombaugh, J., Bittinger, K., Bushman, F.D., Costello, E.K., Fierer, N., Pena, A.G., Goodrich, J.K., Gordon, J.I., Huttley, G.A., 2010. QIIME allows analysis of high-throughput community sequencing data. Nat. Methods 7, 335–336. https://doi.org/10.1038/nmeth.f.303.

Chatterjee, M., Canario, J., Sarkar, S.K., Branco, V., Bhattacharya, A.K., Satpathy, K.K., 2009. Mercury enrichments in core sediments in Hugli–Matla–Bidyadhari estuarine complex, north-eastern part of the Bay of Bengal and their ecotoxicological significance. J. Environ. Geol. 57, 1125–1134. https://doi.org/10.1007/s00254-008-1404-z.

Chaudhuri, K., Manna, S., Sarma, K.S., Naskar, P., Bhattacharyya, S., Bhattacharyya, M., 2012. Physicochemical and biological factors controlling water column metabolism in Sundarbans estuary, India. Aquat. Biosyst. 26, 1–16. https://doi.org/10.1186/2046-9063-8-26.

Dai, Z., Hu, J., Xu, X., Zhang, L., Brookes, P.C., He, Y., Xu, J., 2016. Sensitive responders among bacterial and fungal microbiome to pyrogenic organic matter (biochar) addition differed greatly between rhizosphere and bulk soils. Sci. Rep. 36101, 1–11. https://doi.org/10.1038/srep36101.

Dawoodi, V., Madani, M., Tahmourespour, A., Golshani, Z., 2015. The study of heterotrophic and crude oil-utilizing soil fungi in crude oil contaminated regions. J. Biorem. Biodegrad. 6, 2–5. https://doi.org/10.4172/2155-6199.1000270.

De Santis, T.Z., Hugenholtz, P., Larsen, N., Rojas, M., Brodie, E.L., Keller, K., Huber, T., Dalevi, D., Hu, P., Andersen, G.L., 2006. Greengenes, a chimera-checked 16S rRNA gene database and workbench compatible with ARB. Appl. Environ. Microbiol. 72, 5069–5072. https://doi.org/10.1128/AEM.03006-05.

Dominguez, C., Sarkar, S.K., Bhattacharya, A., Chatterjee, M., Bhattacharya, B.D., Jover, E., Albaiges, J., Bayona, J.M., Alam, M.A., Satpathy, K.K., 2010. Quantification and source identification of polycyclic aromatic hydrocarbons in core sediments from Sundarban Mangrove Wetland, India. Arch. Environ. Contam. Toxicol. 59, 49–61. https://doi.org/10.1007/s00244-009-9444-2.

Edgar, R.C., 2010. Search and clustering orders of magnitude faster than BLAST. Bioinformatics 26, 2460–2461. https://doi.org/10.1093/bioinformatics/btq461.

Froehner, S., Machado, K.S., Dombroski, L.F., Nunes, A.C., Kishi, R.T., Bleninger, T., Sanez, J., 2012. Natural biofilms in freshwater ecosystem: indicators of the presence of polycyclic aromatic hydrocarbons. Water, Air, Soil Pollut. 223, 3965–3973. https://doi.org/10.1007/s11270-012-1164-y.

Gargouri, B., Mhiri, N., Karray, F., Aloui, F., Sayadi, S., 2015. Isolation and characterization of hydrocarbon-degrading yeast strains from petroleum contaminated industrial wastewater. BioMed Res. Int. 1–11. https://doi.org/10.1155/2015/929424, 2015.

Ghosh, A., Dey, N., Bera, A., Tiwari, A., Sathyaniranjan, K.B., Chakrabarti, K., Chattopadhyay, D., 2010. Culture independent molecular analysis of bacterial communities in the mangrove sediment of Sundarban, India. Aquat. Biosyst. 6, 1–11. https://doi.org/10.1186/1746-1448-6-1.

Grula, E.A., Russell, H.H., Bryant, D., Kenaga, M., Hart, M., Donaldson, E., Clark, J., 1982. Isolation and screening of *Clostridia* for possible use in microbially enhanced oil recovery. In: Donaldson, E.C., Clark, J.B. (Eds.), Proceedings of the Microbial Enhanced Oil Recovery. Afton, USA, pp. 43–47.

Guzzella, L., Roscioli, C., Vigano, L., Saha, M., Sarkar, S.K., Bhattacharya, A., 2005. Evaluation of the concentration of HCH, DDT, HCB, PCB and PAH in the sediments along the lower stretch of Hugli estuary, West Bengal, Northeast India. Environ. Int. 31, 523–534. https://doi.org/10.1016/j.envint.2004.10.014.

Hagler, A.N., Santos, S.S., Mendonca-Hagler, L.C., 1979. Yeasts of a polluted Brazilian estuary. Rev. Microbiol. 10, 36–41.

Jaward, F.M., Alegria, H.A., Galindo Reyes, J.G., Hoare, A., 2012. Levels of PAHs in the waters, sediments, and shrimps of Estero de Urias, an estuary in Mexico, and their toxicological effects. Sci. World J. 1–9. https://doi.org/10.1100/2012/687034, 2012.

Ji, D., Yang, Q., Wang, Y., Xi, H., 2015. Estimation of phenanthrene degradation model by *Sphingobacterium multivorum* isolated from municipal sludge. Fresenius Environ. Bull. 24, 48–55.

Jimenez, A., Elner, R.W., Favaro, C., Rickards, K., Ydenberg, R.C., 2015. Intertidal biofilm distribution underpins differential tide-following behavior of two sandpiper species (*Calidris mauri* and *Calidris alpina*) during northward migration. Estuar. Coast Shelf Sci. 155, 8–16. https://doi.org/10.1016/j.ecss.2014.12.038.

Kim, G.B., Maruya, K.A., Lee, R.F., Lee, J.H., Koh, C.H., Tanabe, S., 1999. Distribution and sources of polycyclic aromatic hydrocarbons in sediments from Kyeonggi Bay, Korea. Mar. Pollut. Bull. 38, 7–15. https://doi.org/10.1016/S0025-326X(99)80006-X.

Lafortune, I., Juteau, P., Deziel, E., Lepine, F., Beaudet, R., Villemur, R., 2009. Bacterial diversity of a consortium degrading high-molecular-weight polycyclic aromatic hydrocarbons in a two-liquid phase biosystem. Microb. Ecol. 57, 455–468. https://doi.org/10.1007/s00248-008-9417-4.

Lee, D.W., Lee, H., Lee, A.H., Kwon, B.O., Khim, J.S., Yim, U.H., Kim, B.S., Kim, J.J., 2018. Microbial community composition and PAHs removal potential of indigenous bacteria in oil contaminated sediment of Taean coast, Korea. Environ. Pollut. 234, 503–512. https://doi.org/10.1016/j.envpol.2017.11.097.

Liu, Y.P., Wang, Y.H., Ye, C., Xie, B., Yang, H., 2017. Sedimentary record of polycyclic aromatic hydrocarbons from the Shuanglong catchment, Southwest China. J. Chem. 2017, 1–10. https://doi.org/10.1155/2017/4976574.

MacDonald, D.D., Ingersoll, C.G., Berger, T.A., 2000. Development and evaluation of consensus-based sediment quality guidelines for freshwater ecosystems. Arch. Environ. Contam. Toxicol. 39, 20–31. https://doi.org/10.1007/BF00118995.

MacGillivray, A.R., Shiaris, M.P., 1993. Biotransformation of polycyclic aromatic hydrocarbons by yeasts isolated from coastal sediments. Appl. Environ. Microbiol. 59, 1613–1618.

Mitra, S., Gachhui, R., Mukherjee, J., 2015. Enhanced biofilm formation and melanin synthesis by the oyster settlement-promoting *Shewanella colwelliana* is related to hydrophobic surface and simulated intertidal environment. Biofouling 31, 283–296. https://doi.org/10.1080/08927014.2015.1038705.

Mitra, S., Pramanik, A., Banerjee, S., Haldar, S., Gachhui, R., Mukherjee, J., 2013. Enhanced biotransformation of fluoranthene by intertidally derived *Cunninghamella elegans* under biofilm-based and niche-mimicking conditions. Appl. Environ. Microbiol. 79, 7922–7930. https://doi:10.1128/AEM.02129-13.

Nilsson, R.H., Larsson, K.H., Taylor, A.F., Bengtsson-Palme, J., Jeppesen, T.S., Schigel, D., Kennedy, P., Picard, K., Glockner, F.O., Tedersoo, L., Saar, I., 2018. The UNITE database for molecular identification of fungi: handling dark taxa and parallel taxonomic classifications. Nucleic Acids Res. 47, 259–264. https://doi.org/10.1093/nar/gky1022.

Norkrans, B., 1996. On the occurrence of yeasts in an estuary off the Swedish west coast. Sven. Bot. Tidskr. 60, 463–482.

Oko, B.J., Tao, Y., Stuckey, D.C., 2017. Dynamics of two methanogenic microbiomes incubated in polycyclic aromatic hydrocarbons, naphthenic acids, and oil field produced water. Biotechnol. Biofuels 10, 1–13. https://doi.org/10.1186/s13068-017-0812-2.

Olayinka, O.O., Adewusi, A.A., Olarenwaju, O.O., Aladesida, A.A., 2018. Concentration of polycyclic aromatic hydrocarbons and estimated human health risk of water samples around Atlas Cove, Lagos, Nigeria. J. Health Pollut. 8, 181210. https://doi.org/10.5696/2156-9614-8.20.181210.

Pait, A.S., Whitall, D.R., Jeffrey, C.F., Caldow, C., Mason, A.L., Lauenstein, G.G., Christensen, J.D., 2008. Chemical contamination in southwest Puerto Rico: an assessment of organic contaminants in near shore sediments. Mar. Pollut. Bull. 56, 580–587. https://doi.org/10.1016/j.marpolbul.2008.06.001.

Passarelli, C., Meziane, T., Thiney, N., Boeuf, D., Jesus, B., Ruivo, M., Jeanthon, C., Hubas, C., 2015. Seasonal variations of the composition of microbial biofilms in sandy tidal flats: focus of fatty acids, pigments and exopolymers. Estuar. Coast Shelf Sci. 153, 29–37. https://doi.org/10.1016/j.ecss.2014.11.013.

Potin, O., Veignie, E., Rafin, C., 2004. Biodegradation of polycyclic aromatic hydrocarbons (PAHs) by *Cladosporium sphaerospermum* isolated from an aged PAH contaminated soil. Microb. Ecol. 51, 71–78. https://doi.org/10.1016/j.femsec.2004.07.013.

Qian, X., Liang, B., Fu, W., Liu, X., Cui, B., 2016. Polycyclic aromatic hydrocarbons (PAHs) in surface sediments from the intertidal zone of Bohai Bay, Northeast China: spatial distribution, composition, sources and ecological risk assessment. Mar. Pollut. Bull. 112, 349–358. https://doi.org/10.1016/j.marpolbul.2016.07.040.

Radojevic, M., Bashkin, V., 1999. Practical Environmental Analysis. Royal Society of Chemistry, United Kingdom.

Raza, M., Zakaria, M.P., Hashim, N.R., Yim, U.H., Kannan, N., Ha, S.Y., 2013. Composition and source identification of polycyclic aromatic hydrocarbons in mangrove sediments of Peninsular Malaysia. Environ. Earth Sci 70, 2425–2436. https://doi.org/10.1007/s12665-013-2279-1.

Sarkar, S., Roy, D., Mukherjee, J., 2015. Council of Scientific and Industrial Research and School of Environmental Studies, assignee. Enhanced surface area conico-cylindrical flask (ES-CCF) for biofilm cultivation. U.S. Patent 8, 945,917.

Sarkar, S.K., 2016. Polycyclic aromatic hydrocarbons (PAHs) in sediment cores from Sundarban wetland. In: Sarkar, S.K. (Ed.), Marine Organic Micropollutants. Springer International Publishing, Switzerland, pp. 49–68. https://doi.org/10.1007/978-3-319-43301-1_4.

Sarkar, S.K., Binelli, A., Chatterjee, M., Bhattacharya, B.D., Parolini, M., Riva, C., Jonathan, M.P., 2012. Distribution and ecosystem risk assessment of polycyclic aromatic hydrocarbons (PAHs) in core sediments of Sundarban mangrove wetland, India. Polycycl. Aromat. Comp. 32, 1–26. https://doi.org/10.1080/10406638.2011.633592.

Shilla, D.J., Routh, J., 2018. Distribution, behavior, and sources of polycyclic aromatic hydrocarbon in the water column, sediments and biota of the Rufiji estuary, Tanzania. Front. Earth Sci. 6, 1–12. https://doi.org/10.3389/feart.2018.00070.

Silva, T.R., Verde, L.C., Neto, E.S., Oliveira, V.M., 2013. Diversity analyses of microbial communities in petroleum samples from Brazilian oil fields. Int. Biodeterior. Biodegrad. 81, 57–70. https://doi.org/10.1016/j.ibiod.2012.05.005.

Sojinu, O.S., Wang, J.Z., Sonibare, O.O., Zeng, E.Y., 2010. Polycyclic aromatic hydrocarbons in sediments and soils from oil exploration areas of the Niger Delta, Nigeria. J. Hazard Mater. 174, 641–647. https://doi.org/10.1016/j.jhazmat.2009.09.099.

Sun, J.H., Wang, G.L., Chai, Y., Zhang, G., Li, J., Feng, J., 2009. Distribution of polycyclic aromatic hydrocarbons (PAHs) in henan reach of the yellow river, Middle China. Ecotoxicol. Environ. Saf. 72, 1614–1624. https://doi.org/10.1016/j.ecoenv.2008.05.010.

Tam, N.F.Y., Guo, C.L., Yau, W.Y., Wong, Y.S., 2002. Preliminary study on biodegradation of phenanthrene by bacteria isolated from mangrove sediments in Hong Kong. Mar. Pollut. Bull. 45, 316–324. https://doi.org/10.1016/S0025-326X(02)00108-X.

United States Environmental Protection Agency, 1996a. Method 3540C Soxhlet Extraction.

United States Environmental Protection Agency, 1996b. EPA-method 3630C Silica Gel Cleanup.

United States Environmental Protection Agency, 1996c. Test Method 3510C Separatory Funnel Liquid-Liquid Extraction.

United States Environmental Protection Agency, 1996d. Method 8000B, Determinative Chromatographic Separations.

Walkley, A., Black, I.A., 1934. An examination of the Degtjareff method for determining soil organic matter and a proposed modification of the chromic acid titration method. Soil Sci. 37, 29–38.

Wang, Q., Garrity, G.M., Tiedje, J.M., Cole, J.R., 2007. Naive Bayesian classifier for rapid assignment of rRNA sequences into the new bacterial taxonomy. Appl. Environ. Microbiol. 73, 5261–5267. https://doi.org/10.1128/AEM.00062-07.

Wicke, D., Böckelmann, U., Reemtsma, T., 2007. Experimental and modeling approach to study sorption of dissolved hydrophobic organic contaminants to microbial biofilms. Water Res. 41, 2202–2210. https://doi:10.1016/j.watres.2007.01.039.

Wicke, D., Böckelmann, U., Reemtsma, T., 2008. Environmental influences on the partitioning and diffusion of hydrophobic organic contaminants in microbial biofilms. Environ. Sci. Technol. 42, 1990–1996. https://doi.org/10.1021/es702267s.

Yan, N., Marschner, P., Cao, W., Zuo, C., Qin, W., 2015. Influence of salinity and water content on soil microorganisms. Int Soil Water Conser. Res. 3, 316–323. https://doi.org/10.1016/j.iswcr.2015.11.003.

Yuan, S.Y., Chang, B.V., 2007. Anaerobic degradation of five polycyclic aromatic hydrocarbons from river sediment in Taiwan. J. Environ. Sci. Health B. 42, 63–69. https://doi.org/10.1080/03601230601020860.

Zafra, G., Absalón, Á.E., Cuevas, M.D.C., Cortés-Espinosa, D.V., 2014. Isolation and selection of a highly tolerant microbial consortium with potential for PAH biodegradation from heavy crude oil-contaminated soils. Water Air Soil Pollut. 225, 1–18. https://doi.org/10.1007/s11270-013-1826-4.

Zammit, G., Billi, D., Shubert, E., Kasstovskyy, J., Albertano, P., 2011. The biodiversity of subaerophytic phototrophic biofilms from Maltese hypogea. Fottea 11, 187–201.

Zuloaga, O., Prieto, A., Ahmed, K., Sarkar, S.K., Bhattacharya, A., Chatterjee, M., Bhattacharya, B.D., Satpathy, K.K., 2013. Distribution of polycyclic aromatic hydrocarbons in recent sediments of Sundarban mangrove wetland of India and Bangladesh: a comparative approach. Environ. Earth Sci. 68, 355–367. https://doi.org/10.1007/s12665-012-1743-7.

Zuloaga, O., Prieto, A., Usobiaga, A., Sarkar, S.K., Chatterjee, M., Bhattacharya, B.D., Bhattacharya, A., Alam, M.A., Satpathy, K.K., 2009. Polycyclic aromatic hydrocarbons in intertidal marine bivalves of Sundarban mangrove wetland, India: an approach to bioindicator species. Water, Air, Soil Pollut. 201, 305–318. https://doi.org/10.1007/s11270-008-9946-y.

Journal of Hazardous Materials 437 (2022) 129318

Contents lists available at ScienceDirect

Journal of Hazardous Materials

journal homepage: www.elsevier.com/locate/jhazmat

Polycyclic aromatic hydrocarbon sequestration by intertidal phototrophic biofilms cultivated in hydrophobic and hydrophilic biofilm-promoting culture vessels

Saranya Balu [a], Shantanu Bhunia [a], Ratan Gachhui [b], Joydeep Mukherjee [a,*]

[a] School of Environmental Studies, Jadavpur University, Kolkata 700032, India
[b] Department of Life Science and Biotechnology, Jadavpur University, Kolkata 700032, India

HIGHLIGHTS

- Phototrophic biofilms sequestered 16 priority polycyclic aromatic hydrocarbons (PAHs).
- Biofilms isolated from highest PAH contaminated sites removed PAHs most efficiently.
- Biofilm biomass, photosynthetic pigments, extracellular polymeric substances enhanced.
- PAHs removal, biochemical reactions sensitive to vessel hydrophobicity/hydrophilicity.
- Bound and released exopolysaccharide component of biofilms influenced by PAH exposure.

GRAPHICAL ABSTRACT

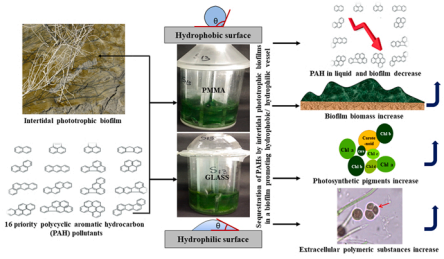

ARTICLE INFO

Editor: María Sonia Rodríguez

Keywords:
Sundarbans
Sediments
Photosynthetic pigments
Exopolysaccharides
Uronic acid

ABSTRACT

Phototrophic biofilms collected from intertidal sediments of the world's largest tidal mangrove forest were cultured in two sets of a biofilm-promoting culture vessel having hydrophilic glass surface and hydrophobic polymethyl methacrylate surface wherein 16 priority polycyclic aromatic hydrocarbons (PAHs) were spiked. Biofilms from three locations of the forest were most active in sequestering 98–100% of the spiked pollutants. PAH challenge did not alter the biofilm phototrophic community composition; rather biofilm biomass production and synthesis of photosynthetic pigments and extracellular polymeric substances (EPS) were enhanced. Photosynthetic pigment and EPS synthesis were sensitive to vessel-surface property. The lowest mean residual amounts of PAHs in the liquid medium as well as inside the biofilm were recorded in the very biofilm cultivated in the hydrophobic flask where highest values of biofilm biomass, total chlorophyll, released polysaccharidic (RPS) carbohydrates, RPS uronic acids, capsular polysaccharidic (CPS) carbohydrates, CPS proteins, CPS uronic acids and EPS hydrophobicity were obtained. Ratios of released RPS proteins: polysaccharides increased during PAH sequestration whereas the ratios of CPS proteins: polysaccharides remained constant. Efficacious PAH removal by the overlying phototrophic biofilm will reduce the entry of these contaminants in the sediments underneath and this strategy could be a model for "monitored natural recovery".

* Corresponding author.
E-mail addresses: sarusaranya.balu@gmail.com (S. Balu), shanu.bhunia@gmail.com (S. Bhunia), ratangachhui@gmail.com (R. Gachhui), joydeep.mukherjee@jadavpuruniversity.in (J. Mukherjee).

https://doi.org/10.1016/j.jhazmat.2022.129318
Received 16 April 2022; Received in revised form 24 May 2022; Accepted 5 June 2022
Available online 9 June 2022

1. Introduction

Polycyclic aromatic hydrocarbons (PAHs) are hydrophobic organic pollutants comprising of two or more fused benzene rings and categorized as priority pollutants by the United States Environmental Protection Agency (USEPA). PAHs enter the environment through partial combustion of carbonaceous materials as well as discharge of petroleum products and alter the biological and physicochemical properties of ecosystems (Lv et al., 2020; Govarthanan et al., 2017a). At the same time, the intertidal zone as a research site, has often been ignored by land and ocean researchers. Intertidal zones have vital ecological and hydrological functions on one hand and high intensity of human activity on the other, thus designating them as fragile and vulnerable to human activities. Urbanization and industrialization have contaminated the intertidal zones over the past several decades, among which, PAHs are prone to be deposited in intertidal sediments because of their excessive hydrophobicity (Lv et al., 2020). Presence of PAHs in intertidal sediments of different geographical regions of the world: China, Taiwan, Qatar, Korea, Malaysia, Japan, Egypt, Tanzania, Spain, Argentina, Chile, Canada, Iran and India was evaluated (Qian et al., 2016; Lv et al., 2020; Wang et al., 2021). Mangrove forests are prominent intertidal ecosystems located along tropical and subtropical coastlines that are exposed to human-derived pollution by PAHs. The typical features of mangroves such as high primary productivity, plentiful detritus, abundant organic carbon and anoxic conditions foster uptake and sediment storage of PAHs from anthropogenic processes (Hong et al., 2008).

Although there is ample evidence on the presence of PAHs contaminants in the intertidal regions, no attention has been focused on the existing natural components of this ecosystem that may be useful in preventing entry of these pollutants in the sediments. Sediment management strategies may implicate non-removal choices such as “monitored natural recovery” where biological processes such as biodegradation, biostabilization and phytoremediation can eradicate the PAHs (Maletic et al., 2019) from the environment without adverse effects (Govarthanan et al., 2020, 2022). We believe efficacious PAH removal from the water by the overlying phototrophic biofilms will reduce the entry of these contaminants in the sediments underneath which could be a model for “monitored natural recovery”: the motivation of this initiating study. These biofilms occur on light-exposed surfaces in a variety of terrestrial and aquatic environments. Oxygenic phototrophs are the main primary producers that reduce carbon dioxide, providing the phototrophic biofilm with organic substrates and oxygen. Photosynthesis drives biochemical reactions in the entire biofilm community, incorporating heterotrophic metabolism as well. Additionally, phototrophs and heterotrophs secrete a matrix of polymeric substances that enhances the surface-attachment of the biofilm community (Roeselers et al., 2008). Recently the role of phototrophic biofilms in the removal of organic pollutants was reviewed by Mandal et al. (2021). Physiological collaboration between the microbes of intertidal communities enhances the ability of PAH pollutants utilization by biofilm-dwelling microorganisms in comparison to mono-species communities. Thus, phototrophic biofilm-based remediation in intertidal zones can be efficacious in the removal of PAHs (Mandal et al., 2021). In this context, Nhi-Cong et al. (2021) described a bacteria-driven carrier system supporting purple phototrophic bacterial biofilm which degraded substantial amounts of PAHs such as phenanthrene (Phe), naphthalene (Nap), anthracene (Ant) and pyrene (Pyr). However, PAH removal from the surrounding water by laboratory-grown multispecies phototrophic biofilms isolated from the field (intertidal regions) has not been verified before.

The distribution of PAHs in the intertidal sediments of the Indian Sundarbans (the world’s largest tidal mangrove forest) was assessed in our previous study (Balu et al., 2020) and total PAH concentration extended from 4880 to 2×10^4 ng g^{-1} dry weight. These values surpassed the Effects Range-Low value and the suggested Effects Range-Median values, indicating the PAHs might negatively influence the biota of the Sundarbans. The capacity of heterotrophic microbial biofilm communities to sequester PAHs in a novel and patented biofilm-promoting vessel was assessed. A modified mixed media was used in our previous study (Balu et al., 2020) to promote concurrent growth of heterotrophic bacteria, eukaryotic microalgae, fungi as well as phototrophic microorganisms. This composite medium circumstantially favored heterotrophic growth and no autotrophic growth was observed. In this perspective, Wyatt et al. (2019) commented that decomposers are often better competitors for nutrients than producers in aquatic environments. Heterotrophs in lake biofilms outcompeted autotrophs for available nutrients unless heterotrophs were constrained by organic carbon afforded by autotrophic constituents of the biofilm. This micro-ecological phenomenon presumably restricted phototrophic growth in our previous investigation. To circumvent this unbalanced growth, we now designed the growth medium supportive towards phototrophic growth.

Attention towards biofilm-based algal cultivation has intensified because of its significance in algal production, nutrient removal of wastewater (Haripriyan et al., 2022) and a prospective route to provide feedstock for microalgae-based biorefinery. In this connection, the research carried out on the influence of material properties on microalgal biofilm growth remains unsettled. Some investigators confirmed positive association between surface hydrophobicity and biofilm formation and growth. Conversely, others established that hydrophilic materials with adequate liquid-holding capacity were superior for algal biofilm-based attached cultivation (Moreno Osorio et al., 2021). Likewise, there are divided opinions on the effect of PAHs on the photosynthetic pigments of phototrophic microalgae. While Chen et al. (2020), Zyszka-Haberecht et al. (2019) and Luo et al. (2015) reported enhancement of chlorophyll *a* (Chl *a*) concentration upon PAH exposure, others Panah et al. (2015) and Patel et al. (2015) demonstrated significant reduction in the photosynthetic and its accessory pigment concentration with the increase in PAHs levels. Then again, biofilm-stemming secretions known as extracellular polymeric substances (EPS) primarily comprised of heteropolysaccharides exuded by cyanobacteria are the center of biofilm-related research. EPS boosts successful survival of cyanobacteria as complex phototrophic biofilms in constrained environments. Presence of environmental stressors not only affects the amount of produced EPS, but also controls the physico-chemical characteristics of the secreted polymer, thus positively shaping the adaptation of the cells to harsh environmental conditions.

There are reports on the removal of PAH contaminants by single-species microalgae as well as the effect of these toxicants on photosynthetic pigment synthesis. Changes in EPS amounts and biochemical characteristic in response to PAH challenge have also been examined. However, phototrophic microorganisms in nature exist in a biofilm consortium, not as individual cells. Notwithstanding, a multifaceted study on the response of field-derived phototrophic biofilms to environmentally realistic PAH concentrations has not been conducted. Therefore, this investigation sought to answer: How efficient are intertidal phototrophic biofilms in sequestration of the PAH contaminants? Does the biofilm biomass, their community composition and photosynthetic pigment production change in response to PAH exposure? Is EPS production and its biochemical composition altered in reaction to the PAH challenge? Does surface hydrophobicity/hydrophilicity of the culture vessel play a role in the sequestration process?

2. Materials and methods

2.1. Cultivation of phototrophic biofilms

Twenty-five estuarine phototrophic biofilm samples were collected by scrapping green and brown colored biomass growth on sediment surfaces in five regions of the Sundarbans (India): Purba Gurguria (Pg), Maipit (Mt), Patharpratima (Pp1 and Pp2), Namkhana (Nk) and Kakdwip (Kk). Please see Balu et al. (2020) for a map of the region. The

biofilm samples were immediately transferred to an enriched growth medium specific for phototrophic microorganisms consisting of ASN III and BG 11 media mixed in equal proportions. Biofilms were maintained at 25 ± 1 °C in fluorescent irradiance (50 μmol photons m^2 s^{-1}) in 14:10 h light: dark photoperiod.

2.2. PAH sequestration by biofilms

Six robustly growing and well-formed phototrophic biofilms were chosen to assess PAH sequestration. Each biofilm represented one of the five different geographical locations: Pg, Mt, Pp1 and Pp2, Nk and Kk. These biofilms were cultured in two sets of the patented (US patent 8 945 917 B2, Sarkar et al., 2015, Fig. 1) enhanced surface conico cylindrical (ES-CCF) flasks with two different surface configurations: hydrophilic glass surface (Set 1) and hydrophobic polymethyl methacrylate (PMMA) (Set 2) surface and further employed for the removal of the PAHs. Roughly 200 mg of phototrophic biofilm was inoculated into the sterile ASN III: BG11 enriched medium. After the growth of the biofilms, different concentrations of the 16 priority PAHs were spiked into the glass and PMMA ES-CCFs: 5 ppm for Pg and Mt, 15 ppm for Pp1, 10 ppm for Pp2 and Nk and 25 ppm for Kk biofilms. Spiking concentrations were the same as the total PAHs sediment concentrations recorded in the different geographical locations described in our previous study (Balu et al., 2020). Another set of biofilms were cultivated in both the ES-CCFs without PAHs as control. Flasks containing sterile ASN III: BG11 enriched media spiked with 5, 10, 15 and 25 ppm of PAHs as well as sterile media without PAHs were incubated as additional controls. The extent of PAHs sequestered from the liquid medium was measured after 21 days in duplicate (n = 2) and denoted as residual PAH (as percentage). PAH removal efficiency (%) was estimated as: $R = (C_i - C_f)/C_i \times 100$, where R indicated the removal efficiency (%), C_i was the initial and C_f was the final PAH concentration.

2.3. Extraction of PAHs from biofilm liquid culture media

After 21 days, the amount of PAH sequestered from the liquid media was measured by extracting PAHs from the media. PAHs were extracted using a separating funnel by applying the USEPA method 3510C liquid-liquid extraction (1996b). To exclude sulfur compound interference in the extract silica gel clean-up method prescribed by the USEPA method 3630C (1996a) was carried out. Collected fractions were concentrated to 4 ml and 2 μl of the concentrates were injected into the gas chromatograph (GC). PAHs were detected using a flame ionization detector or FID (Agilent 7820 A, Agilent Technologies, USA) with nitrogen as the carrier gas as mentioned in USEPA method 8000B (1996c). GC equipment details, limits of detection calibration as well as quantification and quality control methods are described in Balu et al. (2020).

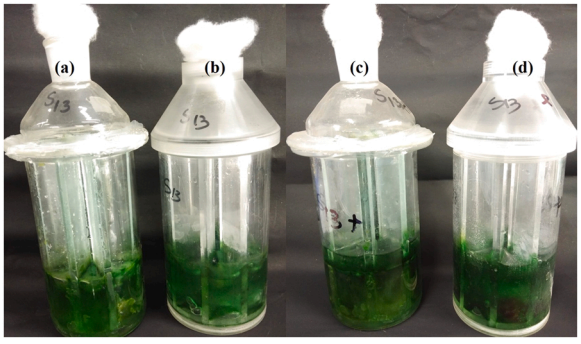

Fig. 1. Phototrophic biofilm cultured in enhanced surface area conico-cylindrical flask (ES-CCF) (a) in hydrophilic glass ES-CCF without PAHs (b) in hydrophobic PMMA ES-CCF without PAHs (c) in hydrophilic glass ES-CCF enriched with PAHs (d) in hydrophobic PMMA ES-CCF enriched with PAHs. All images were obtained after 21 days exposure to PAHs.

2.4. Estimation of PAH concentration inside the biofilms

Phototrophic biofilms were recovered after 21 days, dried by lyophilization (Eyela FDU-1200, Tokyo Rikakikai Co. Ltd, Japan), weighed and biofilm biomasses were recorded. PAHs from dried biofilm samples were extracted following the method of Froehner et al. (2012) by ultrasound sonication using dichloromethane (DCM): methanol (2:1) as the solvent system. The process was repeated thrice, followed by extraction using twice the volume of DCM. All solvent extracts were mixed, concentrated to 2 ml and then put through silica gel clean up and estimation by GC-FID as described in Section 2.3.

2.5. Estimation of photosynthetic pigments

We compared the overall concentration of phototrophic pigments Chl *a*, Chl *b*, Chl *c*, Chl *d*, total Chl and carotenoids from the biofilms cultured in PAH-spiked media with the control biofilms after 21 days incubation. Photosynthetic pigments were extracted in triplicate using reagent-grade methanol. Biofilm samples were weighed, homogenized and the homogenate extract was centrifuged at 1077 × g at 4 °C for 15 min. Pellets were re-suspended in the solvent until they turned colorless. All supernatants were pooled and quantified spectrophotometrically at different absorbances as described by Ritchie (2008):

$$\text{Chl } a\ (\mu g\ ml^{-1}) = -2{\cdot}0780\times(A_{632}\text{-}A_{750}) - 6{\cdot}5079\times(A_{652}\text{-}A_{750}) + 16{\cdot}2127\times(A_{665}\text{-}A_{750}) - 2{\cdot}1372\times(A_{696}\text{-}A_{750})\ (\pm 0{\cdot}0070)$$

$$\text{Chl } b\ (\mu g\ ml^{-1}) = -2{\cdot}9450\times(A_{632}\text{-}A_{750}) + 32{\cdot}1228\times(A_{652}\text{-}A_{750}) - 13{\cdot}8255\times(A_{665}\text{-}A_{750}) - 3{\cdot}0097\times(A_{696}\text{-}A_{750})\ (\pm 0{\cdot}0212)$$

$$\text{Chl } c\ (\mu g\ ml^{-1}) = 34{\cdot}0115\times(A_{632}\text{-}A_{750}) - 12{\cdot}7873\times(A_{652}\text{-}A_{750}) + 1{\cdot}4489\times(A_{665}\text{-}A_{750}) - 2{\cdot}5812\times(A_{696}\text{-}A_{750})\ (\pm 0{\cdot}0120)$$

$$\text{Chl } d\ (\mu g\ ml^{-1}) = -0{\cdot}3411\times(A_{632}\text{-}A_{750}) + 0{\cdot}1129\times(A_{652}\text{-}A_{750}) - 0{\cdot}2538\times(A_{665}\text{-}A_{750}) + 12{\cdot}9508\times(A_{696}\text{-}A_{750})\ (\pm 0{\cdot}0031)$$

$$\text{Total Chl}\ (\mu g\ ml^{-1}) = \text{Chl } a + \text{Chl } b + \text{Chl } c + \text{Chl } d$$

$$\text{Carotenoids}\ (\mu g\ ml^{-1}) = 4\times(A_{480}\text{-}A_{750})$$

2.6. Extraction and characterization of EPS

EPS from control as well as PAH-spiked vessels were measured and characterized. Two fractions of EPS i.e. the released (RPS) as well as the capsular/bound polymeric substances (CPS) from the biofilm samples were extracted. Phototrophic biofilms harvested in the ES-CCFs were centrifuged at 3019 × g for 10 min and the supernatant consisting of the RPS was separated from the pellets which contained the cells and the CPS. EPS from the pellets were quantified by incubating them in 0.1 M sulfuric acid at 95 °C for 1 h. Incubated samples were centrifuged at 1479 × g for 5 min and the supernatant with CPS was separated from the pellet and precipitated in 96% cold ethanol (Di Pippo et al., 2013). RPS from the cell-free culture was quantified following the method prescribed by Gacheva et al. (2013). Collected supernatant was precipitated using 99% chilled ethanol in 1:3 ratio (v/v) and was centrifuged at 10 000 × g for 10 min. Pellets were washed thrice with 65% ethanol to eliminate contaminants, freeze-dried, weighed and stored at − 20 °C for further analysis.

Total carbohydrate contents of RPS and CPS fractions were determined spectrophotometrically by the phenol-sulphuric acid method (Dubois et al., 1956). The standard curve was prepared using glucose. Total protein constituents in EPS fractions were spectrophotometrically measured using Lowry's method (Lowry et al., 1951). Bovine serum albumin was used for preparing the standard curve. Uronic acid contents were determined using carbazole in 80% sulfuric acid with sodium borate. Galacturonic acid served as the standard (Taylor and

Buchanan-Smith, 1992).

2.7. Estimation of EPS and biofilm hydrophobicity

A biphasic system was applied where 5 ml of control as well as test EPS were suspended in 1% w/v phosphate saline buffer in clean test tubes. Hexadecane (300 μl) was added to the test tubes and OD_{550} (A_0) was obtained. All tubes were vortexed for about 1 min and the phases allowed to separate by keeping them still for 15 min. The lower aqueous phase was carefully removed using a sterile Pasteur pipette and OD_{550} (A_1) was quantified. The hydrophobicity of the EPS was calculated using the formula (Bhatnagar et al., 2014):

$$DH = [(A_0 - A_1) / A_0] \times 100$$

Biofilms at the early stationary phase (between 10 and 15 days of growth) before exposure to PAHs were used for testing the hydrophobicity of the biofilms (Zhang et al., 2011; Veerabadhran et al., 2018). Cultures were thoroughly washed twice using the culture medium. Three milliliters of biofilm suspension was taken in a clean sterile test tube and 3 ml of n-hexadecane was added. The contents were manually agitated for about 1 min and after a five-minute pause, the contents were vortexed for 10 s. The tubes were kept stationary for about 10–15 min for the total separation of the two phases. The biofilm cell surface property was assessed by observing adherence to the biphasic (aqueous-hydrocarbon) system as described by Fattom and Shilo (1984).

2.8. Light and scanning electron microscopy of biofilms

Freshly grown biofilms as well as those exposed to PAHs were spread on a clean glass slide, covered with a coverslip and observed at 1000 X magnification using a light microscope (Leica ICC50 HD, Leica Microsystems, Wetzlar, Germany). Biofilm communities growing in control media and media spiked with PAHs were examined by scanning electron microscopy (SEM) using Hitachi FlexSEM 1000 II microscope (Hitachi, Ltd Tokyo, Japan). Biofilms were placed over carbon tape on the SEM sample stub and gold-sputtered (3–5 nm). SEM imaging was done using SEM coupled with detectors for secondary electrons and back-scattered electrons as well as an ultra-variable-pressure detector for imaging non-conductive samples at low vacuum.

2.9. Statistical analyses

Analysis of variance (ANOVA), coefficient of variation for duplicate data (Hyslop and White, 2009; Jones and Payne, 1997) and paired *t*-test was carried out using SPSS software (version 16.0). The statistical significance of the results was verified at $p \leq 0.01$ and $p \leq 0.05$ significance levels.

3. Results

3.1. Sequestration of PAHs from the liquid media by phototrophic biofilms in hydrophobic and hydrophilic vessels

3.1.1. PAHs removal from liquid media

Fig. 1 is representative of the phototrophic biofilms cultivated with and without addition of PAHs. As evident from Table 1, phototrophic biofilms in this study were able to sequester 98–100% of all the individual spiked PAHs in all liquid media except from the medium cultured with the Pg biofilm where the extent of sequestration of the different PAHs ranged from a low 1% to maximum 100%. Significant differences at $p \leq 0.05$ in the mean residual PAHs amounts between the biofilm-cultured vessels with the spiked PAHs and the ones without any spiking were observed (Table 1). The mean residual PAHs retained in the liquid media in the PMMA and glass ES-CCFs indicated that irrespective of the hydrophobic and hydrophilic nature of culture vessels all the PAHs were similarly sequestrated from the liquid media. However, variation from this observation was noted in the sequestration of certain PAHs in the media with the Pg biofilm compared to the other PAH-spiked media with biofilms. PAHs like Nap, Acenaphthene (Ace), benzo(a)anthracene [B(a)A], benzo(k)fluoranthene [B(k)F], benzo(a) pyrene [B(a)P] and benzo (g, h, i) perylene [B(g,*h*,i) P]) showed significant differences in their sequestration in flasks having hydrophilic and hydrophobic surfaces (indicated in bold in Table 1). Except for Ace, all the other PAHs were removed efficiently in the hydrophobic PMMA vessel in comparison to the hydrophilic glass vessel treated with the Pg biofilm. The persistence of low molecular weight PAH (LMW-PAH) contaminants such as Nap, acenaphthylene (Acy), Ace, fluorene (Flu), Phe and Ant was evident in PAH-spiked media with Pg biofilm when compared to the high molecular weight PAHs (HMW-PAH). Four [B(a)A, B(k)F, B(a)P and B(g,*h*,i)P] out of ten HMW-PAHs were recovered. The mean residual LMW-PAHs in Pg biofilms spiked with 5 ppm total PAHs were 51% (0.96 ppm) in glass ES-CCF and 53% (0.99 ppm) in PMMA ES-CCF whereas the mean residual HMW-PAHs were 29% (0.91 ppm) in glass ES-CCF and 12% (0.38 ppm) in PMMA ES-CCF. Additionally, B(g,*h*, i)P when treated with Pp2 biofilm, B(a)P when cultured in Nk biofilm and Ace when cultivated Kk biofilm demonstrated minor differences in sequestration in hydrophobic as well as hydrophilic vessels (indicated in bold in Table 1).

3.1.2. PAHs accumulation inside biofilms

As apparent from Table 2 the mean residual amounts of PAHs inside the phototrophic biofilms after exposure to the PAHs varied between 0% and 100%. Significant differences at $p \leq 0.05$ in the mean residual PAHs amounts between the biofilm-cultured vessels with the spiked PAHs and the ones without any spiking were noticed (Table 2). The ability to remove the 16 priority PAH contaminants by the phototrophic biofilms after 21 days incubation (as evident from the mean residual amount of PAHs) was in the order Pp1 >Kk>Nk>Mt>Pp2 >Pg. The mean residual PAH was higher in the Pg biofilm cultured in the hydrophobic PMMA ES-CCF compared to other biofilms cultured in hydrophobic and hydrophilic vessels, indicating low PAH sequestration potential of the Pg biofilm. Hydrophilic culture of the Pp1 biofilm and hydrophobic culture of the Kk biofilm showed the lowest mean residual amount of PAHs (Table 2). Differences in sequestration arising due to the nature of hydrophobic/hydrophilic surface were more pronounced inside the biofilms (Table 2) compared to liquid media (Table 1). Except for indeno (1, 2, 3 cd) pyrene (Ind) and chrysene (Chry), all the other PAHs showed differences in the extent of removal between the hydrophobic PMMA and hydrophilic glass ES-CCFs for all the biofilms (indicated in bold in Table 2). In case of Pg biofilms, only Ace in PMMA ES-CCF and B(g,*h*,i)P in glass ES-CCF were removed while the remaining PAHs were extracted from the biofilms cultured in both types of flasks. Summing up the mean residual PAHs in the PAH-spiked (5 ppm) liquid media treated with Pg biofilm (Table 1) and the mean residual PAHs obtained from Pg biofilms (Table 2) we recorded a combined 92% (4.6 ppm) mean residual PAHs and a summative 89% (4.4 ppm) mean residual PAHs in the hydrophilic and hydrophobic vessels respectively. In contrast this additive value ranged from 10% to 20% in the other biofilms, indicating the potency of these biofilms to efficiently sequester the PAHs in comparison to the Pg biofilm. Hence, Pp1, Nk and Kk biofilms were selected for further investigations.

3.1.3. Biofilm hydrophobicity and microscopic observations

The hydrophobicity test using n-hexadecane (See Section 2.7) was conducted to establish the surface property (hydrophobic/hydrophilic) of the biofilms. Pp1, Nk and Kk biofilms demonstrated hydrophobic characteristics. Biofilms migrated towards the upper hydrocarbon layer in preference to the lower aqueous layer (Fig. 2). Morphological analyses using light microscope revealed the presence of purple sulfur bacteria, cyanobacteria such as *Gloeocapsa* sp., *Chloroidium* sp., pennate diatoms and *Closterium* sp. like green algae in Pp1 biofilms. Again,

Table 1
Residual amounts (as percent of initial concentrations) of 16 priority spiked PAHs in liquid media after treatment with phototrophic biofilms in glass and PMMA ES-CCF for 21 days. The residual amounts that are at least double of each other (PMMA ES-CCF compared to glass ES- CCF or vice versa) are shown in bold letters. Initial concentration of PAHs spiked: 5 ppm for Pg and Mt, 15 ppm for Pp1, 10 ppm for Pp2 and Nk and 25 ppm for Kk biofilms. Coefficient of variation of duplicate data was 2.89% (n = 192) following Hyslop and White (2009) and Jones and Payne (1997).

Polycyclic aromatic hydrocarbons	Pg		Mt		Pp1		Pp2		Nk		Kk	
	Glass	PMMA	Glass	PMMA	Glass	PMMA	Glass	PMMA	Glass	PMMA	Glass	PMMA
Naphthalene	**77.81**	47.09	0.58	0.33	0.16	0.41	0.00	0.00	0.44	0.55	0.00	0.01
Acenaphthylene	19.42	11.50	0.19	0.00	0.40	0.09	0.00	0.00	0.08	0.09	0.00	0.00
Acenaphthene	15.13	**98.98**	0.98	0.06	0.33	0.00	0.54	0.54	0.11	0.14	**2.06**	0.08
Fluorene	28.30	24.85	0.00	0.10	0.05	0.13	0.03	0.03	0.15	0.14	0.04	0.06
Phenanthrene	78.47	62.09	0.00	0.01	0.04	0.12	0.10	0.10	0.12	0.11	0.02	0.04
Anthracene	89.66	71.26	0.00	0.21	0.16	0.56	0.00	0.00	0.61	0.67	0.05	0.04
Fluoranthene	24.71	18.20	0.00	0.18	0.08	0.33	0.00	0.20	0.09	0.09	0.00	0.01
Pyrene	0.00	0.00	0.00	0.00	0.00	0.00	0.00	0.00	0.06	0.54	0.11	0.24
Benzo(a)anthracene	**57.97**	38.39	0.23	0.49	0.00	0.14	0.10	0.10	0.16	0.13	0.05	0.06
Chrysene	0.00	0.00	0.00	0.00	0.13	0.11	0.00	0.00	0.12	0.11	0.00	0.05
Benzo(b)fluoranthene	0.00	0.00	0.00	0.00	0.00	0.22	0.00	0.00	0.20	0.19	0.07	0.19
Benzo (k)Fluoranthene	**23.65**	0.00	0.00	0.31	0.00	0.00	0.00	0.00	0.00	0.00	0.00	0.00
Benzo (a)pyrene	**83.61**	44.29	0.35	0.68	0.29	0.12	0.16	0.16	0.26	**1.43**	0.27	0.09
Indeno (1,2,3-cd) Pyrene	0.00	0.00	0.00	0.00	0.00	0.11	0.00	0.00	0.16	0.19	0.00	0.14
Dibenz (a,h) anthracene	0.00	0.00	0.00	0.00	0.09	0.14	0.00	0.00	0.00	0.00	0.00	0.00
Benzo (g,h,i) perylene	**95.62**	20.74	0.06	0.73	0.84	0.19	**2.79**	1.57	0.12	0.25	0.79	0.12
Mean PAH residual amounts	37.15	27.34	0.15	0.19	0.16	0.17	0.23	0.17	0.17	0.29	0.22	0.07

Table 2
Residual amounts (as percent of initial concentrations) of 16 priority spiked PAHs inside the biofilms after treatment with phototrophic biofilms in glass and PMMA ES-CCF for 21 days. The residual amounts that are at least double of each other (PMMA ES-CCF compared to glass ES- CCF or vice versa) are shown in bold letters. Initial concentration of PAHs spiked in liquid media: 5 ppm for Pg and Mt, 15 ppm for Pp1, 10 ppm for Pp2 and Nk and 25 ppm for Kk biofilms. Coefficient of variation of duplicate data was 5.77% (n = 192) following Hyslop and White (2009) and Jones and Payne (1997).

Polycyclic aromatic hydrocarbons	Pg		Mt		Pp1		Pp2		Nk		Kk	
	Glass	PMMA	Glass	PMMA	Glass	PMMA	Glass	PMMA	Glass	PMMA	Glass	PMMA
Naphthalene	22.2	**52.9**	13.7	**23.5**	16.5	10.7	10.5	12.5	10.9	18.7	**10.1**	0.0
Acenaphthylene	77.6	88.5	28.2	24.7	5.6	**18.1**	13.4	15.4	35.6	29.0	3.9	**16.4**
Acenaphthene	74.9	0.0	**19.6**	0.0	22.7	**83.2**	33.7	33.7	9.9	**21.8**	98.8	64.4
Fluorene	61.7	65.1	**60.0**	18.0	**14.6**	7.5	7.8	7.8	**13.7**	6.2	4.3	2.9
Phenanthrene	21.5	27.9	5.3	**30.1**	3.5	**10.6**	21.2	19.3	**18.9**	6.1	2.8	3.7
Anthracene	8.3	**18.7**	**83.5**	49.9	10.3	**20.9**	20.0	23.0	27.8	24.7	4.9	10.0
Fluoranthene	65.3	71.8	29.8	24.3	4.4	4.6	29.1	29.1	8.9	**20.3**	**7.0**	0.0
Pyrene	85.4	89.3	0.0	0.0	**12.7**	0.0	0.0	0.0	0.0	**20.2**	13.6	15.5
Benzo(a)anthracene	32.0	41.6	32.0	40.3	0.0	0.0	57.8	57.8	**28.1**	0.0	**6.5**	0.0
Chrysene	89.9	95.0	0.0	0.0	0.0	0.0	0.0	0.0	0.0	0.0	3.2	0.0
Benzo(b)fluoranthene	81.5	34.2	0.0	0.0	0.0	**7.1**	0.0	0.0	0.0	**12.0**	8.7	10.5
Benzo (k)Fluoranthene	66.4	85.3	0.0	**37.0**	0.0	0.0	14.5	14.5	0.0	0.0	0.0	0.0
Benzo (a)pyrene	16.4	**45.7**	13.4	19.2	**37.9**	10.8	52.2	65.6	55.5	45.3	14.8	12.4
Indeno (1,2,3-cd) Pyrene	99.0	100.0	0.0	0.0	0.0	0.0	0.0	0.0	0.0	0.0	0.0	0.0
Dibenz (a,h) anthracene	75.0	86.0	0.0	0.0	0.0	**5.5**	0.0	0.0	9.7	**17.0**	11.3	11.0
Benzo (g,h,i) perylene	0.0	**79.3**	0.0	0.0	30.5	26.1	11.5	15.5	**67.4**	23.6	**38.0**	5.4
Mean PAH residual amounts	54.8	61.4	17.8	16.7	9.9	12.8	17.0	18.4	17.9	15.3	14.2	9.5

cyanobacteria such as *Gloeocapsa* sp., *Microcystis* sp. and purple sulfur bacteria were observed in Nk biofilms whereas Kk biofilms showed the occurrence of purple sulfur bacteria, cyanobacteria such as *Gleocapsa* sp. *Microcystis* sp. and *Phormidium* sp., *Closterium* sp. like green algae as well as pennate diatoms (Fig. 3). PAH-treated biofilms also showed the presence of similar phototrophic microorganisms. SEM observations (Fig. 4) and comparisons with similar published images (Boelee, 2013; Cole et al., 2014) were suggestive of the biofilm being composed predominantly of filamentous cyanobacteria where the algal cells occurred in clusters embedded in the EPS matrix. Filaments with the associated EPS were observed in the control biofilms. Heterotrophic bacteria formed close association with filamentous phototrophic microorganisms (Fig. 4b). In the PAH-treated biofilms cells were found as clusters and embedded firmly within the produced EPS in response to xenobiotic challenge. Biofilm structures were largely unchanged after 21days of incubation with PAHs. Salt crystals appeared as cube-like structures in SEM images.

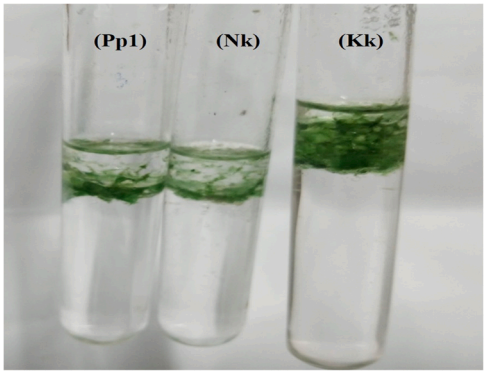

Fig. 2. Partitioning of phototrophic biofilms in the biphasic system. Pp1, Nk and Kk biofilms preferentially adhered to the hydrocarbon layer indicating the hydrophobicity of biofilms. For experimental method see Section 2.7.

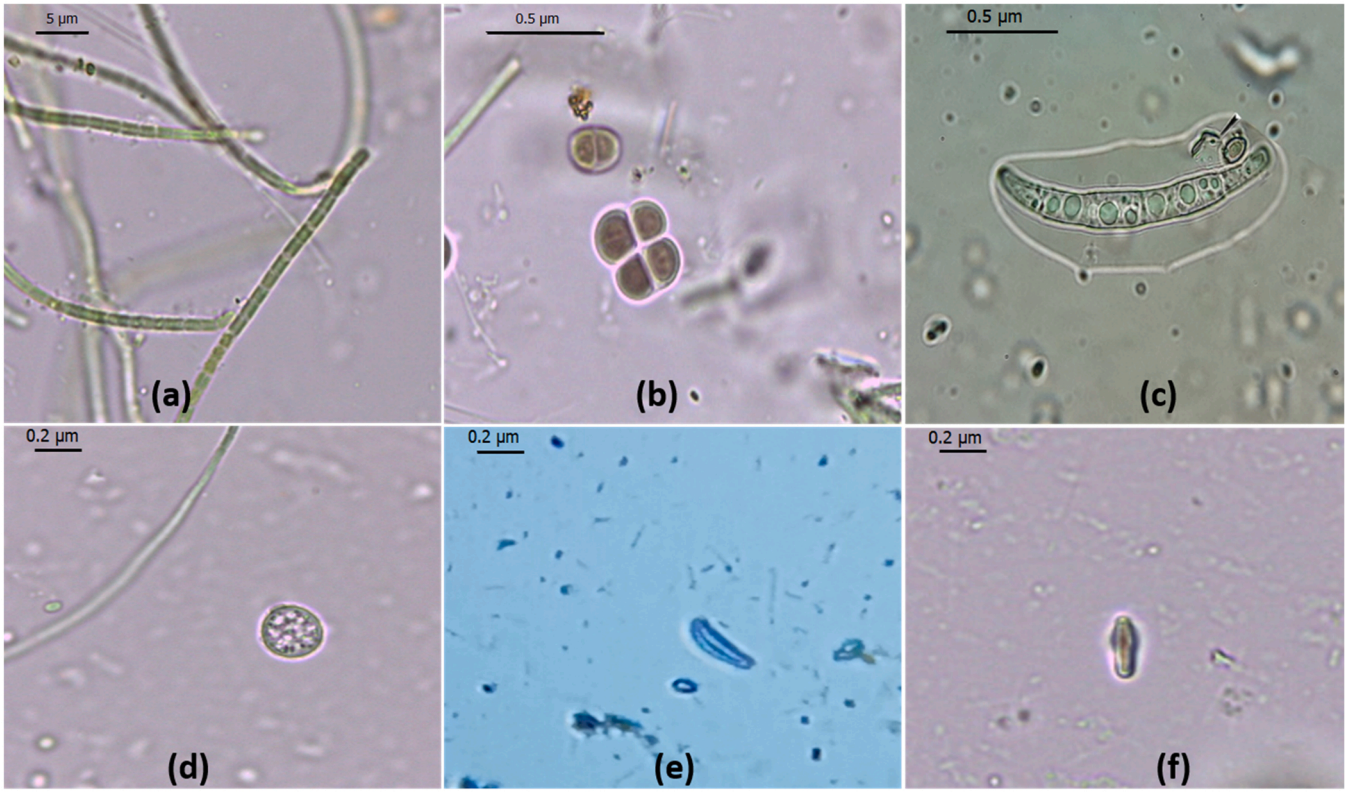

Fig. 3. Morphological analyses of PAH degrading phototrophic biofilms showed presence of (a) *Phormidium* sp. (b) *Gloeocapsa* sp. (c) *Closterium* sp. (d) *Microcystis* sp. (e) and (f) pennate diatoms (magnification of 100 ×10 X).

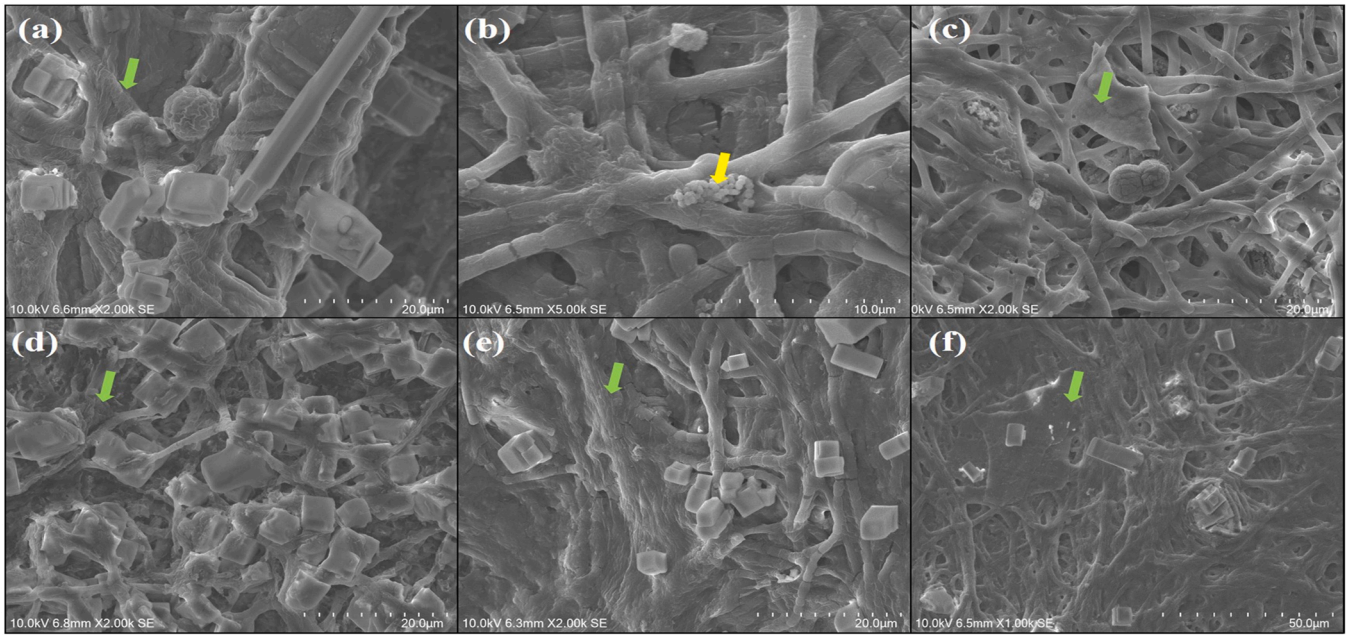

Fig. 4. Scanning electronic microscope (SEM) micrographs of (a) Pp1 (b) Nk (c) Kk phototrophic biofilms without PAHs and (d) Pp1 (e) Nk (f) Kk phototrophic biofilms treated with PAHs. Yellow arrow indicates bacteria associated with the biofilm and green arrows denote the EPS matrix.

3.2. Effect of PAHs on the biofilm biomass and photosynthetic pigments in hydrophobic and hydrophilic vessels

3.2.1. Increase in biofilm biomass

Addition of PAHs in the phototrophic biofilm growth media showed significant biomass increase in hydrophobic as well as hydrophilic flasks at $p \leq 0.05$ as shown in Table 3. Biomass accrued by the Pp1 biofilm in the presence of PAHs was higher in the hydrophilic glass flask in comparison to the hydrophobic PMMA flask. The increase in the Pp1 biomass in the presence of PAHs was 100% in glass ES-CCF and 58% in the PMMA flask. Compared to control biofilms, 19% and 22% increase in Nk biofilm biomass were recorded in the glass and PMMA ES-CCFs

respectively. For Kk biofilms, increase in biofilm biomass was 12% (glass ES-CCF) and 33% (PMMA ES-CCF). The mean residual PAH amounts were lowest in the liquid medium as well as inside the biofilms in the hydrophobic flask where the Kk biofilm was cultivated (Tables 1 and 2). Interestingly, highest biofilm biomass was recorded in this cultivation (Table 3, indicated in bold).

3.2.2. Increase in photosynthetic pigments

Total Chl contents in the biofilms cultured with PAHs increased when compared to the controls (Table 3). The highest total Chl content was measured in the hydrophilic culture of Pp1 biofilm and hydrophobic culture of Kk biofilm cultivated in PAH-spiked media. The enhanced total Chl content in these two flasks was well correlated with the lowest mean residual amount of PAHs (Table 2). Thus, elevated chlorophyll concentrations in PAH-treated biofilms implied an increased photosynthetic efficiency compared to control biofilms that in turn played a role in reducing PAH pollutant levels. Total Chl amounts in PAH-treated Nk biofilms were higher in hydrophobic PMMA flasks compared to hydrophilic glass vessels. Additionally, according to paired *t*-test concentrations of photosynthetic pigments (Chl *a*, *b*, *c*, *d* and carotenoids) in all three biofilms (Pp1, Nk and Kk) were significantly higher ($p \leq 0.05$) than their respective control treatments (Table 3).

After spiking with PAHs, Pp1 biofilm in the hydrophobic PMMA ES-CCF showed substantial increase in concentrations of all pigments (25–100% increase) compared to biofilms cultivated in hydrophilic glass ES-CCF (1–38%). Enhancement of all pigment concentrations (except Chl *d*) were noticeably higher in the hydrophilic glass ES-CCF cultured with the Nk biofilms spiked with the PAH contaminants in comparison with the hydrophobic PMMA ES-CCF. On the contrary, enhanced concentrations of all photosynthetic pigments were recorded in the hydrophobic PMMA ES-CCF compared to hydrophilic flasks where Kk biofilms were cultivated. As a further insight, carotenoids, among all the pigments showed a relatively lower increase in the biofilm samples spiked with PAHs in comparison to the controls. Enhancement of carotenoid contents in the hydrophilic glass ES-CCF with the spiked PAHs compared to its equivalent control was negligible (1.9% and 0.02%) when Pp1 and Kk biofilms were tested; whereas hydrophobic PMMA ES-CCF showed 29.4% increase when Pp1 biofilm was cultivated and 21.7% increase when Kk biofilm was grown. About 25% enhancement in carotenoid content was recorded in Nk biofilm cultured in the hydrophilic glass ES-CCF spiked with PAH pollutants while 16.2% increase in carotenoid content was measured when the biofilm was grown in the hydrophobic PMMA ES-CCF.

3.3. Production of exopolymeric substances (EPS) in hydrophobic and hydrophilic vessels

3.3.1. Released (RPS) and capsular/bound polymeric substances (CPS)

RPS and CPS were extracted separately from the PAH-spiked as well as control experiments to evaluate EPS production by the phototrophic biofilms when challenged with the 16 PAHs after 21 days incubation (Table 4). Increased production of the RPS as well as CPS was observed in the biofilms spiked with different concentrations of PAHs. Highest production of RPS was observed in Nk biofilms (compared to Pp1 and Kk biofilms) cultured in presence of PAHs in glass ES-CCF and PMMA ES-CCF. Mean RPS production by the phototrophic biofilms when challenged with PAHs was in the order Pp1 <Kk<Nk. RPS formation was higher in the hydrophobic flask cultured with Pp1 and Kk biofilms compared to the glass ES-CCFs but the reverse was observed in Nk biofilm cultures. Compared to the control biofilms, RPS production increased by 42.3%, 43.2% and 46% respectively in Pp1, Nk and Kk biofilms cultured in the hydrophilic flasks after 21 days incubation; whereas in the hydrophobic PMMA flasks 22.9%, 30.8% and 17.4% enhancements in RPS production were recorded in Pp1, Nk and Kk biofilms respectively.

Similar to RPS, the production of CPS by the biofilms increased but to a relatively lesser degree compared to RPS production after 21 days incubation with PAH contaminants (Table 4). In the presence of PAHs, highest CPS formation was observed in the Kk biofilms followed by Pp1 and Nk biofilms. Pp1 and Kk biofilms cultured in glass hydrophilic flask with PAHs showed greater CPS production compared to hydrophobic flask cultures whereas CPS production in Nk biofilms was higher in PMMA flask in comparison to glass ES-CCF vessel. The increase in the CPS production in the presence of PAH compared to the control was less in the glass ES-CCF for Pp1 biofilm (3.9%) and Kk biofilm (4.9%). In contrast, the enhancement of CPS production in the PMMA ES-CCF was 50.9% (Pp1 biofilm) and 20.6% (Kk biofilm). Compared to the Nk control biofilms, CPS production in the hydrophilic flask incubated with PAHs was enhanced negligibly (0.84%), while 12.3% increase in CPS production in the PMMA hydrophobic flask was recorded. Changes in RPS and CPS production were significant at $p < 0.05$ between the controls and their respective PAH-treated samples (Table 4).

3.3.2. EPS carbohydrates

Carbohydrates, proteins and uronic acid present in the EPS which have characteristic roles in biofilm growth and attachment were determined (Table 4). The concentration of protein was rather low, less than 15 mg g^{-1} of EPS on average, which accounted for only a small portion of the EPS constituents (less than 9% in RPS and 5% in CPS), while uronic acid and carbohydrates were the major biochemical components

Table 3
Biomass (g), concentration of total Chl, Chl *a*, Chl *b*, Chl *c*, Chl *d*, and carotenoid pigments (μg g^{-1}) extracted from biofilm biomass cultured with and without 16 priority PAH contaminants after 21 days incubation (values are means ± SD; n = 3). Bold figures indicate the highest values obtained. * * represents $p < 0.01$, * denotes $p < 0.05$ and ns stands for non-significant. Differences evaluated through paired *t*-test.

Parameters	Pp1 control		Pp1 +PAH		Nk control		Nk +PAH		Kk control		Kk +PAH	
	GLASS	PMMA	GLASS	PMMA	GLASS	PMMA	GLASS	PMMA	GLASS	PMMA	GLASS	PMMA
Biomass	0.94 ± 0.01	1.16 ± 0.02	1.96 ± 0.04 * *	1.85 ± 0.01 * *	1.59 ± 0.03	1.55 ± 0.06	1.90 ± 0.00 * *	1.91 ± 0.01 *	1.71 ± 0.04	1.53 ± 0.13	1.90 ± 0.06 ns	**1.97 ± 0.02***
Total Chl	1374.4 ± 13.2	965.9 ± 14.0	1495.0 ± 9.7 *	1397.7 ± 10.5 * *	897.8 ± 6.1	1024.2 ± 13.7	1323.9 ± 6.7 * *	1408.3 ± 6.4 * *	1221.2 ± 14.7	1153.6 ± 3.5	1381.7 ± 13.3 *	**1568.5 ± 8.3*** *
Chl a	868.4 ± 10.1	709.1 ± 3.6	903.2 ± 9.9 *	889.2 ± 4.7 * *	658.2 ± 10.4	722.4 ± 11.8	846.8 ± 2.7 * *	898.3 ± 8.2 * *	842.4 ± 8.2	789.5 ± 2.8	896.2 ± 3.2 *	**933.4 ± 9.4*** *
Chl b	181.5 ± 9.8	68.3 ± 8.2	247.2 ± 6.2 *	194.2 ± 5.6 * *	47.0 ± 2.9	78.1 ± 8.4	181.9 ± 7.9 * *	221.2 ± 20.2 * *	88.4 ± 3.7	112.2 ± 7.3	172.5 ± 7.3 * *	**268.2 ± 7.9*** *
Chl c	284.7 ± 5.7	176.4 ± 15.3	**338.5 ± 6.5***	295.7 ± 4.3 *	188.0 ± 0.4	217.0 ± 2.4	268.5 ± 9.6 * *	301.4 ± 6.0 * *	280.6 ± 6.1	240.8 ± 3.5	299.3 ± 1.3 ns	332.7 ± 10.6 * *
Chl d	19.9 ± 2.2	12.1 ± 0.7	**22.8 ± 3.4 ns**	18.5 ± 3.1 ns	4.6 ± 1.9	6.7 ± 1.7	11.5 ± 1.1 ns	17.1 ± 1.7 * *	9.8 ± 1.2	11.1 ± 1.7	13.6 ± 1.6 *	17.6 ± 1.6 *
Carotenoids	344.3 ± 5.6	275.1 ± 4.9	351.0 ± 14.6 ns	**355.9 ± 10.1***	231.3 ± 2.4	252.6 ± 1.4	289.4 ± 5.7 * *	293.4 ± 8.3 ns	315.5 ± 2.2	283.4 ± 8.6	315.5 ± 12.7 ns	344.7 ± 6.2 *

Table 4
RPS and CPS (mg g^{-1} of dry weight of biomass); carbohydrate, protein and uronic acid contents (mg g^{-1} of dry weight of RPS/CPS) and protein/polysaccharide ratio as percentage (%) in control and experimental biofilms cultured in hydrophilic glass and hydrophobic PMMA ES-CCFs (values are means ± SD; n = 3). Protein/ polysaccharide ratios of RPS and CPS were estimated by summing up the carbohydrate and uronic acid contents as total polysaccharide. Bold figures indicate the highest values obtained. * * represents $p < 0.01$, * denotes $p < 0.05$ and ns stands for non-significant. Differences evaluated through paired *t*-test.

Parameters	Pp1 control		Pp1 +PAH		Nk control		Nk +PAH		Kk control		Kk +PAH	
	GLASS	PMMA	GLASS	PMMA	GLASS	PMMA	GLASS	PMMA	GLASS	PMMA	GLASS	PMMA
RPS	55.9 ± 0.2	63.1 ± 8.7	78.7 ± 2.5 * *	82.3 ± 3.0 ^{ns}	83.9 ± 6.0	85.7 ± 1.3	**122.0 ± 3.5****	111.4 ± 7.3 *	59.0 ± 3.7	81.2 ± 3.4	90.6 ± 7.4 ^{ns}	96.6 ± 8.4 *
Carbohydrate	47.6 ± 0.9	50.9 ± 1.8	63.7 ± 2.3 *	52.6 ± 2.6 ^{ns}	77.8 ± 2.3	84.7 ± 1.9	92.5 ± 11.4 ^{ns}	100.3 ± 2.3 *	78.6 ± 6.2	88.3 ± 3.1	90.8 ± 2.8 ^{ns}	**128.2 ± 3.2***
Protein	6.6 ± 0.1	7.4 ± 0.2	**11.4 ± 0.3****	9.4 ± 0.6 ^{ns}	5.7 ± 0.1	5.9 ± 0.1	9.2 ± 0.6 * *	10 ± 0.6 *	5.5 ± 0.0	5.6 ± 0.0	9.8 ± 0.2 * *	10.4 ± 0.2 * *
Uronic acid	43.1 ± 2.8	33.7 ± 3.4	54.8 ± 2.0 * *	48.8 ± 0.9 *	36.2 ± 1.8	43.1 ± 2.0	64.1 ± 3.7 * *	68.5 ± 5.9 *	31.9 ± 1.6	37.3 ± 0.8	63.7 ± 2.2 * *	**90.2 ± 7.4****
Protein/ polysaccharide	7.2	8.7	**9.6****	9.3 ^{ns}	5.0	4.6	5.9 ^{ns}	5.8 ^{ns}	4.8	4.5	6.3 *	5.0 ^{ns}
CPS	51.2 ± 0.9	27.9 ± 1.4	53.2 ± 3.1 ^{ns}	42.2 ± 6.2 ^{ns}	22.5 ± 1.2	31.6 ± 1.2	25.2 ± 2.1 ^{ns}	31.8 ± 6.2 ^{ns}	65.1 ± 2.2	44.2 ± 4.3	**68.3 ± 6.0 ^{ns}**	53.3 ± 10 ^{ns}
Carbohydrate	148.3 ± 5.9	169.6 ± 3.2	297.8 ± 4.7 * *	274.6 ± 4.8 * *	126.0 ± 4	136.2 ± 1.9	232.6 ± 5.2 * *	294.6 ± 2.2 * *	208.0 ± 10.1	178.7 ± 3.0	325.1 ± 0.5 *	**398.4 ± 9****
Protein	5.5 ± 0.8	5.0 ± 0.1	11.1 ± 0.7 * *	8.1 ± 0.6 *	4.7 ± 0.5	4.9 ± 0.9	8.8 ± 0.9 * *	10.7 ± 0.3 *	5.8 ± 3.3	6.2 ± 0.4	9.1 ± 1.0 *	**14.1 ± 3.5****
Uronic acid	30.1 ± 2.8	32.2 ± 0.3	40.9 ± 3.5 *	55.0 ± 8.6 *	54.1 ± 4.5	56.3 ± 2.6	59.0 ± 0.9 * *	61.6 ± 5.6 ^{ns}	34.6 ± 2.4	55.2 ± 4.2	66.1 ± 4.9 * *	**90.2 ± 8.4****
Protein/ Polysaccharide	3.0	2.5	3.3 ^{ns}	2.5 ^{ns}	2.6	2.6	3.0 ^{ns}	3.0 ^{ns}	2.4	2.7	2.4 ^{ns}	2.9 ^{ns}

of the EPS, having proportions of above 91% in RPS and over 95% in CPS. In general, protein, carbohydrates and uronic acid contents increased in both RPS and CPS in the presence of PAHs in the cultivation media. RPS and CPS carbohydrates in biofilms spiked with PAHs increased significantly ($p \leq 0.05$) compared to the controls as evident from Table 4. Additionally, highest carbohydrate concentration was recorded in the RPS and CPS extracted from Kk biofilms cultured in the PMMA flask. CPS carbohydrate was present in the order Kk>Pp1 >Nk whereas RPS carbohydrates were obtained in the order Kk>Nk>Pp1 after 21 days incubation with PAHs. In the presence of PAHs, the carbohydrates were higher in the EPS extracted from hydrophilic vessels in comparison to hydrophobic vessels cultured with Pp1 biofilms. Carbohydrate content (in RPS and CPS) from the Nk biofilm-EPS was higher in EPS extracted from the hydrophobic flasks than the corresponding hydrophilic flasks. RPS carbohydrate contents extracted from the Kk biofilms were similar to that obtained from Nk biofilms. With PAHs as pollutants, increase of CPS carbohydrates in Kk biofilms was estimated to be lower in glass vessels compared to PMMA vessels.

3.3.3. *EPS proteins*

Measured values of proteins were low compared to the corresponding carbohydrates and uronic acids. Despite their low contents proteins are important because they constitute the enzymes required for metabolism, photosynthesis as well as CO_2 fixation. Similar to RPS and CPS carbohydrates the RPS and CPS proteins increased significantly in glass and PMMA ES-CCFs spiked with PAHs ($p \leq 0.05$) as evident from Table 4 The RPS and CPS protein contents in Pp1 biofilms were higher in the hydrophilic flasks in the presence of PAHs compared to hydrophobic flasks. In comparison with glass ES-CCFs, PMMA flask showed higher RPS and CPS protein concentrations in Nk as well as Kk biofilms. Protein concentration in the RPS was measured in the order Pp1 >Kk>Nk whereas for the CPS protein the series was Kk>Nk>Pp1. Moreover, the ratio of protein to polysaccharides (as percentage) upon exposure to PAHs pollutants was evaluated to decipher the specific character of EPS excretion (Table 4). In general, CPS protein to polysaccharides ratios showed no significant difference ($p > 0.05$) in the presence of PAHs for all the biofilms after 21 days incubation. The ratios of RPS protein to polysaccharides for Pp1 and Kk biofilms incubated with PAHs in hydrophilic vessels increased significantly at $p < 0.05$ (Table 4).

3.3.4. *EPS uronic acids*

Highest concentrations of CPS carbohydrates, uronic acid as well as RPS carbohydrates, proteins and uronic acids in the PMMA flasks cultured with the PAH-treated Kk biofilms was correlated with the lowest mean residual amount of PAHs in the hydrophobic culture of the Kk biofilm (Tables 1 and 2). In presence of PAH pollutants, uronic acid contents in RPS as well as CPS in all the biofilms increased significantly ($p \leq 0.05$). RPS uronic acids extracted from Nk and Kk biofilms as well as CPS uronic acids obtained from all three biofilms showed enhanced uronic acid concentration in the PMMA vessel spiked with PAHs. Only RPS uronic acids recovered from the Pp1 biofilms was an exception. The order of RPS as well as CPS uronic acids were Kk>Nk>Pp1. Uronic acid content of EPS (comprising of RPS and CPS) corroborated with the hydrophobicity of the EPS. Hydrophobicity of the EPS increased significantly after spiking with PAHs. Similar to uronic acid contents, hydrophobicity of RPS extracted from the Pp1 biofilms, hydrophobicity of RPS from Nk and Kk biofilms as well as CPS hydrophobicity from all the three biofilms were higher in the PMMA vessel for PAH exposed biofilms (Fig. 5).

4. Discussion

Differences in the sequestration of PAHs in the liquid media and biofilm biomass can be attributed to the geographical location from where the biofilms were sourced as well as the hydrophobicity/hydrophilicity of the culture vessel. No difference in the microbial community composition in biofilms collected from different geographical locations or changes in the microbial community composition in response to PAH exposure were noted. PAH challenge did not alter the community composition, rather biofilm biomass production and biochemical reactions (photosynthetic pigments and EPS synthesis) which also depended on the surface property of the culture vessel were affected. Despite being a toxicant, PAHs enhanced growth and Chl synthesis in biofilms. Photosynthetic pigment synthesis was very sensitive to surface property. Enhanced EPS synthesis was a major response to PAH challenge. The synthesis of the EPS components (RPS and CPS) as well as their biochemical constituents (proteins, carbohydrates and uronic acids) was highly influenced by the surface property of the cultivation vessel. These results are discussed in light of published literature under three sub-sections.

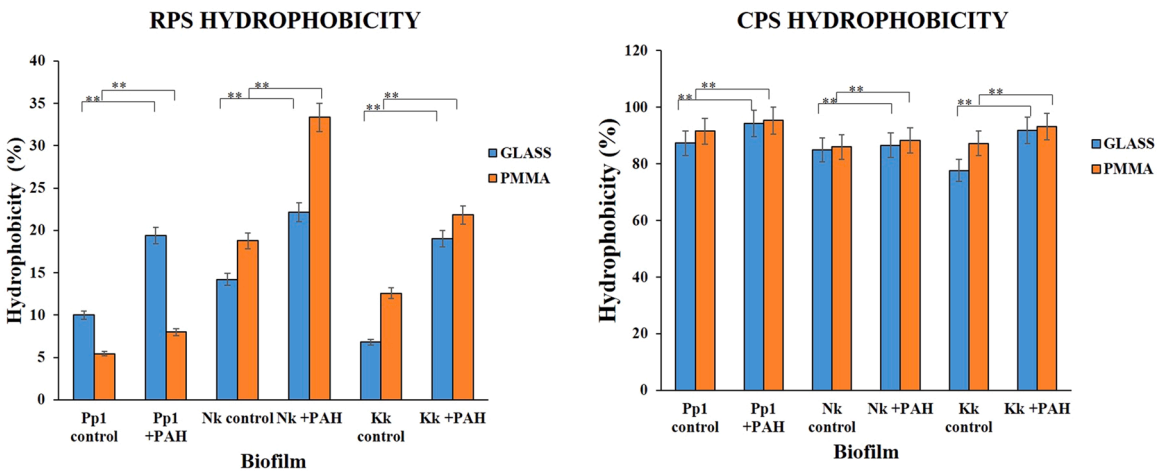

Fig. 5. Hydrophobicity of released (RPS) as well as capsular (CPS) extracellular polymeric substances. While RPS hydrophobicity is altered in response to PAH exposure, CPS hydrophobicity remained constant. For experimental method see Section 2.7. Significance determined through paired *t*-test at $p < 0.01$.

4.1. Growth and PAH sequestration by phototrophic biofilms

Phototrophic biofilms isolated from Patharpratima followed by Kakdwip and Namkhana showed the lowest mean PAH recoveries, which interestingly, were the same geographical locations of the Indian Sundarbans from where the isolated heterotrophic biofilms also demonstrated maximum PAH sequestration activity. Similar to this investigation, there was no substantial divergence between the mean residual PAHs remaining in the liquid media between hydrophobic and hydrophilic vessels. However, residual amounts of specific PAHs showed dissimilarities in their sequestration when cultivated in flasks having different surface properties (Balu et al., 2020). Initial layers of microalgal cells are more likely to adhere to hydrophobic surfaces than to hydrophilic surfaces (Wang et al., 2018). According to Mantzorou and Ververidis (2019) cell adhesion is favored by hydrophobic materials, although there are arguments disapproving the role of surface hydrophobicity in microalgae adhesion. For example Zhuang et al. (2018) noted that hydrophilic support media was more readily inclined to form the initial conditioning algal biofilm. Our results on the extent of PAH removal (Section 3.1) and formation of biofilm biomass (Section 3.2.1) in hydrophobic/hydrophilic vessels indicated that no generalizations could be made on the preference of surface hydrophobicity/hydrophilicity towards biofilm growth and PAH sequestration. Presence of PAHs in the liquid medium and the physico-chemical properties of the individual PAHs were influential in determining the role of the surface hydrophobicity/hydrophilicity in biofilm biomass formation and pollutant sequestration.

Hong et al. (2008) studied the accumulation and biodegradation of Phe and fluoranthene (Fla) by diatoms collected from mangroves of the Jiulong river estuary (China). Authors observed higher biomass provided more cell surface area and cell volume for adsorption and absorption of the PAHs, leading to enhanced removal in a shorter time period. These inferences were supported by Chan et al. (2006) and Lei et al. (2007) and are in consonance with the present study (see Section 3.2.1) because highest biofilm biomass was correlated with lowest mean residual PAHs. Usually, natural environments are polluted by multiple PAHs. Thus, Hong et al. (2008) remarked that in the presence of two or more PAHs, one PAH influenced the rate and extent of biodegradation of the other. This positive interaction was again supported by Chan et al. (2006) and Lei et al. (2007). Such positive influences presumably occurred amongst the 16 PAHs in the present investigation as well which led to their enhanced extent of sequestration.

In the environment, it is extremely rare to find a single microorganism that can degrade or completely remove the xenobiotic compound under different environmental conditions, therefore combined action of microalgae along with other phototrophic microbes play important role in the elimination of these contaminants (Semple et al., 1999). Consortia of the microbial population can exhibit functions that are challenging and require numerous steps to carry out for single species. Furthermore, mixotrophs are capable of assimilating both organic carbon and CO_2 simultaneously and autotrophic biofilms of the present investigation favored mixotrophic metabolism by assimilating PAHs with concomitant photosynthetic activity. Given their tolerance towards extreme environmental conditions, mixotrophic culture of algae/cyanobacteria was found to have an advantage over heterotrophic culture when cultivated at low nutrient concentration (Hamouda et al., 2016). Phototrophic biofilms of the present study were more active in the sequestration of PAHs compared to equivalent heterotrophic biofilms of our previous study. The average of mean residual PAH amounts in the phototrophic biofilms of this study were 22% while the same in heterotrophic biofilms was 35% (Balu et al., 2020).

Phormidium sp., *Gloeocapsa* sp., *Closterium* sp., *Microcystis* sp. and diatoms were identified as photosynthetic organisms in the biofilms. These organisms possess PAH degradation capability as well as the potential to degrade other pollutants including metals. For example, Ant was degraded by hypersaline *Phormidium tenue* (Zyszka-Haberecht et al., 2019). Abed et al. (2002) also reported presence of *Phormidium* sp. as the predominant cyanobacterium in indigenous microbial communities inhabiting a heavily polluted site in a coastal stream (Wadi Gaza) as well as its PAH degradation potential, especially Phe. Ibraheem (2010) and Kumar et al. (2009) demonstrated Phe, Ant and Nap degradation activity of *Phormidium* sp. *Gloeocapsa* sp. has not yet been known as a PAH degrader but it is widely applied in the removal of lead (Pb^{2+}) as reported by Raungsomboon et al. (2006). Mohamed (2001) also determined the capacity of *Gloeocapsa* sp. to adsorb cadmium and manganese. Nap, Phe and Pyr were degraded by the cyanobacterium *Microcystis aeruginosa* (Rath, 2012). The biosorption of Phe by the EPS of *Microcystis aeruginosa* was studied by Bai et al. (2016). Ichor et al. (2016) identified *Phormidium* sp. and *Microcystis* sp. as Phe degrading microorganisms. *Closterium* sp. degraded the crude oil in the polluted environment, especially in dark (Uzoh et al., 2015) but its PAH degradation capacity is not yet known.

4.2. Photosynthetic pigment production upon PAH exposure

The present study showed an increase in the photosynthetic pigment concentrations in all the three biofilm samples after growing in media spiked with 16 priority pollutants for 21 days. Increase in Chl *a* content can augment algal photosynthesis, which can accelerate greater energy accretion in the algae and stimulate algal reproduction and growth

(Chen et al., 2020). Similar inferences were drawn by several other workers in other phototrophic microorganisms such as the saline cyanobacterium *Phormidium tenue* (Zyszka-Haberecht et al., 2019), *Selenastrum capricornutum* (Luo et al., 2015, 2014; Traczewska et al., 1999), *Chlorella vulgaris* and *Chlorella* sp (Luo et al., 2015) and *Oscillatoria* sp. (Aldaby and Mawad, 2019).

Although these authors reported enhancement of chlorophyll levels in photoautotrophs upon PAH exposure, the reasons for such increase were not discussed. PAHs inhibited photosystem II in wild-type *Arabidopsis thaliana* plants (Jajoo et al., 2014). However, the action of PAHs on the photosynthetic mechanism of microalgae has not been examined. On the other hand, Ricart et al. (2009) reported herbicide diuron exposure enhanced Chl *a* content of a riverine biofilm community. Chl *a* increased with high diuron exposure, similar to our observations. At low diuron concentrations, electron flow in photosystem II during the light reaction of photosynthesis is disrupted and stimulates the formation of shade-type chloroplasts. Microalgae may regulate the intracellular levels of photosynthetic pigments in response to changing environmental situations. "Shade-adaptation" response involves enhancement in photosynthetic pigments in reaction to decreased light intensity. This acclimatization may recompense for the lowered photosynthetic efficiency. Higher diuron concentrations inhibit photosystem I and can lead to the photodestruction of pigments. However, reduction of pigment concentration was not detected in our study. In agreement with the mechanism proposed by Ricart et al. (2009) our results indicate the formation of shade-type chloroplasts corroborative with the correlated increase in Chl *a* in response to PAH exposure. Additionally, the accessory light harvesting pigment (Chl *b*) content of *Nephroselmis pyriformis* increased significantly when exposed to three photosystem II–inhibiting herbicides; while another accessory pigment (Chl *c*) enhanced marginally in the presence of these herbicides (Magnusson et al., 2008) which is supportive of our contemplated photosystem II disruption hypothesis. Carotenoids play a key role in light-protection reactions and contribute towards cell wall stabilization. Enhanced synthesis of carotenoids in phototrophic biofilms as observed in the presence of PAHs in this study is an indicator of suboptimal cultivation conditions (Stiefelmaier et al., 2020).

Our experiments underscored the difference in the pigment synthesis when biofilms were cultured in hydrophobic/hydrophilic flasks surfaces. There is scant literature on the influence of surface hydrophobicity/hydrophilicity on photosynthetic pigment synthesis. Five microalgal species (*Amphora coffeaeformis, Navicula incerta, Cylindrotheca fusiformis, Chaetoceroups* sp. and *Nannochloropsis* sp.) were cultivated on hydrophobic and hydrophilic surfaces by Poad and Derek (2019). Authors observed higher attachment of the microalgae on the hydrophilic cellulose acetate and polyacrylamide membranes compared to the hydrophobic polytetrafluoroethylene membrane. Concomitant chlorophyll concentrations were higher in the microalgae attached to hydrophilic membranes compared to the hydrophobic membrane. Similarly, biofilm wet weight as well as Chl *a* contents of *Synechocystis salina* and *Cyanobium* sp. were higher on hydrophilic glass than on hydrophobic epoxy-coated glass (Faria et al., 2020). Variability in the concentration of each type of pigment (Chl *a*, *b*, *c*, *d* and carotenoids) was dependent on the geographical location from where the biofilm was sourced (Pp, Nk and Kk) as well as surface hydrophobicity/hydrophilicity of the culture flask.

4.3. Influence of PAH exposure on EPS synthesis

More condensed fractions of the EPS are usually designated as "sheaths" and "capsules" [capsular polysaccharides (CPSs)] which enclose cells or cell groups. CPSs increase microbial adhesion to solid surfaces and the aggregation of crude substrates. Less condensed EPS fractions, lightly bound to cells, are generally defined as "slime" and are not indicative of cellular shape. Released polysaccharides (RPSs) constitute the polysaccharidic external layers that are partially released in the surrounding medium. Anionic and sticky characters of the EPS macromolecules are imparted by the presence of sulfate groups and uronic acids. Hydrophobic nature of the EPS is conferred by deoxysugars (rhamnose and fucose), peptides and ester-linked acetyl groups, significantly influencing their ability to adhere to solid substrates (Rossi and De Philippis, 2015).

A high production of EPS is generally regarded as a protective mechanism against stress factors (Stiefelmaier et al., 2020). Environmental stressors, such as the presence of PAHs in this investigation, affect not only the quantity of produced EPSs, but also the physico-chemical characteristics of the secreted polymer, thus strengthening the adaptation capacity of the biofilm to severe environmental conditions (Rossi and De Philippis, 2015). In this perspective, a mechanism to be considered for the enhancement of the bioavailability of PAHs to the degradative enzymes is the production of biosurfactants and high molecular weight EPS can function as biosurfactants (McGenity et al., 2012). Microbial biosurfactants are also produced in response to heavy metal challenge (Govarthanan et al., 2017b). Produced EPS can reduce interfacial tension and interact with hydrophobic PAHs thus enhancing their solubility in water. Solubilization of PAHs enhanced with augmented surfactant levels and reduced interfacial tension (Zhang et al., 2011), commensurate with this study. The cell surface produced polysaccharides contain hydrophobic as well as hydrophilic moieties. The hydrophobic constituents are possibly accountable for the enhancement of PAH solubility in the bulk water by interactions between the hydrophobic components and the PAH molecules (Zhang et al., 2011). In agreement with this interpretation, the hydrophobicity of the RPS fraction of the EPS secreted in our experiments increased upon exposure to PAHs (Fig. 5). CPS hydrophobicity was maintained above 80% irrespective of PAH exposure which was also confirmed by the hexadecane partition test, suggesting that the tested biofilms were inherently hydrophobic.

Microbes control their EPS constitution and components for acclimatization to growth with hydrophobic substrates such as PAHs. EPS polysaccharide contents increased in the presence of PAH pollutants, which is favorable for the removal of the toxicant through accumulation, adsorption or degradation (Chen et al., 2020). The alteration of EPS composition can be assessed by determining the ratio of proteins to polysaccharides (Zhang et al., 2011). In our study, the ratio of RPS proteins to polysaccharides increased for all the biofilms, indicating that RPS proteins increased faster than RPS polysaccharides when hydrophobic PAHs were used as the substrate. However, the ratios of CPS proteins to CPS polysaccharides remained constant during PAH exposure for all the biofilms, showing that there was no modification in the biochemical composition of CPS. Moreover, the RPS protein to polysaccharide ratio of Pp1 biofilm cultured in hydrophilic as well as hydrophobic flasks increased, signifying that Pp1 biofilms regulated their EPS constituents more effectively than Nk and Kk biofilms during adaptation to PAH exposure. RPS played a greater role than CPS during growth of Pp1, Nk and Kk biofilms in presence of PAHs. The hydrophobic domains of EPS (mainly consisting of proteins) adsorb organic petroleum hydrocarbons such as Phe and benzene. The relative abundance of protein to polysaccharides can be considered as the key parameter that controls the hydrophobicity/ hydrophilicity of EPS (Xu et al., 2018). Additionally, EPS with higher protein and polysaccharide ratios possessed higher enzymatic activities (Nikolova and Gutierrez, 2021). Yet another biochemical component of the EPS, uronic acid effectively emulsifies hydrocarbons. High uronic acids containing EPS have lower amounts of carbohydrates and proteins (Uzoigwe et al., 2015). Uronic acids bestow the capability of EPS to interact with hydrophobic substrates such as PAHs. The EPS-mediated solubilization enhancement of hydrocarbons with lower log *P* values may be associated with the polarity of these compounds, permitting them to modestly unite with the negatively-charged residues of uronic acids (Gutierrez et al., 2013).

In our experiments production of CPS, RPS, carbohydrate, protein,

uronic acids, protein/polysaccharide ratios also varied depending on the source of the biofilm (Pp, Nk, Kk) as well as with the type of culture vessel (hydrophobic/hydrophilic). No generalizations on specific reasons for such influences can be made because there is very limited knowledge of the effect of surface hydrophobicity/hydrophilicity on the synthesis of EPS. Few reports demonstrated that EPS production was influenced by available nutrients and/or surface hydrophobicity/hydrophilicity of the culture vessel. For example, *Botryococcus braunii* produced higher EPS concentration in a modified basal medium (MB) when cultivated on glass fiber reinforced plastic (hydrophilic surface) in a multilayered photobioreactor compared to culture on polyethylene foam (hydrophobic surface). The protein secreted from the biofilm cells was pivotal for robust biofilm adhesion on glass fiber reinforced plastic (as reviewed by Cheah and Chan, 2021). In another study by Becker (1996), highest EPS production by diatoms and bacteria was observed on hydrophilic substrata and lowest EPS production was recorded on hydrophobic substrata. Authors remarked that exopolysaccharides are produced in greater amounts when diatoms and bacteria are in contact with those materials on which EPS provides superior adhesion. It should also be considered that different EPS concentrations determined on the different substrata are connected with several other functions beyond adhesion (Becker, 1996). As discussed previously in this sub-section, the adaptive response of biofilms to PAH exposure as tested in the present investigation was also influential in determining the EPS levels in addition to surface hydrophobicity/hydrophilicity of the cultivation vessel.

5. Conclusions and prospects

Our observations underline surface hydrophobicity/hydrophilicity as a major influencing factor in investigations involving phototrophic biofilms. The choice of the vessel will affect experimental results and inferences drawn therefrom. It may also be concluded that heterotrophic and phototrophic biofilms community from the sites having highest PAH sediment concentration (Nk and Kk) adapted themselves by elaborate biochemical responses to the presence of high levels of PAHs. For better understanding of the sequestration process, the determination of the water/biomass organic carbon distribution coefficients and diffusion coefficients of the individual PAHs (Wicke et al., 2007) is essential. The composition of the biofilm and the role of external effects on the partitioning of the individual PAHs inside the biofilm and the transformation of the individual PAHs (Wicke et al., 2008) are also necessary. Contaminated sediments present difficult remediation and management challenges, as standard sediment quality preservation techniques are intrusive, costly, and occasionally ineffective or difficult to apply to large and diverse sediment sites (Maletic et al., 2019). This study revealed the prospective of phototrophic biofilms in field applications for sequestering PAH contaminants in mangrove forest intertidal sediments. These films should be propagated in preference to heterotrophic ones due to their enhanced extent of PAH removal compared to heterotrophic biofilms. In future we wish to translate this laboratory study to the field where PAH sequestration will be evaluated through bioaugmentation and biostimulation approaches. Simultaneously, phototrophic and heterotrophic microbial diversity will be determined. Prospective investigations may also be concentrated upon metagenomics (Prakash et al., 2021), electrochemical treatments (Silambarasan et al., 2021) and bioelectrokinetic remediation (Vaishnavi et al., 2021).

Environmental implication

Polycyclic aromatic hydrocarbon (PAH) pollutants are mutagenic, carcinogenic, teratogenic and immunotoxicogenic to humans, plants and animals hence regarded as hazardous. The USEPA recognizes 16 PAHs as priority pollutants considering their higher prevalence, greater exposure, recalcitrance and toxicity. Enhanced deposition of PAHs occurs in sediments owing to their low aqueous solubility and high hydrophobicity. PAH accretion in intertidal sediments is due to economic activity and conventional energy usage. Bioaugmentation, biostimulation, bioreactors, phytoremediation and composting are the current popular biological methods applied for PAH bioremediation. Application of indigenous phototrophic biofilms for PAH preclusion in intertidal sediments is a new and innovative approach.

CRediT authorship contribution statement

Saranya Balu: Data curation, Formal analysis, Investigation, Methodology, Writing – original draft. **Shantanu Bhunia:** Data curation, Formal analysis, Investigation, Methodology, Writing – original draft. **Ratan Gachhui:** Funding acquisition, Resources, Software, Supervision. **Joydeep Mukherjee:** Conceptualization, Funding acquisition, Project administration, Resources, Software, Supervision, Validation, Visualization, Writing – review & editing.

Declaration of Competing Interest

The authors declare that they have no known competing financial interests or personal relationships that could have appeared to influence the work reported in this paper.

Acknowledgments

Authors thank the Department of Biotechnology, Government of West Bengal, India [72 (Sanc.)-BT/P/Budget/RD-34/2017] for financial support and Mr. Sanjoy Mondal (Sundarbans Safari) for organizing the field trip.

References

Abed, R.M., Safi, N.M., Köster, J., De Beer, D., El-Nahhal, Y., Rullkötter, J., Garcia-Pichel, F., 2002. Microbial diversity of a heavily polluted microbial mat and its community changes following degradation of petroleum compounds. Appl. Environ. Microbiol. 68 (4), 1674–1683. https://doi.org/10.1128/AEM.68.4.1674-1683.2002.

Aldaby, E.S.E., Mawad, A.M.M., 2019. Pyrene biodegradation capability of two different microalgal strains. Glob. Nest J. 21 (3), 291–296. https://doi.org/10.30955/gnj.002767.

Bai, L., Xu, H., Wang, C., Deng, J., Jiang, H., 2016. Extracellular polymeric substances facilitate the biosorption of phenanthrene on cyanobacteria *Microcystis aeruginosa*. Chemosphere 162, 172–180. https://doi.org/10.1016/j.chemosphere.2016.07.063.

Balu, S., Bhunia, S., Gachhui, R., Mukherjee, J., 2020. Assessment of polycyclic aromatic hydrocarbon contamination in the Sundarbans, the world's largest tidal mangrove forest and indigenous microbial mixed biofilm-based removal of the contaminants. Environ. Pollut. 266, 115–270. https://doi.org/10.1016/j.envpol.2020.115270.

Becker, K., 1996. Exopolysaccharide production and attachment strength of bacteria and diatoms on substrates with different surface tensions. Microb. Ecol. 32 (1), 23–33. https://doi.org/10.1007/BF00170104.

Bhatnagar, M., Parwani, L., Sharma, V., Ganguly, J., Bhatnagar, A., 2014. Exopolymers from *Tolypothrix tenuis* and three *Anabaena* sp. (Cyanobacteriaceae) as novel blood clotting agents for wound management. Carbohydr. Polym. 99, 692–699. https://doi.org/10.1016/j.carbpol.2013.09.005.

Boelee, N.C., 2013. Microalgal Biofilms for Wastewater Treatment. Wageningen University. ISBN: 978-94-6173-666-6.

Chan, S.M.N., Luan, T., Wong, M.H., Tam, N.F.Y., 2006. Removal and biodegradation of polycyclic aromatic hydrocarbons by *Selenastrum capricornutum*. Environ. Toxicol. Chem. 25 (7), 1772–1779. https://doi.org/10.1897/05-354R.1.

Cheah, Y.T., Chan, D.J.C., 2021. Physiology of microalgal biofilm: a review on prediction of adhesion on substrates. Bioengineered 12 (1), 7577–7599. https://doi.org/10.1080/21655979.2021.1980671.

Chen, S., Li, J., Feng, W., Yuan, M., Zhang, W., Xu, H., Zheng, X., Wang, L., 2020. Biochemical responses of the freshwater microalga *Dictyosphaerium* sp. upon exposure to three sulfonamides. J. Environ. Sci. 97, 141–148. https://doi.org/10.1016/j.jes.2020.05.018.

Cole, J.K., Hutchison, J.R., Renslow, R.S., Kim, Y.M., Chrisler, W.B., Engelmann, H.E., Dohnalkova, A.C., Hu, D., Metz, T.O., Fredrickson, J.K., Lindemann, S.R., 2014. Phototrophic biofilm assembly in microbial-mat-derived unicyanobacterial consortia: model systems for the study of autotroph-heterotroph interactions. Front. Microbiol. 5, 109. https://doi.org/10.3389/fmicb.2014.00109.

Di Pippo, F., Ellwood, N.T., Gismondi, A., Bruno, L., Rossi, F., Magni, P., De Philippis, R., 2013. Characterization of exopolysaccharides produced by seven biofilm-forming cyanobacterial strains for biotechnological applications. J. Appl. Phycol. 25 (6), 1697–1708. https://doi.org/10.1007/s10811-013-0028-1.

Dubois, M., Gilles, K.A., Hamilton, J.K., Rebers, P.T., Smith, F., 1956. Colorimetric method for determination of sugars and related substances. Anal. Chem. 28 (3), 350–356. https://doi.org/10.1021/ac60111a017.

Faria, S.I., Teixeira-Santos, R., Romeu, M.J., Morais, J., Vasconcelos, V., Mergulhão, F.J., 2020. The relative importance of shear forces and surface hydrophobicity on biofilm formation by coccoid cyanobacteria. Polymers 12 (3), 653. https://doi.org/10.3390/polym12030653.

Fattom, A., Shilo, M., 1984. Hydrophobicity as an adhesion mechanism of benthic cyanobacteria. Appl. Environ. Microbiol. 47, 135–143. https://doi.org/10.1128/aem.47.1.135-143.1984.

Froehner, S., Machado, K.S., Dombroski, L.F., Nunes, A.C., Kishi, R.T., Bleninger, T., Sanez, J., 2012. Natural biofilms in freshwater ecosystem: indicators of the presence of polycyclic aromatic hydrocarbons. Water Air Soil Poll. 223 (7), 3965–3973. https://doi.org/10.1007/s11270-012-1164-y.

Gacheva, G., Gigova, L., Ivanova, N., Iliev, I., Toshkova, R., Gardeva, E., Kussovski, V., Najdenski, H., 2013. Suboptimal growth temperatures enhance the biological activity of cultured cyanobacterium *Gloeocapsa* sp. J. Appl. Phycol. 25 (1), 183–194. https://doi.org/10.1007/s10811-012-9852-y.

Govarthanan, M., Fuzisawa, S., Hosogai, T., Chang, Y.C., 2017a. Biodegradation of aliphatic and aromatic hydrocarbons using the filamentous fungus *Penicillium* sp. CHY-2 and characterization of its manganese peroxidase activity. RSC Adv. 7 (34), 20716–20723. https://doi.org/10.1039/C6RA28687A.

Govarthanan, M., Mythili, R., Selvankumar, T., Kamala-Kannan, S., Choi, D., Chang, Y.C., 2017b. Isolation and characterization of a biosurfactant-producing heavy metal resistant *Rahnella* sp. RM isolated from chromium-contaminated soil. Biotechnol. Bioprocess Eng. 22 (2), 186–194. https://doi.org/10.1007/s12257-016-0652-0.

Govarthanan, M., Khalifa, A.Y., Kamala-Kannan, S., Srinivasan, P., Selvankumar, T., Selvam, K., Kim, W., 2020. Significance of allochthonous brackish water *Halomonas* sp. on biodegradation of low and high molecular weight polycyclic aromatic hydrocarbons. Chemosphere 243, 125389. https://doi.org/10.1016/j.chemosphere.2019.125389.

Govarthanan, M., Liang, Y., Kamala-Kannan, S., Kim, W., 2022. Eco-friendly and sustainable green nano-technologies for the mitigation of emerging environmental pollutants. Chemosphere 287 (2), 132234. https://doi.org/10.1016/j.chemosphere.2021.132234.

Gutierrez, T., Berry, D., Yang, T., Mishamandani, S., McKay, L., Teske, A., Aitken, M.D., 2013. Role of bacterial exopolysaccharides (EPS) in the fate of the oil released during the Deep-water Horizon oil spill. PLos One 8 (6), e67717. https://doi.org/10.1371/journal.pone.0067717.

Hamouda, R.A.E.F., Sorour, N.M., Yeheia, D.S., 2016. Biodegradation of crude oil by *Anabaena oryzae*, *Chlorella kessleri* and its consortium under mixotrophic conditions. Int. Biodeterior. Biodegrad. 112, 128–134. https://doi.org/10.1371/journal.pone.0067717.

Haripriyan, U., Gopinath, K.P., Arun, J., Govarthanan, M., 2022. Bioremediation of organic pollutants: a mini review on current and critical strategies for wastewater treatment. Arch. Microbiol. 204 (5), 1–9. https://doi.org/10.1007/s00203-022-02907-9.

Hong, Y.W., Yuan, D.X., Lin, Q.M., Yang, T.L., 2008. Accumulation and biodegradation of phenanthrene and fluoranthene by the algae enriched from a mangrove aquatic ecosystem. Mar. Pollut. Bull. 56 (8), 1400–1405. https://doi.org/10.1016/j.marpolbul.2008.05.003.

Hyslop, N.P., White, W.H., 2009. Estimating precision using duplicate measurements. J. Air Waste Manag. Assoc. 59 (9), 1032–1039. https://doi.org/10.3155/1047-3289.59.9.1032.

Ibraheem, I.B.M., 2010. Biodegradability of hydrocarbons by cyanobacteria. J. Phycol. 46 (4), 818–824. https://doi.org/10.1111/j.1529-8817.2010.00865.x.

Ichor, T., Gberikon, G.M., Nevkaa, D., 2016. Biodegradation of phenanthrene by a consortium of aerobic heterotrophic bacteria and cyanobacteria in petroleum hydrocarbon polluted brackish water of Bodo Creek. J. Microbiol. 6, 1–8. https://doi.org/10.3923/mj.2016.1.8.

Jajoo, A., Mekala, N.R., Tomar, R.S., Grieco, M., Tikkanen, M., Aro, E.M., 2014. Inhibitory effects of polycyclic aromatic hydrocarbons (PAHs) on photosynthetic performance are not related to their aromaticity. J. Photochem. Photobiol. B Biol. 137, 151–155. https://doi.org/10.1016/j.jphotobiol.2014.03.011.

Jones, R., Payne, R., 1997. Clinical Investigation and Statistics in Laboratory Medicine. ACB Venture Publications, London, pp. 53–64.

Kumar, M.S., Muralitharan, G., Thajuddin, N., 2009. Screening of a hypersaline cyanobacterium, *Phormidium tenue*, for the degradation of aromatic hydrocarbons: naphthalene and anthracene. Biotechnol. Lett. 31 (12), 1863–1866. https://doi.org/10.1007/s10529-009-0085-3.

Lei, A.P., Hu, Z.L., Wong, Y.S., Tam, N.F.Y., 2007. Removal of fluoranthene and pyrene by different microalgal species. Bioresour. Technol. 98 (2), 273–280. https://doi.org/10.1016/j.biortech.2006.01.012.

Lowry, O.H., Rosebrough, N.J., Farr, A.L., Randall, R.J., 1951. Protein measurement with the Folin phenol reagent. J. Biol. Chem. 193, 265–275.

Luo, L., Wang, P., Lin, L., Luan, T., Ke, L., Tam, N.F.Y., 2014. Removal and transformation of high molecular weight polycyclic aromatic hydrocarbons in water by live and dead microalgae. Process. Biochem. 49 (10), 1723–1732. https://doi.org/10.1016/j.procbio.2014.06.026.

Luo, L., Lai, X., Chen, B., Lin, L., Fang, L., Tam, N.F., Luan, T., 2015. Chlorophyll catalyse the photo-transformation of carcinogenic benzo [a] pyrene in water. Sci. Rep. 5 (1), 1–11. https://doi.org/10.1038/srep12776.

Lv, M., Luan, X., Liao, C., Wang, D., Liu, D., Zhang, G., Jiang, G., Chen, L., 2020. Human impacts on polycyclic aromatic hydrocarbon distribution in Chinese intertidal zones. Nat. Sustain. 3 (10), 878–884. https://doi.org/10.1038/s41893-020-0565-y.

Magnusson, M., Heimann, K., Negri, A.P., 2008. Comparative effects of herbicides on photosynthesis and growth of tropical estuarine microalgae. Mar. Pollut. Bull. 56 (9), 1545–1552. https://doi.org/10.1016/j.marpolbul.2008.05.023.

Maletic, S.P., Beljin, J.M., Rončević, S.D., Grgić, M.G., Dalmacija, B.D., 2019. State of the art and future challenges for polycyclic aromatic hydrocarbons is sediments: sources, fate, bioavailability and remediation techniques. J. Hazard. Mater. 365, 467–482. https://doi.org/10.1016/j.jhazmat.2018.11.020.

Mandal, A., Dutta, A., Das, R., Mukherjee, J., 2021. Role of intertidal microbial communities in carbon dioxide sequestration and pollutant removal: a review. Mar. Pollut. Bull. 170, 112626 https://doi.org/10.1016/j.marpolbul.2021.112626.

Mantzorou, A., Ververidis, F., 2019. Microalgal biofilms: a further step over current microalgal cultivation techniques. Sci. Total Environ. 651, 3187–3201. https://doi.org/10.1016/j.scitotenv.2018.09.355.

McGenity, T.J., Folwell, B.D., McKew, B.A., Sanni, G.O., 2012. Marine crude-oil biodegradation: a central role for interspecies interactions. Aquat. Biosyst. 8 (1), 1–19. https://doi.org/10.1186/2046-9063-8-10.

Mohamed, Z.A., 2001. Removal of cadmium and manganese by a non-toxic strain of the freshwater cyanobacterium *Gloeothece magna*. Water Res. 35 (18), 4405–4409. https://doi.org/10.1016/S0043-1354(01)00160-9.

Moreno Osorio, J.H., Pollio, A., Frunzo, L., Lens, P.N.L., Esposito, G., 2021. A review of microalgal biofilm technologies: definition, applications, settings and analyzing. Front. Chem. Eng. 43. https://doi.org/10.3389/fceng.2021.737710.

Nhi-Cong, L.T., Lien, D.T., Mai, C.T.N., Linh, N.V., Lich, N.Q., Ha, H.P., Show, P.L., 2021. Advanced materials for immobilization of purple phototrophic bacteria in bioremediation of oil-polluted wastewater. Chemosphere 278, 130464. https://doi.org/10.1016/j.chemosphere.2021.130464.

Nikolova, C., Gutierrez, T., 2021. Biosurfactants and their applications in the oil and gas industry: current state of knowledge and future perspectives. Front. Bioeng. Biotechnol. 46. https://doi.org/10.3389/fbioe.2021.626639.

Panah, B.A., Najafi, F., Soltani, N., Nejad, R.A., Babaei, S., 2015. Biodegradation ability and physiological responses of cyanobacterium *Leptolyngbya* sp. ISC 25 under naphthalene treatment. Algologia 25 (2), 125–134. https://doi.org/10.15407/alg25.02.125.

Patel, J.G., Kumar, J.N., Khan, S.R., 2015. Consequences of environmentally hazardous polycyclic aromatic hydrocarbon-anthracene treatment on cyanobacteria. Int. J. Appl. Sci. Biotechnol. 3 (3), 381–386. https://doi.org/10.3126/ijasbt.v3i3.11654.

Poad, S.M. and Derek, C.J.C., 2019. Microalgae adhesion on polymeric membrane. In AIP Conference Proceedings. AIP Publishing LLC. 2124(1), pp. 020061. https://doi.org/10.1063/1.5117121.

Prakash, A.A., Rajasekar, A., Sarankumar, R.K., AlSalhi, M.S., Devanesan, S., Aljaafreh, M.J., Govarthanan, M., Sayed, S.R., 2021. Metagenomic analysis of microbial community and its role in bioelectrokinetic remediation of tannery contaminated soil. J. Hazard. Mater. 412, 125133 https://doi.org/10.1016/j.jhazmat.2021.125133.

Qian, X., Liang, B., Fu, W., Liu, X., Cui, B., 2016. Polycyclic aromatic hydrocarbons (PAHs) in surface sediments from the intertidal zone of Bohai Bay, Northeast China: spatial distribution, composition, sources and ecological risk assessment. Mar. Pollut. Bull. 112 (1–2), 349–358. https://doi.org/10.1016/j.marpolbul.2016.07.040.

Rath, B., 2012. Microalgal bioremediation: current practices and perspectives. J. Biochem. Technol. 3 (3), 299–304.

Raungsomboon, S., Chidthaisong, A., Bunnag, B., Inthorn, D., Harvey, N.W., 2006. Production, composition and Pb^{2+} adsorption characteristics of capsular polysaccharides extracted from a cyanobacterium *Gloeocapsa gelatinosa*. Water Res. 40 (20), 3759–3766. https://doi.org/10.1016/j.watres.2006.08.013.

Ricart, M., Barceló, D., Geiszinger, A., Guasch, H., de Alda, M.L., Romaní, A.M., Vidal, G., Villagrasa, M., Sabater, S., 2009. Effects of low concentrations of the phenylurea herbicide diuron on biofilm algae and bacteria. Chemosphere 76 (10), 1392–1401. https://doi.org/10.1016/j.chemosphere.2009.06.017.

Ritchie, R.J., 2008. Universal chlorophyll equations for estimating chlorophylls a, b, c, and d and total chlorophylls in natural assemblages of photosynthetic organisms using acetone, methanol, or ethanol solvents. Photosynthetica 46 (1), 115–126. https://doi.org/10.1007/s11099-008-0019-7.

Roeselers, G., Van Loosdrecht, M.C., Muyzer, G., 2008. Phototrophic biofilms and their potential applications. J. Appl. Phycol. 20 (3), 227–235. https://doi.org/10.1007/s10811-007-9223-2.

Rossi, F., De Philippis, R., 2015. Role of cyanobacterial exopolysaccharides in phototrophic biofilms and in complex microbial mats. Life 5 (2), 1218–1238. https://doi.org/10.3390/life5021218.

Sarkar, S., Roy, D., Mukherjee, J., 2015. Enhanced surface area conico cylindrical flask (ES-CCF) for biofilm cultivation. U.S. Patent 8, 945,917.

Semple, K.T., Cain, R.B., Schmidt, S., 1999. Biodegradation of aromatic compounds by microalgae. FEMS Microbiol. Lett. 170 (2), 291–300. https://doi.org/10.1111/j.1574-6968.1999.tb13386.x.

Silambarasan, P., Ramu, A.G., Govarthanan, M., Jung, K.D., Moon, I.S., 2021. Enhanced sustainable electro-generation of a Ni (I) homogeneous electro-catalyst at a silver solid amalgam electrode for the continuous degradation of N_2O, NO, DCM, and CB pollutants. J. Hazard. Mater. 420, 126564 https://doi.org/10.1016/j.jhazmat.2021.126564.

Stiefelmaier, J., Strieth, D., Di Nonno, S., Erdmann, N., Muffler, K., Ulber, R., 2020. Characterization of terrestrial phototrophic biofilms of cyanobacterial species. Algal Res. 50, 101996 https://doi.org/10.1016/j.algal.2020.101996.

Taylor, K.A., Buchanan-Smith, J.G., 1992. A colorimetric method for the quantitation of uronic acids and a specific assay for galacturonic acid. Anal. Biochem. 201 (1), 190–196. https://doi.org/10.1016/0003-2697(92)90194-C.

Traczewska, T.M., Woźniak, B., Moskal, J., 1999. Application of bioassay with *Selenastrum capricornutum* to evaluation of toxicity of anthracene and phenanthrene in water. Environ. Prot. Eng. 25 (4), 51–59.

United States Environmental Protection Agency, 1996a. EPA-Method 3630C, Silica gel cleanup.

United States Environmental Protection Agency, 1996b. Test Method 3510C: Separatory funnel liquid-liquid extraction.

United States Environmental Protection Agency, 1996c. Method 8000B, Determinative chromatographic separations.

Uzoh, C.V., Ifeanyi, V.O., Okwuwe, C.I., Oranusi, S.U., Braide, W., Iheukwumere, I.H., Anyanwuocha, C.E., Ntamzor, B.G., 2015. Effect of light on the biodegradation of crude oil by the algae *Closterium* species. J. Nat. Sci. Res. 5 (22), 112–118.

Uzoigwe, C., Burgess, J.G., Ennis, C.J., Rahman, P.K., 2015. Bioemulsifiers are not biosurfactants and require different screening approaches. Front. Microbiol. 6, 245. https://doi.org/10.3389/fmicb.2015.00245.

Vaishnavi, J., Devanesan, S., AlSalhi, M.S., Rajasekar, A., Selvi, A., Srinivasan, P., Govarthanan, M., 2021. Biosurfactant mediated bioelectrokinetic remediation of diesel contaminated environment. Chemosphere 264, 128377. https://doi.org/10.1016/j.chemosphere.2020.128377.

Veerabadhran, M., Chakraborty, S., Mitra, S., Karmakar, S., Mukherjee, J., 2018. Effects of flask configuration on biofilm growth and metabolites of intertidal cyanobacteria isolated from a mangrove forest. J. Appl. Microbiol. 125 (1), 190–202. https://doi.org/10.1111/jam.13761.

Wang, J.H., Zhuang, L.L., Xu, X.Q., Deantes-Espinosa, V.M., Wang, X.X., Hu, H.Y., 2018. Microalgal attachment and attached systems for biomass production and wastewater treatment. Renew. Sustain. Energy Rev. 92, 331–342. https://doi.org/10.1016/j.rser.2018.04.081.

Wang, Y.S., Wu, F.X., Gu, Y.G., Huang, H.H., Gong, X.Y., Liao, X.L., 2021. Polycyclic Aromatic Hydrocarbons (PAHs) in the intertidal sediments of Pearl River Estuary: characterization, source diagnostics, and ecological risk assessment. Mar. Pollut. Bull. 173, 113140 https://doi.org/10.1016/j.marpolbul.2021.113140.

Wicke, D., Böckelmann, U., Reemtsma, T., 2007. Experimental and modeling approach to study sorption of dissolved hydrophobic organic contaminants to microbial biofilms. Water Res. 41 (10), 2202–2210. https://doi.org/10.1016/j.watres.2007.01.039.

Wicke, D., Böckelmann, U., Reemtsma, T., 2008. Environmental influences on the partitioning and diffusion of hydrophobic organic contaminants in microbial biofilms. Environ. Sci. Technol. 42 (6), 1990–1996. https://doi.org/10.1021/es702267s.

Wyatt, K.H., Seballos, R.C., Shoemaker, M.N., Brown, S.P., Chandra, S., Kuehn, K.A., Rober, A.R., Sadro, S., 2019. Resource constraints highlight complex microbial interactions during lake biofilm development. J. Ecol. 107 (6), 2737–2746. https://doi.org/10.1111/1365-2745.13223.

Xu, C., Zhang, S., Beaver, M., Lin, P., Sun, L., Doyle, S.M., Sylvan, J.B., Wozniak, A., Hatcher, P.G., Kaiser, K., Yan, G., 2018. The role of microbially-mediated exopolymeric substances (EPS) in regulating Macondo oil transport in a mesocosm experiment. Mar. Chem. 206, 52–61. https://doi.org/10.1016/j.marchem.2018.09.005.

Zhang, Y., Wang, F., Yang, X., Gu, C., Kengara, F.O., Hong, Q., Lv, Z., Jiang, X., 2011. Extracellular polymeric substances enhanced mass transfer of polycyclic aromatic hydrocarbons in the two-liquid-phase system for biodegradation. Appl. Microb. Biotechnol. 90 (3), 1063–1071. https://doi.org/10.1007/s00253-011-3134-5.

Zhuang, L.L., Yu, D., Zhang, J., Liu, F.F., Wu, Y.H., Zhang, T.Y., Dao, G.H., Hu, H.Y., 2018. The characteristics and influencing factors of the attached microalgae cultivation: a review. Renew. Sustain. Energy Rev. 94, 1110–1119. https://doi.org/10.1016/j.rser.2018.06.006.

Zyszka-Haberecht, B., Niemczyk, E., Lipok, J., 2019. Metabolic relation of cyanobacteria to aromatic compounds. Appl. Microbiol. Biotechnol. 103 (3), 1167–1178. https://doi.org/10.1007/s00253-018-9568-2.

CONFERENCE

6th Annual International E-Conference of
Indian Network for Soil Contamination Research (INSCR)

Certificate of Appreciation

This is presented to

Saranya Balu, School of Environmental Studies, Jadavpur University, Kolkata

for POSTER PRESENTATION under the theme

Microbial Ecology and Biotechnology

at the 6th Annual International Conference of INSCR on

"MICROBES IN SUSTAINABLE DEVELOPMENT"

organized in association with the Department of Zoology (DU), Acharya Narendra Dev College (DU), Deen Dayal Upadhyaya College (DU), Gargi College (DU), Kirori Mal College (DU), PG Department of Zoology (MU), Maitreyi College (DU), Ramjas College (DU), Sri Venkateswara College (DU), C.M.P. College (AU), SGTB Khalsa College (DU), COCAS (PU) & PhiXgen Pvt. Ltd., Gurugram from November 15 to 18, 2021.

Rup Lal

PROF. RUP LAL
President, INSCR

Yogendra Singh

PROF. YOGENDRA SINGH
General Secretary, INSCR

Thesis

ORIGINALITY REPORT

10%
SIMILARITY INDEX

PRIMARY SOURCES

1	Saranya Balu, Shantanu Bhunia, Ratan Gachhui, Joydeep Mukherjee. "Assessment of polycyclic aromatic hydrocarbon contamination in the Sundarbans, the world's largest tidal mangrove forest and indigenous microbial mixed biofilm-based removal of the contaminants", Environmental Pollution, 2020 Crossref	1188 words — 4%
2	aquafishcrsp.oregonstate.edu Internet	127 words — < 1%
3	dspace.unive.it Internet	119 words — < 1%
4	www.frontiersin.org Internet	119 words — < 1%
5	www.researchgate.net Internet	115 words — < 1%
6	wydoe.state.wy.us Internet	112 words — < 1%
7	iiseagrant.org Internet	111 words — < 1%
8	epdf.tips Internet	100 words — < 1%